2002

Faculteit Wetenschappen

The polymerisation behaviour of *p*-quinodimethane systems : verification of radical and anionic mechanisms in the Sulfinyl and the Gilch route

Proefschrift voorgelegd tot het behalen van de graad van
Doctor in de Wetenschappen, richting Scheikunde,
te verdedigen door

Lieve HONTIS

Promotoren : Prof. dr. D. Vanderzande
Prof. dr. J. Gelan

LIMBURGS
UNIVERSITAIR
CENTRUM
PARTNER IN DE UNIVERSITEIT LIMBURG

Voorwoord

Dit onderdeel van de thesis is vanuit wetenschappelijk oogpunt misschien niet het belangrijkste deel, maar het blijkt wel het meest gelezen te worden. Hier mag ik de wetenschappelijke termen achterwege laten en het gevoel de bovenhand laten krijgen. Veel mensen hebben hun eigen steentje bijgedragen aan het tot stand komen van dit werk en nu is het ogenblik aangebroken om duidelijk te maken wat die steentjes (stenen) zijn en wat ze voor mij betekenen.

Laat ik beginnen met die personen die meestal aan het eind vermeld worden, maar die eigenlijk op de eerste plaats komen. Pa en ma, dank je voor de kans om verder te studeren; hoewel het soms vanzelfsprekend lijkt, besef ik dat dit niet zo is. Zonder jullie nooit-aflatende steun en liefde zou ik dit niet hebben kunnen verwezenlijken. Ik hou van jullie.

Ook Moniek en Marc, Ketty en Erik, Joëlle en Jacky, Jacky en Caroline (mijn zussen, broer en hun partners) hebben samen met mij naar dit moment toegeleefd. Ik zou kunnen uitweiden over het soms kleine verschil tussen scheikunde en biologie, maar ik zal me hier beperken tot het getuigen van mijn diepe genegenheid voor jullie allen.

Twee andere kanjers die mijn geluk en leven compleet maken zijn mijn twee mannen in huis: Mirko en Sander. Mirko, ongelooflijk hoe je steeds (soms meer dan ikzelf) in mijn kunnen hebt geloofd. Als jij niet zo'n geduldige, lieve man en papa was, zouden er nu heel wat minder letters op papier hebben gestaan. Zo'n kleine uk vraagt immers heel wat aandacht. Sander (ook al beseft hij het nu waarschijnlijk nog niet) heeft me geleerd te relativeren; als ik naar hem kijk, weet ik wat belangrijk is. Ik heb jullie beiden o zo lief.

Inge, Rolf, Niklas en Karen, ook jullie wil ik bedanken voor de sterke interesse en steun tijdens de voorbije jaren. Ik zou me geen betere schoonfamilie en derde thuis kunnen wensen.

Hoewel nonkel Wim deze wereld al enkele jaren verlaten heeft, toch weet ik dat hij nu trots zou zijn. Ik ben hem (mijn engel) nog niet vergeten en draag dit werk gedeeltelijk aan hem op.

Piet, bedankt dat je ondanks de vele werkvakanties toch tijd hebt vrijge-maakt om het eerste hoofdstuk na te lezen. Jouw positieve feedback en blijk van interesse waren voor mij een teken dat het goed zat.

Gedurende die 4 à 5 jaren van doctoreren aan het LUC heb ik heel wat mensen leren kennen en grenzen verlegd. Het meeste tijd heb ik doorgebracht met de leden van de onderzoeksgroep organische en polymeerscheikunde en die lijst van mensen is over de jaren aangegroeid: Anne I., Mik, Margreet, Ben, Albert, Henk, Laurence, Wim, Dirk, Iwona, (Maria,) Pawel, Pierre-Henry, Roel, Liesbet, Robby, Anne P., Iris, Hugette, Tom, Stijn, Anja, Hilde, Filip, Joachim, Els, Veerle en Noura. Gedachten verbonden aan hen en de leden van de andere onderzoeksgroepen (anorganische, theoretische en toegepaste scheikunde) betreffen discussies en babbels, gehouden in de koffiekamer, in het labo, op de gang, in de Ardennen, tijdens feestjes, culinaire avonden.... Ik zal de goede werksfeer en collegialiteit missen en hoop met heel mijn hart dat de opgebouwde vriendschappen blijven duren en nieuwe banden worden aangehaald.

Ook alle overige vrienden, namen zijn hier overbodig, wil ik bedanken voor hun steun, interesse en gewoon omdat ze er zijn.

Dit alles heeft van dit doctoraat een ervaring gemaakt die ik niet had willen missen en voor de rest van mijn leven meedraag. Ik hoop dat ik de juiste woorden heb gevonden om mijn dank, genegenheid en respect uit te drukken voor al die mensen. Eigenlijk vat de volgende combinatie van drie lettergroepen ongeveer samen wat ik hen hier heb proberen te zeggen: dank je wel.

Contents

Contents

Chapter Three   Mechanistic Study on the Sulfinyl and Gilch Route
                 towards OC_1C_{10}-PPV

Contents

Chapter Four   Characterisation of Polymers by means of SEC-LS

1 | General Introduction

1.1 CONDUCTIVE POLYMERS

We are used to polymers – that is, plastics – that, unlike metals, insulate and do *not* conduct electricity. Electric wires are coated with polymers, such as polyethylene and poly(vinyl chloride) to protect them – and us – from short-circuits. Yet Alan J. Heeger, Alan G. MacDiarmid and Hideki Shirakawa were rewarded with the year 2000 Nobel Prize in Chemistry "*for the discovery and development of electrically conductive polymers*". In 1977 this trio of scientists discovered – accidentally - that oxidation with iodine vapour made polyacetylene (PA) films several orders of magnitude more electrically conductive than they were originally[1]. The "doped" form of PA had a conductivity of 10^5 Siemens per meter (S m^{-1}), which was higher than that of any previously known polymer. As a comparison, Teflon has – like quartz – an electrical conductivity of 10^{-16} S m^{-1}, while the conductivity of silver or copper equals 10^8 S m^{-1}.

The discovery of the highly conductive doped PA generated considerable excitement, from which a new research field of conductive polymers, rich in new physics and chemistry, emerged. Since then, various polymers have been devised with a remarkably wide range of electrical conductivities (figure 1.1). Most current commercial applications of conductive polymers utilise intermediate conductivity levels of between 10^0 and 10^4 S m^{-1}.
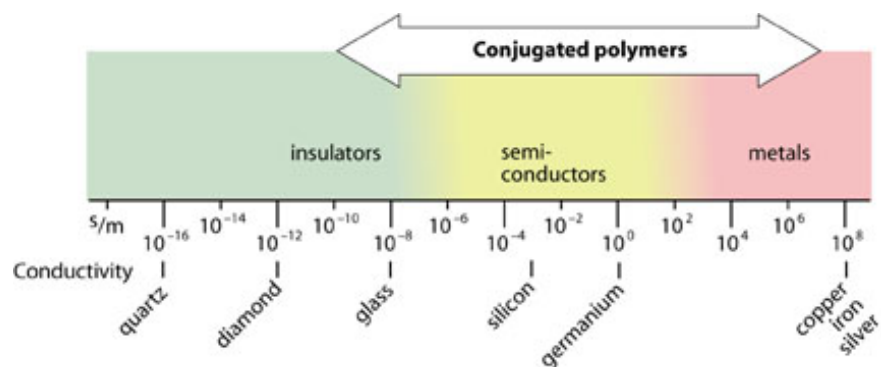
Figure 1.1: The range of electrical conductivities of conjugated polymers
compared to those of other materials

A key property of a conductive polymer is the extended π-conjugated
system, a sequence of alternating single and double bonds along the backbone of
the polymer. The chemical structure of several common conjugated polymers
with their repeat units is depicted in figure 1.2.

| Polyacetylene (PA) | Polythiophene (PT) | Poly(*p*-phenylene) (PPP) |

| Poly(p-phenylene vinylene) (PPV) | Poly(ethylenedioxythiophene) (PEDOT) |
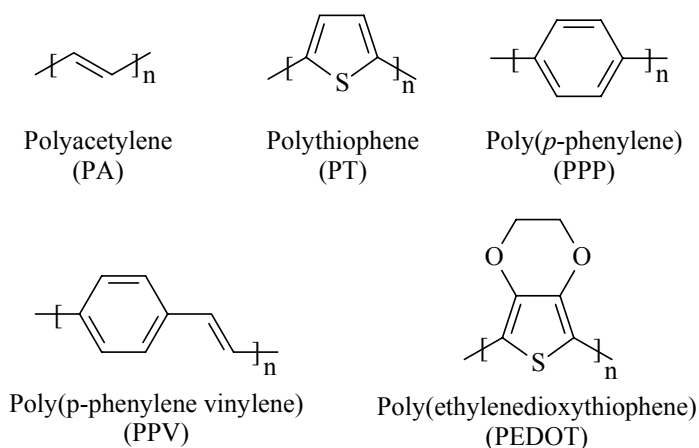
Figure 1.2: The chemical structure of several common conjugated polymers

However, conjugation is not enough to make the polymer material
conductive. In addition, the plastic has to be disturbed - either by removing
electrons from (oxidation), or inserting them into (reduction) the material. This

process is respectively known as p- and n-doping. The created "holes" and extra electrons can move along the molecule - it becomes electrically conductive.

The electrical properties of a material are determined by its electronic structure. The simple band theory can provide some useful information on the doping-induced changes in electronic structure. Overlap of adjacent atomic p_z-orbitals yields lower energy bonding (π) and higher energy anti-bonding ($\pi*$) molecular orbitals. When many molecular orbitals are spaced together in a given range of energy, the π-orbitals generate an apparently continuous, occupied valence band (VB), while the $\pi*$-orbitals produce the conduction band (CB). The energy spacing between the highest occupied molecular orbital (HOMO) and the lowest unoccupied molecular orbital (LUMO) is called the band gap (E_g). The size of this band gap, which in general lies between 1 and 4 eV for conjugated polymers, determines the electrical and optical properties of the material. Within the polymer material, charge-carrying species (solitons, polarons and bipolarons) can be created through doping or optical absorption[2]. Associated with these species are localised electronic states with energy levels within the otherwise forbidden band gap ("mid-gap" states). Figure 1.3 can help to understand.

At first, the poor processability and environmental stability of the first conductive polymers hampered commercial success. But during the 1980s, excitement was renewed because chemists learned how to solubilise these conductive polymers in various aqueous and organic solvents (more about this in section 1.4), while maintaining their electrical properties. These materials now can be processed much like the common polymers of the plastics industry. They can be moulded into parts, drawn into long fibres and cast into flexible films, and this offers potential for substantial cost-savings compared to conventional inorganic semiconductors (compare spin coating to epitaxial growth).

The discovery of conductive polymers has led to an impressive list of intended applications among which electromagnetic shielding[3], capacitors[4], electrostatic discharge coatings[4], polymer batteries[5], smart windows[6], sensors[7], photodetectors[8], lasers[9], field-effect transistors (FETs)[10], light-emitting electrochemical cells (LECs)[11], photovoltaic (solar) cells[12], and polymer light-emitting devices (P-LEDs). A major future goal for conductive polymers will be

replacement of copper for interconnects on printed circuit boards. Improved stability is the major technical milestone that needs to be achieved for this application.

By now, the number of publications concerning conductive polymers is enormous and promising results are obtained in more than one field of application. Although PA served as the prototype conjugated polymer, it was not the first to be commercialised due to its instability in air and its sensitivity to humidity. The much greater stability of other conjugated materials with somewhat lower conductivities - but still sufficient for many applications – has made them more interesting for commercialisation. The following list of some already commercially available materials illustrates the success of the field of conductive polymers in optical, electronic and opto-electronic devices.

Polythiophene derivatives are promising for FETs[13]. They may possibly find a use in supermarket checkouts.

Poly(phenylene vinylene) and derivatives have been major candidates for the active layer in the pilot production of electroluminescent displays (mobile telephone displays), and recently serves as a useful system for elucidating the working principle of polymer photovoltaic cells.

Poly(ethylenedioxythiophene) doped with polystyrenesulfonic acid (PSS) is manufactured as an antistatic coating material to prevent electrical discharge exposure on photographic emulsions and also serves as a hole-injecting electrode material in P-LEDs[14].

The major interest in the use of polymers is in low-cost solution-processing making use of the film-forming properties of such polymers. Light displays and integrated circuits, for example, could theoretically be manufactured using simple inkjet printer techniques[15].

1.2. ELECTROLUMINESCENCE

With sufficient current, electrically conducting metal wires can light up – as we are reminded of every time we switch on a light bulb. Polymers can also be made to light up, but by another principle, namely *electroluminescence* (EL), which is used in photodiodes. These photodiodes are more energy saving and generate less heat than light bulbs.

Electroluminescence – the conversion of an electrical current into visible light – is at present a major research topic in the field of semi conductive polymers[16]. It can be explained in analogy to *photoluminescence* (PL), which is defined as the conversion of (UV-) light into visible light. These two processes are depicted in figure 1.3 using a conjugated polymer as active material. A comparison of PL- and EL-spectra of polymer films has shown that in both cases identical excited states are involved[17].
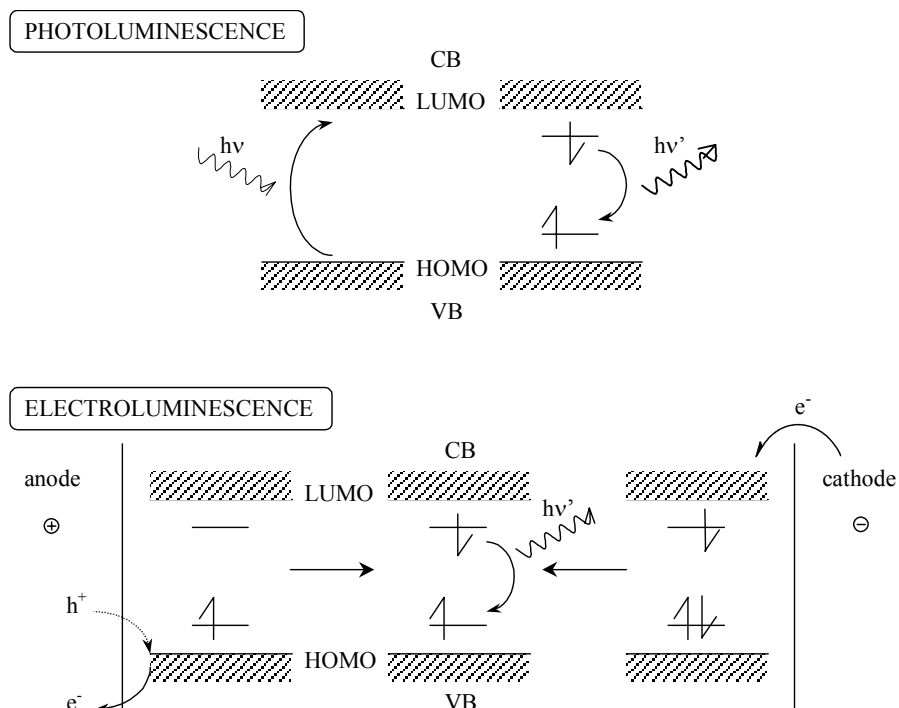
Figure 1.3: Schematic representation of photoluminescence (top) and electroluminescence (bottom) in conjugated polymers

In the case of PL, the action of an incident photon excites an electron from the HOMO into the LUMO of a fluorescent polymer. In a typical conjugated polymer, the partial delocalisation causes the formation of two new mid-gap states, each filled with an electron of opposite spin, forming a singlet excited state. Radiative decay of this singlet exciton to the ground state produces emission of light – luminescence - at a longer wavelength than that absorbed and is called PL.

EL works under a similar general principle. On application of an electrical voltage, electrons are injected from the cathode in the LUMO to generate negatively charged polarons (radical anions). At the anode electrons are extracted from the HOMO, or in other words holes are injected, to form positive polarons (radical cations). Under the influence of the applied electric field electrons and holes migrate in opposite directions within the polymer layer. Charge carrier recombination somewhere in the bulk of the polymer, results in the formation of an exciton, which can emit light by relaxation to the ground state.

This phenomenon led to the light-emitting device technology that has proven to be a multidisciplinary field: it challenges the skills of synthetic chemists, applied physicists, theoreticians, and materials scientists. As a consequence the number of publications is enormous and it would lead too far to discuss all literature on the subject. Therefore section 1.3 should not be regarded as a complete survey, but merely as an introduction to the broad and complex field.

1.3 POLYMER LIGHT-EMITTING DEVICES

1.3.1 The Working Principle

The development of electroluminescent devices based on inorganic semiconductors and organic compounds has been an active research area for decades. The first reports on EL of organic compounds date back to 1963 when Pope et al. described EL in anthracene single crystals using liquid electrolytic electrodes and high voltages (400-2000 V)[18]. In the 1980s development of

organic EL devices was spurred on through the work of Tang and Van Slyke, who demonstrated efficient EL – a luminance of over 1000 Candela per m² (Cd/m²) at an operating voltage below 10 V - in two-layer sublimed molecular film devices[19]. These devices consisted of a hole-transporting layer of an aromatic diamine and an emissive layer of the fluorescent organic dye 8-hydroxyquinoline aluminium (Alq$_3$) between two electrodes.

A major breakthrough came only in 1990, when the Cambridge group reported the observation of EL in the conjugated polymer poly(*p*-phenylene vinylene), PPV[20]. The faint glow was bright enough to illuminate an entire research field and move the dream to create a generation of "plastic electronics" closer to reality. Since, intensive research was driven by the outlook on possible advantages of polymer light-emitting diodes (P-LEDs): cheap processing, small thickness, low weight, versatility for fabrication (especially over a large area), low driving voltages and flexibility. The research in P-LEDs at both academic and industrial research institutes grew exponentially and a lot of effort was exposed to design stable P-LEDs in which mainly PPV and its derivatives are used as active layer.

In figure 1.4 the device layout of a single-layer P-LED is schematically represented. On top of a glass substrate a high-work-function transparent electrode (mostly indium-tin-oxide, ITO) is deposited to allow the generated light to leave the device. A thin layer of the emissive polymer is sandwiched between this anode and a low-work-function cathode (mostly calcium, aluminium or magnesium). Proper encapsulation prevents diffusion of water and oxygen into the active area of the device.
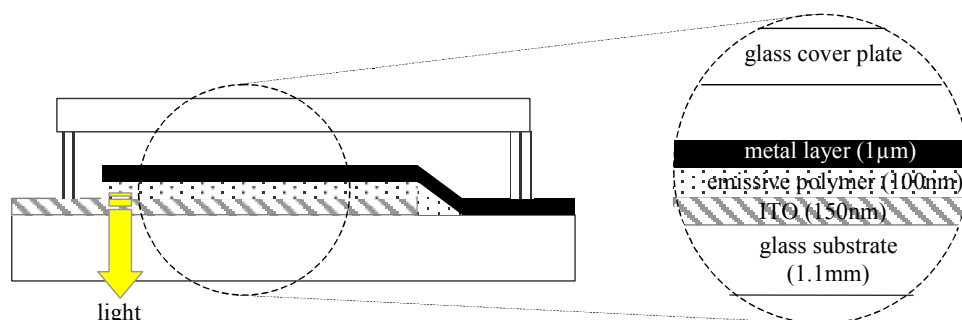
Figure 1.4: A cross section of a single-layer P-LED

By exhibiting a voltage the conjugated polymer starts emitting light by the phenomenon of EL. As shown in figure 1.5 three electronic processes can be distinguished that determine the device operation of a P-LED[21]: charge injection, charge transport and recombination, and these will now be discussed briefly.
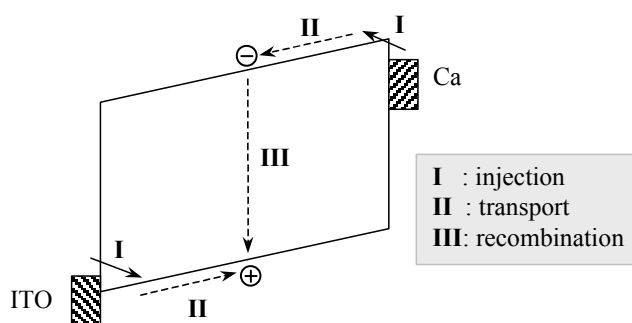
Figure 1.5: A schematic band diagram of a PPV-based LED

Charge injection

For the majority of conjugated polymers investigated so far, electron injection has proven more difficult than hole injection. That is, the polymers are more easily oxidised than reduced. The energy barrier for charge injection depends on the relative positions of the energy levels of the active layer and the work functions of the electrode materials used. Or, in other words: the work function of the anode material should match the ionisation potential of the polymer as good as possible, whereas the same holds for the work function of the cathode and the electron affinity of the polymeric compound.

Consequently, improvement of charge injection, hence device efficiency, can involve variation of electrode materials or adjustment of HOMO-LUMO levels of the polymer layer(s) by chemical modification[22].

Charge transport

It has been found that the mobility of electrons and holes in PPV are highly asymmetric: electrons are, in contrast to holes, severely trapped[23]. The use of an electron transport layer (e.g. oxadiazoles) will shift the recombination area away from the cathode, resulting in an efficiency increase at low voltages[24].

Mobilities are low due to the largely amorphous nature of conjugated polymer films[25]. Charge carrier transport across thin films is limited by the mobility values. The hole mobility in PPV is of order 10^{-4} cm² V^{-1} s^{-1} allowing transport across a 100 nm layer with typical fields of 5 x 10^5 V/cm in 0.5 μs (compare to amorphous silicon mobilities of between 0.1 and 1 cm² V^{-1} s^{-1}). Nevertheless, these switching times are quite adequate for use in many diode devices, such as P-LEDs, detectors and photovoltaic cells.

Recombination

A major factor determining the luminescence efficiency of P-LEDs is the competition between radiative and non-radiative decay of the recombined electron-hole pairs within the polymer layer. Because of the spin statistics to form singlet excitons, it has been hypothesised that the EL quantum efficiency (QE) – the proportion of emitted photons to the electrons transported through the device – would be only about one fourth of the PL QE[26]. In order to achieve high EL efficiencies, compounds with a high PL efficiency in the solid state are therefore necessary.

1.3.2 Important Characteristics

The number of publications on P-LEDs – physical as well as chemical - is impressive and it's not the intention to cover all aspects in this introduction. But to give an idea of the work that is done by the various research teams all over the world a few issues are discussed briefly in this section. In order to discuss the possibilities of light-emitting polymers for large-area applications the following items are important: solubility, colour tuning, brightness and lifetime, efficiency, stability, and purity. The numeric data are based on Philips publications[27], unless stated otherwise.

Solubility

An interesting technique in polymer processing technology is the spin coating technique: a drop of the polymer solution falls onto a rapidly rotating substrate, and spreads out immediately into an almost perfectly homogeneous

film. This way, after solvent evaporation, the substrate is coated with a polymer film with a thickness of about 100 to 200 nm. In order to apply the spin coating technique for the deposition of the material, it is necessary to have a soluble polymer material. However, most regular conjugated materials are insoluble and therefore two successful methods to enable processing have been proposed[28].

One possibility is to prepare films from a soluble precursor material, and convert it by thermal treatment. A disadvantage of this process - which makes it less attractive for industrial application - is the lack of good reproducibility, because of entrapped elimination products in the polymer film.

Another approach involves the introduction of flexible side-chains to yield completely soluble conjugated polymers. The advantage of this strategy is that elimination procedures can be performed before the spin coating procedure. A drawback is the difficulty to engineer mutually exclusive solvents for the different polymer layers in a multilayer device, which leads to poor interface quality.

Colour tuning

The richness of organic chemistry allows the fabrication of new materials with different emission properties, including a wide range of colours. The colour of the emitted light depends on the band gap of the polymer material, and is usually identical to the colour of its fluorescence[29]. The intensively studied polymer PPV has a band gap of about 2.4 eV and produces yellow-green luminescence. With P-LEDs the full spectrum of colours – from deep blue to even the infrared – has now been shown to be feasible[30]. In traditional semiconductor LEDs this took 20 years.

An important advantage of polymeric materials is that the band gap and redox potential can be tuned by the chemical modification of the polymer chain. Control of the effective conjugation length by the introduction of steric side-chains, which force the backbone to twist[31] and the design of copolymers that comprise well-defined conjugated segments[32] are illustrative examples of how the emission colour can be varied over a wide range. Another important tool for colour control is the variation of the aromatic ring or the introduction of electron withdrawing or electron donating side-chains[33]. Alkoxy side-chains lead to a

lowering of the band gap, and thus to a red-shifted emission, whereas the use of alkyl or aryl side-chains results in a blue-shifted colour of emission. These examples demonstrate the possibility to cover the entire visible spectrum by choosing the appropriate side-chains.

Brightness and lifetime

High values for brightness – or more exactly luminance – can now be reached at a low voltage. According to Philips, orange P-LEDs with 50 nm thick emissive layers have an onset of emission at 1.8 V (just above the band gap). With these devices a luminance of 100 Cd/m² can already be reached at 2.5 V. This may be compared with a typical luminance of 60 Cd/m² of lap top computer displays and 100 Cd/m^2 of a TV screen.

Lifetime is also a big concern when considering commercial applications of the P-LED technology. Significant activity is taking place to improve material lifetimes both through use of materials that are resistant to oxidation and through improved encapsulation. Storage lifetimes of at least 5 years are typically required by most consumer and business products, and operating lifetimes of over 20 000 hours are relevant for most applications. For orange and green emitting devices lifetimes of more than 10 000 hours (417 days) have been reported. Some of the most interesting blue emitting materials are based on polyphenylene and polyfluorene derivatives. Serious industrial evaluation still has to be carried out; hence no data on blue devices with very long lifetimes are available yet.

Efficiency

Different definitions are applied to describe the efficiency of an EL polymer. A common measure is the internal EL efficiency, which is defined as the amount of photons generated within the device per electron injected (expressed in %), and is based on the assumption that all light generated is received by the viewer. External efficiencies are a factor of 2n² smaller – n being the refractive index of the polymer[34]. Most external quantum efficiencies for the family of PPV polymers fall within the range of 0.1-5%. Device engineers are used to express luminous efficiency in terms of Lumen per Watt (Lm/W), a value that takes

account of the fact that the eye is more sensitive to green than to red and blue light.

The levels of internal quantum efficiency on the first, simple PPV-based LEDs fabricated with aluminium cathodes were of the order of 0.01%[20]. These values progressed rapidly over the last decade as improved understanding of the operation of these devices – utilising device engineering techniques of inorganic LEDs, such as the use of a heterostructure - has allowed considerable optimisation of the device characteristics. Recently, for a P-LED where green light is emitted at 550 nm wavelength, external efficiency values - measured in forward direction – as high as 17 Lm/W are reported. This value compares favourably with values of 20 Lm/W for ordinary light bulbs. To compare with existing display technologies: a cathode ray tube has an efficiency of around 1 Lm/W and an active matrix liquid-crystal display (LCD) with a backlight has an efficiency of 1 to 3 Lm/W. With 17 Lm/W the efficiency of a P-LED is far superior.

Stability

One of the main question marks concerning this P-LED technology has been stability, and a lot of effort has been exposed in this field in search for answers. Operating lifetimes in excess of 3 000 hours, and in general, in excess of 10 000 hours, are required for most applications, together with storage times of 5 years or more. Important progress has been reported in this area. Improvement of the anode stability was, for example, obtained by covering the ITO-layer with a transparent and conductive polymer (PEDOT / PSS), which has been found to increase device lifetime by a factor 10 to 100. Proper device encapsulation to prevent ingress of water and oxygen has been found to prevent oxidation for devices based on glass.

Fully flexible LEDs - using poly(ethyleneterephthalate), PET as the substrate instead of glass, and polyaniline (PANI) instead of ITO - suffer rapid corrosion of cathode materials caused by water diffusion through the plastic film, resulting in a short lifetime (about 1 day) in an ambient atmosphere[35]. To improve their stability plastic films with improved water barriers are being investigated.

Purity

The performance and lifetime of P-LEDs are governed by many factors, of which one is the purity of the material. During polymer synthesis a large number of impurities and defects may be formed – depending on the synthetic route used. Purification procedures can remove impurities such as salts, monomer residues and low molecular weight reaction products. However, defects in the polymer structure are an integral part of the polymer and affect the device performance considerably. The intrinsic purity of the polymer can only be improved by variation of reaction conditions, such as type of solvent, reaction temperature, and concentration. A careful control of these parameters can lead to polymers of higher purity and therefore improved performance of the devices.

The electronics industry traditionally relied on inorganic chemicals for many of its devices – e.g. computer chips and visual displays. However, in the constant drive for better performance, the big industry players – like Covion, Philips, Bayer and Cambridge Display Technology (CDT) – started to look at the use of polymers in certain applications. By now, P-LED displays can meet customer specifications in the case of orange emitting materials.

Because of their high brightness, P-LEDs could be used in all kinds of signalling applications like warning signs, indicators, decorative light sources, advertising, rear lights and brake lights for cars, and LCD backlights (e.g. mobile phones, car radios and stereo sets). Expectations are that P-LED technology will ultimately offer an alternative to the cathode ray tube – the display in conventional televisions and computer monitors.

Extension to a full-colour graphic display (for computer monitors and video display) is very attractive, not at least because organic and polymeric LEDs provide full viewing angle and video-rate response times (in contrast to current LCD technology). In 1998, CDT unveiled a prototype television screen – measuring 5 cm square and only 2 mm thick - using the green light emitting PPV[36]. June 2000, Seiko-Epson and CDT presented already a prototype colour display, made using CDT's red, green and blue polymer materials and an industry first ink-jet process developed for the project[37]. This prototype display measures 2.5 inch square, and has a resolution of 200 by 150 pixels.

A big goal for P-LEDs remains large area flat panel displays, where there is no established commercial technology, and where the polymer approach promises a low cost solution. But large P-LEDs still have problems associated with the loss of charge along the lines, which can give problems with colour and image uniformity.

Solution processing of polymers offers new methods for colour patterning, among which there is particular interest in ink-jet printing, to place separated pixels of red-, green-, and blue-emitting polymers onto the prepared substrate. This technique is being developed by Seiko-Epson, CDT and also by other groups[38].

The use of conductive polymers offers several advantages over the classical semiconductors both in terms of the ease of fabrication, as well as the design of new materials with different band gaps, ionisation potentials and electron affinities. The principal disadvantages are lifetime and mobility, but significant activity to improve has been taken and still is taking place.

The new P-LED technology is attractive for flat and thin light sources. After about three decades of development, an inorganic standard commercial red LED has a luminescence efficiency of about 1-2%. Because of the progress made in recent years – better materials, improved device preparation, process conditions and understanding - P-LEDs have reached in one decade comparable and even higher values.

1.4 PRECURSOR ROUTES TO PPVS

As discussed in previous sections, conjugated polymers have a wide range of potential applications in opto-electronic devices. As solution processing is in most cases the preferable method for device fabrication, soluble forms of conjugated polymers are highly desirable for both practical applications and fundamental studies. However, before the early 1980s no conjugated conducting polymer had been shown to be soluble in any solvent without decomposition, and they were regarded as intrinsically intractable (i.e. insoluble and infusible). Since,

research in this field has been extended to the synthesis and study of soluble conducting polymers and has led to two important approaches to the preparation of conjugated polymer thin films: the precursor and the side-chain approach[28].

The side-chain approach involves the polymerisation of a substituted monomer into a soluble conjugated polymer with the advantage that it can be directly solution-processed into thin films. Disadvantages are that the substituents used to provide solubility frequently lead to a reduction in mechanical properties, reduced T_g (assumed T_g of PPV = 220°C)[39] and photochemical instability – they greatly affect device performance. Also, interface quality in multilayer devices can be poor due to the difficult engineering of mutually exclusive solvents for the various polymer layers.

The precursor approach relies on the design and synthesis of an intermediate, soluble precursor polymer that can be cast into thin films, before solid-state conversion to the final conjugated polymer. A disadvantage of this approach is that incomplete solvent removal and / or liberation of volatile leaving group species after film deposition can cause delamination of electrodes, formation of voids and chemical reactivity. Precursor routes do offer the advantage of processability without sacrificing any of the desirable physical, electronic or optical properties in the final polymer and multilayer LEDs can be easily produced as the polymer can be rendered insoluble after film deposition.

This section focuses on the progress in the synthesis of PPVs. These conjugated polymers were initially prepared by means of Wittig olefination[40], Heck reaction[41] or Knoevenagel condensation[42]. These various, so-called direct routes gave essentially low molecular weight, insoluble and infusible oligomers that precipitated in an early stage of the reaction. A fundamental step in the development of conjugated polymers occurred with the soluble precursor route. While PPV is an intractable material with a rigid-rod microcrystalline structure, the precursor polymer is solution processable and can be converted into the conjugated structure by thermal treatment.

During the years several clever synthetic precursor routes - of which the most important are discussed below - were developed to solubilise these polymers.

1.4.1 The Wessling-Zimmerman route

This route is also called the sulfonium (polyelectrolyte) precursor route and was patented by Wessling and Zimmerman[43]. The precursor is produced in aqueous solution by the base-induced polymerisation of an appropriate monomer – a bis-sulfonium salt of *p*-xylene (figure 1.6). The principal derivatives used in initial polymerisations have been the dimethyl and diethyl sulfonium salts with either chlorine or bromine counter ions. Although this route allows preparation of high molecular weight polymers, the obtained yields were rather low (10–20%) due to undesired side reactions. Other sulfonium salt monomers were evaluated and the tetrahydrothiophenium (THT) derivative was found to be more stable. Optimised reaction conditions – to minimise premature elimination - involve the use of low temperatures (T $\leq$ 0°C), fairly dilute monomer solutions (0.05 to 0.2 mM) and equimolar or lower base to monomer ratios[44].
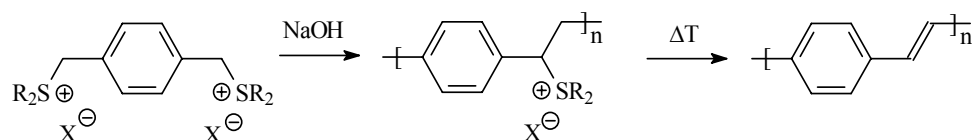
Figure 1.6: The Wessling-Zimmerman route

The polymerisation reaction is terminated by the addition of dilute HCl and the solution is then dialysed against water for a week or longer in order to separate the high molecular weight fraction from monomer residues, salts and oligomeric material. The precursor solutions generally show a weak blue / green fluorescence, which is attributed to very short conjugated sequences arising from an unavoidable limited amount of preliminary elimination. Under normal circumstances the molecular weight of the precursor is found to be relatively high ($M_w \geq 1 \times 10^5$ g/mol), but molecular weight measurements are very difficult due to irreversible interactions between the ionic precursor and the chromatography columns. For this reason the precursor is sometimes methoxy converted – leading to a higher stability at room temperature and solubility in tetrahydrofuran (THF)

or chloroform - to make size exclusion chromatography (SEC) and NMR-measurements possible[45].

The precursor polymer solution is then spin casted onto substrates to form thin films, and conversion to PPV is normally achieved by a thermal treatment under vacuum or inert gas atmosphere to avoid formation of carbonyl moieties through oxidation of the vinylic bond. It involves the elimination of dialkylsulfide (SR_2) and hydrogen halide (HX) of which the latter may react with ITO electrodes, leading to poor device performance. The temperature and the time of heating primarily determine the degree of conversion. Full conversion requires an elimination temperature of 160-300°C during 2 to 20 hours, whereas polymer decomposition occurs at approximately 550°C[46].

As mentioned before, the Wessling precursor suffers from instability and can undergo all kinds of side reactions during polymerisation or storage leading to gel formation and eventually insoluble precursor polymers. This is due to the good leaving group properties of the sulfonium groups – even at room temperature - and connected nucleophilic substitution. In figure 1.7 a possible defective structure of a sulfonium precursor is presented. The extreme sensitivity of the symmetric monomer to polymerisation conditions limits the possibilities of this precursor route for device manufacturing.
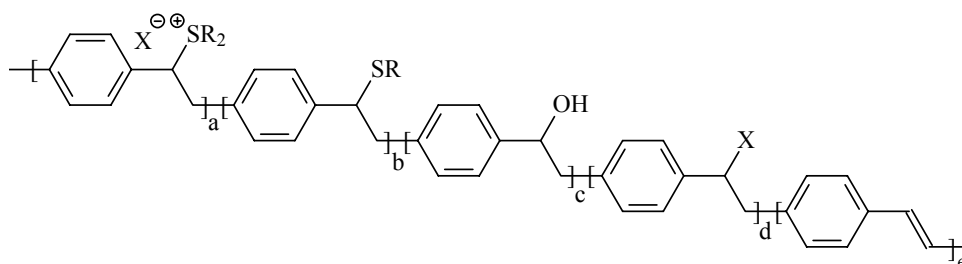
Figure 1.7: A possible defective structure of a
Wessling-Zimmerman precursor polymer

Chapter One

1.4.2 The Xanthate Route

This route was developed at AT&T Bell Laboratories and actually is a modification of the Wessling route as an attempt to circumvent the problems inherent to the latter[47]. The goal was to synthesise organic soluble precursors with improved film quality and a leaving group that would not easily undergo nucleophilic substitution and would produce a mixture of *cis-* and *trans-*vinylic bonds upon elimination in order to reduce crystallinity.

A base-induced polymerisation in THF at 0°C of a symmetric xanthate substituted *p*-xylene monomer yields the xanthate precursor polymer (figure 1.8), that is soluble in common organic solvents like THF, 1,4-dioxane, chloroform, cyclohexanone and toluene. Size exclusion chromatography against polystyrene standards results in an M_w of $6x10^5$ g/mol with a polydispersity of 3.4 - yields are not mentioned. Elimination takes place between 180 and 250°C and IR-frequencies around 868 cm^{-1} are assigned to the presence of *cis*-double bonds. However, until now these *cis*-structures could not be confirmed by other characterisation techniques and the competitive explanation of incomplete elimination should be kept in mind.
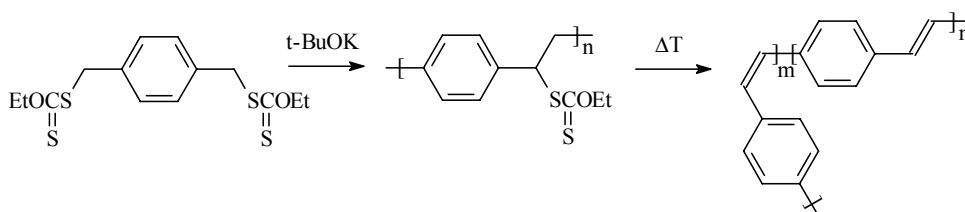
Figure 1.8: The Xanthate route

Although this route should offer certain advantages - like stability and solubility - over the Wessling-Zimmerman route, the number of publications on this subject is rather limited. It is striking that in some publications silence is kept about polymer yields, while others mention yields of 60-70%[48]. However, it appears that this route could not fulfil the expectance of a commercial synthetic method.

1.4.3 The Gilch route

In 1944 Kharasch et al. observed nearly quantitative yields of trans-stilbene from the reaction of benzylhalides with sodium amide in liquid ammonia[49]. Some two decades later, Hoeg and his co-workers obtained insoluble and infusible PPV after a similar reaction of α,α'-dichloro-*p*-xylene in dry THF at –35°C[50].

Following this model Gilch and Weelwright reported in 1966 on the polymerisation of bis(halomethyl)benzenes – again a symmetrical monomer - in benzene in the presence of large excess (10 equivalents) of potassium *t*-butoxide (*t*-BuOK) to PPVs[51]. To prevent premature precipitation Swatos *et al.* presented a modification of the Gilch route – the chlorine precursor route (CPR) – that uses about one equivalent of *t*-BuOK instead of an excess of base, to yield a soluble precursor polymer that can be converted to the conjugated form[52]. The chlorine PPV-precursor is insoluble in most common organic solvents such as acetone, chloroform and THF. Conversion of chlorine precursors to conjugated material can be obtained by heat treatment (300°C, 1h) or in case of soluble PPV-derivatives by basic elimination.

In literature no real distinction is made between the two routes (figure 1.9) - it is always referred to as the Gilch route and this appellation is kept throughout this thesis.
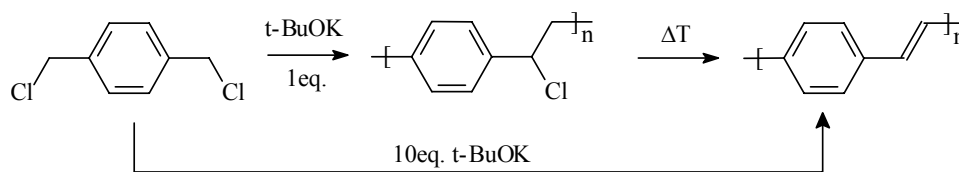
Figure 1.9: The Gilch route

For the synthesis of PPV this Gilch precursor route has no real advantages over the Wessling-Zimmerman route - both of them involve the liberation of HCl gas, which may react with ITO electrodes, leading to poor device performance. Nevertheless, at present, the Gilch route is in industry the most common used,

because in comparison with the Wessling method it allows easier access to a large range of substituted PPV derivatives, soluble in organic solvents.

1.4.4 The Sulfinyl route

The use of symmetrical monomers – chemical identical functionalities on both benzylic monomer positions – in the precursor routes discussed previously, implies unstable or defective precursor polymers. The demand to have an efficient monomer formation for efficient polymerisation leads to the use of good leaving groups, like sulfonium or chlorine substituents, which yield consequently highly reactive precursor polymers. In contrast, the wish to accomplish a relatively stable precursor implies a compromise in the leaving group capability and in consequence more severe reaction conditions for the polymerisation reaction.

To control the polymerisation process and simultaneously the stability of precursor polymers, there is a necessity for a chemical differentiation between both functionalities and that is exactly why the Sulfinyl route was developed in our laboratory. It makes use of un-symmetrical monomers bearing two different functionalities on the benzylic positions: a polariser and a leaving group. As leaving group halides were chosen, because of their high leaving group capacity and the lack of enhancement of the acidity of the benzylic position. Sulfinyl groups introduce the opposite behaviour and fulfil the function of polarisers, which is in fact, threefold (section 1.5.2). One of these functions is the well-documented concerted thermal conversion to a double bond[53], while a high stability against nucleophilic reagents is retained.

The Sulfinyl precursor route (figure 1.10) again uses a base (1.0-1.3 equivalents) to induce polymerisation of α-chloro-α'-alkyl(or aryl)sulfinyl-*p*-xylenes yielding high molecular weight precursor polymers, soluble in simple organic solvents. According to IR and UV-vis measurements these stable precursors can be very conveniently converted at low temperature (70-100°C) to the fully conjugated polymer[54] and this adds to the advantages of this precursor route. The precursor stability at room temperature makes a thorough

characterisation using spectroscopic techniques and SEC measurements possible, also opening opportunities to study the reaction mechanism.
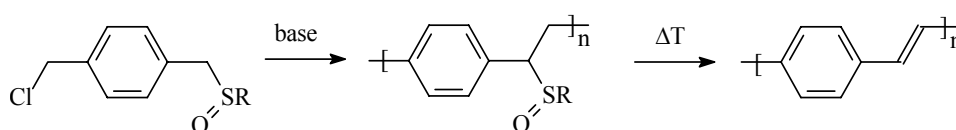
Figure 1.10: The Sulfinyl route

Partial reduction or oxidation of the sulfinyl group in the precursor can lead to a conjugated polymer with a restricted conjugation length. Due to the higher elimination temperatures of obtained sulfanyl (S) and sulfonyl ($S(O)_2$) functionalities respectively, careful tuning of the elimination conditions can lead to a selective removal of the sulfinyl groups. The resulting partially conjugated copolymers show an enhanced PL efficiency compared to standard PPV[55].

Altering the R-group of the sulfinyl functionality offers opportunities to tune solubility characteristics of both monomer and precursor polymer. This way an impressive spectrum of solvents, ranging from apolar (e.g. toluene) to polar solvents (like alcohols and water) becomes available for processing and facilitates optimisation of e.g. spin coating conditions[56]. Especially alcohols could be interesting from environmental viewpoint.

Due to this flexibility of the Sulfinyl route, monomers with electron withdrawing and donating substituents can be polymerised. Moreover, unlike the Wessling-Zimmerman route, also polymerisation of monomers with extended aromatic systems, like the 2,6-naphthalene and the 4,4'-biphenyl derivatives is feasible. Suitable solvent-base systems to overcome losses of resonance energies can be found as function of the monomers, by altering leaving group and/or polariser[57]. More about this in chapter two.

1.5 PRECURSOR ROUTE MECHANISMS

In this section of the introduction, literature on the mechanism of the precursor routes will be discussed on the basis of a general scheme. But first the

Chapter One

chemistry of poly(*p*-xylylenes) will be reviewed, because it paved the way to PPV precursors and its mechanism is more or less agreed on.

1.5.1 The Chemistry of Poly(*p*-xylylenes)

Szwarc was the first to observe that fast flow pyrolysis of *p*-xylene at 900-950°C and low pressure (4 mm Hg) yields a white polymeric material (max. 25%) having the postulated structure of poly(*p*-xylylene), PPX, the saturated analogue of PPV[58]. The high temperature was necessary to cleave the methylene carbon-hydrogen bonds leading to the formation of *p*-xylylene, more recently called *p*-quinodimethane (*p*-QM). The existence of this reactive intermediate was demonstrated by detection of *p*-xylylene diiodide among the pyrolysis products after injection of iodine vapour into the pyrolysate. Furthermore, addition of elementary chlorine or bromine shows a similar reaction, yielding the corresponding dihalides.

The *p*-QM molecule is the prototype of a class of hydrocarbons known as Chichibabin hydrocarbons and can be represented either by a quinonoid or a benzenoid resonance structure (figure 1.11)[59]. Coulson et al. calculated the energy difference for unsubstituted *p*-QM between the singlet ground state and the triplet excited state to be only 8-9 kcal/mol[60]. The corresponding value for ethene is much higher: 82 kcal/mol[61]. The unusual low energy difference implies an unexpected high contribution of the diradical (benzenoid) resonance structure, possessing two uncoupled electrons, to the ground or singlet state of the *p*-quinodimethane[62]. It is responsible for the extreme reactivity of *p*-QMs in condensed phase and implies that 1,6-addition by free radical mechanism should occur readily at the two terminal methylene groups[60].

quinonoid   benzenoid
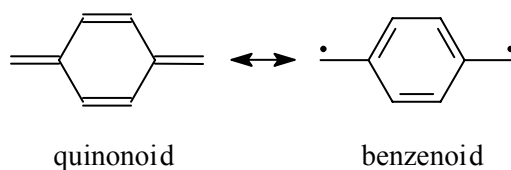
Figure 1.11: *p*-Quinodimethane

22

Introduction of electron withdrawing substituents like the cyano group at the methylene positions leads to a stabilisation of QMs. Therefore, substituted QMs become less reactive (more stable) and more easily obtainable as crystals at room temperature – e.g. 7,7,8,8-tetracyanoquinodimethane is an isolable crystalline compound. These monomers are expected to exhibit unique polymerisation behaviour[63]. It was found that captodative substituted QMs are stable compounds that are homopolymerisable with free radical and anionic initiators and copolymerisable with styrene in a random fashion[64].

Errede refined the fast flow pyrolysis technique by subsequent quenching of the pyrolysate directly into a solvent maintained at –78°C to obtain relatively stable *p*-QM solutions, which allowed their chemistry to be studied more in detail[65]. The usual inhibitors like amines, phenols, and quinones - even if present as major component of the solution – did not improve the solution stability. Chain transfer only occurred - with difficulty - with mercaptans and compounds of comparable reactivity, while the common chain transfer agents – chloroform, carbon tetrachloride, phenol, anilines, nitrobenzene, benzoquinones - did not exhibit an effect[66]. The free radical reactivity of the *p*-QM is so high that polymerisation takes place as if it were in an inert medium, even at this low temperatures[67]. Reaction of *p*-QM with monoradicals (NO_2 and NO), halogen molecules and diphenyl picryl hydrazine (DPPH) was found to afford linear telomeric products by addition at the two terminal methylene groups[68]. Bubbling oxygen or air through a fresh monomer solution resulted in an unstable, insoluble alternating copolymer with oxygen[69], but numerous attempts to copolymerise *p*-QM with various olefins like styrene, butadiene or acrylonitrile were unsuccessful. Even if the olefin acted as solvent, the QM pseudo-radical seemed too reactive to afford cross propagation with these monomers, because the only polymeric material formed was PPX[70].

All these experiments and the characterisation of the side-products led to the scheme of Errede (figure 1.12) - a mechanism proposal[71]. Isothermal reaction at –78°C presumably involves formation of diradical n-mers, which continue to grow at both ends by successive addition of *p*-QM monomer and / or by coupling until all monomer is consumed or the free radical chain ends are entrapped in the chain mesh. A molecular weight of about $2x10^5$ g/mol was calculated from the number

of radioactive iodine groups incorporated into the polymer after quenching with labelled iodine at 95% conversion (this is an approximation, because of the uncertainty in removing last traces of adsorbed radioactive iodine). Subjection to non-isothermal reaction (rapid heating from −78°C to room temperature) increases the amount of low molecular weight side-products. Due to the temperature increase the rate of propagation as well as initiation increases, favouring formation of dimers, trimers and tetramers. Cyclisation occurs most easily at the trimer stage, and becomes increasingly less probable with each new monomer addition.

Isothermal polymerisation at low temperature
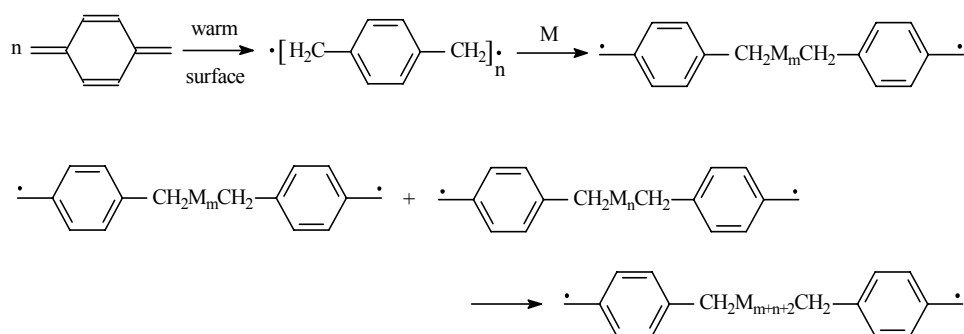
Non-isothermal polymerisation
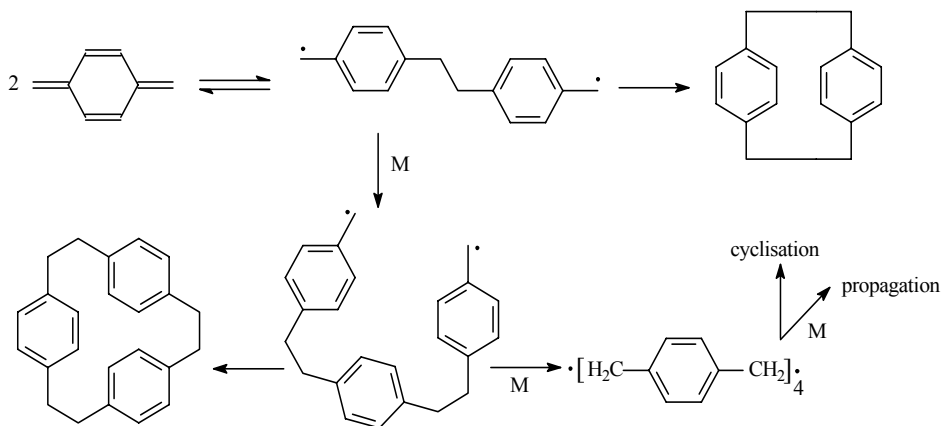
Figure 1.12: The scheme of Errede[71]

In 1966 Gorham reported on a new, general synthetic route to PPX and substituted derivatives by pyrolysis of *p*-cyclophane – cleavage into two *p*-QM molecules - at 600°C[72]. These intermediates spontaneously polymerise upon condensation on glass or metal surfaces maintained below 30°C at low pressure (< 1 mbar), yielding a tough transparent PPX film. Due to the milder pyrolysis temperature this process can be applied to the preparation of a variety of substituted PPXs[73]. The vapour-coating process – now called chemical vapour deposition (CVD) – was the key to industrial application of high molecular weight PPXs as insulating or protective coatings, because wet chemistry only resulted in low molecular weight materials, due to insolubility[74].

Conclusive evidence that the final pyrolysis products of *p*-cyclophanes are *p*-QMs has been obtained from a study of the pyrolytic polymerisation of unsymmetrical substituted *p*-cyclophanes[72]. Electron Spin Resonance (ESR) measurements determined a radical concentration of 5 to 10×10^{-4} per mol QM, representing the radical chain ends in PPX films. These observations led to the proposal of a free radical mechanism, similar to the scheme of Errede: initiation by coupling of two *p*-QM molecules (dimerisation) and chain growth at both ends by addition of QM monomers[75].

Experiments of *p*-cyclophane pyrolysis at 600°C and subsequent condensation of the resulting *p*-QM vapour in a toluene / 2,2,6,6-tetramethyl-piperidinoxyl (TEMPO) solution at −78°C confirm this free radical polymerisation mechanism (figure 1.13)[76]. Upon heating the solution slowly to room temperature, its colour lightened from orange to yellow, indicating a decrease in TEMPO concentration. No polymer was formed, while NMR and mass spectroscopy pointed at the formation of the dinitroxide of the *p*-QM dimer, rather than the monomer.
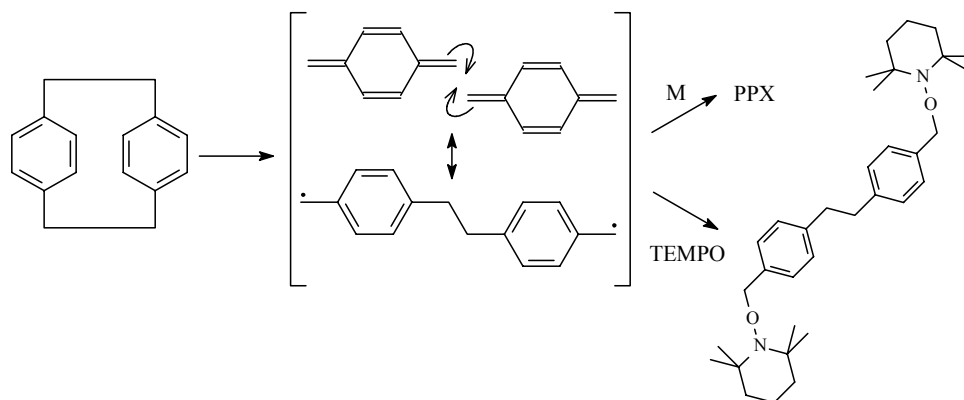
Figure 1.13: Proposed free radical mechanism of *p*-cyclophane CVD[76]

Regarding the analogy between substituted PPXs and PPV precursors it is important to keep the proposed free radical polymerisation mechanism in mind during the following discussion on the polymerisation mechanism of the PPV precursor routes.

1.5.2 A General Scheme for the PPV Precursor Routes

The earlier discussed precursor routes (section 1.4) are based on similar chemistry, and because of this similarity they can all be described by a general scheme of *p*-QM based polymerisations consisting of three steps (figure 1.14). The first step is a base induced 1,6-elimination from a *p*-xylene derivative **1** leading to the *in situ* formation of the actual monomer – the *p*-QM system **2**. Secondly, this intermediate – which can be represented by three structures contributing differently to the character of the molecule[77] - polymerises spontaneously to the precursor polymer **3**. The conjugated structure **4** is obtained in a third step, directly or after thermal treatment depending on the specific chemical structure of the starting monomer and the polymerisation conditions.
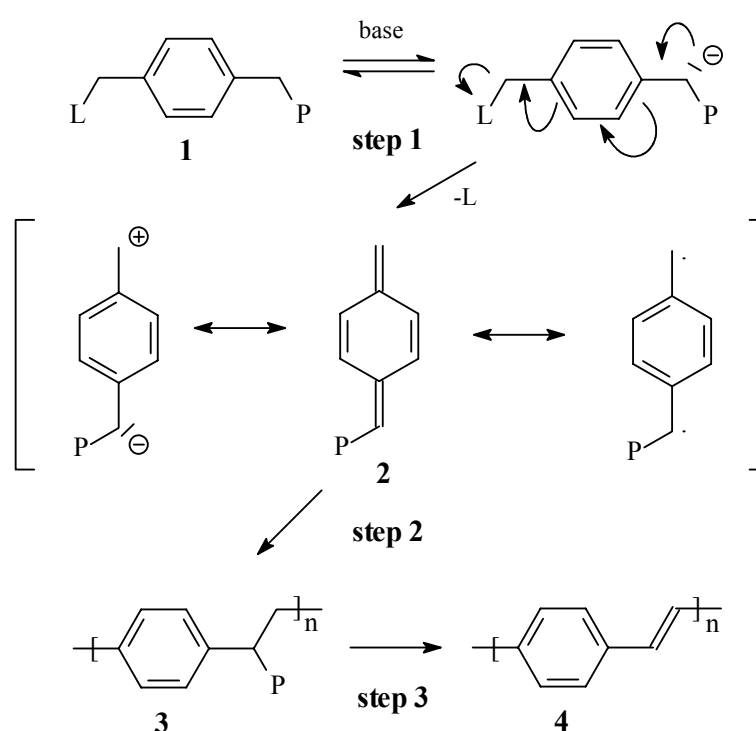
Figure 1.14: A general scheme for the PPV precursor routes;
Wessling-Zimmerman: $L = P = {}^+SR_2\,X^-$; Xanthate: $L = P = SC(S)OEt$;
Gilch: $L = P = Cl$; Sulfinyl: $L = X$, $P = S(O)R$

At the benzylic positions the *p*-xylene derivative is functionalised with a leaving group (L) and a polariser (P). The function of the polariser is in fact threefold: preferential stabilisation of the anion formed in the first step of the process, polarisation of the *p*-QM system in such a way that regular head-to-tail addition results, and provision of the specific chemistry to allow formation of a double bond. Notice that the Sulfinyl route differs from the other routes in that a chemical differentiation is introduced between the two functionalities L and P, implying a better control over the whole process.

The remainder of this introduction will be involving the literature on the mechanisms behind steps one and two of the general scheme, because knowledge

of these mechanisms implies more control on the polymerisation process. For further information on the elimination mechanism (step 3), the reader is referred to more specific literature (references in 1.4).

1.5.3 *p*-Quinodimethane Formation (Step 1)

It is agreed on that these precursor routes all proceed via a *p*-QM intermediate. This is mainly based on the occurrence of a new UV-vis band around 320 nm during polymerisation observed by different research teams[78]. The new band is assigned to the absorption of the *p*-QM system, which in all cases initially increases to a maximum intensity, indicating accumulation, before gradual fading due to polymerisation.

The *in situ* formation of the *p*-QM system involves a base-induced 1,6-elimination, characterised by a loss of HL. Three limiting mechanisms can be envisaged for HL-eliminations, differing in the timing of C-H and C-L bond breaking (figure 1.15), but in fact, a continuous mechanistic spectrum in the relative time of bond breaking is available. If it concerns a concerted – one-step – process passing through one transition state, this is referred to as the E_2 mechanism. Alternatively, the C-H and C-L bonds can be broken separately in two-step processes. Initial C-L bond breakage involves a carbocationic intermediate and is referred to as the E_1 mechanism. When the C-H bond is broken first, a carbanion intermediate is involved and it is referred to as the E_{1cb} mechanism (cb: conjugate base).

Considering the basic conditions for the QM formation, the E_1 mechanism is improbable, which leaves E_{1cb} and E_2. These are not easy to distinguish and are on top sensitive to structural changes of the substrate and to reaction conditions.

Issaris performed some kinetic measurements on the Sulfinyl route to trace the mechanism behind the QM formation[79]. When polymerisation is followed by ^{1}H-NMR in d-MMF at low temperatures (-45°, -40°, -35°C) no exchange between H- and D-atoms is observed, meaning that the proton abstraction process is slow under these conditions. Experiments with various monomers – differing in leaving group (L) and polariser (P) – show a P-dependence and an L-independence in the polymerisation results. Especially the latter observation

negates an E_2 mechanism, while the combination of all results supports an E_{1cb} mechanism.
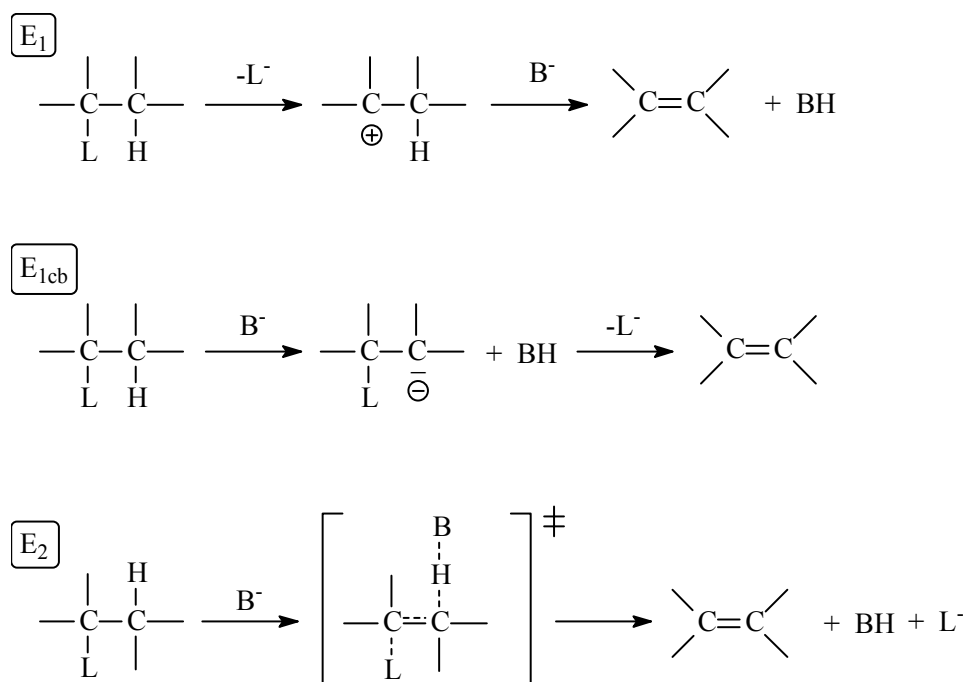
Figure 1.15: Mechanisms for HL-elimination

NMR-measurements on the Wessling-Zimmerman route, conducted by Lahti et al., showed complete conversion of the benzylic C-H bonds to C-D bonds at –50°C, before polymerisation[80]. Extensive kinetic studies of Cho et al. confirm these results, indicating that the deprotonation step must be reversible and proceed at a much faster rate than the QM-formation[81]. The obtained rate data also reveal that an E_{1cb} mechanism is operative.

No publications on kinetic studies on the Xanthate and the Gilch route were found, but it can be concluded that for all precursor routes the E_{1cb} mechanism is generally adopted for describing the first step of the process, the *p*-QM-formation.

1.5.4 *p*-Quinodimethane Polymerisation (Step 2)

Polymerisations can be divided into three main categories: chain, living, and stepwise polymerisations. They each have their own characteristics, and a parameter common used to distinguish them is the molecular weight as a function of the monomer conversion (figure 1.16).
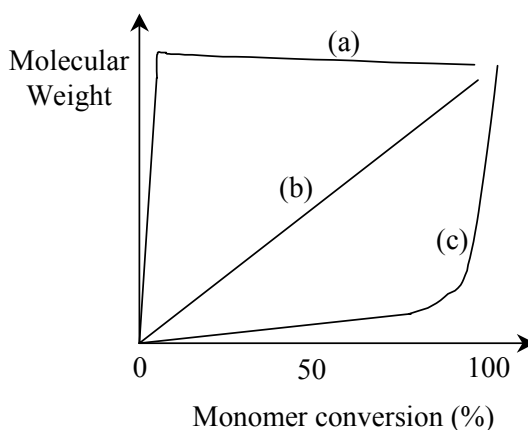
Figure 1.16: Molecular weight as function of conversion for:
(a) chain, (b) living, and (c) stepwise polymerisation

The precursor routes belong to the category of chain polymerisations, because experiments show the presence of high molecular weight polymer even at low monomer conversion, while for a stepwise mechanism high molecular weights are only formed at high conversion[82].

A further differentiation in mechanism is necessary, because a chain polymerisation can be of cationic, switterionic, anionic or radical nature. A switterionic mechanism is improbable for the QM-based precursor routes due to the calculated negligible switterionic character of the *p*-QM system[77]. Regarding the basic conditions of the polymerisations also a cationic mechanism can be excluded, leaving only the anionic and radical as possible polymerisation mechanisms.

Distinction between these two possibilities (figure 1.17) has proven hard to achieve, leading to a still ongoing argument on the exact nature of the second step mechanism. The difficulty lies in the presence of the equilibrating carbanion chemistry involved in the basic 1,6–elimination towards *p*-QM formation. As a result, conditions aimed at quenching anionic chains could also inhibit the reaction through suppression of the *in situ p*-QM formation (step 1) rather than through inhibiting *p*-QM polymerisation (step 2).
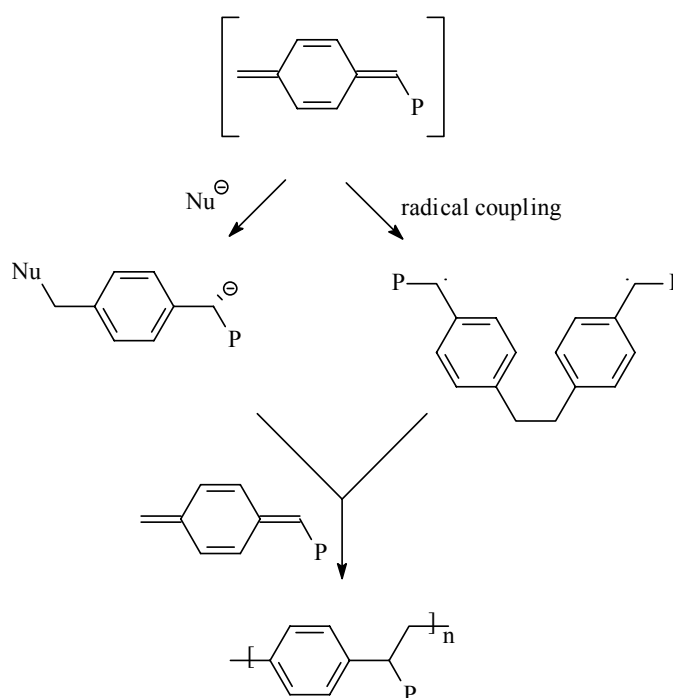
Figure 1.17: A radical or anionic chain mechanism for step 2

Wessling proposed a radical chain mechanism that is most likely initiated by spontaneous head-to-head dimerisation of the *p*-QM[83]. In 1988 researchers at the Polymer Science department of the University of Massachusetts published results of ESR and trapping studies, which did not show evidence for the postulated radical mechanism[80]. A Wessling polymerisation in the ESR cavity at −10°C in the presence of 0.1 to 1.0 equivalents of the radical scavenger TEMPO did not result in a decrease in ESR signal intensity. Addition of a nitrone to trap transient

radicals as stable nitrosyl radicals didn't produce any ESR signal, and no copolymer with styrene could be obtained, leading to a proposal for a putative anionic chain polymerisation.

In 1992 the same group reinvestigated the effect of radical trapping agents on molecular weight and its distribution under typical Wessling conditions (H_2O, 0°C, NaOH) more thoroughly[84]. They found out it is discomfiting to rely too heavily upon negative evidence in postulating a reaction mechanism. ESR measurements with only 0.00025 equivalents of TEMPO resulted in a complete disappearance of the TEMPO signal, indicating the trapping of TEMPO by a radical. The most convincing demonstration of the presence of radical chemistry during polymerisation was the complete suppression of polymer formation by 0.1 equivalents of TEMPO, while UV-vis measurements showed no effect of TEMPO upon *p*-QM formation rate. However, initiation and termination mechanisms remain unclear.

The research team of Cho performed extensive kinetic studies on the Wessling polymerisation[81]. Results of addition of various carbanions, and quenching experiments with HCl were inconsistent with an anionic polymerisation mechanism and gave strong indications for a reactive species other than an anion that reacts with *p*-QM. The observed rate of disappearance of the *p*-QM intermediate was decreased by TEMPO-addition, confirming the proposal of a radical polymerisation mechanism. Although direct evidence for the dimer biradical has never been observed by the researchers - probably due to its high reactivity - it seems difficult to rule out the possibility that it may be the initiator in the polymerisation reaction.

Researchers at the Xerox Corporation studied the Gilch polymerisation towards MEH-PPV and DP-PPV in THF at room temperature[85]. A standard polymerisation yields an insoluble gel, while resulting polymer solutions of intermittent base addition could not be filtered through 0.5-1.0 μm filters, indicating microgel formation. Use of 0.06 equivalents of the 'non-polymerisable acidic additive' 4-*t*-butylbenzylchloride results in soluble polymers of which the molecular weight is inversely proportional to the additive concentration. This is claimed to indicate involvement of an anionic polymerisation process, where nucleophilic attack by the deprotonated additive on the *p*-QM initiates and

nucleophilic attack by the propagating anionic chain on the additive terminates polymerisation. However, to explain the formation of high molecular weight in the presence of a large amount of additive, stilbene formation or a radical polymerisation mechanism is suggested.

In a recent publication of Neef and Ferraris the effects of the chain transfer agent (cta) anthracene and the nucleophile 4-methoxyphenol on the molecular weight of the resulting polymer were evaluated[86]. During each Gilch polymerisation towards MEH-PPV the torque was monitored in order to detect changes in viscosity. Torque measurements for polymerisations where the base solution was slowly added to a solution of monomer and 0.02 to 0.5 equivalents of anthracene, were similar to polymerisation without the cta. Similar torque measurements were performed for polymerisations where the monomer solution was slowly added to a solution of base and 0.005 to 0.02 equivalents of 4-methoxyphenol. They showed an inverse proportional relation between molecular weight of the resulting polymer and the amount of nucleophile added, suggesting an anionic polymerisation mechanism.

In the early stages of Sulfinyl route development an investigation into the possibility of an anionic mechanism for the polymerisation of α-leaving group-α'-polariser-*p*-xylene in the solvent *N*-methyl pyrrolidinone (NMP) was set up[87]. The use of LDA or BuLi as base resulted in an oligomeric fraction of which NMR and MS characterisation pointed at the presence of NMP endgroups. This led to the proposal of an anionic polymerisation mechanism, with the solvent anion acting as initiator. Because polymerisation in NMP resulted in bimodal molecular weight distributions (MWD) - which complicated a mechanistic study – the focus was shifted to the solvent *N*-methyl formamide (MMF)[88]. Polymerisation in this polar, protic solvent is possible, leading to high molecular weight polymer with a monomodal MWD, even in the presence of 10% water. These observations made an anionic polymerisation mechanism improbable, resulting in a focus on the radical mechanism.

Many experiments on the Sulfinyl route in MMF were performed to check for a radical polymerisation mechanism[89]; only a selection will be mentioned here. ESR measurements with the spin trap 5,5-dimethyl-1-pyrroline-*N*-oxide (DMPO) showed signals of a DMPO-adduct, proving the presence of radicals

Chapter One

during polymerisation. Another argument was the addition of 0.5 equivalents of the radical transfer agent carbon tetrabromine (CBr$_4$) to the reaction mixture resulting in a decrease in molecular weight, but leaving yield unchanged[90]. Also addition of amounts less than 0.1 equivalents of the well-known radical trappers TEMPO and diphenylpicryl hydrazyl (DPPH) resulted in a substantial decrease in molecular weight and polymer yield, while 0.5 equivalents of TEMPO totally inhibited polymer formation[89]. All these results strongly indicate a radical character of the *p*-QM polymerisation and even yielded an indication for the initiating particle: a biradical dimer similar to the one proposed by Wessling[83]. These findings have been an important basis for the present work and some will be discussed in more detail in chapter two and three.

1.6 AIM AND OUTLINE OF THE THESIS

The aim of the research described in this thesis is to contribute to the ongoing discussion on the polymerisation mechanism of *p*-quinodimethane based routes towards PPV derivatives. Understanding the polymerisation mechanism may provide the means to control molecular weight and circumvent problems such as gelation or precipitation during polymerisation.

In chapter two results of a mechanistic study on the Sulfinyl route towards PPV in the dipolar aprotic solvent NMP are presented. Together with earlier results an overview of the Sulfinyl route is made. Chapter three describes the results concerning a comparative mechanistic study on the Gilch and the Sulfinyl route towards OC$_1$C$_{10}$-PPV in apolar, aprotic solvents. In chapter four the SEC-LS characterisation technique is used to characterise various PPV precursor and OC$_1$C$_{10}$-PPVs. Branching studies are performed to detect possible conformational differences between OC$_1$C$_{10}$-PPV synthesised using the Gilch and the Sulfinyl route. This thesis is concluded with summaries and perspectives in English and in Dutch.

34

1.7 REFERENCES

1. a) H. Shirakawa, E.J. Louis, A.G. MacDiarmid, C.K. Chiang, A.J. Heeger, *J. Chem. Soc., Chem. Commun.* (1977) 578; b) C.K. Chiang, C.R. Fincher, Y.W. Park, A.J. Heeger, H. Shirakawa, E.J. Louis, S.C. Gau, A.G. MacDiarmid, *Phys. Rev. Lett.*, **39** (1977) 1098.

2. J.-L.Brédas, G.B. Street, *Acc. Chem. Rev.*, **18** (1985) 309.

3. a) A. Wirsén, *"Electroactive Polymer Materials"*, Technomic publishing AG, Switzerland, 1987; b) S. Roth, *"One-Dimensional Metals"*, Weinheim VCH, 1995, p. 209-231; c) G. Horowitz, *Adv. Mater.*, **10(5)** (1998) 365.

4. a) J. Miller, *Adv. Mater.*, **5(9)** (1993) 671; b) S. Roth, *"One-Dimensional Metals"*, Weinheim VCH, 1995, p. 209-231.

5. a) P. Nigrey, D. MacInnes, D. Nairns, A. MacDiarmid, A. Heeger, *J. Electrochem. Soc.*, **128(8)** (1981) 1651; b) A. Wirsén, *"Electroactive Polymer Materials"*, Technomic publishing AG, Switzerland, 1987; c) M.G. Kanatzidis, *C&EN*, **3** (1990) 36; d) J. Miller, *Adv. Mater.*, **5(9)** (1993) 671; e) S. Roth, *"One-Dimensional Metals"*, Weinheim VCH, 1995, p. 209-231.

6. a) M.G. Kanatzidis, *C&EN*, **3** (1990) 36; b) S. Roth, *"One-Dimensional Metals"*, Weinheim VCH, 1995, p. 209-231.

7. a) S. Roth, *"One-Dimensional Metals"*, Weinheim VCH, 1995, p. 209-231; b) J. Barisci, C. Conn, G. Wallace, *TRIP*, **4(9)** (1996) 307 ; c) A. MacDiarmid, W. Zhang, Z. Huang, P.-C. Wang, F. Huang, S. Xie, *Polym. Prepr.*, **38(1)** (1997) 333; d) H. Geise, *Natuur & Techniek*, **april** (2000) 28.

8. a) G. Yu, J. Wang, J. McElvain, A.J. Heeger, *Adv. Mater.*, **10** (1998) 1431; b) E. Miyasaki, S. Itami, T. Araki, *Rev. Sci. Instrum.*, **69(11)** (1998) 3751.

9. a) B. Schwartz, M. Diaz-Garcia, F. Hide, M. Andersson, Q. Pei, A. Heeger, *Polym. Prepr.*, **38(1)** (1997) 325; b) N. Tessler, *Adv. Mater.*, **11(5)** (1999) 363; c) M. McGehee, A. Heeger, *Adv. Mater.*, **12(22)** (2000) 1655.

10. a) D. Bloor, *Chemistry in Britain*, **may** (1995) 385; b) S. Roth, *"One-Dimensional Metals"*, Weinheim VCH, 1995, p. 209-231.

11. a) Q. Pei, G. Yu, C. Zhang, Y. Yang, A.J. Heeger, *Science*, **269** (1995) 1086; b) R.F. Service, *Science*, **269** (1995) 1042; c) Q. Pei, G. Yu, C. Zhang, Y. Yang, A. Heeger, *Science* **269** (1995) 1086; d) D.J. Dick, A.J. Heeger, Y. Yang, Q. Pei, *Adv.*

Mater., **8(12)** (1996) 985; e) Y. Yang, Q. Pei, *Polym. Prepr.*, **38(1)** (1997) 335; f) H. Schoo, R. Demandt, J. Vleggaar, C. Liedenbaum, *Polym. Prepr.*, **38(1)** (1997) 337; g) Y. Greenwald, F. Hide, J. Gao, F. Wudl, A.J. Heeger, *J. Electrochem. Soc.*, **144(4)** (1997) L70; h) J.-L. Brédas, J. Cornil, A. Heeger, *Adv. Mater.*, **8(5)** (1998) 447; i) L. Holzer, B. Winkler, F.P. Wenzl, S. Tasch, L. Dai, A.W.H. Mau, G. Leising, *Synth. Met.*, **100** (1999) 71.

12. a) J.J.M. Halls, C.A. Walsh, N.C. Greenham, E.A. Morseglia, R.H. Friend, S.C. Moratti, A.B. Holmes, *Nature*, **376** (1995) 498; b) G. Yu, J. Gao, J.C. Hummelen, F. Wudl, A.J. Heeger, *Science*, **270** (1995) 1789; c) R.F. Service, *Science*, **269** (1995) 91; d) L. Dai, *J.M.S. - Rev. Macromol. Chem. Phys.*, **C39(2)** (1999), 273; e) G.G. Wallace, P.C. Dastoor, D.L. Officer, C.O. Too, *Chemical Innovation*, **april** (2000) 15; f) L. van der Ent, *Kunststof magazine*, **april(3)** (2001) 38.

13. Z. Xie, M.S.A. Abdou, X. Lu, M.J. Deen, S. Holdcroft, *Can. J. Phys.*, **70** (1992) 1171.

14. a) S.J. Campbell, S. Carter, S. Karg, M. Angelopoulos, *Polym. Prepr.*, **38(1)** (1997) 384; b) P.K.H. Ho, J.-S. Kim, J.H. Burroughes, H. Becker, S.F.Y. Li, T.M. Brown, F. Cacialli, R.H. Friend, *Nature*, **404** (2000) 481.

15. T.R. Hebner, C.C. Wu, D. Marcy, M.H. Lu, J.C. Strum, *Appl. Phys. Lett.*, **72** (1998) 519.

16. J. Salbeck, *Ber. Bunsenges. Phys. Chem.*, **100(10)** (1996) 1667.

17. a) D.D.C. Bradley et al., *Synth. Met.*, **41-43** (1991) 3135; b) R. Friend, D. Bradley, A. Holmes, *Physics World*, **november** (1992) 42; c) Y. Yang, *Mrs. Bulletin*, **june** (1997) 31.

18. M. Pope, H.P. Kallmann, P. Magnante, *J. Chem. Phys.*, **38** (1963) 2042.

19. C.W. Tang, S.A. Van Slyke, *Appl. Phys. Lett.*, **51** (1987) 913.

20. J. Burroughes, D. Bradley, A. Brown, R. Marks, K. Mackay, R. Friend, P. Burns, A. Holmes, *Nature*, **347** (1990) 539.

21. a) D.D.C. Bradley, *Synth. Met.*, **54** (1993) 401; b) R.H. Friend, R.W. Gymer, A.B. Holmes, J.H. Burroughes, R.N. Marks, C. Taliani, D.D.C. Bradley, D.A. Dos Santos, J.-L. Brédas, M. Lögdlund, W.R. Salaneck, *Nature*, **397** (1999) 121.

22. S. Moratti, D. Bradley, R. Friend, N. Greenham, A. Holmes, *Polym. Prepr.*, **35(1)** (1994) 214.

23. Z. Peng, Z. Bao, M.E. Galvin, *Chemtech*, **may** (1999) 41.

24. a) Q. Pei, Y. Yang, *Chem. Mater.*, **7** (1995) 1568; b) M. Strukelj, F. Papadimitra-kopoulos, T.M. Miller, L.J. Rothberg, *Science*, **267** (1995) 1969; c) Y. Yang, *Mrs. Bulletin*, **june** (1997) 31.

25. P. Blom, M. de Jong, M. van Munster*, Physical Review B*, **55(2)** (1997) r656.

26. S. Karg, M. Meier, W. Riess, *J. Appl. Phys.*, **82(4)** (1997) 1951.

27. a) C. Liedenbaum, Y. Croonen, P. van de Weijer, J. Vleggaar, H. Schoo, *Synth. Met.*, **91** (1997) 109; b) R.J. Visser, *Philips J. Res.*, **51(4)** (1998) 467; c) P.W.M. Blom, M.J.M. de Jong, *Philips J. Res.*, **51(4)** (1998) 479; d) M.J.M. de Jong, M.C. J.M. Vissenberg, *Philips J. Res.*, **51(4)** (1998) 495; e) A.J.M. Berntsen, P. van de Weijer, Y. Croonen, C.T.H.F. Liedenbaum, J.J.M. Vleggaar, *Philips J. Res.*, **51(4)** (1998) 511; f) H.F.M. Schoo, R.C.J.E. Demandt, *Philips J. Res.*, **51(4)** (1998) 527.

28. R. Friend, D. Bradley, A. Holmes, *Physics World*, **november** (1992) 42.

29. D. Clery, *Science*, **263** (1994) 1700.

30. J.L. Segura, *Acta Polym.*, **49** (1998) 319.

31. a) B. Xu, S. Holdcroft, *Macromol.*, **26** (1993) 4457; b) N.C. Greenham, R.H. Friend, *Solid State Phys.,* **49** (1995) 1; c) J. Salbeck, F. Weissörtel, J. Bauer, *Macromol. Symp.*, **125** (1997) 121; d) N. Johansson, D.A. dos Santos, S. Guo, J. Cornil, M. Fahlman, J. Salbeck, H. Schenk, H. Arwin, J.L. Brédas, W.R. Salanek, *J. Chem. Phys.*, **107(7)** (1997) 2542.

32. a) M. Hay, F.L. Klavetter, *J.Am. Chem. Soc.*, **117** (1995) 7112; b) J. Kim, S. Hong, H. Cho, D. Kim, C. Kim, *Polym. Bull.*, **38** (1997) 169; c) H.N. Cho, D.Y. Kim, J.K. Kim, C.Y. Kim, S*ynth. Met.*, 91 (1997) 293; d) H.N. Cho, J.K. Kim, D.Y. Kim, C.Y. Kim, N.W. Song, D. Kim, *Macromol.*, **32** (1999) 1476.

33. B. Cumpston, K. Jensen, *TRIP*, **4(5)** (1996) 151.

34. A. Kraft, A.C. Grimsdale, A.B. Holmes, *Angew. Chem. Int. Ed.*, **37** (1998) 402.

35. a) G. Gustafsson, Y. Cao, G.M. Treacy, F. Klavetter, N. Colaneri, A.J. Heeger, *Nature*, **357** (1992) 477; b) E. Harlev, T. Gulakhmedova, I. Rubinovich, G. Aizenshtein, *Adv. Mater.*, **8(12)** (1996) 994.

36. *European Plastics News*, **march** (1998) 21.

37. http://www.ctdltd.co.uk/NR-InkJetDisplay.html

38. a) T.R. Hebner, C.C. Wu, D. Marcy, M.H. Lu, J.C. Sturm, *Appl. Phys. Lett.*, **72** (1998) 519; b) J. Bharathan, Y. Yang, *Appl. Phys. Lett.*, **72** (1998) 2660.

39. O. Schafer, A. Greiner, J. Pommerehne, W. Guss, H. Vestweber, H.Y. Tak, H. Bassler, C. Schmidt, G. Lussem, B. Schartel, V. Stumpflen, J.H. Wendorff, S. Spiegel, C. Moller, H.W. Spiess, *Synth. Met.*, **82** (1996) 1.

40. R.N. McDonald, T.W. Campbell, *J. Am. Chem. Soc.*, **82** (1960) 4669.

41. R.F. Heck, *Org. React.*, **27** (1982) 345.

42. a) R.W. Lenz, C.E. Handlovits, *J. Org. Chem.*, **25** (1960) 813; b) H.-H. Hörhold, D. Gräf, J. Opfermann, *J. Plaste und Kauschuk*, **17** (1970).

43. a) R.A. Wessling, R.G. Zimmerman, *U.S. Patent No 3 401 152* (1968) ; b) R.A. Wessling, R.G. Zimmerman, *U.S. Patent No 3 706 677* (1972).

44. a) D.D.C. Bradley, *J. Phys. D: Appl. Phys.*, **20** (1987) 1389; b) R.W. Lenz, C.-C. Han, J. Stenger-Smith, F.E. Karasz, *J. Polym. Sci.*, **26** (1988) 3241.

45. M.J. Cherry, S.C. Moratti, A.B. Holmes, P.L. Taylor, J. Grüner, R.H. Friend, *Synth. Met.*, **69** (1995) 493.

46. a) D.D.C. Bradley, *J. Phys. D: Appl. Phys.*, **20** (1987) 1389; b) R.O. Garay, U. Baier, C. Bubeck, K. Mullen, *Adv. Mat.*, **5** (1993) 561; c) C. Zhang, D. Braun, A.J. Heeger, *J. Appl. Phys.*, **73** (1993) 5177.

47. a) S. Son, A. Dodabalapur, A.J. Lovinger, M.E. Galvin, *Science*, **269** (1995) 376; b) S. Son, A.J. Lovinger, M.E. Galvin, *Polym. Mater. Sci. and Engin.*, **72** (1995) 567.

48. a) J. Yang, H. Hong, M.E. Thompson, *Polym. Prepr.*, **40(2)** (1999) 1244; b) S.-C. Lo, A.K. Sheridan, I.D.W. Samuel, P.L. Burn, *J. Mater. Chem.*, **9** (1999) 2165; c) G. Arbuckle-Keil, Y. Liszewski, J. Peng, B. Hsieh, *Polym. Prepr*, **41(1)** (2000) 826.

49. M.S. Kharasch, W. Nudenberg, E.K. Fields, *J. Am. Chem. Soc.*, **66** (1944) 1276.

50. D.F. Hoeg, D.I. Lusk, E.P. Goldberg, *Polym. Lett.*, **2** (1964) 697.

51. H.G. Gilch, W.L. Wheelwright, *J. Polym. Sci.*, **4** (1966) 1337.

52. W.J. Swatos, B. Gordon III, *Polym. Prepr.*, **31(1)** (1990) 505.

53. a) C.A. Kingsbury, D.J. Cram, *J. Am. Chem. Soc.*, **82** (1960) 1810 ; b) J.R. Shelton, K.E. Davis, *Int. J. Sulfur Chem.*, **8(2)** (1973) 197 ; c) J.R. Shelton, K.E. Davis, *Int. J. Sulfur Chem.*, **8(2)** (1973) 205.

54. E. Kesters, L. Lutsen, D. Vanderzande, J. Gelan, T.P. Nguyen, P. Molinié, submitted to and accepted for Thin Solid Films.

55. M.M. de Kok, *Ph.D. Dissertation*, 1999, Limburgs Universitair Centrum, Diepenbeek, België.

56. A.J.J.M. van Breemen, *Ph.D. Dissertation*, 1999, Limburgs Universitair Centrum,

Diepenbeek, België.

57. M. Van Der Borght, *Ph.D. Dissertation*, 1998, Limburgs Universitair Centrum, Diepenbeek, België.

58. a) M. Szwarc, *Faraday Soc. Disc.*, **2** (1947) 46; b) M. Szwarc, *J. Chem. Phys.*, **16** (1948) 128; c) M. Szwarc, *J. Polym. Sci.*, **6(3)** (1951) 319.

59. L.A. Errede, M. Szwarc, *Quart. Rev.*, **12** (1958) 301.

60. C.A. Coulson, D.P. Craig, A. Maccoll, A. Pullman, *Faraday Soc. Disc*, **2** (1947) 36.

61. D.F. Evans, *J. Chem. Soc.*, (1959) 2753.

62. L. Salem, C. Rowland, *Angew. Chem. Int. Ed. Engl.*, **11** (1972) 92.

63. a) S. Iwatsuki, H. Kamiya, *Macromol.*, **7(6)** (1974) 732; b) T. Itoh, S. Iwatsuki, *Macromol. Chem. Phys.*, **198** (1997) 1997.

64. a) S. Iwatsuki, T. Itoh, T. Sato, T. Higuchi, *Macromol.*, **20** (1987) 2651; b) S. Iwatsuki, T. Itoh, I. Miyashita, *Macromol.*, **21** (1988) 557.

65. L.A. Errede, B.F. Landrum, *J. Am. Chem. Soc.*, **79** (1957) 4952.

66. L.A. Errede, R.S. Gregorian, J.M. Hoyt, *J. Am. Chem. Soc.*, **82** (1960) 5218.

67. L.A. Errede, J.M. Hoyt, R.S. Gregorian, *J. Am. Chem. Soc.*, **82** (1960) 5224.

68. L.A. Errede, J.M. Hoyt, *J. Am. Chem. Soc.*, **82** (1960) 436.

69. L.A. errede, S.L. Hopwood, *J. Am. Chem. Soc.*, **79** (1957) 6507.

70. a) L.A. Errede, M. Szwarc, *Quart. Rev.*, **12** (1958) 301; b) L.A. Errede, J.M. Hoyt, R.S. Gregorian, *J. Am. Chem. Soc.*, **82** (1960) 5224 ; c) T. Itoh, S. Iwatsuki, *Macromol. Chem. Phys.*, **198** (1997) 1997.

71. a) L.A. Errede, M. Szwarc, *Quart. Rev.*, **12** (1958) 301; b) L.A. Errede, R.S. Gregorian, J.M. Hoyt, *J. Am. Chem. Soc.*, **82** (1960) 5218; c) S. Iwatsuki, *Adv. in Polym. Sci.*, **58** (1984) 93.

72. W.F. Gorham, *J. Polym. Sci., Part A-1*, **4** (1966) 3027.

73. S. Iwatsuki, "*The Chemistry of Quinonoid Compounds Vol. II*", Edited by S. Patai and Z. Rappoport, 1988, p. 1067-1111.

74. A. Greiner, S. Mang, O. Schäfer, P. Simon, *Acta Polymer.*, **48** (1997) 1.

75. A. Greiner, *TRIP*, **5(1)** (1997) 12.

76. I. Li, B.A. Howell, *Polym. Prepr.*, **37(3)** (1996) 517.

77. a) C.R. Flynn, J. Michl, *J. Am. Chem. Soc.*, **96(10)** (1974) 3280; b) D. Döhnert, J. Koutecký, *J. Am. Chem. Soc.*, **102(6)** (1980) 1789; c) P.C. Hiberty, P. Karafiloglou, *Theoret. Chim. Acta (Berl.)*, **61** (1982) 171.

78. a) R.A. Wessling, *J. Polym. Sci.: Polym. Symp.*, **72** (1985) 55; b) P.M Lahti, D.A. Modarelli, F.R. Denton, R.W. Lenz, F.E. Karasz, *J. Am. Chem. Soc.*, **110** (1988) 7258; c) B.R. Cho, M.S. Han, Y.S. Suh, K.J. Oh, S.J. Jeon, *J. Chem. Soc., Chem. Commun.*, (1993) 564; d) M. Van Der Borght, *Ph.D. Dissertation*, 1998, Limburgs Universitair Centrum, Diepenbeek, België.

79. a) A. Issaris, *Ph.D. Dissertation*, 1997, Limburgs Universitair Centrum, Diepenbeek, België; b) A. Issaris, D. Vanderzande, P. Adriaensens, J. Gelan, *Macromol.*, **31(14)** (1998) 4426.

80. P.M Lahti, D.A. Modarelli, F.R. Denton, R.W. Lenz, F.E. Karasz, *J. Am. Chem. Soc.*, **110** (1988) 7258.

81. a) B.R. Cho, M.S. Han, Y.S. Suh, K.J. Oh, S.J. Jeon, *J. Chem. Soc., Chem. Commun.*, (1993) 564; b) B.R. Cho, Y.K. Kim, M.S. Han, *Macromol.*, **31** (1998) 2098.

82. a) H.G. Gilch, W.L. Wheelwright, *J. Polym. Sci.*, **4** (1966) 1337; b) R.A. Wessling, *J. Polym. Sci.: Polym. Symp.*, **72** (1985) 55; c) F. Louwet, *Ph.D. Dissertation*, 1993, Limburgs Universitair Centrum, Diepenbeek, België.

83. R.A. Wessling, *J. Polym. Sci.: Polym. Symp.*, **72** (1985) 55.

84. F.R. Denton III, P.M. Lahti, F.E. Karasz, *J. Polym. Sci. Part A: Polym. Chem.*, **30** (1992) 2223.

85. a) B.R. Hsieh, Y. Yu, A.C. VanLaeken, H. Lee, *Macromol.*, **30** (1997) 8094; b) Y. Yu, C. VanLaeken, H. Lee, B.R. Hsieh, *Polym. Prepr.*, **39(1)** (1998) 161; c) B.R. Hsieh, Y. Yu, G.M. Schaaf, W.A. Fled, *Polym. Prepr.*, **39(1)** (1998) 163; d) B.R. Hsieh, Y.Yu, E.W. Forsythe, G.M. Schaaf, W.A. Feld, *J. Am. Chem. Soc.*, **120** (1998) 231.

86. C.J. Neef, J.P. Ferraris, *Macromol.*, **33** (2000) 2311.

87. F. Louwet, *Ph.D. Dissertation*, 1993, Limburgs Universitair Centrum, Diepenbeek, België.

88. A. Issaris, D. Vanderzande, J. Gelan, *Polymer*, **38(1)** (1997) 2571.

89. A. Issaris, *Ph.D. Dissertation*, 1997, Limburgs Universitair Centrum, Diepenbeek, België.

90. D.J. Vanderzande, A.C. Issaris, M.J. Van Der Borght, A.J. van Breemen, M.M. de Kok, J.M. Gelan, *Macromol. Symp.*, **12** (1997) 189.

2 | Mechanistic Study on the Sulfinyl Route towards PPV Precursors in DAS

2.1 INTRODUCTION

The development of precursor routes for conjugated polymers has paved the way to applications of organic semiconductors in opto-electronic devices. As discussed in section 1.4 of the general introduction most of the precursor routes suffer from instability and defective structures due to the symmetrical substitution pattern of the monomer used. The challenge to overcome this drawback led in our laboratory to the development of a new precursor route – the Sulfinyl route. The ongoing work in our research group has shown it to be a very versatile route that *e.g.*, unlike the Wessling-Zimmerman route, also allows polymerisation of monomers with extended aromatic systems, like the 2,6-naphthalene and the 4,4'-biphenyl derivatives.

In order to exhibit control over the polymerisation process and the stability of the precursor, a chemical differentiation is made between a polariser and a leaving group, leading to an unsymmetrical substituted monomer. Because two different monomer syntheses were used in the course of this PhD work, both will be briefly discussed in section 2.2.

The remainder of the chapter concerns the nature of the polymerisation reaction, which could be considered as a black box: you only see the input and outcome. By studying the end products at various reaction conditions an attempt was made to disclose the nature of the underlying polymerisation mechanism in dipolar aprotic solvents (DAS). To this class of solvents belong: dimethylsulfoxide (DMSO), N,N-dimethylformamide (DMF) and 1-methyl-2-pyrrolidinone (NMP) (figure 2.1).

DMSO   DMF   NMP
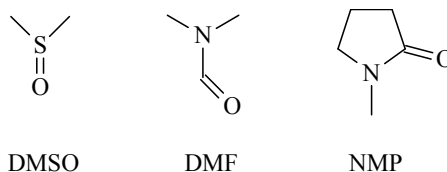
Figure 2.1: Dipolar aprotic solvents

The choice for this type of solvents has to be seen in an historical context. In the beginning of the 1990s, at the start of the Sulfinyl route development, the general accepted opinion on *p*-quinodimethane based polymerisations assumed an anionic mechanism. Therefore DAS, known to enhance nucleophilicity, seemed most suited for the investigation of the new route. However, primary experiments did show a strange bimodal molecular weight distribution (MWD) (section 2.4.1), which complicated research[1]. Further exploration of the route's possibilities revealed that the bimodal MWD becomes monomodal, changing solvent from e.g. DMF to MMF (N-methylformamide). On this basis dr. A. Issaris chose the latter solvent – a protic polar solvent - to perform a mechanistic study. Her findings raised the possibility and probability of the occurrence of a radical polymerisation mechanism[2]. In view of these results it was decided to reinvestigate the polymerisation behaviour in DAS and possibly find an explanation for the awkward bimodal MWD.

The results obtained in this study made it possible to gain insight in other features of the route. This will be subject of section 2.8 where an extension is made to other monomers and solvents, leading to an overall discussion on the Sulfinyl route.

2.2 THE MONOMER SYNTHESES

Keeping the general scheme for PPV-precursor routes (figure 1.13) in mind, the choice for an unsymmetrical substituted monomer can easily be defended. To promote sufficient *p*-quinodimethane (QM) formation a halide is introduced on one of the benzylic positions because of their high leaving group capacity, while

affecting the benzylic position's acidity negligible. The other benzylic position bears a sulfinyl group fulfilling the triple function of a polariser: preferential stabilisation of the anion formed in the first step of the process, polarisation of the *p*-QM system in such a way that regular head-to-tail addition results, and provision of the specific chemistry to allow double bond formation (step 3). As a consequence the Sulfinyl route is linked to a somewhat more extended – multistep - monomer synthesis (figure 2.2).

i: RSH, NaOH (aq), Aliquat 336, toluene
ii: RSH, Na*t*BuO, MeOH
iii: petroleumether (100-130°C), Δ
iv: H$_2$O$_2$, TeO$_2$, MeOH
a: R = *n*-C$_8$H$_{17}$; b: R = *n*-C$_4$H$_9$
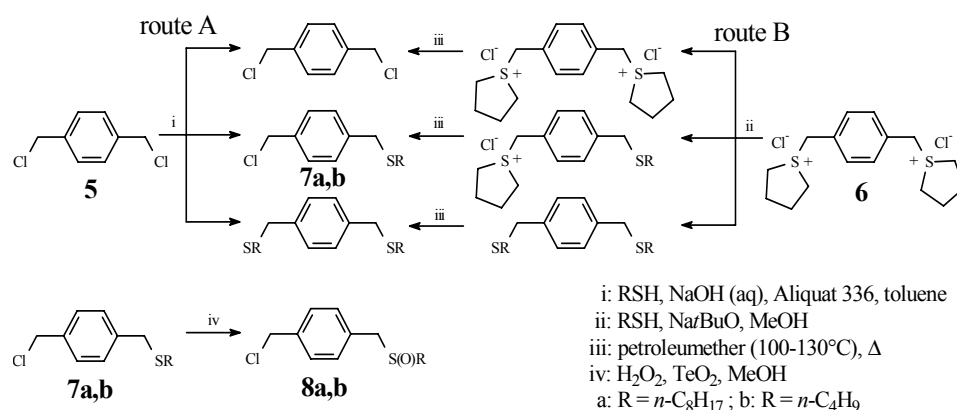
Figure 2.2: The monomer syntheses: route A and B

Until 1999 a classical phase-transfer synthetic procedure (route A) was used for producing monosubstituted thioethers as the first step towards sulfinyl monomers. In order to avoid unwanted disubstitution a large excess (2 to 3 equivalents) of the α,α'-dichloride-*p*-xylene **5** has to be used, leading to a relatively poor overall yield for monosubstituted product **7**. In the course of the last five years dr. A. van Breemen developed a new monomer synthetic procedure (route B) with a much higher selectivity for the monosubstituted thioether **7**, leading to a doubling of the overall yield[3]. Because of the major importance of using equimolar amounts of reagents starting from the hygroscopic α,α'-bissulfonium-*p*-xylene **6**, ^{1}H-NMR is used to determine the water content of the latter, prior to reaction.

A tellurium dioxide (TeO$_2$) catalysed selective oxidation of the thioether **7** with hydrogen peroxide as oxidant yields the corresponding sulfoxide **8** and prevents overoxidation to sulfones[4].

2.3 OPTIMISATION OF THE EXPERIMENTAL POLYMERISATION PROCEDURE IN NMP

During the mechanistic study in MMF by dr. Issaris, the polymerisation appliance depicted in figure 2.3, which allows a continuous nitrogen stream through the base and the monomer solution at a constant temperature, was found best to obtain reproducible results[2].

Previous research has led to a general polymerisation procedure in which a freshly prepared base solution is added in one portion to a monomer solution after degassing for 1 hour by passing through a continuous stream of nitrogen. The total monomer concentration is set at 0.1 M. After one hour of reaction under nitrogen atmosphere the mixture is poured out in ice water and neutralised with aqueous hydrogen chloride (1 M). After extraction with chloroform, the combined organic layers are concentrated *in vacuo*. The crude product is dissolved in chloroform, precipitated in a non-solvent, collected and dried *in vacuo*. The residual fraction is concentrated *in vacuo*.

This study is performed in the solvent NMP – a dipolar aprotic solvent. Preliminary experiments show that working with DAS presents new problems and requires some adjustments of the general procedure. For example, the use of the usual 1.3 equivalents of base results in this type of solvents in a yellow coloured precursor, indicating the presence of conjugated segments in the polymer. To avoid this premature basic elimination of sulfinyl groups, caused by the enhanced base strength in DAS compared to e.g. MMF, the amount of base is reduced to 1.1 equivalents. Further optimisation of the experimental polymerisation procedure is based on experiments with the two most common sulfinyl monomers, represented in figure 2.2 as **8a** and **8b**, differing only in the alkyl group of the polariser.
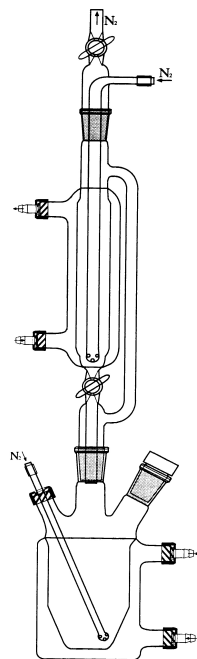
Figure 2.3: The polymerisation appliance

2.3.1 Experiments on 1-(chloromethyl)-4-[(*n*-octylsulfinyl)-methyl]benzene (**8a**)

Primary experiments are conducted on the monomer 1-(chloromethyl)-4-[(*n*-octylsulfinyl)methyl]benzene **8a,** immediately resulting in a new feature in work up: emulsion formation after pouring in ice water and neutralisation with aqueous hydrogen chloride. This white emulsion proves difficult to disturb and makes simple extraction impossible, due to NMP's solubility both in water and in chloroform. Attempts to promote or induce phase separation of the aqueous and the organic layer by addition of DMSO – as emulsion disturber – and use of a centrifuge are fruitless, pointing at a strong solvatation of both monomer and polymer by NMP. At this point, the combination of sodium chloride addition with vigorous stirring or shaking seems to be the best solution to the emulsion problem, but still lacks ease and elegance.

The presence of NMP during work up holds besides formation of an emulsion another difficulty in the form of an extra washing procedure of the

combined organic layers. These consecutive steps are necessary to remove the high boiling NMP from the polymer fraction, but cause at the same time uncontrollable losses and therefore irreproducibility and a lowering of yields. Inevitable, all fractions obtained still contain an amount of NMP.

Listed in table 2.1 are the yields and the molecular weights – determined by size exclusion chromatography (SEC) – of the polymer fractions obtained from standard polymerisations of **8a**. In a SEC chromatogram the refractive index detector response is plotted as a function of elution time or volume. The corresponding SEC chromatograms – an example is shown in figure 2.4 - clearly present a bimodal molecular weight distribution, making two sets of values for molecular weight and polydispersity necessary for characterisation. These numbers are only estimates because the peaks are not fully baseline separated. The peak situated most to the right originates from toluene, which is used as flow rate marker.

The low molecular weight polymer with a M_w-value of about 3000 g/mol will from now on be referred to as the oligomer (OM) fraction, while the higher molecular weight fraction – in this case of about 70 000 g/mol – will be referred to as polymer and abbreviated as PM. The corresponding peaks are indicated in figure 2.4 together with their peak areas.

Table 2.1: Results of standard polymerisations of **8a**

	Yield (%)	M_w (PM) (g/mol)	PD (PM)	% PM	M_w (OM) (g/mol)	PD (OM)
standard 1	38	77 000	1.9	68	3 200	1.0
standard 2	28	68 000	2.1	66	2 900	1.0

To have an idea about the amount of polymer in comparison to the amount of oligomer present in the sample, the sum of their corresponding peak areas is considered 100% (or in symbols: % PM + % OM = 100%). The molecular weight values listed in table 2.1 originate from experiments where the signal of the polymer fraction covers about 67% of the total peak area. The relative amounts of PM (expressed in percentage) are listed in the third column from the right of the table.

The M_w/M_n-value – called polydispersity, PD – of about 1 for the second (OM) peak is possibly caused by an early cut off due to the occurrence of a negative peak – water or air signal - around an elution time of 19 minutes. Another explanation for the low PD-value could be the reaching of the non-linear dynamic range (in the plot of log MW versus elution volume) of the SEC-columns, but the corresponding calibration curves seem to rule out this possibility.
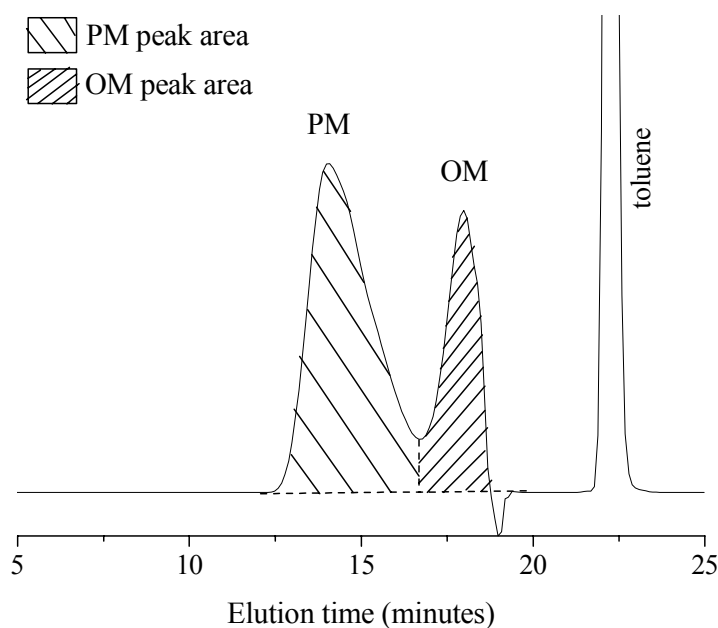
Figure 2.4: An example of a corresponding SEC chromatogram showing a bimodal MWD

It is checked if perhaps a more vigorous stirring while pouring in ice water could prevent emulsion formation and hence increase yields and enhance reproducibility. This turns out not to be the case, but – rather by accident - another elegant solution to the impediment is found. Standard polymerisation procedure prescribes neutralisation after pouring the reaction mixture in ice water to a pH-value of 6 to 7. But, prolonged addition of a 1 M aqueous solution of

hydrogen chloride until a pH-value of 4 to 5 is reached – acidification - results in a disturbance of the emulsion, hence precipitation of both monomer and polymer(s). This permits omission of the irksome extraction / washing procedure, making way for a single filtration step. Apparently, in the case of this octylmonomer **8a** a higher degree of acidity is necessary to cancel the solvatation, possibly by protonation of NMP's nitrogen. Next, the crude product is dissolved in chloroform and precipitated in a solvent mixture of hexane / diethyl ether 1/1.

In table 2.2 the obtained yields and molecular weights – at about 90% PM peak area coverage – starting from the octylmonomer are listed. An obvious increase in yield is perceived comparing these results of the adjusted polymerisation procedure with those of the primary experiments (table 2.1).

Table 2.2: Results of the improved polymerisation procedure on **8a**

	Yield (%)	M_w (PM) (g/mol)	PD (PM)	% PM	M_w (OM) (g/mol)	PD (OM)
standard 3	61	170 000	2.5	87	3 500	1.1
standard 4	69	182 000	2.6	90	3 000	1.1

The OM fractions again have a weight average molecular weight value of about 3 000 g/mol, while the PM fractions have an M_w-value of about 175 000 g/mol. The reason for the significant distinction in the molecular weights of these reactions and those of standard 1 and 2 lies in a variation in starting concentrations of the base and the monomer solution. This will be discussed and examined in more detail in section 2.7.

2.3.2 Experiments on 1-(chloromethyl)-4-[(*n*-butylsulfinyl)-methyl]benzene (8b)

Pouring the reaction mixture in ice water, followed by neutralisation, when 1-(chloromethyl)-4-[(*n*-butylsulfinyl)-methyl]benzene **8b** is used as monomer, immediately results in precipitation. Continuation with extraction again leads to the formation of a white emulsion and difficulties that go with it. Therefore the

extraction / washing procedure is again replaced by a single filtration step, at the same time offering an elegant solution to get rid of the NMP. Next, the crude product is dissolved in chloroform and precipitated in diethyl ether. This adjusted procedure leads to significantly higher yields (table 2.3).

Table 2.3: Results of standard polymerisations of **8b**

	Yield (%)	M_w (PM) (g/mol)	PD (PM)	% PM	M_w (OM) (g/mol)	PD (OM)
standard 5	79	148 000	2.1	86	2 700	1.1
standard 6	85	132 000	2.0	83	2 500	1.0

SEC-measurements again show a bimodal molecular weight distribution, consequently leading to two sets of values for molecular weight and polydispersity for each sample. The listed molecular weight values originate from about 85% relative PM peak area coverage.

Focussing on the resulting ^{1}H-NMR spectra, the fact that these NMR spectra show two chemical shift values for each proton signal – as is also the case for spectra of poly{[1,4-phenylene]-[1-(*n*-octylsulfinyl)ethylene]} - is striking. One set of signals shows a fine structure – pointing at a lower molecular weight polymer (the oligomer) – while another group consists of broader signals – typical for high molecular weight polymers. Apparently this is strongly dependent on the concentration and the molecular weight of the polymer fractions present in the NMR sample tube, because the fine structure could not always be perceived to the same extent. These NMR-spectra will be shown and discussed more in detail in section 2.6. The residual fractions are also subjected to ^{1}H-NMR analysis, but the spectra are overcrowded – too many signals are overlapping. Hence, apart from the observation that monomer and a small amount of NMP are still present and several new signals between 9.95 and 10.60 ppm have emerged, no conclusions can be drawn.

This study in NMP permits to make some adjustments of the general polymerisation procedure in order to obtain reproducible results. The optimisation is performed for the two most common used sulfinyl monomers **8a**

and **8b**, yielding similar results, thus justifying a mixed use of both in further experiments to investigate the polymerisation mechanism. It is found that the results of distinct polymerisations may be compared as long as initial base and monomer concentrations are kept constant. The origin of this feature will be examined and discussed in more detail in section 2.7.

2.4 A *P*-QUINODIMETHANE-BASED POLYMERISATION

2.4.1 Observation of *p*-quinodimethane using
UV-vis spectroscopy

As depicted in the general scheme (figure 1.13) precursor routes – like the Sulfinyl route - are believed to be *p*-quinodimethane based polymerisations. As a consequence, an efficient conversion of monomer to the *p*-quinodimethane (*p*-QM) system is essential for a high polymer yield. UV-vis spectroscopy has proven to be a most convenient technique to monitor the concentration of *p*-QM systems[5]. Differentiation is based on the distinction between the absorption wavelength for a benzoic (at about 278 nm) and a quinoid (at about 316 nm) structure[6]. This difference in λ_{max} was confirmed by UV-vis measurements of dr. Van Der Borght by observing the reaction of a solution of a blocked monomer (0.025 M) – a monomer with a structure similar to **8b**, only this time the leaving group is omitted – in MMF with a base (1.3 equivalents). No absorption is observed at 316 nm since only the benzylic anion and not the QM system can be formed[7].

In this work, the *in situ* UV-vis technique is used to check if polymerisation reactions in DAS also involve *p*-QMs. The objective is to monitor the appearance and depletion of the *p*-QM intermediate during polymerisation of **8a** in NMP, DMSO and DMF. Very low concentrations are used (in the order of 10^{-3}-10^{-4} mM) to prevent polymerisation and thus enhance the lifetime of the *p*-QM systems. The resulting plot from the experiment in DMSO is depicted in figure 2.5. Similar plots are obtained for the experiments in DMF and NMP. However, a general observation is the much lower maximum concentration – derived from

the observed absorption (Abs) respecting the same monomer and base concentrations - of *p*-QM in DAS compared to for example *s*-butanol. In the latter solvent high concentrations of the intermediate are easily formed[8]. This probably explains the lower molecular weights obtained for polymerisations in DAS.
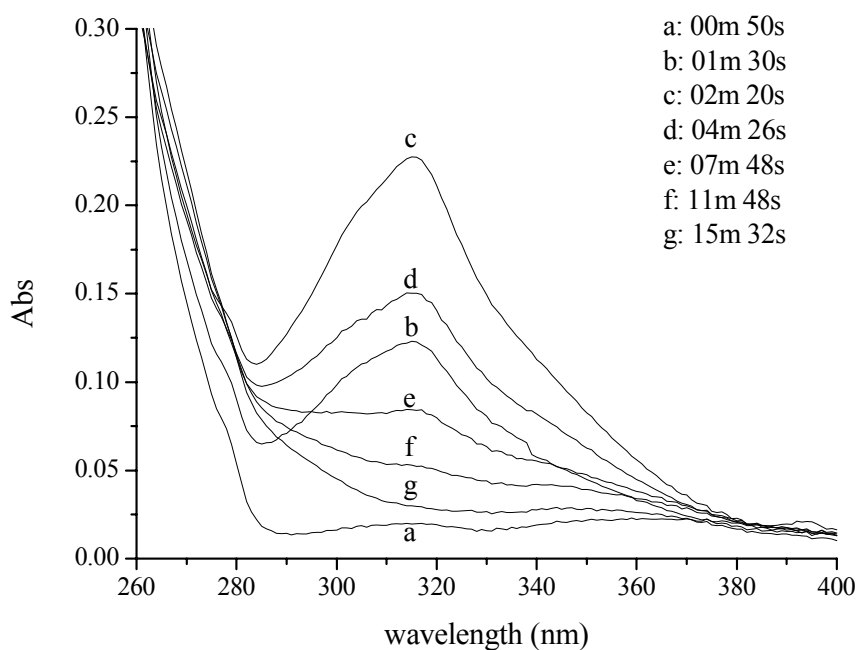
Figure 2.5: UV-vis monitoring of the formation and consumption of the quinodimethane intermediate for **8a** in DMSO

When the spectrophotometer is focussed at a constant wavelength of 316 nm the intensity evolution of the quinodimethane signal in time can be visualised. This is represented in figure 2.6 by plotting the absorption at 316 nm as a function of time.
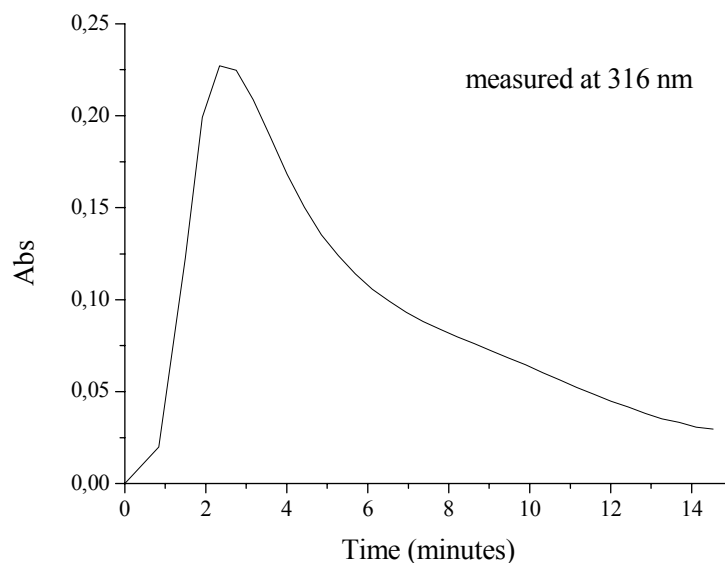
Figure 2.6: UV-vis monitoring of the *p*-QM signal in time at 316 nm

In this experiment the maximum concentration of *p*-QM is reached after about 2 minutes and then gradually fades. Probably the depletion of the signal involves consumption of the intermediate by a nucleophilic attack of the base, because in these conditions no polymer is formed. The absorption of this adduct would possibly lie underneath the monomer signal (at about 270 nm).

2.4.2 Observation of *p*-Quinodimethane using NMR Spectroscopy

Although *p*-QMs are the intermediates in this type of polymerisations, the number of reports on their NMR spectroscopic characteristics is very limited. Structural studies are complicated by the high reactivity of these intermediates. In fact, an on-line chemical abstracts (CA) search on *p*-QM (CAS registry number 502-86-3) combined with NMR led to only one hit: a publication by Williams dated 1970[9]. This group of researchers observed for the first time the NMR spectrum of unsubstituted *p*-QM, which unequivocally established its structure. Pyrolytic cleavage of the corresponding paracyclophane and trapping of the

intermediates at liquid nitrogen temperature (-169°C) prepared the solution of the reactive species. To permit the *p*-QM to be taken into solution distilled deuterated tetrahydrofuran (d-THF) was added at –80°C. The NMR spectrum was also taken at this temperature, but no concentrations are mentioned. Two specific signals were found: the olefinic protons at 6.49 ppm and the methylenic protons at 5.10 ppm.

Other, more recent publications containing NMR data on *p*-QMs do exist, but they concern stable derivatives – anthraquinodimethanes[10] and *p*-QMs bearing strong electron withdrawing (mostly cyano) groups on the vinyl carbons[11]. Therefore these data cannot serve as a reference for the experiments on the Sulfinyl route. Nonetheless an attempt is made to visualise *p*-QM systems during Sulfinyl polymerisation by ^{1}H-NMR.

2.4.2.1 In d-THF

For initial experiments d-THF - an apolar aprotic solvent - is chosen as solvent, because in comparison to DAS the extra complication of a bimodal molecular weight distribution is avoided[3b]. Thus, a system to check the feasibility of the idea and at the same time potentially optimise experimental conditions is offered.

The general polymerisation procedure prescribes that the base is added in solution to the monomer, but primary experiments show this causes problems with fast shimming – tuning of the magnetic field to obtain good resonance - of the instrument. Too much time passes during the making of parameter adjustments after base addition (in solution). The best procedure turns out to be: shimming of the instrument with 800 μL of monomer **8a** solution (with a concentration of about 1 mM), ejecting the NMR tube, adding the base as a solid, shake, and reinserting the tube. This way the shimming parameters should be all right. When 1.3 equivalents of base are added no reaction is observed; the monomer signals are unchanged. Next, an excess of base (approximately 10 equivalents) is added and this time reaction is initiated. A mediated spectrum is taken every thirty seconds allowing a follow up of the polymerisation in time, but implying at the same time a loss of quantitative information.

In figure 2.7 an example of such NMR experiments in time is visualised, focussing on the region between 7.4 and 4.5 ppm, because in this range the most interesting signals to follow the reaction are positioned. Polymer (PM), monomer (MM), and *p*-QM signals are marked to obtain a more direct overview.
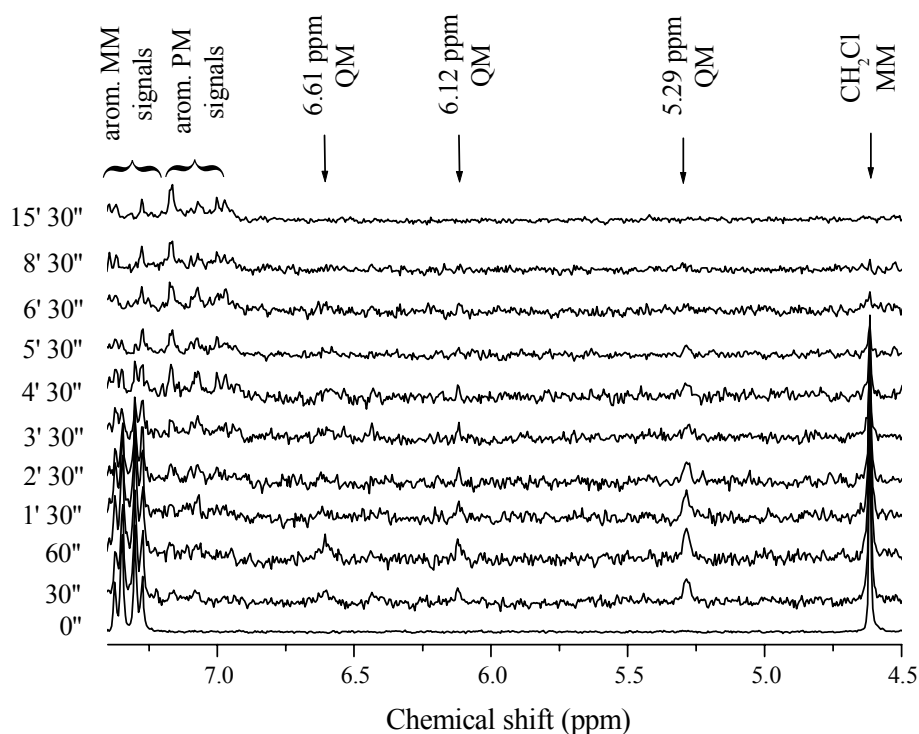
FIGURE 2.7: Reaction progress followed by ^{1}H-NMR –
focussed on the region between 4.5 and 7.5 ppm

Immediately after addition of the excess base, three new signals appear in the region between 5 and 7 ppm (5.29, 6.12 and 6.61 ppm), which are ascribed to the presence of a *p*-QM. These signals have a relatively low signal to noise ratio - probably due to their low concentration – but they are nevertheless observable. During the first five minutes they gradually fade away. At the same time monomer signals decrease in intensity – most clearly demonstrated by the gradual disappearance of the ϕCH_2Cl-signal at 4.62 ppm – and polymer signals

show up in the spectra between 7.0 and 7.3 ppm. These results demonstrate that polymerisation in these conditions is over in about 15 minutes.

In table 2.4 the experimental (from figure 2.7) and the calculated – using two different reference tables - chemical shift values (δ) of the involved *p*-QM system are listed and actually show rather good conformity. They are also in agreement with the values in reference 9.

Table 2.4: Calculated and experimental values for chemical shifts
of the involved *p*-QM
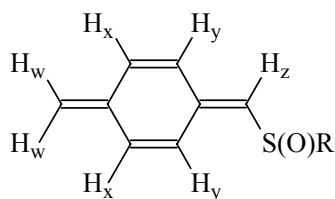
Proton	δ exp. (ppm)	δ calc.[12] (ppm)	δ calc.[13] (ppm)
H_w	5.29	5.35	5.22
$H_x = H_y$	6.12	6.05	6.02
H_z	6.61	6.35 (SR)*	6.49
		6.93 (SO$_2$)*	

* This reference does not contain correction values for SOR substituents,
therefore SR and SO$_2$ values are used as estimates.
SOR substituents are expected to give a value in between.

These experiments are an affirmation of the results of UV-vis measurements in THF[7] and justify the assignment of the absorption at 316 nm to the presence of a *p*-QM system. Considering the limited number of publications on this subject, the obtained NMR results are rather unique.

2.4.2.2 In d-DMSO

In an effort to visualise the *p*-QM system in a DAS, a similar experiment as in d-THF is set up: identical concentrations, solid base and similar experimental NMR parameters (e.g. delay time). Spectra are recorded immediately after addition of base. However, although monomer signals disappear in time making room for polymer signals, no proof for *p*-QM intermediates is found – nor for other intermediates. In the region between 5 and 7 ppm the signal to noise ratio is too low to distinct new signals. Hence, the idea to obtain direct evidence for *p*-QM systems during polymerisation by NMR turned out not to be feasible when working in DAS. The restriction is probably the low – too low - concentration of *p*-QMs – as observed in the UV-vis experiments.

However, the ^{1}H-NMR results in d-THF substantiate the assignment of the UV-vis absorption at about 316 nm to *p*-QM formation. Hence, although the attempt to visualise these intermediates during polymerisation in DAS by NMR failed, the observation of a signal at 316 nm in UV-vis measurements is considered enough and plausible proof for the classification of the Sulfinyl route as a *p*-QM based polymerisation.

2.5 OBSERVATION OF RADICAL SPECIES USING ESR-SPECTROSCOPY

Electron spin resonance spectroscopy (ESR) – also called electron paramagnetic resonance spectroscopy (EPR) – is a technique to identify the presence and nature of species containing unpaired electrons (radicals, paramagnetic molecules or ions). The principle is similar to that of NMR: appropriate detection equipment monitors the amount of radiation absorbed by the sample at slowly varying magnetic field. Because of the relatively broad signals – due to relatively short relaxation times compared to proton relaxation - most instruments use a phase-sensitive method of detection, and hence produce the first derivative of the absorption spectrum[14].

For this PhD work, ESR measurements are used to verify a radical nature of the polymerisation reaction. In all experiments solutions are flushed with helium

to remove dissolved oxygen, which is paramagnetic and can contribute to line-broadening. A primary experiment consisting of a recording of a monomer solution in NMP, immediately after addition of the base solution, did not result in an ESR signal. This can be due to concentration or lifetime problems, because qualitative ESR analyses are only possible on condition that the radicals are present in a minimum detectable concentration (mostly about 10^{-6} M) and have a lifetime of at least 10^{-6} s.

Interesting for the detection of short-lived radicals is the technique of spin trapping. In spin trapping, the ESR spectrometer detects the radical addition product – called the spin adduct – of the reaction between a radical and a spin trap. A widely used spin trap is 5,5-dimethyl-1-pyrroline-N-oxide (DMPO)[15]. DMPO rapidly scavenges free radicals generating relatively persistent spin adducts (figure 2.8).
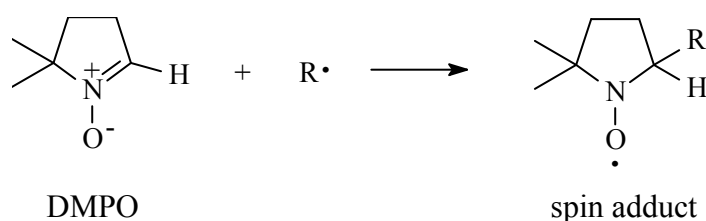
DMPO   spin adduct

Figure 2.8: The formation of DMPO spin adducts

ESR spectra recorded from solutions consisting of DMPO, DAS and base contain minor (in case of NMP) or no signals (in case of DMF and DMSO). However, stable ESR-signals are obtained in experiments in which spectra are recorded after addition of the base solution to a solution of monomer and DMPO, respecting a global monomer concentration of about 0.1 M. A typical pattern of a DMPO spin adduct, containing six characteristic signals, is for instance found in the ESR spectrum obtained in NMP (figure 2.9). The main feature is the relatively large doublet of triplets, due to a splitting of the oxygen radical signal by coupling with the neighbouring β-hydrogen and nitrogen nucleus. Further splitting is not observed, typical for a spin adduct of DMPO and a carbon radical. Similar experiments using the solvents DMF and DMSO yield similar spectra.
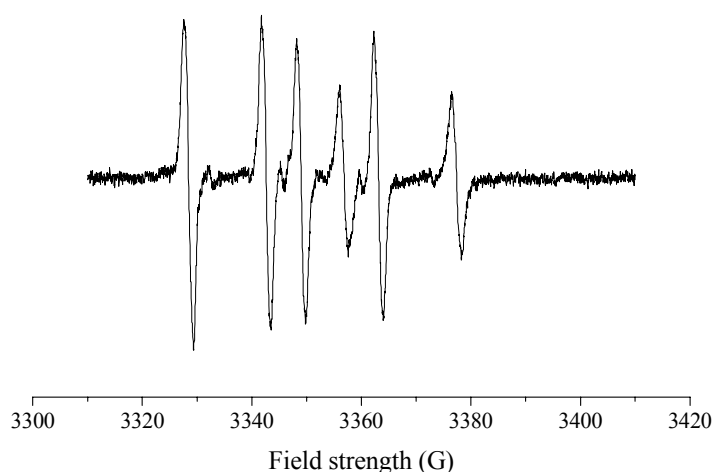
Figure 2.9: ESR spectrum of a DMPO spin adduct observed during
polymerisation in NMP

Important characteristics of the ESR spectral lines are the intensity
(concentration dependent), the position or g-value (similar to chemical shift
values) and the multiplicity. The latter term is expressed in values of hyperfine
splitting constants (hfsc's, linked to nuclear spin-spin coupling) and is used to
describe the magnetic coupling that can occur between the spin of the unpaired
electron and those of nearby magnetic nuclei in the molecule.

For DMPO spin adducts, the identification of the radical trapped is derived
from the magnitude of the nitrogen (α_N) and β-hydrogen (α_H) splitting constants
and the g-value. Theoretically, differences in hfsc's of 0.5 Gauss (G; $1\ G = 10^{-4}$
T)) can point at different DMPO spin adducts. Calculated values from the spectra
obtained in the various solvents using monomer **8a** or **8b** are listed in table 2.5.

Table [2.5]: Resulting g-values and hyperfine splitting constants

	g-value	α_H (G)	α_N (G)
NMP, **8b**	2.0059	20.59	14.21
DMSO, **8b**	2.0057	20.65	14.48
DMF, **8b**	2.0057	20.61	14.22
DMF, **8a**	2.0059	20.52	14.28

An important conclusion of these ESR measurements is that the results point at the presence of radicals during polymerisation in DAS, indicating the possibility of a radical nature of the polymerisation mechanism. For the calculated hfsc-values no differences above 0.3 Gauss are observed; hence most probably in all cases a similar spin adduct is formed – possibly the initiating particle. However, the experimental set up used does not allow a more detailed identification of the DMPO spin adduct.

2.6 INFLUENCE OF ADDITIVES ON A STANDARD POLYMERISATION[16]

From the mechanistic study in MMF it was concluded that the Sulfinyl route towards PPV precursor polymers in polar, protic solvents proceeds via a radical polymerisation mechanism. One of the experimental results that led to this conclusion was the effect of the radical scavenger 2,2,6,6-tetramethylpiperinoxyl (TEMPO, figure 2.10) on the reaction. Addition of a small amount (0.01 equivalents) decreased yields and molecular weights, whereas addition of 0.5 equivalents TEMPO totally inhibited polymerisation[2].
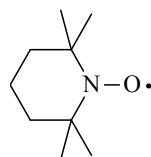
Figure 2.10: The structure of TEMPO

This experience is used in this work to verify the radical nature of a standard polymerisation reaction in NMP. The influence of a couple of additives is checked to gain knowledge on the underlying polymerisation mechanisms. It is started from a standard polymerisation of monomer **8b** in NMP, based on initial monomer and base concentrations of 0.14 and 0.37 M respectively, yielding 43% of polymer with a bimodal molecular weight distribution in SEC analysis – shown in figure 2.12. The molecular weights and polydispersities obtained are M_w = 44 600 g/mol, PD = 1.8 and M_w = 2 500 g/mol, PD = 1.0, for the polymer

and the oligomer fraction respectively. Because the peaks are not baseline separated these values should be considered as estimates. The corresponding ^{1}H-NMR spectrum – containing two pairs of similar signals: one pair of broad signals and one pair of signals showing a finestructure - is shown in figure 2.13.

2.6.1 Addition of TEMPO

To check the influence of TEMPO addition on the standard polymerisation it was chosen to add 0.5 equivalents. In contrast with the results obtained in MMF not all polymer formation is blocked by this addition. However, yield is seriously affected and decreases to about 10%. SEC analysis of the polymer shows a monomodal distribution on the low molecular weight side of the chromatogram (M_w = 3 000 g/mol, *PD* = 1.1, hence an oligomer) at about the same elution volume as the OM peak of the standard bimodal distribution (figure 2.12). The higher molecular weight polymer fraction has disappeared. The corresponding ^{1}H-NMR analysis (figure 2.13) only shows the pair of polymer signals possessing a fine structure – thus pointing at the lower molecular weight of the obtained oligomer.

In a separate experiment it is checked if any reaction between base and TEMPO occurs, but in the end pure TEMPO was collected, hence no evidence for a side reaction is found.

^{1}H-NMR analysis of the residual fraction leads to an overcrowded spectrum (figure 2.11), where a lot of signals overlap, hampering a detailed characterisation of products present. Hence, unfortunately this analysis merely can lead to some vague determinations and assignments. The monomer constitutes the main product of the residual fraction, suppressing other signals. However, at a relatively low intensity some oligomer signals containing a fine structure are neighbouring the monomer signals. Also chemical shift values corresponding to NMP are present. In the region between 9.90 and 10.15 ppm several minor new signals emerge – possibly originating from carbonyl and / or carboxyl groups – and between 5 and 6 ppm signals of indistinct origin appear.
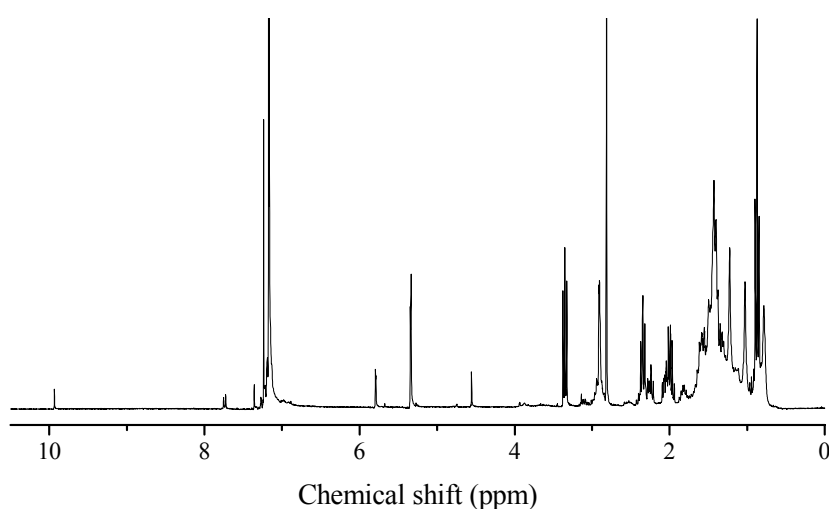
Figure 2.11: ^{1}H-NMR spectrum of the residual fraction
of the TEMPO experiment

The most intense downfield signal emerges at 9.98 ppm. Integration values show a correspondence with signals at 7.80, 7.30, and 2.95 ppm - a set in good accordance with signals assigned to the dialdehyde perceived by A. Issaris, who has also put forward a proposal for its formation[2]. A schematic representation of this proposal can also be found in chapter three (figure 3.4). In fact, the dialdehyde has been regarded as a possible derivative of the dimer initiator as indication of the radical polymerisation. Putting the monomer intensity at 100%, this product has a relative intensity of 15%, which is relatively high compared to other signals present. Further, some signals of TEMPO can be detected between 2 and 3 ppm, but currently no adduct-structures could be revealed, due to overcrowding.

It seems that addition of TEMPO only inhibits formation of higher molecular weight polymer, leaving the oligomer formation unaffected. The experimental results point to the occurrence of a radical mechanism, being responsible for the formation of high molecular weight polymer in NMP.

2.6.2 <u>Addition of Water</u>

From the previous experiment the origin of the low molecular weight polymer is not clear, but the results seem to point to a non-radical mechanism for its formation because it is not affected by TEMPO. When the nature of the solvent is taken into account, an anionic mechanism seems to be probable. Indeed NMP belongs to the class of dipolar, aprotic solvents (DAS) which specifically solvate cations very efficiently and enhance the reactivity of anions. Hence, if an anionic mechanism is postulated for these *p*-quinodimethane-based polymerisations it is most probable to take place in this class of solvents.

To check if any anionic polymerisation mechanism does take place in NMP, 5 vol% of water is added to the standard reaction mixture, as water is known to prevent anionic polymerisation. The result is consistent with our expectations: SEC-analysis shows that the higher molecular weight polymer (M_w = 61 000 g/mol, PD = 1.7) is still present, but the oligomer formation is blocked (figure 2.12). The corresponding ^{1}H-NMR spectrum (figure 2.13) shows a pair of broad polymer signals harmonizing with one set of signals of the standard spectrum.

Also this time the NMR analysis of the residual fraction results in an overcrowded spectrum, where overlapping of signals hampers product characterisation, leading to similar restrictions as with the discussion of the previous residual fraction. The monomer definitely constitutes the main product and also NMP signals are present. The minor signals neighbouring those of the monomer and containing a fine structure again point at some oligomer (low molecular species). Once more, several signals emerge in the spectral region between 9.90 and 10.15 ppm – some with similar chemical shift values as for the previous residual fraction. Currently, more than a vague assignment to carbonyl or carboxyl groups cannot be offered. At 10.05 ppm the most important signal is situated, but the corresponding structure could not be traced.
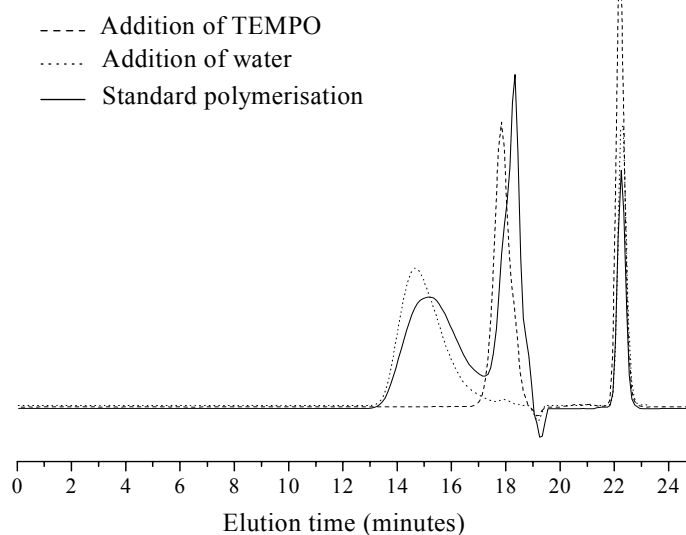
Figure 2.12: Overlay of SEC chromatograms of the various polymer fractions
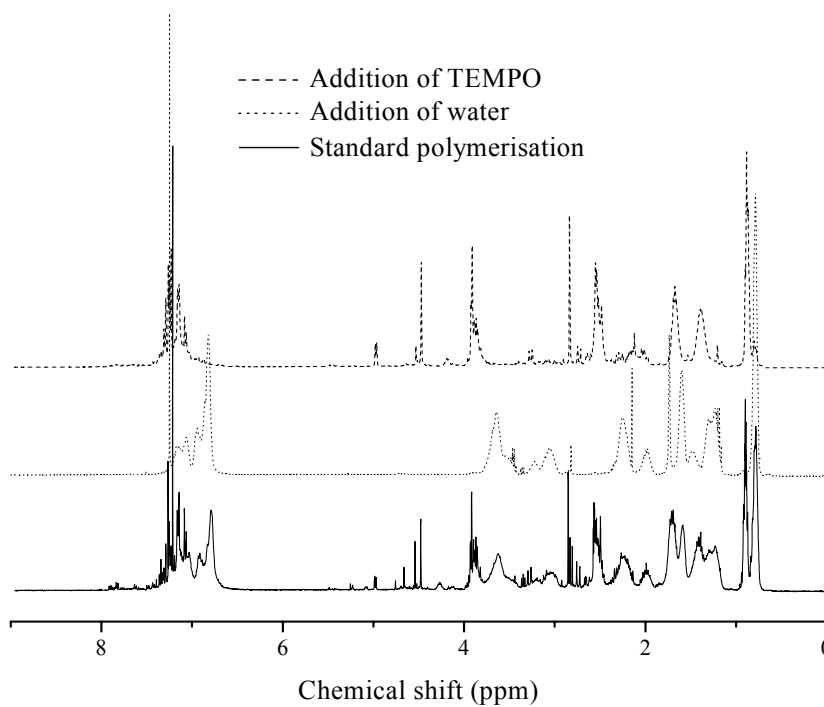
Figure 2.13: Overlay of ^{1}H-NMR spectra of the various polymer fractions

The water addition does not seem to have much influence on the yield of the reaction: about 48%, in good accordance with the 43% yield under standard conditions. Using pro analysis (p.a.) NMP yields similar results: a monomodal molecular weight distribution of high molecular weight polymer. Hence, if at the start of the Sulfinyl route development the global opinion on the nature of the polymerisation mechanism hadn't been anionic – implying the importance of dry conditions - perhaps the feature of a bimodal molecular weight distribution would never have been observed.

More information on whether this anionic mechanism is of a chain- or step-growth nature is provided by results of the monitoring of the polymerisation in function of time using SEC, as will be discussed in section 2.8.

Standard characterisation of the higher molecular weight polymer by ^{1}H-NMR does not yield additional information on the progress of the polymerisation - the high molecular weight prevents determination of end groups. However, taking the analysis of the residual fraction into consideration a proposal for the radical polymerisation is put forward (figure 2.14).
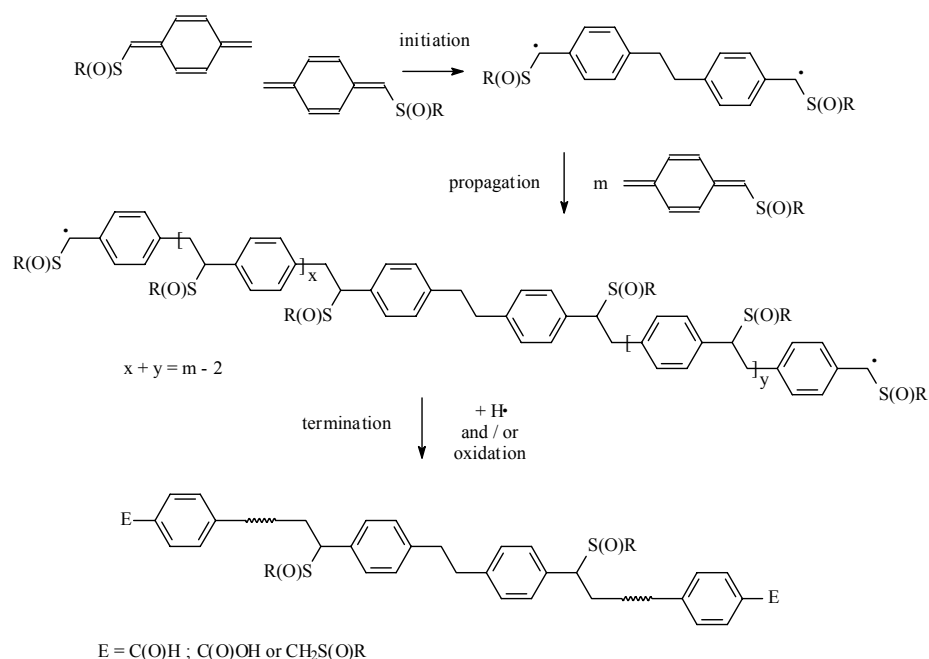
Figure 2.14: Proposal for the radical polymerisation mechanism yielding high MW polymer

The presence of the dialdehyde in the residual fraction of the TEMPO experiment (section 2.6.1) is an indication that initiation consists of a spontaneous head-to-head dimerisation of *p*-QM systems yielding a diradical species. This is in agreement with the proposal of Wessling[17], the scheme of Errede[18] and some principles of free radical polymerisation[19]. Both sides of the diradical can propagate independently by reaction with *p*-QM intermediates, probably by a chain type reaction, as will be demonstrated in section 2.8.

Currently, the nature of the termination reaction remains indefinite, but two pathways are proposed. Possibly, hydrogen atom transfer terminates the active polymer chain. On the other hand, the presence of carbonyl and / or carboxyl signals in the NMR spectrum of the residual fraction can point at oxidation as termination reaction(s). Another member of our research group (H. Roex) is currently investigating this by working with ^{13}C enriched or labelled compounds. Initial experiments confirm the presence of carboxyl and / or carbonyl entities.

2.6.3 ^{13}C-NMR analysis of the oligomer fraction

A more detailed ^{13}C-NMR study of the oligomer fraction of the TEMPO experiment (with a M_w–value of about 3 000 g/mol) can possibly reveal a more detailed structure of the oligomer by detection of end groups. Hence it could lead to a proposal for the anionic polymerisation mechanism by which it is made. At first, it was looked for NMP-endgroups, because they were mentioned in previous work[1,3b], and indeed NMP signals are observed. An Attached Proton Test (APT) analysis shows that NMP is possibly not only present as traces of free solvent, but actually also acts as end group. One of the original CH_2 carbons has probably become a CH carbon, implying that an adduct is formed. However, the rather low signal intensity causes this to be not irrefutable. In figure 2.15 both ^{13}C- and ^{13}C-APT spectra are presented.

On top of the NMP signals, two signals corresponding to original monomer signals are still present in the spectrum. These signals correspond to the CH_2 carbons neighbouring the sulfoxide: one is the benzylic carbon, while the other is positioned first in the R-group (carbon 4 and 5 – see figure 2.23 in the experimental part). APT mode confirms that both are CH_2 carbons, thus providing an

indication that the S(O)R functionality also acts as end group. The other, more distant carbons of the alkyl group experience little or no effect of possible benzylic (C4) substitution, resulting in an overlap of corresponding end group with backbone signals. No residual CCl signal, which is normally positioned at about 45.1 ppm, can be observed, implying that the chloride has fulfilled its function of leaving group well.
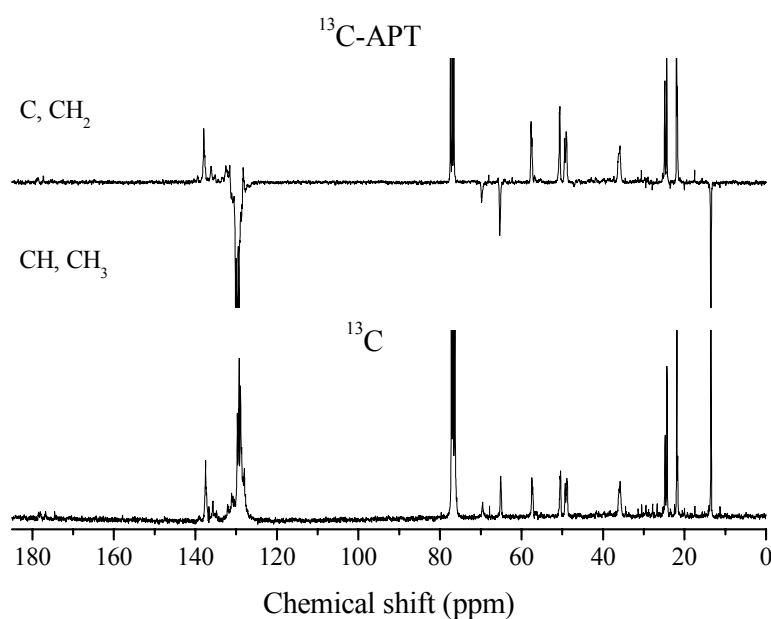
Figure 2.15: NMR spectra of the oligomer fraction
top: ^{13}C-APT spectrum; bottom: [13]C spectrum

No ethylene signals are visible around 30.9 ppm – the signal at 30.5 ppm is assigned to a NMP signal - contradicting the head-to-head dimerisation of *p*-QM systems as initiation of the polymerisation – as in Wesslings mechanism proposal[17] and the scheme of Errede[18]. However, this is conforming to the proposal of an anionic mechanism for oligomer formation – as presented in figure 2.16.

Unfortunately, integration values do not irrefutable confirm the structure of the oligomer presented – the ratio between end group signals of the sulfoxide and NMP does not equal unity. The intensity of the NMP signals is about one fifth of the sulfoxide end signals. This is possibly due to initiation other than attack by the solvent, but more direct indications for this assumption are not found. However the ratio between sulfoxide ends and oligomer signals yield a value of about 15 as conjugation length of the oligomer. This number is obtained by comparison of the integration value of the sulfoxide ends (C4 or C5) with that of a benzyl group (summation of the 6 C-atoms).
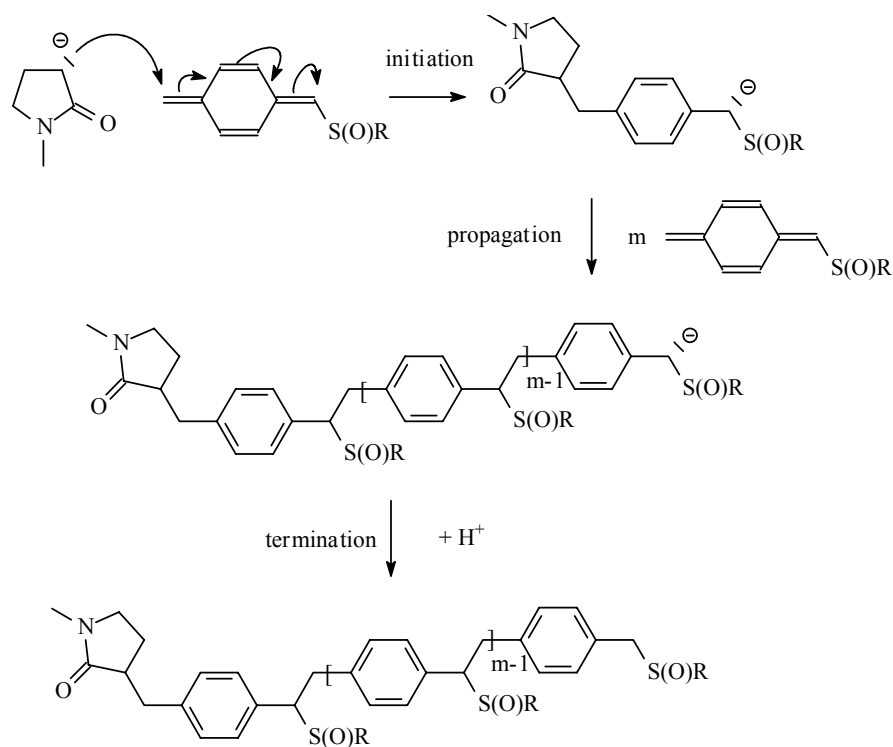
Figure 2.16: Proposal for the anionic polymerisation mechanism yielding oligomers

2.6.4 <u>Confirmation of the additive effects on a monomer</u>
<div align="right"><u>with an extended π-system</u></div>

In collaboration with dr. M. Van Der Borght, a second example comprising the polymerisation in NMP of 4-chloromethyl-4'-(*n*-butylsulfinyl)methyl-biphenyl – containing a more extended π-system in the direction of the polymer axis (inset figure 2.17) - is included in the study. The Wessling route does not allow polymerising this type of monomers, again demonstrating the versatility of the Sulfinyl route. In spite of the anticipated higher resonance energy to be broken, *in situ* UV-vis spectroscopy shows a new signal at about 445 nm, which quickly diminishes in time, pointing at the formation of the corresponding *p*-QM system[20].

Because of the low solubility of the monomer in NMP the reaction is performed at 35°C. Standard polymerisation results in a bimodal molecular weight distribution shown in SEC analysis (figure 2.17). At a yield of 25% a polymer with an M_w of 21 000 g/mol and a polydispersity of 1.9 is isolated. These numbers originate from calculations where the two peaks are taken as a whole.

The addition of 0.5 equivalents TEMPO yields an oligomer with a monomodal molecular weight distribution (M_w = 8 000 g/mol, *PD* = 1.1). In accordance to the experiment described in section 2.6.1, the yield of the reaction is seriously affected by this addition and decreases to 5%.

Addition of 5 vol% water to the polymerisation mixture results in the formation of a monomodal higher molecular weight polymer fraction with a M_w of 40 000 g/mol and a polydispersity of 1.5. The corresponding SEC chromatogram is shown in figure 2.17. The yield of this reaction is rather low (2%) - possibly due to a difficult separation / precipitation or by an effect of the water on the base strength.
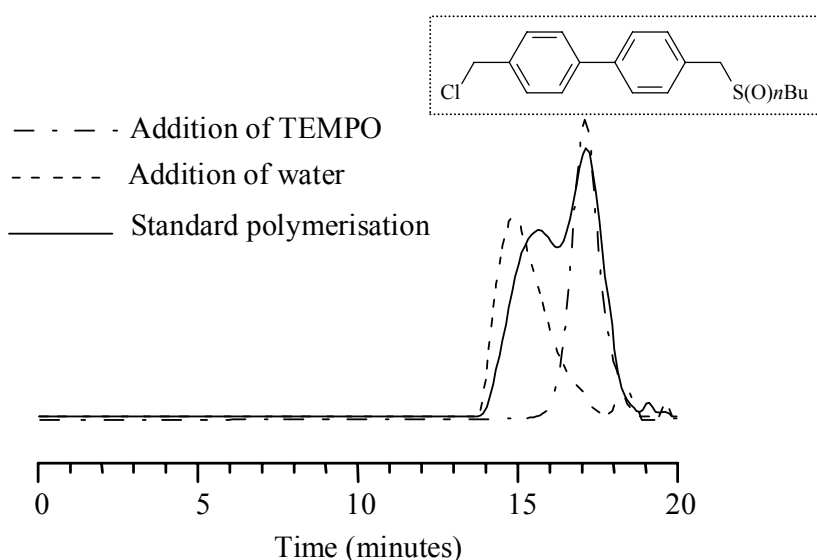
Figure 2.17: Overlay of SEC chromatograms
confirming the effect of the additives

These experimental results are in good agreement with the ones presented in section 2.6.1 and 2.6.2 and confirm that an extension of the conclusions of the previous sections to other monomers yielding a bimodal molecular weight distribution can be made.

2.7 INFLUENCE OF CONCENTRATION AND TEMPERATURE

2.7.1 The effect of concentration variation

An important remark has to be made regarding the molecular weight (MW) values mentioned in the previous sections. A first overview on the various reactions of for example monomer **8a** shows a large spread of calculated molecular weights ranging from about 70 000 to 170 000 g/mol. A more detailed study of the SEC results – focussing on relative percentages of peak areas – yields a correlation between the amount of oligomer (derived from the area of the OM peak) and the MW value of the higher MW polymer (PM peak). An increasing amount of oligomer seems to correlate with a lower molecular weight

value of the polymer. This is represented in figure 2.18 by plotting the weight average molecular weight as a function of relative % PM peak area. Remember that for the calculations of the relative amounts of OM and PM the sum of the two peak areas is considered 100%. Similar observations can be made for the various reactions of monomer **8b**.

A difference between the various reactions of monomer **8a** (standards 1 and 2 compared to standards 3 and 4) is the division of the solvent (20 mL) over the monomer and the base solutions prior to reaction, hence on their initial concentrations. Remember that the polymerisation procedure only mentions a global monomer concentration of 0.1 M - that is after base addition. The first experiments (standards 1 and 2) were performed respecting a ratio between both solutions of 14 over 6, respectively. This means that the monomer is dissolved in 14 mL (0.14 M) and the base in 6 mL of solvent (0.37 M), and these concentrations are generally applied as starting conditions.

In order to prevent a possible origin of irreproducibility due to solubility problems of the base, it was changed to a 10 over 10 ratio (standards 3 and 4), thus providing more solvent to dissolve the base and leading to initial monomer and base concentrations of 0.2 and 0.22 M, respectively. The significant differences in the obtained results of both sets of reactions point at a great importance of the first seconds of polymerisation, right after base addition.

Hence, the origin of the spread in molecular weights appears to be a variation in initial concentrations, implying major consequences for the molecular weight value of the higher molecular weight polymer and the ratio between the amount of OM and PM. To check if this is due to a variation in initial monomer concentration, base concentration or both, two other polymerisations are performed using the optimised procedure respecting a 14 over 8 ratio leading to a monomer and a base solution with a concentration of 0.14 M and 0.28 M, respectively. This way, the initial monomer concentration is kept constant in comparison with standard 1 and 2, while the starting base concentration is lowered. Inevitably, the global monomer concentration – after base addition – is affected (lowered to 0.09 M), but this change is considered negligible. The corresponding results are listed in table 2.6 and originate from

about 80% relative PM peak area coverage. The corresponding data points are also displayed in figure 2.18 and lie surprisingly well in the line of expectation.
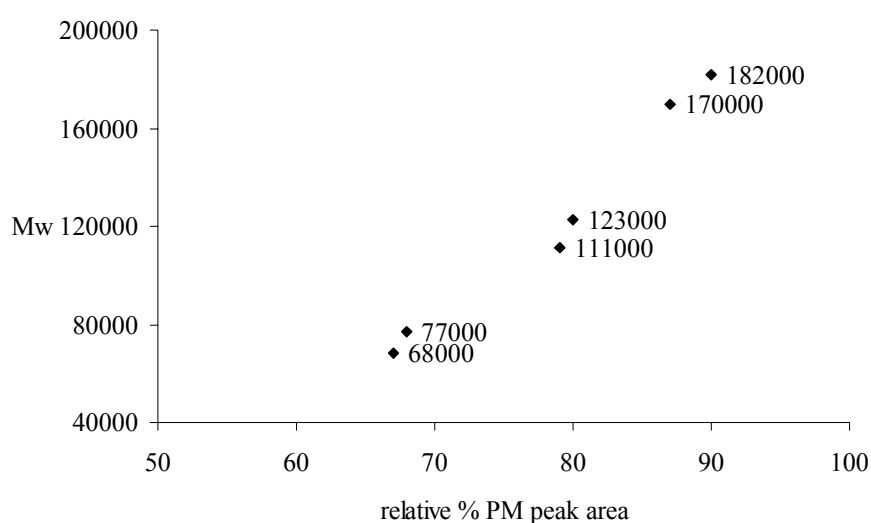
Figure 2.18: Molecular weight of PM peak as a function of % PM

Table 2.6: Results of polymerisations of **8a** using a 14 / 8 ratio

	Yield (%)	M_w (PM) (g/mol)	PD (PM)	% PM	M_w (OM) (g/mol)	PD (OM)
14 / 8 (1)	47	111 000	2.1	79	3 300	1.1
14 / 8 (2)	40	123 000	2.4	80	2 900	1.0

These data indicate that the initial base concentration definitely exhibits an influence on several polymerisation characteristics. An increase of initial base concentration results in a decrease in the polymer molecular weight, and an increase in the relative amount of oligomer present. This could be interpreted as an indication that the mechanisms of polymer and oligomer formation are in competition with each other. To summarise and visualise these effects an overview of some select data is listed in table 2.7 laying the emphasis on differences in initial concentrations.

Table 2.7: Overview of results of polymerisations of **8a** using various initial concentrations

Ratio	$[B]_i$ (mol/L)	$[MM]_i$ (mol/L)	$\dfrac{[B]_i}{[MM]_i}$	M_w (PM) (g/mol)	% OM	M_w (OM)
14 / 6	0.37	0.14	2.6	77 000	33	3 200
14 / 8	0.28	0.14	2.0	123 000	20	2 900
10 / 10	0.22	0.20	1.1	182 000	13	3 000

[B]: base concentration; [MM]: monomer concentration; i: initial

This overview clearly shows the significant decrease in molecular weight of the polymer when the initial base concentration is increased, while the molecular weight of the oligomer is hardly influenced. The rise in the amount of oligomer fraction is probably due to an increased initiation, favoured at higher momentary base concentrations.

All this seems to fit well within the framework of a competition between two polymerisation mechanisms – anionic as well as radical. Based on the mechanistic proposals, depicted in figure 2.14 and 2.16, reaction kinetics can now be included in the discussion. Kinetically, the speed of dimerisation initiation (of the radical mechanism) depends on the quinodimethane concentration to the square (~ $[QM]^2$), while the anionic initiation is supposed to depend on the first power of the QM concentration ([QM]) times the concentration of the nucleophile ([Nu]). This is schematically represented in figure 2.19.
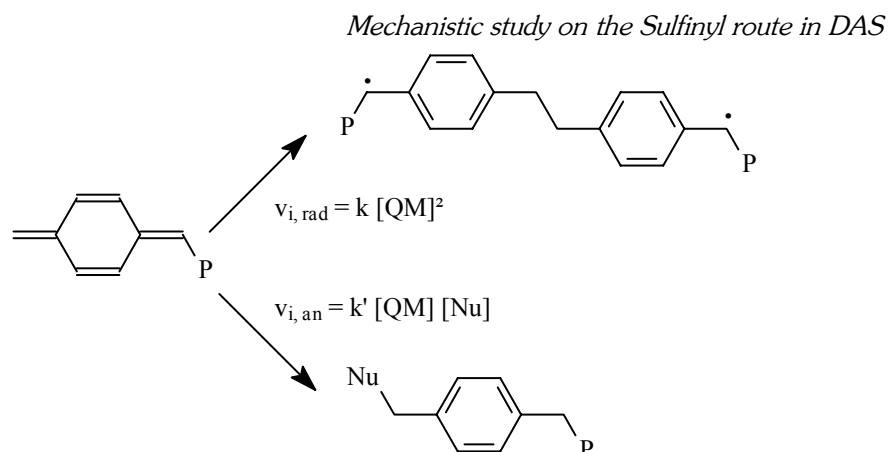
Figure 2.19: Schematic representation of initiation kinetics based on the
proposals for the anionic and radical polymerisation mechanisms

This would imply that a rise in momentary base concentration results in a relative increase in anionic initiation compared to radical initiation, yielding an increased amount of anionically formed oligomer at the cost of the amount of polymer formed by the radical polymerisation mechanism. The obtained results are in good agreement with this, supporting the underlying mechanistic proposals.

Apparently, the termination reaction of the oligomer formation – anionic polymerisation - is not much – if at all – influenced by this change in reaction conditions, explaining the more or less constant molecular weights found.

2.7.2 The effect of reversed addition

The previous experimental results indicate that an increasing initial base concentration causes the reactions for anionic OM formation to gain importance and apparently to compete stronger with the radical processes of PM formation. To check for an affirmation of this effect of the initial base concentration another experiment – expressing a rather extreme case - is set up. This time the addition is reversed, meaning that the monomer solution is now added to the base solution, in one portion. Starting concentrations similar to standards 3 and 4 (using a 10 / 10 ratio) are applied implying monomer and base concentrations of

0.2 and 0.22 M, respectively. This way the momentary base concentration is very high compared to the momentary monomer concentration.

Addition of the monomer to the base solution results in a bright yellow coloration of the reaction mixture, which faints after a few seconds. Pouring in ice water, after one hour of reaction, yields a white emulsion, which is disturbed by acidification. An attempt to purify the crude product - obtained by filtration and dissolved in chloroform - by precipitation in a mixture of hexane / diethyl ether 1/1 is unsuccessful. Only a small amount of precipitate could be collected and the corresponding NMR and SEC analyses show the presence of oligomer, polymer as well as monomer. The obtained molecular weights are listed in table 2.8. Similar results are obtained analysing the residual fraction. Because of the very low molecular weight of the so-called PM fraction, the OM and PM peaks overlap even more as usual and they are thus not baseline separated. Hence the calculated values should be regarded as estimates. Actually, the PM peak can be seen as a large shoulder of the OM peak. When both peaks are taken as a whole to perform calculations upon, an M_w-value of 5 500 g/mol and a polydispersity of 1.6 result.

Repeated attempts to precipitate and separate the various fractions (monomer, oligomer and polymer) failed - possibly due to the very similar molecular weights of all distinct fractions. Therefore, the precipitate and the residual fraction are recombined and again analysed by SEC to get an idea of relative yields. These are calculated by setting the sum of the peak areas equal to 100% (% MM + % OM + % PM = 100%). As a consequence, these values should be considered as rough estimates.

Table 2.8: Results of polymerisations of **8a** –
reversed compared to regular addition

Addition	Yield (%)	M_w (PM) (g/mol)	PD (PM)	% PM	M_w (OM) (g/mol)	PD (OM)
Reversed	41	10 400	1.2	36	2 900	1.1
Regular	61	170 000	2.5	87	3 500	1.1

Again, the results are conforming to the expectations and support the idea of two competing mechanisms. The reversed addition (relatively high initial base concentration compared to the monomer concentration during the first moment of reaction / addition) results in a significant increase in amount of OM. These conditions apparently favour anionic initiation over radical dimerisation; hence oligomer formation increases at the cost of high molecular weight polymer formation. Similar kinetic considerations as for the previous experiments can be made. The higher $[B]_i$ the stronger the initiation of the oligomer formation competes with radical initiation resulting in a higher relative amount of oligomer formed, and a lower polymer molecular weight.

2.7.3 The effect of temperature variation

To check the influence of temperature, a polymerisation with a 10 to 10 ratio - between the volume of solvent used for initial monomer and base solutions respectively - is executed at 0°C. The special polymerisation appliance allows cooling of both monomer and base solution. The corresponding results originate from about 52% relative PM peak area coverage and are listed in table 2.9 together with the results of standard 4 – a similar polymerisation performed at ambient temperature.

Table 2.9: Results of polymerisations of **8a** at 0 and 25°C (using a 10 / 10 ratio)

Temp.	Yield (%)	M_w (PM) (g/mol)	PD (PM)	% PM	M_w (OM) (g/mol)	PD (OM)
0°C	43	54 000	2.1	52	3 300	1.2
25°C	68	182 000	2.6	90	3000	1.1

As a consequence of the lower polymerisation temperature, the relative amount of oligomer has increased significantly to about 48% - compare to a value of 10% for the polymerisation at ambient temperature - and the molecular weight of the PM decreased. This again supports the idea of a competition between and the proposals for the radical and the anionic polymerisation mechanism. The observation that oligomer formation is favoured at low

temperature is in agreement with the supposition of an anionic mechanism *as well as* the dimerisation initiation proposal of the radical mechanism. By decreasing temperature quinodimethane formation is slowed down and consequently the speed of initiation is lowered. Kinetically, the speed of the radical dimerisation initiation is hereby more affected ($\sim$ [QM]^2) than the speed of anionic initiation ($\sim$ [QM] [Nu]). This presents a plausible explanation for the results obtained from this temperature experiment.

Another way to explain the lowering of the PM molecular weight by a temperature decrease is the presumption of an increased initiation, leading to shorter chains. This should go along with a higher QM concentration. However, earlier research on the Sulfinyl route has shown that for polymerisations in secondary butanol the molecular weight increases as temperatures decrease, making this explanation less probable[21].

2.8 Monitoring the Polymerisation Process
as a Function of Time by means of SEC

In an attempt to check if the oligomer is formed simultaneous with or sequential to the higher molecular weight polymer the polymerisation of **8a** in NMP is followed in time. In practice, sampling is performed using a glass syringe and a septum to preserve the nitrogen atmosphere inside the appliance. Pouring in ice water and acidification until precipitation occurs stops the reaction. The precipitate is then recovered by filtration, dried *in vacuo*, and processed in a SEC sample.

A first specimen is taken from the reaction mixture at about 30 seconds after the base addition. For the next ten minutes samples are taken about each 60 seconds. The last two samples are taken 30 minutes and one hour after the start of the polymerisation. Evolution of the polymerisation in time is evaluated by SEC analysis considering molecular weights, polydispersities and relative peak areas. The corresponding results are listed in table 2.10, while figure 2.20 represents evolution of molecular weight in time.

Table 2.10: Results of timed samples using SEC analysis

sample	M_w (PM) (g/mol)	PD (PM)	% PM[a]	M_w (OM) (g/mol)	PD (OM)	% OM[a]	% MM[b]
30''	190 000	1.7	85	2 400	1.1	15	56
1'	180 000	1.7	84	2 400	1.1	16	48
2'	164 000	2.0	83	2 400	1.1	17	41
3'	155 000	2.2	85	2 400	1.1	15	37
4'	159 000	2.2	86	2 500	1.1	14	36
5'	160 000	2.2	85	2 500	1.1	15	34
6'	162 000	2.2	85	2 500	1.1	15	33
7'	163 000	2.2	82	2 500	1.1	18	34
8'	160 000	2.2	81	2 600	1.1	19	33
9'	154 000	2.2	79	2 400	1.1	21	32
10'	159 000	2.2	84	2 700	1.1	16	28
30'	158 000	2.3	84	2 600	1.1	16	22
60'	155 000	2.3	86	3 000	1.1	14	20

The calculations are based on [a]: % PM + % OM = 100%;

[b]: % PM + % OM + % MM = 100%

These results demonstrate that the Sulfinyl route belongs to the category of chain polymerisations: high molecular weight polymer is present at an early stage of the reaction. The M_w-value of the oligomer stays more or less constant in time; the differences in molecular weight values are low taking analysis errors in account. Probably also in this case a chain polymerisation is involved, which is terminated at a much earlier stage of propagation than is the case for the higher molecular weight polymer.
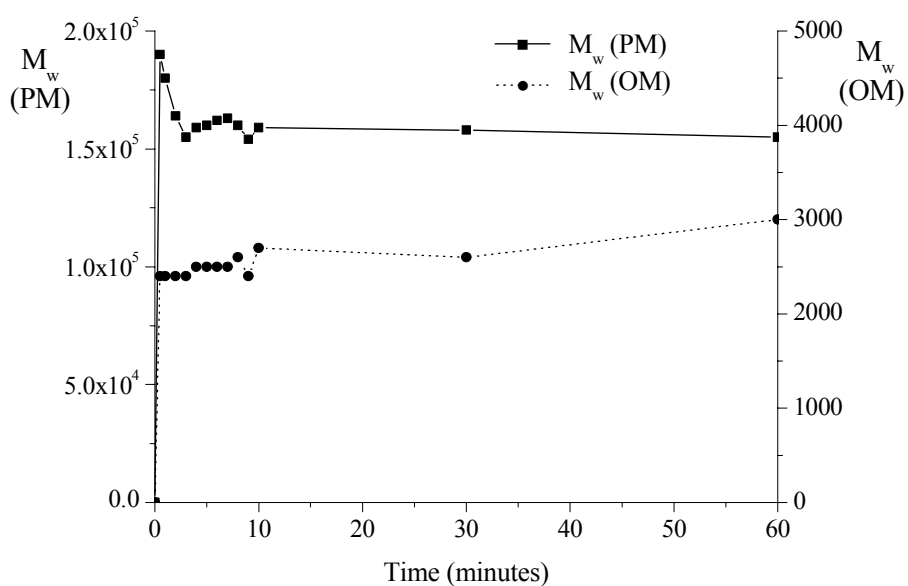
Figure 2.20: Evolution of molecular weight in time

Polymer and oligomer are formed simultaneously; the ratio between both quantities is determined in the beginning and retained in the course of the polymerisation. Combined with the results presented in figure 2.18 it can be concluded that there is a competition between the formation of oligomer and polymer, but the extent to which this happens seems to be defined in the first moments of reaction.

Actually, for this plot to be similar to the original plot type, such as figure 1.15, molecular weights should be expressed as function of monomer conversion – not time - but the experimental set up did not allow exact quantitative data on monomer conversion. However, relative values for monomer conversion can be obtained by following changes in relative peak area. For this purpose the peak area of the polymer, the oligomer and the monomer are summed and set equal to 100%. In the column most to the right in table 2.10 the calculated values of relative percentage monomer peak area (% MM) are listed. From these values it can be concluded that an early stage of the reaction corresponds with a relatively low monomer conversion, hence conclusions drawn from figure 2.20 can be

defended. The decrease in monomer concentration as a function of time is plotted in figure 2.21 and can be fitted with an exponential decay function. Hence, although the molecular weight of the polymer remains more or less constant after two minutes of reaction, this does not inherently mean polymerisation is over. The inset of figure 2.19 shows the molecular weight of the polymer as function of the calculated relative monomer conversion and shows similarity with figure 2.20.
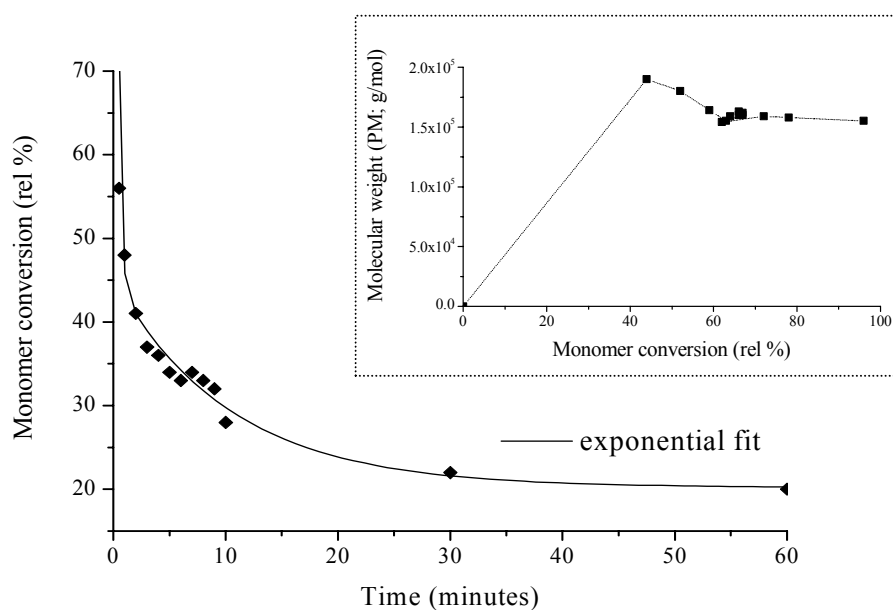
Figure 2.21: Relative monomer conversion as a function of time; Inset: molecular weight as function of monomer conversion (PM)

2.9 EXTENSION TO OTHER MONOMERS AND SOLVENTS

The results obtained in the mechanistic study in DAS help to gain insight in a number of features of the Sulfinyl route – e.g. the bimodal molecular weight distribution. Over the years, a large amount of data is gathered in our research group and now these results can be put in perspective in a compilation and extension to other monomers and solvents[22]. New insights in the mechanism of

the Sulfinyl precursor route towards PPV derivatives are presented by studying the polymerisation reaction in various solvents and by evaluating the influence of both electron donor and acceptor substituents. This is possible thanks to the use of unsymmetrical monomers – as stated before - which allows a broad range of solvents to become available for investigation.

Especially the introduction of electron acceptors is of interest towards the use of PPV derivatives as active layers in P-LEDs, because of their higher electron affinity. Although the electroluminescence efficiency is high in P-LEDs with calcium as cathode, the lifetime is rather limited due to the reactivity of calcium[23]. In that view, aluminium - a less reactive metal - is a more interesting electrode material. Its work function is higher - compared to calcium - requiring a higher electron affinity of the conjugated polymer in order to retain the high P-LED efficiencies.

Table 2.11 shows an overview of polymer yields, molecular weights and molecular weight distributions of different precursor polymers obtained via the Sulfinyl precursor route in several solvents starting from various monomers differing in leaving group (L), polariser ($S(O)R_2$) and / or ring substituents R_1 (figure 2.22).

L = leaving group;
R_1 = aromatic ring substituents;
R_2 = *n*-alkyl group of the polariser.
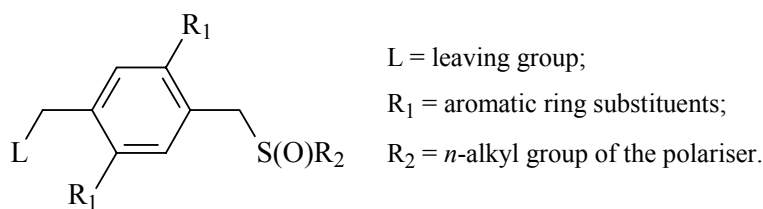
Figure 2.22: general structure of the monomers used

With chlorine as leaving group the polymerisation in methanol only takes place if electron donor substituents are present (entries 1-3). Replacement of the chlorine by an iodine leaving group makes polymerisation of unsubstituted monomer possible in methanol (entry 4).

In MMF, another protic, polar solvent, polymerisation occurs except in the presence of electron acceptors (entries 5-7). In both solvents a rather low yield and a monomodal molecular weight distribution is obtained.

In protic, more apolar solvents like *s*-butanol, polymerisation always takes place with a high yield and a monomodal molecular weight distribution (entries 8-10). Electron acceptors however also seem to reduce polymer yield.

Table 2.11: Overview of the polymer yield, molecular weight and molecular weight distribution of different precursors obtained via the Sulfinyl route in various solvents

Entry	Solvent	L	R_2	R_1	Yield (%)	M_w (g/mol)	PD
1	MeOH	Cl	*n*-Bu	OMe	40	88 000	1.7 (m)
2	MeOH	Cl	*n*–Bu	H	0	-	-
3	MeOH	Br	*n*–Oct	Cl	0	-	-
4	MeOH	I	*n*–Bu	H	25	74 000	1.7 (m)
5	MMF	Cl	*n*–Bu	Me	25	620 000	2.9 (m)
6	MMF	Cl	*n*–Bu	H	25	803 000	2.7 (m)
7	MMF	Br	*n*–Oct	Cl	0	-	-
8	*s*-BuOH	Cl	*n*–Bu	Me	90	773 000	2.6 (m)
9	*s*-BuOH	Cl	*n*–Bu	H	87	540 000	2.5 (m)
10	*s*-BuOH	Br	*n*–Oct	Cl	65	678 000	3.3 (m)
11	THF	Cl	*n*–Oct	Me	65	989 000	3.4 (m)
12	THF	Cl	*n*–Oct	H	80	735 000	3.9 (b)
13	THF	Br	*n*–Oct	Cl	50	121 000	6.2 (b)
14	NMP	Cl	*n*–Bu	Me	55	192 000	1.9 (m)
15	NMP	Cl	*n*–Bu	H	45	28 000	5.3 (b)
16	NMP	Br	*n*–Oct	Cl	35	26 000	3.4 (b)

(m) points at a monomodal and (b) at a bimodal molecular weight distribution

In aprotic, apolar solvents like THF polymerisation also occurs (entries 11-13) but a monomodal molecular weight distribution is only observed in the presence of electron donor substituents. The case of unsubstituted monomers is somewhat dubious. The SEC peak seems to contain a shoulder on the low

molecular weight side of the chromatogram. However, this could also be an artefact, because the molecular weight of the shoulder seems rather high compared to other oligomer peaks. The use of electron acceptor substituted monomers results in a bimodal molecular weight distribution, which complicates comparison of polymer yields.

In aprotic, more polar solvents like NMP similar trends are observed. A monomodal molecular weight distribution is only observed if electron donor substituents are used (entry 14), while unsubstituted and electron withdrawing substituted monomers result in bimodal molecular weight distribution (entries 15-16).

Research has proven the polymerisation reaction to be a complicated process in which the different steps are highly linked. However, the combination and comparison of all the presented experimental results – using various solvents and distinct aromatic ring substituents – allows deduction of the following interesting points.
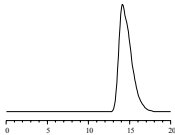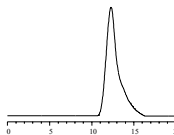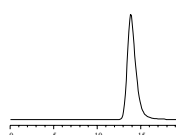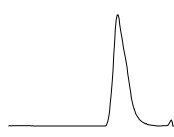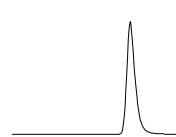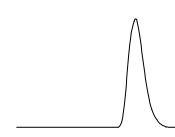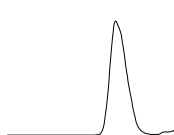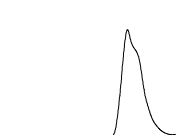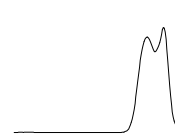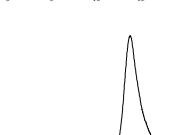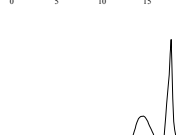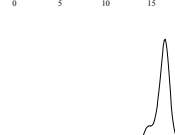
The absence of polymerisation in case of unsubstituted and electron acceptor substituted monomers in methanol (entry 2-3) and electron acceptor substituted monomers in MMF (entry 7) can be ascribed to the inability of quinoid formation as was already demonstrated by UV-vis spectroscopy for unsubstituted monomers in methanol[8]. However, if the chlorine group is replaced by an iodine functionality (entry 4), polymerisation in methanol occurs even without electron donors. This is a strong indication that in alcohols the expulsion of the leaving group is involved in the rate limiting step of the reaction - the p-quinodimethane formation.

However, not only the leaving group but also the substituents and type of solvent play a major role in the rate-limiting step. Electron donor substituents seem to enhance the rate of formation of the p-quinodimethane system probably because they facilitate the expulsion of the leaving group (e.g. entry 1).

The feature of a bimodal molecular weight distribution for standard polymerisation in NMP is found to extend to a larger domain: polymerisation reactions of unsubstituted and electron acceptor substituted monomers in aprotic solvents all yield a bimodal molecular weight distribution. Table 2.12 presents an

overview of the influence of the solvent and substituents on the molecular weight distribution found in SEC analysis.

Table 2.12: Overview of the influence of the solvent and substituents on the formation and molecular weight distribution of precursor polymers

Solvent	Electron Donors (Me)	No Substituents	Electron Acceptors (Cl)
MeOH protic polar	[chromatogram] [a]	no polymer formed	no polymer formed
MMF protic polar	[chromatogram]	[chromatogram]	no polymer formed
s-BuOH protic apolar	[chromatogram]	[chromatogram]	[chromatogram]
THF aprotic apolar	[chromatogram]	[chromatogram]	[chromatogram]
NMP aprotic polar	[chromatogram]	[chromatogram]	[chromatogram]

X-axes are given in minutes; [a]: electron donors are OMe functionalities

Note: The solvents with a dielectricity constant lower than 20 are – although this is unusual - called apolar, to emphasise the difference with the other more polar solvents used in the investigation.

High molecular weight polymers of unsubstituted PPV precursors are formed via a radical polymerisation as is demonstrated by addition of the radical scavenger TEMPO to the reaction mixture. Addition of 0.5 equivalents of

TEMPO to the reaction mixture in MMF totally inhibits the polymerisation reaction. Similar results are even obtained in *s*-butanol, a solvent in which normally high polymer yields are obtained (entry 8-10)[8]. On the other hand, addition of TEMPO to the reaction mixture in NMP, where normally a bimodal molecular weight distribution is observed, results in a monomodal distribution at the same elution time as the low molecular weight fraction of the standard bimodal distribution. TEMPO only inhibits the formation of the high molecular weight polymer.

2.10 CONCLUSIONS

2.10.1 The polymerisation mechanism in DAS

Polymerisations in DAS present new features and complications – premature basic elimination, emulsion formation, irreproducibility, and bimodal molecular weight distribution - and therefore require some adjustments of the general polymerisation procedure. These adjustments are made based on the results of a sequence of experiments on the two most common Sulfinyl monomers: **8a** and **8b**, and made a mechanistic study in DAS possible.

Several experiments are set up to reveal the nature of the polymerisation mechanism of *p*-quinodimethane based polymerisations – which is still under discussion. UV-vis and NMR experiments provide proof that the Sulfinyl route indeed belongs to this class of polymerisations, as does the well-known Wessling-Zimmerman route. The presence of radicals during polymerisation is demonstrated by ESR measurements – supporting the idea of a radical polymerisation mechanism. This idea is more founded and specified by addition reactions in NMP, which on top provide an explanation for the awkward bimodal molecular weight distribution. Addition of a radical inhibitor shows that high molecular weight polymer is formed via a radical mechanism. Furthermore, the results of a water addition experiment point to the presence of an anionic polymerisation mechanism - responsible for the formation of an oligomer fraction.

This idea of an occurrence of two types of mechanism (radical and anionic) is conform to the conclusions drawn from experiments where variations of initial monomer and base concentrations, sequence of addition and temperature demonstrate a competition between the formation of an oligomer and a polymer fraction. The observation that oligomer formation is favoured at low temperature is in agreement with the supposition of an anionic mechanism *as well as* the dimerisation initiation proposal of the radical mechanism. By decreasing temperature quinodimethane formation is slowed down and consequently the speed of initiation is lowered. However, kinetically, the speed of dimerisation initiation (of the radical mechanism) depends on the quinodimethane concentration to the square ($\sim [QM]^2$), while the anionic initiation probably depends on the first power of the QM concentration ([QM]) times the concentration of a nucleophile ([Nu]). This would explain the results obtained from the temperature experiment.

The results of the experiments with variation in initial base concentration are also in agreement with the idea of two competing mechanisms. Similar kinetic conclusions as for the temperature experiment can be drawn. The higher the momentary concentration of base the stronger the initiation of the oligomer formation competes with polymer initiation resulting in a higher relative amount of oligomer formed, and a lower polymer molecular weight. At a low momentary initial base concentration the radical polymerisation mechanism consumes the present quinodimethane more rapidly than the anionic initiation, thus yielding a large relative amount of high molecular weight polymer at the cost of oligomer formation. On the contrary, a higher initial base concentration is in favour of anionic initiation and results in a rise in relative amount of oligomer together with a decrease in the molecular weight and the amount of polymer.

According to ^{1}H-NMR analyses both polymer and oligomer fractions possess a similar structure. However, a more detailed ^{13}C-NMR study of the OM fraction revealed the presence of end groups and results in proposals for its structure and for the anionic polymerisation mechanism.

All these results combined with the outcome of the experiment where polymerisation is monitored in time lead to the conclusion that two different mechanisms – a radical as well as an anionic - can occur simultaneously in this

type of *p*-quinodimethane based polymerisations, mostly dependent on the solvent. These polymerisations have proven to be rather complex, hence it was and is not our objective to claim a complete knowledge of the processes occurring. However, the obtained results do permit to put forward a proposal for the two possible polymerisation mechanisms and allow a more profound understanding of the reaction processes.

2.10.2 Extension to other monomers and solvents

A compilation of a large amount of data gathered over the years helped to extend the insights on the Sulfinyl route - obtained in the mechanistic study in DAS - to other monomers and solvents. New knowledge on the mechanism is gained by studying the polymerisation reaction in various solvents and by evaluating the influence of both electron donor and withdrawing substituents. A strong indication is presented that in alcohols the expulsion of the leaving group is involved in the rate-limiting step of the reaction, the formation of the *p*-quinodimethane intermediate. However, not only the leaving group but also the substituents and type of solvent play an important role in the rate-limiting step. Electron donor substituents seem to enhance the rate of formation of the *p*-quinodimethane system - probably because they facilitate the expulsion of the leaving group in the transition or intermediate state.

Protic solvents like MMF and alcohols suppress the anionic mechanism resulting in a monomodal molecular weight distribution independent of the type of substituent. In aprotic, apolar solvents like THF the anionic mechanism - hence the bimodal molecular weight distribution - is observed in the absence of electron donors. It only becomes the main mechanism in the presence of electron acceptors, but yields even in a solvent well suited for this kind of polymerisation only a low molecular weight material (M_w < 10 000 g/mol) – an oligomer. In aprotic, polar solvents like NMP, the anionic mechanism can only be suppressed if electron donors or water are present.

A general conclusion is that the competition between the anionic and radical mechanism is found to depend strongly on the reaction conditions, more specific on the solvent and monomer substituents. The anionic mechanism – always yielding oligomers - is not observed in protic solvents and is promoted by electron withdrawing substituents. Hence a bimodal molecular weight distribution is observed only for the polymerisation of unsubstituted and electron acceptor substituted monomers in aprotic solvents. On the other hand do electron donor substituents suppress the anionic polymerisation in each type of solvent. In our opinion the main polymerisation mechanism of the Sulfinyl route and hence also for other *p*-quinodimethane based polymerisation routes is radical of nature leading to a high(er) molecular weight polymer.

2.11 EXPERIMENTAL SECTION

General Remarks and Instrumentation

Melting points were determined on an Electrothermal 9100 and are uncorrected. The centrifuge experiment was executed on a Heraeus-Christ Labofuge II at 3 000 rotations / minute. ^{1}H-NMR spectra were obtained in $CDCl_3$ (unless stated otherwise) at 400 MHz on a Varian Inova spectrometer using a 5 mm probe. Chemical shifts (δ) are expressed in ppm relative to the $CHCl_3$ absorption (7.24 ppm). All spectra were recorded at room temperature. The ^{13}C-NMR experiments are recorded at 100 MHz on the same spectrometer. Chemical shifts are determined relative to the ^{13}C resonance shift of $CHCl_3$ (77.0 ppm). Fourier transform Infra Red Spectroscopy was performed on a Perkin Elmer 1600 FT-IR (nominal resolution 2 cm^{-1}, summation of 16 scans). Direct Insert Probe Mass Spectrometry (DIP-MS) analyses were carried out on a Finnigan TSQ 70, electron impact mode, mass range 35-550 and an interscan time of 2 s. The electron energy was 70 eV. Molecular weights and molecular weight distributions were determined relative to polystyrene standards (Polymer Labs) by Size Exclusion Chromatography (SEC). Chromatograms were recorded on a Spectra series P100 (Spectra Physics) equipped with two MIXED-B columns (10

μm, 2 x 30 cm, Polymer Labs) and a refractive index (RI) detector (Shodex) at 70 °C. A DMF solution of oxalic acid (1 mM) is used as the eluent at a flow rate of 1.0 ml/min. Toluene is used as flow rate marker.

Water determination by ^{1}H-NMR

To determine the amount of water on the bissulfonium salt, a blank D_2O sample (750 μL) was recorded quantitatively using a delay time of 60 s and the water signal was integrated (A). Using the same conditions, a product sample (15 mg) was recorded and again the water signal was integrated (B). Subtraction of A from B gave the integration (C) corresponding to the amount of water on the product. Correlation of C to another known proton signal of the product (e.g. aromatic H) leads to a formula of the type: product.xH_2O.

UV-vis measurements

UV-vis measurements were performed on a Varian Cary Scan 500 spectrophotometer. To allow continuous stirring for efficient mixing of the reagents, a magnetic stirrer is placed inside the quartz cell of the spectrometer. Solutions: 14.2 mg of monomer **8a** in 10 mL of solvent (= 4.7 mM) and 40 mg of NatBuO in 10 mL of solvent (= 42 mM). Backgrounds are recorded after addition of 100 μL base solution to 4 mL pure solvent (base concentration $\approx 1\text{x}10^{-3}$ mM). Measurements start when 100 μL of monomer solution is added (monomer concentration $\approx 1\text{x}10^{-4}$ mM). The scan range was set from 260 to 400 nm and a scan is taken every 0.1 seconds.

ESR measurements

ESR measurements were executed by Tonny Bosman at the Technical University of Eindhoven, in co-operation with professor Jansen. The ESR spectrometer (Bruker ER 200 D SRC X-band) was equipped with an ER 4111 variable temperature unit, and spectra were recorded at 300K using a flat cell, after purging the sample solution with Helium. The spin trap DMPO was purchased from Aldrich Chemical Co., Inc. Spectra were recorded starting from solutions containing 1 mL monomer solution (0.6 mmol in 3 mL), 1 mL NatBuO solution (1.1 eq, 1.1 mmol, 0.1056 g in 5 mL), and one drop of DMPO, in order

to have a global monomer concentration of about 0.1 M in the recorded sample. G-values were calculated using the formula: $h \times \nu = \mu_B \times B \times g$, where $h = 6.63 \times 10^{-34}$ J.s , $\mu_B = 9.3 \times 10^{-28}$ J.G^{-1}, $\nu = 9.4$ GHz and B is obtained from the mean value of the two main doublet signals, expressed in kG.

Materials
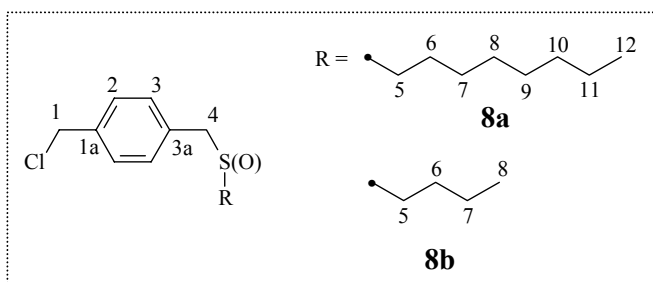
Figure 2.23: Atomic numbering of sulfinyl monomers

Monomer syntheses

1-(Chloromethyl)-4-[(n-octylsulfinyl)methyl]benzene (via route A) (8a)

At ambient temperature a solution of *n*-octane thiol (0.248 mol, 36.2 g) in toluene (300 mL) is added dropwise over a time period of 24 hours to a stirred mixture of 1,4-di(chloromethyl)benzene (0.57 mol, 100 g) in toluene (1000 mL), aqueous sodium hydroxide (1.5 mol in 1000 mL H_2O) and phase transfer catalyst trioctyl methyl ammonium chloride, Aliquat 336, (6 mmol, 2.5g). The organic layer is separated, washed with water (3 x 500 mL), dried over magnesium sulfate and concentrated *in vacuo*.

To a solution of the resulting mixture and tellurium dioxide (0.03 mol, 4.6 g) in methanol (1200 mL), an aqueous (35 wt%) solution of hydrogen peroxide (0.57 mol) is added dropwise. After 6 hours the reaction is quenched by addition of a saturated aqueous sodium chloride solution (800 mL). After extraction with chloroform (3 x 400 mL), the combined organic layers are dried over magnesium sulfate and concentrated *in vacuo*. The reaction mixture is purified by means of column chromatography (eluent chloroform, $R_f = 0.20$) and subsequent crystallisation from dichloromethane / hexane. The monomer was obtained as a white solid at a yield of 32% compared to the amount of 1,4-

di(chloromethyl)benzene used. Mp: 109.5-110.5°C. ^{1}H NMR (CDCl$_3$, 400 MHz): δ 0.84 (t, J = 6.8 Hz, 3H, H12), 1.23 (m, 8H, H8-11), 1.36 (m, 2H, H7), 1.70 (m, 2H, H6), 2.55 (t, J = 7.8 Hz, 3H, H5), 3.91 + 3.93 (dd, J$_{AB}$ = 13.0 Hz, 2H, H4), 4.56 (s, 2H, H1), 7.28 (d, J = 8.0 Hz, 2H, H3), 7.39 (d, J = 8.0 Hz, 2H, H2) ppm. IR (KBr): 2959, 2916, 2846, 1443, 1070, 847 cm^{-1}. MS (EI, m/z, rel. int. (%)): 300 ([M]$^+$, 3), 265 ([C$_{16}$H$_{25}$OS]$^+$, 80), 139 ([C$_8$H$_8$Cl]$^+$, 100), 104 ([C$_8$H$_8$]$^+$, 46), 77 ([C$_6$H$_5$]$^+$, 3).

1,4-Bis(tetrahydrothiofeniomethyl)xylene dichloride (6)

A solution of 1,4-di(chloromethyl)benzene (0.29 mol, 50g) and tetrahydrothiofene (THT, 1.15 mol, 101 mL) in methanol (110 mL) is stirred for 60 hours at ambient temperature. The reaction mixture is precipitated in acetone (420 mL) at −10°C. The precipitate is recovered by filtration and washed with cold acetone (600 mL). After evaporation of the solvent a white hygroscopic solid could be collected (92.5 g, 92%). Water determination by ^{1}H-NMR revealed the formula: product.6H$_2$O (92.5 g, 0.20 mol, 70%). ^{1}H NMR (D$_2$O, 400 MHz): δ 2.12-2.30 (m, 8H, SCH$_2$C$\underline{H}_2$), 3.31-3.50 (m, 8H, SC$\underline{H}_2$), 4.48 (s, 4H, ArC$\underline{H}_2$S), 7.53 (s, 4H, ArH) ppm.

1-(Chloromethyl)-4-[(n-butylsulfinyl)methyl]benzene (via route B) (8b)

A mixture of Na*t*BuO (19.3 g, 0.20 mol) and *n*-butane thiol (0.20 mol, 18 g) in MeOH (700 mL) is stirred for 30 minutes at ambient temperature. The clear solution is added in one portion to a stirred solution of 1,4-bis(tetrahydrothiofeniomethyl)xylene dichloride (0.20 mol, 92.5 g) in methanol (1750 mL) at 25°C. After one hour the reaction mixture was neutralised with aqueous hydrogen chloride (1 M), and concentrated *in vacuo*. The crude product is diluted with chloroform (mL) and the precipitate was filtered off. The filtrate is concentrated in vacuo. The obtained oil is diluted with petroleum ether (boiling range 100-130°C, mL) and concentrated to remove tetrahydrathiofene by means of an azeotropic destillation. This sequence is repeated three times.

To a solution of the resulting mixture (63.4 g) and tellurium dioxide (0.024 mol, 3.7 g) in methanol (1600 mL), an aqueous (35 wt%) solution of hydrogen peroxide (0.46 mol) is added dropwise. After 6 hours the reaction is quenched by

addition of a saturated aqueous sodium chloride solution (980 mL). After extraction with chloroform (3 x 500 mL), the combined organic layers are dried over magnesium sulfate and concentrated *in vacuo*. The reaction mixture is purified by means of column chromatography (eluent chloroform, $R_f = 0.17$) and subsequent crystallisation from dichloromethane / hexane. The monomer is obtained as a white solid at a yield of 65% compared to the amount of 1,4-di(chloromethyl)benzene used. Mp: 111-112°C. ^{1}H NMR (CDCl$_3$, 400 MHz): δ 0.90 (t, J = 7.2 Hz, 3H, H8), 1.41 (m, 2H, H7), 1.72 (m, 2H, H6), 2.54 (t, J = 8.0 Hz, 2H, H5), 3.93 + 3.95 (dd, J_{AB} = 13.2 Hz, 2H, H4), 4.56 (s, 2H, H1), 7.27 (d, J = 8.0 Hz, 2H, H3), 7.38 (d, J = 8.0 Hz, 2H, H2) ppm. ^{13}C NMR (CDCl$_3$, 100 MHz) : δ 13.1 (C8), 21.3 (C7), 23.8 (C6), 45.1 (C1), 50.2 (C5), 56.9 (C4), 128.4 (C2), 129.8 (C3), 129.9 (C3a), 136.8 (C1a) ppm. IR (KBr): 2957, 2922, 2859, 1020, 849 cm^{-1}. MS (EI, m/z, rel. int. (%)): 244 ([M]$^+$, 2), 209 ([C$_{12}$H$_{17}$OS]$^+$, 3), 139 ([C$_8$H$_8$Cl]$^+$, 100), 104 ([C$_8$H$_8$]$^+$, 16), 77 ([C$_6$H$_5$]$^+$, 5).

Drying procedure of NMP

To remove the water from the p.a. NMP an azeotropic distillation with toluene, followed by a fractionated vacuum distillation is necessary. The azeotropic distillation is performed after addition of 50 mL toluene to 500 mL NMP. This is repeated two times. In the fractionated vacuum distillation dry NMP is collected at a temperature of about 76°C. ^{1}H NMR (CDCl$_3$, 400 MHz): δ 1.99 (m, 2H, NCH$_2$C$\underline{H}_2$), 2.33 (t, J_{AB} = 8.0 Hz, 2H, C$\underline{H}_2$C(O)N), 2.80 (s, 3H, NC$\underline{H}_3$), 3.34 (t, J_{AB} = 7.2 Hz, 2H, NC$\underline{H}_2$CH$_2$) ppm. ^{13}C NMR (CDCl$_3$, 100 MHz): δ 16.1 (NCH$_2$$\underline{C}H_2$), 29.0 ($\underline{C}H_2$CO), 27.7 (N$\underline{C}H_3$), 47.6 (N$\underline{C}H_2CH_2$), 172.9 ($\underline{C}$O) ppm.

Polymerisation in NMP

Poly{[1,4-phenylene]-[1-(n-octylsulfinyl)ethylene]} - primary experiments

A freshly prepared Na*t*BuO-solution (2.2 mmol, 0.211 g in 6 mL NMP = 0.37 M) is added in one portion to a solution of **8a** (2 mmol, 0.60g in 14 mL NMP = 0.14 M) after degassing for 1 hour by passing through a continuous stream of nitrogen. After one hour reaction under nitrogen atmosphere the mixture is poured in ice water (200 mL) and neutralised with aqueous hydrogen

chloride (1 M). Sodium chloride (p.a.) is added to make extraction with chloroform (3 x 200 mL) possible. The combined organic layers are concentrated *in vacuo* and washed with water (3 x 100 mL). After another concentration *in vacuo* of the organic layer, some chloroform is added and the crude product is precipitated in a solvent mixture hexane / diethyl ether 1/1, collected and dried *in vacuo*. The residual fraction is concentrated *in vacuo*. ^{1}H NMR (CDCl$_3$, 400 MHz, two pair of signals overlapping): δ 0.75-0.88 (3H, br, CH$_2$C$\underline{H}_3$), 1.1-1.45 (10H, br, C$\underline{H}_2$C$\underline{H}_2$C$\underline{H}_2$C$\underline{H}_2$C$\underline{H}_2$CH$_3$), 1.5-1.75 + 1.75-2.1 (2H, br, S(O)CH$_2$C$\underline{H}_2$), 1.9-2.1 + 2.1-2.4 + 2.4-2.6 (2H, br, S(O)C$\underline{H}_2$CH$_2$), 3.8-4.0 (1H, br, φC$\underline{H}$S(O)R), 3.1-3.3 + 3.4-3.8 (2H, br, φC$\underline{H}_2$CHS(O)R), 6.76-7.0 + 7.0-7.3 (4H, br, arom. H) ppm.

Poly{[1,4-phenylene]-[1-(n-octylsulfinyl)ethylene]} - adjusted procedure

A freshly prepared NatBuO-solution (2.2 mmol, 0.211 g in 10 mL NMP = 0.22 M) is added in one portion to a solution of **8a** (2 mmol, 0.601g in 10 mL NMP = 0.2 M) after degassing for 1 hour by passing through a continuous stream of nitrogen. After one hour reaction under nitrogen atmosphere the mixture is poured in vigorously stirred ice water (200 mL) and acidified to a pH-value of 5 with aqueous hydrogen chloride (1 M). The precipitate is recovered by filtration using a glass filter, collected and dried *in vacuo*. The precipitate is then redissolved in chloroform, and concentrated *in vacuo* until approximately 5 mL solution is left. Afterwards this solution is precipitated in 50 mL of the cooled solvent mixture hexane / diethyl ether 1/1, collected and dried *in vacuo*. The residual fraction is concentrated *in vacuo*. Characterisation is identical to that of the primary experiments.

Poly{[1,4-phenylene]-[1-(n-butylsulfinyl)ethylene]} - standard procedure

A freshly prepared NatBuO-solution (2.2 mmol, 0.211 g, in 10 mL NMP = 0.22 M) is added in one portion to a solution of **8b** (2 mmol, 0.489 g in 10 mL NMP = 0.2 M) after degassing for 1 hour by passing through a continuous stream of nitrogen. After one hour reaction under nitrogen atmosphere the mixture is poured in ice water (200 mL) and neutralised with aqueous hydrogen chloride (1 M). After some time for coagulation the precipitate is recovered by filtration over

a P3 glass filter and washed with cold water. The precipitate is dissolved in chloroform, precipitated in pure diethyl ether, collected and dried *in vacuo*. The residual fraction is concentrated *in vacuo*. ^{1}H NMR (CDCl$_3$, 400 MHz, two pair of signals overlapping): δ 0.75-0.85 + 0.85-0.95 (3H, br, CH$_2$C$\underline{H}_3$), 1.16-1.34 + 1.34-1.52 (2H, br, C$\underline{H}_2$CH$_3$), 1.54-1.64 + 1.64-1.8 (2H, br, S(O)CH$_2$C$\underline{H}_2$), 1.9-2.1 + 2.1-2.4 + 2.46-2.6 (2H, br, S(O)C$\underline{H}_2$CH$_2$), 3.8-4.0 (1H, br, φC$\underline{H}$S(O)R), 2.96-3.3 + 3.4-3.8 (2H, br, φC$\underline{H}_2$CHS(O)R), 6.7-7.0 + 7.0-7.35 (4H, br, arom. H) ppm.

Following polymerisation by NMR

^{1}H-NMR spectra are acquired at 300 MHz on a Varian Inova spectrometer using a 5 mm probe. The instrument is shimmed with an 800 μL monomer **8a** (0.32 mg) solution (≈ 1 mM). After addition of an undefined amount (a tip of the spatula ≈ 1 mg) base, mixing and injecting the nmr tube back in the instrument, spectra are recorded respecting an acquisition time of 1 second between scans. One spectrum is build out of a summation of 32 scans. Chemical shifts (δ) are expressed in ppm relative to the characteristic solvent signals (d-THF: 3.57 and 1.71 ppm; d-DMSO: 2.50 and water signal in d-DMSO: 3.35). Na*t*BuO signals are positioned at 1.13 and 3.21 ppm. All spectra are recorded at room temperature.

Estimations for *p*-QM chemical shift values:

$$\delta_H = 5.28 + z_{gem} + z_{cis} + z_{trans}\ ^{[12]}$$

H_w = 5.28 + 0 + 0.08 - 0.01 = 5.35 ppm; gem: H; cis: C=C conj; trans: C=C conj / H_x = H_y = 5.28 + 0.98 + 0 - 0.21 = 6.02 ppm; gem: C=C solo; cis: H; trans: C=C solo / H_z = 5.28 + 1.00 + 0.08 – 0.01 = 6.35 ppm; gem: SR; cis: C=C conj; trans: C=C conj / H_z = 5.28 + 1.58 + 0.08 – 0.01 = 6.93 ppm; gem: SO$_2$; cis: C=C conj; trans: C=C conj

$$\delta_H = 5.25 + z_{gem} + z_{cis} + z_{trans}\ ^{[13]}$$

H_w = 5.25 + 0 + 0.02 + 0.05 = 5.22 ppm; gem: H; cis: C=C conj; trans: C=C conj / H_x = H_y = 5.25 + 1.00 + 0 - 0.23 = 6.02 ppm; gem: C=C solo; cis: H; trans: C=C solo / H_z = 5.25 + 1.27 + 0.02 – 0.05 = 6.49 ppm; gem: H; cis: C=C conj; trans: C=C conj

in d-THF:

^{1}H NMR (monomer **8a**, d-THF, 300 MHz): δ 0.87 (t, J = 6.5 Hz, 3H, H12), 1.13 (m, 8H, H8-11), 1.28 (m, 2H, H7), 1.60-1.80 (m, 2H, H6), 2.48 (t, J = 7.8 Hz, 3H, H5), 3.80-3.96 (dd, J_{AB} = 13.0 Hz, 2H, H4), 4.62 (s, 2H, H1), 7.30 (d, J = 8.1 Hz, 2H, H3), 7.37 (d, J = 8.1 Hz, 2H, H2) ppm. ^{1}H NMR (polymer, d-THF, 300 MHz): δ 0.80-0.95 (3H, br, CH₂CH₃), 0.95-1.40 (10H, br, CH₂CH₂CH₂CH₂-CH₂CH₃), 1.6-1.7 (2H, br, S(O)CH₂CH₂), 2.3-2.6 (2H, br, S(O)CH₂CH₂), 3.4-3.7 (1H, br, φCHS(O)R), 3.1-3.3 (2H, br, φCH₂CHS(O)R), 6.8-7.1 (4H, br, arom. H) ppm.

in d-DMSO:

^{1}H NMR (monomer **8a**, d-DMSO, 300 MHz): δ 0.85 (t, J = 6.6 Hz, 3H, H12), 1.24 (m, 8H, H8-11), 1.34 (m, 2H, H7), 1.62 (m, 2H, H6), 2.59 (t, J = 7.8 Hz, 3H, H5), 3.91-4.15 (dd, J_{AB} = 12.9 Hz, 2H, H4), 4.77 (s, 2H, H1), 7.31 (d, J = 7.2 Hz, 2H, H3), 7.43 (d, J = 7.2 Hz, 2H, H2) ppm. ^{1}H NMR (polymer, d-DMSO, 300 MHz): δ 0.85 (3H, br, CH₂CH₃), 1.11 (2H, br, CH₂CH₃), 1.24 (10H, br, CH₂CH₂CH₂CH₂CH₂CH₃), 1.59 (2H, br, S(O)CH₂CH₂), 2.99 (2H, br, S(O)CH₂CH₂), 3.95 (1H, br, φCHS(O)R), 3.95 + 3.4 (2H, br, φCH₂CHS(O)R), 7.10-7.25 (4H, br, arom. H) ppm.

Influence of additives

Poly{[1,4-phenylene]-[1-(n-butylsulfinyl)ethylene]} - standard reaction (1)

A freshly prepared Na*t*BuO-solution (2.2 mmol, 0.211 g, in 6 mL NMP = 0.37 M) is added in one portion to a solution of **8b** (2 mmol, 0.489 g in 14 mL NMP = 0.14 M) after degassing for 1 hour by passing through a continuous stream of nitrogen. After one hour reaction under nitrogen atmosphere the mixture is poured in ice water (200 mL) and neutralised with aqueous hydrogen chloride (1 M). Further work up is similar to the standard procedure described earlier, as is polymer characterisation.

Addition of TEMPO (1)

A freshly prepared Na*t*BuO-solution (2.2 mmol, 0.211 g, in 6 mL NMP) is added in one portion to a 14 mL NMP solution of **8b** (2 mmol, 0.489 g) and 0.5 equivalents TEMPO (1 mmol, 0.156 g) after degassing for 1 hour by passing

through a continuous stream of nitrogen. After one hour reaction under nitrogen atmosphere the mixture is poured in ice water (200 mL) and neutralised with aqueous hydrogen chloride (1 M). Further work up is similar to the standard procedure described earlier. ^{1}H NMR (CDCl$_3$, 400 MHz): δ 0.83-0.93 (3H, br, CH$_2$C$\underline{H}_3$), 1.28-1.48 (2H, br, C$\underline{H}_2$CH$_3$), 1.6-1.76 (2H, br, S(O)CH$_2$C$\underline{H}_2$), 2.45-2.6 (2H, br, S(O)C$\underline{H}_2$CH$_2$), 3.8-3.95 (1H, br, φC$\underline{H}$S(O)R), 3.0-3.2 + 3.8-3.95 (2H, br, φC$\underline{H}_2$CHS(O)R), 7.06-7.2 + 7.24-7.32 (4H, br, arom. H) ppm.
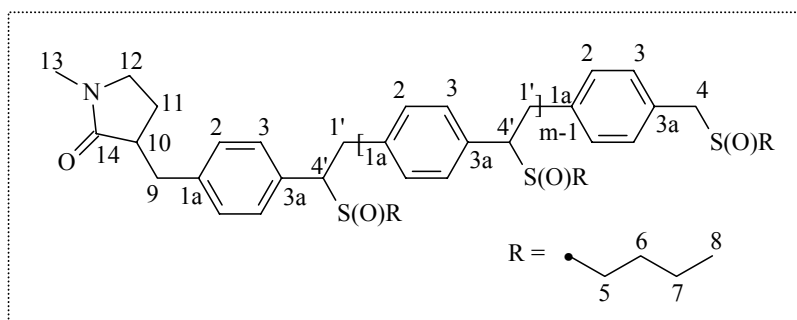
Figure 2.24: Atomic numbering of a possible oligomer

^{13}C NMR (CDCl$_3$, 100 MHz) : δ 13.6 (C8), 21.9 (C7), 24.5 (C6), 36.0 (C1'), 49.3 (C5'), 50.6 (C5, end sulfoxide), 57.7 (C4 end sulfoxide), 65.3 + 69.8 (C4'), 129.3 + 129.7 (C2 + C3), 131.7 (C3a), 137.9 (C1a), 30.6 (C9), 29.5 (C10), 17.5 (C11), 49.3 (C12), 27.9 (C13), 174.9 (C14) ppm.

Addition of water (1)

A freshly prepared Na*t*BuO-solution (2.2 mmol, 0.211 g, in 6 mL NMP) is added in one portion to a mixture of **8b** (2 mmol, 0.489 g in 14 mL NMP) and 5 vol% water (1 mL) after degassing for 1 hour by passing through a continuous stream of nitrogen. After one hour reaction under nitrogen atmosphere the mixture is poured in ice water (200 mL) and neutralised with aqueous hydrogen chloride (1 M). Further work up is similar to the standard procedure described earlier. ^{1}H NMR (CDCl$_3$, 400 MHz): δ 0.74-0.84 (3H, br, CH$_2$C$\underline{H}_3$), 1.16-1.38 (2H, br, C$\underline{H}_2$CH$_3$), 1.4-1.54 + 1.54-1.68 (2H, br, S(O)CH$_2$C$\underline{H}_2$), 2.1-2.4 + 1.9-2.1

(2H, br, S(O)C$\underline{H}_2$CH$_2$), 3.4-3.8 (1H, br, ϕC$\underline{H}$S(O)R), 3.4-3.8 + 2.94-3.3 (2H, br, ϕC$\underline{H}_2$CHS(O)R), 6.74-7.0 + 7.0-7.2 (4H, br, arom. H) ppm.

Poly{[4,4'-biphenylene]-[1-(n-butylsulfinyl)ethylene] } - standard reaction (2)

A freshly prepared Na*t*BuO-solution (1.3 mmol in 3 mL NMP) is added in one portion to a solution of chloromethyl-4'-(*n*-butylsulfinyl)methylbiphenyl (1 mmol in 7 mL NMP) after degassing for 1 hour by passing through a continuous stream of nitrogen. After one hour reaction at 35°C under nitrogen atmosphere the mixture is poured in ice water (100 mL) and neutralised with aqueous hydrogen chloride (1 M). The precipitate is recovered by filtration over a P3 glass filter and washed with cold water, dissolved in chloroform, precipitated in a mixture diethyl ether / THF 9/1, collected and dried *in vacuo*. The residual fraction is concentrated *in vacuo*. Characterisation is described elsewhere[7].

Addition of TEMPO (2)

Procedure similar to standard reaction (2), but this time 0.5 equivalents TEMPO is added to the monomer solution. Characterisation is described elsewhere[7].

Addition of water (2)

Procedure similar to standard reaction (2), but this time 0.5 mL of water is added to the monomer solution at 40°C. Characterisation is described elsewhere[7].

Poly{[1,4-phenylene]-[1-(n-octylsulfinyl)ethylene] } - 14 / 8 ratio

A polymerisation procedure similar to that described under the heading 'poly{[1,4-phenylene]-[1-(*n*-octylsulfinyl)ethylene]} - adjusted procedure' is used, only this time the concentration of the base and the monomer solutions are adjusted as follows: a freshly prepared Na*t*BuO-solution (2.2 mmol, 0.211 g in 8 mL NMP = 0.28 M) is added in one portion to a solution of **8a** (2 mmol, 0.601g in 14 mL NMP = 0.14 M). Characterisation is identical to that of the primary experiments.

Influence of concentration and temperature
Poly{[1,4-phenylene]-[1-(n-octylsulfinyl)ethylene]} - reversed addition

This time a solution of **8b** (2 mmol, 0.489 g in 10 mL NMP = 0.2 M) is added in one portion to a freshly prepared Na*t*BuO-solution (2.2 mmol, 0.211 g, in 10 mL NMP = 0.22 M) after passing through a continuous stream of nitrogen for 1 hour. After one hour reaction under nitrogen atmosphere the mixture is poured in ice water (200 mL) and acidified with aqueous hydrogen chloride (1 M) to a pH-value of about 5. The precipitate is recovered by filtration, washed with cold water and redissolved in a few mL of chloroform. Repeated attempts to precipitate in hexane / diethyl ether 1/1 and pure diethyl ether did not lead to a purification or separation of the different fractions (OM, PM, MM). Next, precipitation is performed in pure hexane, the resulting product is dried under reduced pressure and yield is calculated based on relative peak areas in SEC chromatograms. Characterisation is identical to that of the primary experiments.

Poly{[1,4-phenylene]-[1-(n-octylsulfinyl)ethylene]} - at 0°C

Apart from the lowering of the temperature to 0°C, a polymerisation procedure identical to that described under the heading 'poly{[1,4-phenylene]-[1-(n-octylsulfinyl)ethylene]} - adjusted procedure' is applied (using a 10 / 10 ratio between the volume of solvent used to prepare the monomer and the base solutions, respectively). Characterisation is identical to that of the primary experiments.

Polymerisation in time

A freshly prepared Na*t*BuO-solution (6.6 mmol, 0.634 g in 30 mL NMP) is added in one portion to a solution of **8a** (6 mmol, 0.180 g in 30 mL NMP) after degassing for 1 hour by passing through a continuous stream of nitrogen. One arm of the standard polymerisation appliance is sealed with a septum, and a long needle pierces the septum during the course of the reaction to prevent incoming air by sampling. By means of a glass syringe approximately 3 mL of the reaction mixture is at definite times (see section 2.7) poured in 30 mL of vigorously stirred ice water using a mechanical stirrer. Next, the mixture (a white emulsion) is acidified to a pH-value of 5 with aqueous hydrogen chloride (1M). The

precipitate is recovered by filtration using a glass filter, collected and dried *in vacuo*. In the case of the last sample (after one hour reaction) all residual polymerisation mixture is poured in ice water (respecting a 1/10 ratio) and worked up similar to the other samples.

All SEC-samples were made using p.a. DMF and respecting a concentration between 1 and 3 mg/mL. SEC analysis took place in one day keeping columns at a constant temperature of 70°C and maintaining a 1 mL/min flow rate. Toluene is used as flow rate marker.

Extension to other monomers and solvents

The syntheses of the starting unsymmetrically substituted monomers are described elsewhere[24]. Also for the analyses of the polymer compounds it is referred to other literature[7,8,25].

General procedure for polymerisation

A solution of monomer (1 mmol) in solvent (7 mL) and a solution of NaO*t*Bu in solvent (3 mL) are flushed with nitrogen under stirring for 1 hour before mixing. After 1 hour reaction under nitrogen atmosphere the reaction mixture is poured in 100 mL water, neutralised with a 1 M hydrogen chloride solution and extracted with 2 x 100 mL CHCl$_3$. The combined organic layers are concentrated *in vacuo*; the crude product is redissolved in 10 mL chloroform and precipitated in 100 mL non-solvent. The polymer is collected and dried *in vacuo*. The standard amount of 1.3 equivalents of NaO*t*Bu was sometimes slightly reduced to prevent basic elimination of sulfinyl groups. The type of reaction solvent, precipitation solvent, amount of base and reaction temperature is given below for each of the precursor polymers. The polymer yields, molecular weights and molecular weight distributions are given in table 2.7.

Poly{[1,4-phenylene]-[1-(n-butylsulfinyl)ethylene]}.

This compound is synthesised according to the general procedure starting from **8b**. With chlorine as leaving group: reaction in MeOH: 20°C, 1.3 eq. base; in MMF: 20°C, 1 eq. base; in *s*-BuOH: 30°C, 1.3 eq. base; and in NMP: 20°C, 1.1 eq. base. With iodine as leaving group: reaction in MeOH: 20°C, 1.3 eq. base. The polymers were precipitated in ether. NMP is used as eluent for SEC except for the polymers obtained in NMP for which DMF is used.

Poly{[1,4-phenylene]-[1-(n-octylsulfinyl)ethylene]}.

This compound is synthesised according to the general procedure starting from **8a**. Reaction in THF: 30°C, 1 eq. base. The polymers are precipitated in ether / hexane 1/1.

Poly{[2,5-dimethyl-1,4-phenylene]-[1-(n-butylsulfinyl)ethylene]}.

This compound is synthesised according to the general procedure starting from the appropriate monomer. Reaction in *s*-BuOH: 20°C, 1.3 eq. base; in MMF: 20°C, 1.3 eq. base; in NMP: -10°C, 1.3 eq. base. All polymers are precipitated in ether. DMF is used as eluent for SEC.

Poly{[2,5-dimethyl-1,4-phenylene]-[1-(n-octylsulfinyl)ethylene]}

This compound is synthesised according to the general procedure starting from the appropriate monomer. Reaction in THF: 20°C, 1 eq. base. The polymer is precipitated in ether / hexane 1/1. DMF is used as eluent for SEC.

Poly{[2,5-dimethoxy-1,4-phenylene]-[1-(n-butylsulfinyl)ethylene]}

This compound is synthesised according to the general procedure starting from the appropriate monomer. Reaction in MeOH: 35°C, 1.3 eq. base. The polymer is precipitated in ether. DMF is used as eluent for SEC.

Poly{[2,5-dichloro-1,4-phenylene]-[1-(n-octylsulfinyl)ethylene]}

This compound is synthesised according to the general procedure starting from the appropriate monomer. Reaction in MMF: 20°C, 1.1 eq. base; in THF: 20°C, 1 eq. base; in NMP: 20°C, 1eq. base; in MeOH: 20°C, 1.3 eq. base; and in *s*-BuOH: 20°C, 1 eq. base. The polymers are precipitated in ether / hexane 1/1. THF is used as eluent for SEC at 40°C and maintaining a flow rate of 1mL/min.

2.12 REFERENCES

1. F. Louwet, *Ph.D. Dissertation*, 1993, Limburgs Universitair Centrum, Diepenbeek, België.

2. A. Issaris, *Ph.D. Dissertation*, 1997, Limburgs Universitair Centrum, Diepenbeek, België.

3. a) A.J.J.M. van Breemen, D.J.M. Vanderzande, P.J. Adriaensens, J.M.J.V. Gelan, *J. Org. Chem.*, **64** (1999) 3106; b) A.J.J.M. van Breemen, *Ph.D. Dissertation*, 1999, Limburgs Universitair Centrum, Diepenbeek, België.

4. a) J. Drabowicz, M. Mikolajczyk, *Synth. Comm.*, **11(12)** (1981) 1025; b) K.S. Kim, H.J. Hwang, C.S. Cheong, C.S. Hahn, *Tetrahedron Letters*, **31(20)** (1990) 2893.

5. F.R. Denton III, P.M. Lahti, F.E. Karasz, *J. Pol. Sci. A: Pol. Chem.*, **30** (1992) 2223.

6. a) B.R. Cho, M.S. Han, Y.S. Suh, K.J. Oh, S.J. Jeon, *J. Chem. Soc., Chem. Commun.*, (1993) 564; b) V. Massardier, J.C. Beziat, A. Guyot, *Eur. Polym. J.*, **31(3)** (1995) 291; c) A. Issaris, D. Vanderzande, J. Gelan, *Polymer*, **38(10)** (1997) 2571; d) B.R. Cho, Y.K. Kim, M.S. Han, *Macromolecules*, **31** (1998) 2098.

7. M. Van Der Borght, *Ph.D. Dissertation*, 1998, Limburgs Universitair Centrum, Diepenbeek, België.

8. A.J.J.M. van Breemen, A.C.J. Issaris, M.M. de Kok, M.J.A.N. Van Der Borght, P.J. Adriaensens, J.M.J.V. Gelan, D.J.M. Vanderzande, *Macromolecules*, **32** (1999) 5728.

9. D.J. Williams, J.M. Pearson, M. Levy, *J. Am. Chem. Soc.*, **92(5)** (1970) 1436.

10. W.J.Y. Cheng, N.R. Janosy, J.M.C. Nadeau, S. Rosenfeld, M. Rushing, J.P. Jasinski, V. Rotello, *J. Org. Chem.*, **63** (1998) 379.

11. a) M.W. Brandt, J.E. Mulvaney, H.K. Hall Jr., G.D. Green, *Journal of Polymer Science: part A: Polymer Chemistry*, **27** (1989) 1957; b) T. Itoh, H.K. Hall Jr., *Macromolecules*, **23** (1990) 2836.

12. NMR chemical shift tables from the course of J. Gelan, D. Vanderzande and P. Adriaensens entitled: "Organische Scheikunde en beginselen van biochemie 1 – Organische Chemie (Spectroscopie)", 2nd year
    Chemistry, Faculty of Sciences, Limburgs Universitair Centrum, Diepenbeek.

13. D.H. Williams & I. Fleming, *Spectroscopic Methods in Organic Chemistry*, 5th ed., The McGraw-Hill Companies London, 1995, p. 158.

14. a) M. Symons, *Chemical and biochemical aspects of electron-spin resonance*, Van Nostrand Reinhold Company: New York, 1978, p. 1-25; b) G.D. Christian, J.E. O'Reilly, *Instrumental analysis*, Prentice-Hall: Englewood Cliffs, 1986, p. 395-411; c) G. Moad, D.H. Solomon, *The chemistry of free radical polymerisation*, Elsevier Science Ltd, Oxford, 1995, p. 116-124

15. E.G. Janzen, Y.-K. Zhang, *J. Org. Chem.*, **60** (1995) 5441.

16. L. Hontis, M. Van Der Borght, D. Vanderzande, J. Gelan, *Polymer*, **40** (1999) 6615.

17. R.A. Wessling, *J. Polym. Sci.: Polym. Symp.*, **72** (1985) 55.

18. L.A. Errede, J.M. Hoyt, *J. Am. Chem. Soc.*, **82** (1960) 436.

19. G. Moad & D.H. Solomon, *The chemistry of free radical polymerisation*, Elsevier Science Ltd, Oxford, 1995, a.o. p. 92.

20. M. Van Der Borght, P. Adriaensens, D. Vanderzande, J. Gelan, *Polymer*, **41** (2000) 2743.

21. Personal communication with D. Van Den Berghe.

22. P. Adriaensens, M. Van Der Borght, L. Hontis, A. Issaris, A. van Breemen, M. de Kok, D. Vanderzande, J. Gelan, *Polymer*, **41** (2000) 7003.

23. a) N.C. Greenham, S.C. Moratti, D.D.C. Bradley, R.H. Friend, A.B. Holmes, *Nature*, **365** (1993) 628; b) W.R. Salaneck, J.-L. Brédas, *Adv. Mater.*, **8(1)** (1996) 48.

24. a) A. Issaris, D. Vanderzande, P. Adriaensens, J. Gelan, *Macromolecules*, **31(14)** (1998) 4426; b) A.J.J.M. van Breemen, D.J.M. Vanderzande, P.J. Adriaensens, J.M.J.V. Gelan, *J. Org. Chem.*, **64** (1999) 3106; c) M. Van Der Borght, D. Vanderzande, P. Adriaensens, J. Gelan, *J. Org. Chem.*, 65 (2000) 284.

25. a) A. Issaris, D. Vanderzande, J. Gelan, *Polymer*, **38(10)** (1997) 2571; b) A. Issaris, D. Vanderzande, P. Adriaensens, J. Gelan, *Macromolecules*, **31(14)** (1998) 4426.

3
Mechanistic Study on the Sulfinyl and the Gilch Route towards OC_1C_{10}-PPV

3.1 INTRODUCTION

The synthetic route commonly used in industry (e.g. at Covion Organic Semiconductors and Philips) to obtain poly(p-phenylene vinylenes) (PPVs) is the dehydrohalogenation or Gilch route. As discussed in section 1.5 of the general introduction, the mechanism of the second step of the polymerisation is still under discussion. However, to gain more control over the polymerisation process, it is of importance to know which processes are occurring during reaction. Recent publications on the Gilch route - involving addition of the "*acidic*" additive 4-*tert*-butylbenzyl chloride[1] and the nucleophile 4-methoxyphenol[2] - state or favour an anionic polymerisation mechanism.

The mechanistic study on the Sulfinyl route towards PPV - described in chapter 2 – led to the conclusion that apparently both radical and anionic mechanism can occur simultaneously. However, experiments with for example the radical inhibitor TEMPO indicated that even in solvents that enhance the reactivity of anions, the main pathway occurs via radicals, while the anionic mechanism merely yields oligomers[3]. On top of this, the probability of an anionic mechanism turned out to be strongly dependent on the choice of monomer – the type of ring substituents - and the solvent used.

The present mechanistic study was set up to link the Sulfinyl and the Gilch route, because in our opinion both routes proceed via similar mechanisms involving the *in situ* formation and polymerisation of p-quinodimethane (p-QM) systems. A general scheme consisting of three steps is represented in figure 3.1.

The first step - a basic 1,6-elimination - leads to the formation of intermediate *p*-QM systems. These species are the actual reactive monomers and they polymerise in a second step spontaneously to the precursor polymer. The question is if this involves an anionic or a radical mechanism. In a third step the precursor is converted into the conjugated polymer.
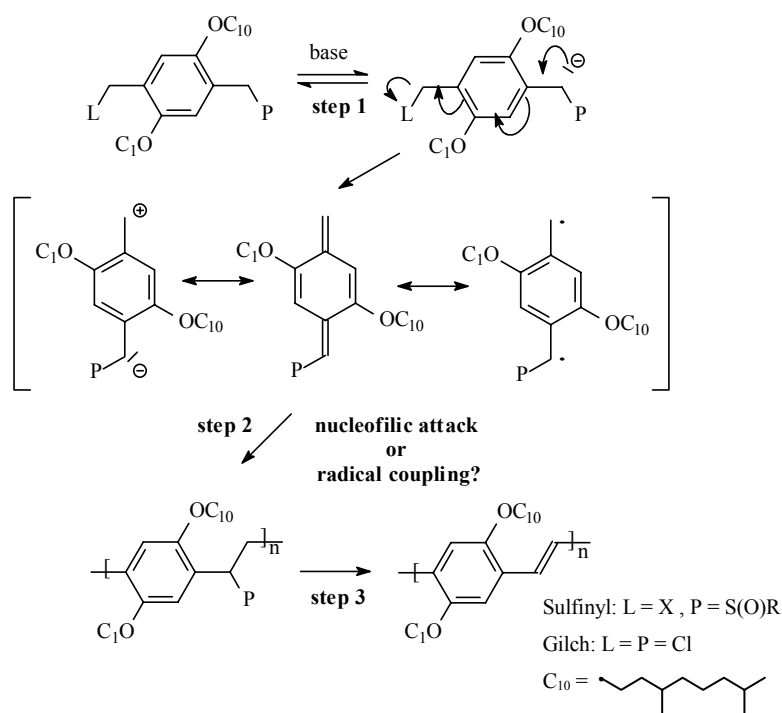
Figure 3.1: Schematic representation of the Gilch and the Sulfinyl route towards OC_1C_{10}-PPV

Because of stability problems of the Gilch precursor polymers the side-chain approach - the polymerisation of a substituted monomer into a soluble conjugated polymer - is applied. In the present study poly[2-(3,7-dimethyloctyloxy)-5-methoxy-1,4-phenylene vinylene] is used. This PPV-derivative is commercially known as OC_1C_{10}-PPV and also as MDMO-PPV - the abbreviations are derived from the alkoxy side-chains. In the following the former appellation will be used. These side-chains on the aromatic ring give the conjugated polymer the property

of solubility in common organic solvents and lead together with the backbone to a material that emits an orange colour of light.

A reason for the industrial interest in this polymer lies in its solubility in the conjugated state. As such, drawbacks of film conversion, like remaining elimination products or degradation of the ITO electrode - connected to the use of the insoluble and intractable regular PPV - are bypassed. On top of this, OC_1C_{10}-PPV exhibits very good properties - like luminescence efficiency, high brightness at low voltage - and therefore finds common use as active layer in polymer LEDs[4]. Even more recently promising results are obtained for its use in photovoltaic devices[5].

As mentioned in the first paragraph of this chapter recent publications on the Gilch route – which is mostly performed in THF or dioxane - support the idea of an anionic mechanism. The mechanistic study described in chapter 2 (Sulfinyl route – PPV precursors) indicated that both radical and anionic mechanisms could occur simultaneously, depending on the type of monomer and the solvent used.

By placing the starting data of the present mechanistic study: THF or dioxane as solvents, and monomers bearing alkoxy ring substituents, in the elaborated line of thought developed in chapter 2, a radical polymerisation mechanism is anticipated. However, already at the start of the study it is realised that very complex chemistry is involved - as is demonstrated by related literature - undermining straightforward, irrefutable conclusions.

In an attempt to elucidate the mechanism of the Sulfinyl and the Gilch polymerisation towards OC_1C_{10}-PPV several experiments with different types of additives were performed. These additives and some available data thereof are presented in section 3.2. Further division in sections of this chapter (section 3.3 to 3.5) is based on the synthetic route and the solvent used. Prior to the formulation of conclusions the feature of phase separation and / or gelation is investigated and discussed in section 3.6.

3.2 PRESENTATION OF THE ADDITIVES

A common way to investigate a polymerisation mechanism is to look at the influence of additives on the reaction and its products. There are different kinds of additives: some affect anionic processes, while others exhibit an effect on radical processes. For this study it is not only relied on experimental results of the additive TEMPO, but this time a combination of additives - depicted in figure 3.2 - is used in an attempt to distinguish between anionic and radical polymerisation mechanisms. The reason why the choice fell on this combination will be discussed in this section. The additives **5**, **6** and **7** were added in a finishing stadium of the research, in response to a publication of Ferraris and co-workers[2]. As a consequence, they are not used to the same extent in every section. The effects of the additives on the molecular weight of the polymer are evaluated by size exclusion chromatography (SEC).
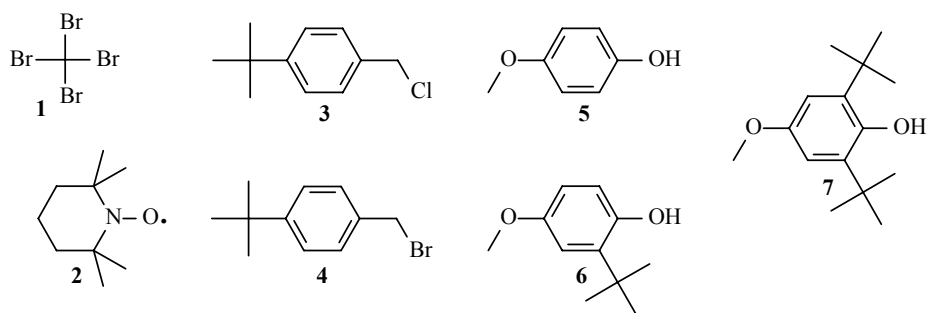
Figure 3.2: Representation of the additives used

*Carbon tetrabromine (CBr₄, **1**)*

This compound is known to be an effective radical transfer agent, due to the weak carbon-bromine bond[6]. This bond is especially weak because of the excellent stabilisation of the tribromocarbon radical formed by resonance involving the bromine free pairs of electrons. In its function as chain transfer agent carbon tetrabromine reacts with the growing radical polymer chain, resulting in the formation of a premature terminated chain and a new radical (figure 3.3). Hence, an effect on the degree of polymerisation – a decrease in molecular weight - is expected, at the same time leaving the yield unaffected.

$$M_n^{\bullet} \;+\; CBr_4 \longrightarrow M_n\text{-}Br \;+\; {}^{\bullet}CBr_3$$

$$^{\bullet}CBr_3 \;+\; M \longrightarrow CBr_3\text{-}M^{\bullet}$$
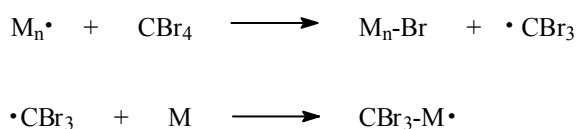
Figure 3.3: Carbon tetrabromine as a chain transfer agent

In the research of dr. Issaris it was found that addition of 0.5 equivalents of CBr$_4$ to the reaction mixture results in a decrease in molecular weight, while the yield is not altered[7]. Similar experiments with the transfer agent carbon tetrachloride (CCl$_4$), which is slightly less reactive, did not demonstrate any effect. This is in agreement with the results of Errede, who also found that CCl$_4$ does not exhibit an effect on the fast flow pyrolysis of p-xylene[8]. He argued that this is due to the high free radical reactivity of the *p*-QM.

*2,2,6,6-tetramethylpiperinoxyl (TEMPO, **2**)*

The compound TEMPO is a common radical scavenger. Addition of radical scavengers to a reaction mixture suppresses polymerisation by reacting with the initiating and propagating radicals and converting them either to non-radical species or to radicals with a reactivity that is too low to undergo propagation. Such polymerisation suppressors are classified in inhibitors and retarders, according to their effectiveness. Inhibitors stop every radical and polymerisation is completely halted until they are consumed. Retarders are less efficient and stop only a portion of the radicals, resulting in polymerisation at a slower rate[9].

In 1992 researchers at the Polymer Science department of the University of Massachusetts reinvestigated the effect of radical trapping agents on molecular weight and its distribution under typical Wessling conditions[10]. ESR measurements with only 0.00025 equivalents of TEMPO resulted in a complete disappearance of the TEMPO signal, indicating the trapping of TEMPO by a radical. The most convincing demonstration of the presence of radical chemistry during polymerisation was the complete suppression of polymer formation by 0.1 equivalents of TEMPO, while UV-vis measurements showed no effect of TEMPO upon the *p*-QM formation rate.

Results of dr. Issaris show that addition of amounts less than 0.1 equivalents of the radical scavengers TEMPO and diphenylpicryl hydrazyl (DPPH) to a Sulfinyl polymerisation in MMF results in a substantial decrease in molecular weight and polymer yield[7,11]. Moreover, a concentration of 0.5 equivalents TEMPO totally inhibits polymer formation. In the residual fraction of the latter experiment a dialdehyde was characterised. Its formation can be explained by the coupling of two *p*-QM molecules, resulting in a biradical dimer, which reacts with two TEMPO molecules. Rearrangement with the geminal sulfoxide or hydrolysis of the dinitroxide could explain the formation of the dialdehyde (figure 3.4).
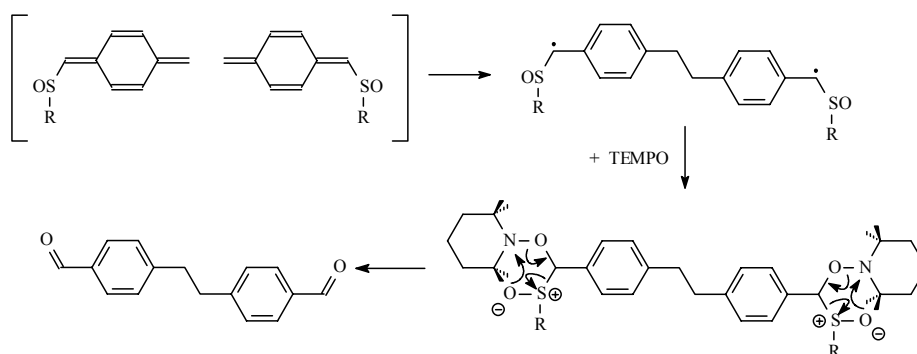
Figure 3.4: Proposed mechanism for the formation of the dialdehyde

4-tert-butylbenzyl chloride (tBuφCH₂Cl, 3)

Various publications of Hsieh and his co-workers of the Xerox Corporation (NY, USA) concern the use of the non-polymerisable 'acidic' additive **3** as anionic initiator and / or terminator[1,12,13]. They report that the molecular weight of another dialkoxy PPV derivative poly[2-(2'-ethylhexyloxy)-5-methoxy-1,4-phenylene vinylene], MEH-PPV, can be controlled by varying the amount of compound **3**. Table 3.1 shows a selection of their results on MEH-PPV synthesised via the Gilch route in THF at room temperature using a monomer concentration of 0.03M.

Table 3.1: Results of addition of **3** on MEH-PPV Gilch synthesis, published by Hsieh et al.[1,12]

amount of **3** (equivalents)	M_w / M_n (x 10^3 g/mol)[a]	poly-dispersity	yield (%)
0	gel	/	/
0.006	gel	/	/
0.06	331 / 66.5	5.0	35
0.12	172 / 15.1	11.4	20
0.61	85 / 11.3	7.5	17

[a] Relative to polystyrene in THF

An insoluble MEH-PPV "microgel" is obtained in the absence of or with an insufficient amount of tBuϕCH$_2$Cl (**3**). Soluble products are obtained by adding larger amounts of the additive. According to the authors, the fact that molecular weight depends inversely proportional to the amount of compound **3**, could be interpreted as a consequence of the involvement of an anionic polymerisation process.

4-tert-butylbenzyl bromide (tBuφCH₂Br, 4)

This compound is expected to exhibit similar effects as compound **3**. If an anionic process is involved, this additive should be more effective than **3**, as bromine presents a better leaving group than chlorine. A second reason for including this additive in the study is out of economic aspects. At present, the cost of this compound is one third of the cost of the chloride derivative **3**, hence it could be an interesting substitute, if successful.

4-methoxyphenol (MeOPhOH, 5)

In a recent publication of Ferraris and co-workers of the University of Texas at Dallas (USA) the effect of compound **5** on the molecular weight of MEH-PPV is evaluated by torque measurements[2]. They use a somewhat modified Gilch polymerisation for these experiments in the sense that the order of addition is reversed: this time a 0.24 M monomer solution is added over 1 hour to a 1.0 M

base solution in dry THF. A rheostat is used as mechanical stirrer to detect *in situ* changes in viscosity during the polymerisation process. In table 3.2 a selection of their results is presented.

Table 3.2: Results of addition of **5** on MEH-PPV Gilch synthesis, published by Ferraris et al.[2]

amount of **5** (equivalents)	M_n (x 10^3 g/mol)	poly-dispersity	yield (%)
0	125.7	1.06	72
0.005	118.2	1.04	68
0.01	86.2	1.52	67
0.015	57.7	1.43	56
0.02	51.3	1.14	50

An inverse relationship between the amount of additive **5** and the molecular weight of the resulting polymer is found. Hence, it is concluded that compound **5** acts as an anionic initiator. This effect led to their conclusion that a 'Gilch' polymerisation of MEH-PPV in THF proceeds via an anionic mechanism. In their view the low polydispersity values even point to a living polymerisation process.

2-tert-butyl-4-methoxyphenol (tBuMeOPhOH, 6)

This compound **6** is incorporated in our study to clarify the effect of the non-butylated derivative **5**; to obtain a more founded interpretation of its results. This butylated derivative **6** is expected to possess similar radical inhibiting, but different nucleophilic properties compared to compound **5**. If additive **5** exhibits an effect while compound **6** does not, than this is an indication for anionic processes. If both of them exhibit a similar effect, this is rather an indication for a radical polymerisation process.

2,6-di-tert-butyl-4-methoxyphenol (ditBuMeOPhOH, 7)

Additive **7** is incorporated in the study as an extension of compound **6**. As catalogues state that the latter has anti-oxidant properties as well as a synergism with acids[14], a new species is necessary to prevent a dubiousness of explanations of its effect. The nucleophilic properties of this compound **7** are expected to be negligible compared to those of **5**, due to the sterical hindrance exercised by the bulky tertiary butyl substituents. On top of this, species **6** and **7** are widely used antioxidant food additives in biochemistry[15], and are therefore expected to act as radical scavengers rather than anionic initiators or terminators.

Before proceeding to the results of this study, again I would like to stress that a study of the polymerisation process is rather complicated, as noticed in chapter two. The ongoing ambiguity on the nature of the polymerisation mechanism demonstrates this difficulty. The equilibrating carbanion chemistry involved in the first step of the polymerisation process can intervene inconspicuous. Hence, conditions aimed at quenching anionic chains could also inhibit the reaction through suppression of the QM-formation (step 1) rather than through inhibiting QM–polymerisation (step 2). Consequently, additives meant to affect an anionic polymerisation reaction could also interfere with the *p*-QM formation. One should therefore be very careful in interpreting the effects of these additives. The complexity of the chemistry involved in the whole polymer synthesis severely complicates a study into the nature of the polymerisation mechanism, anionic or radical.

3.3 MECHANISTIC STUDY ON THE SULFINYL ROUTE IN THF

3.3.1 The polymerisation procedure

The polymerisation procedure used for this study is based on the one applied by Covion Organic Semiconductors[16], combined with parts of the PPV Sulfinyl procedure. The polymerisation appliance (figure 3.5) consists of a 100 mL three-neck flask with Teflon stirrer, reflux condenser and elbow to add the base as a

solid. Prior to reaction the appliance is flushed with nitrogen gas to create a nitrogen atmosphere. To degas the solvent the flask is charged with dry THF and N_2 gas is passed for about 15 minutes.
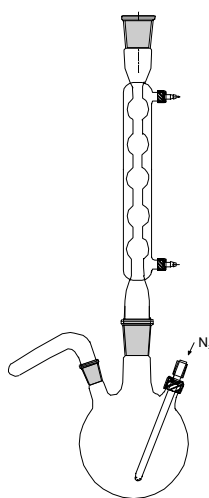
Figure 3.5: The polymerisation appliance

Dry THF is used to rinse in solid monomer providing a monomer concentration of 0.02 M. This concentration is rather low for the Sulfinyl route, because normally a concentration of 0.1 M is applied without encountering problems[17]. However, the lower concentration is chosen to enable comparison with Gilch experiments – while for this route gelation problems are expected to occur even at concentrations of 0.03 M[13]. All additives are added in an amount of 0.5 equivalents to the monomer solution.

Polymerisation is initiated by addition of 1.3 equivalents of solid potassium *tert*-butoxide, maintaining a nitrogen atmosphere. After 2 hours at ambient temperature, pouring the mixture in ice water stops the reaction. Excess of base is neutralised by addition of 1.0 M aqueous hydrochloric acid, followed by extraction with chloroform. The combined organic layers are concentrated under reduced pressure, and the precursor polymer is redissolved in toluene. Thermal elimination to the conjugated polymer takes place during 3 hours of reflux. The solution is cooled to about 40°C and a dropwise addition of methanol causes the

polymer to precipitate. The precipitated polymer is recovered by filtration, washed with methanol and dried under reduced pressure at room temperature. Residual fractions are concentrated *in vacuo*.

3.3.2 Results and discussion

In table 3.3 the results of standard Sulfinyl polymerisations together with those of additive experiments are listed. Experiments are performed in duplo and ad random – to cancel possible time influences - at ambient temperature in dry THF and show a rather good reproducibility. All SEC analyses present a monomodal molecular weight distribution. ^{1}H-NMR analyses of the polymer fractions all are identical: they contain the same set of signals corresponding to poly[2-methoxy-5-(3,7-dimethyloctyloxy)-*p*-phenylene vinylene]. In none of these spectra indications for end groups are detected.

Table 3.3: Results of standard and additive experiments
on the Sulfinyl route in THF

	Yield (%)	M_w (g/mol)	M_n (g/mol)	PD
Standard (1)	35	178 300	47 300	3.7
Standard (2)	55	226 000	46 500	4.9
*t*BuφCH$_2$Cl (1)	53	213 100	52 100	4.1
*t*BuφCH$_2$Cl (2)	55	205 400	50 300	4.0
*t*BuφCH$_2$Br (1)	34	140 600	47 300	3.0
*t*BuφCH$_2$Br (2)	51	130 100	39 600	3.3
TEMPO (1)	0	/	/	/
TEMPO (2)	0	/	/	/
CBr$_4$ (1)	6	25 300	10 500	2.4
CBr$_4$ (2)	7	38 500	19 400	2.0
*t*BuMeOPhOH (1)	7	11 900	4 900	2.4
*t*BuMeOPhOH (2)	6	12 400	4 600	2.7

As for ^{1}H-NMR analysis of the residual fractions similar remarks as in chapter 2 have to be made. The spectra show an overlap of signals, hampering a detailed characterisation of products present, and therefore merely lead to some vague determinations and assignments. However, a common feature is the emergence of several minor signals in the region between 10.30 and 10.50 ppm – possibly originating from carbonyl and / or carboxyl groups as a result of oxidation. Also signals of indistinct origin and low intensity emerge in each spectrum between 2.90 and 3.10 ppm. These possibly point at saturated ethylene entities in between phenyl rings. As far as possible, more details of the spectra will be given in the following discussion.

For a standard reaction a polymer with an M_w of about 200 000 is obtained at a moderate yield. ^{1}H-NMR analysis of the residual fraction demonstrates that the monomer constitutes the main product of the residual fraction, suppressing other signals. However, at a relatively low intensity some oligomer signals containing a fine structure are neighbouring the monomer signals. Thin Layer Chromatography (TLC) confirms this by a tailing of the starting spot that shows fluorescence by exposure of light of 366 nm, hereby supporting the idea of the presence of oligomers.

Addition of *t*-butylbenzyl chloride doesn't exhibit the effect experienced by Hsieh[1,12] - molecular weight is not lowered although a large amount is added. In the ^{1}H-NMR spectra of the residual fractions the monomer again constitutes the main product. Also original additive signals are found with a relative intensity of 75% when the monomer intensity is put at 100%. Between 7.00 and 7.60 ppm new signals emerge which lie in the region of aromatic oligomer protons – confirmed by tailing in TLC analysis. Also stilbene vinylene bonds – made by the coupling of two additive molecules – can be expected to appear in this range, but due to overcrowding exact determination and / or quantification could not take place. However, mass spectrometry confirms the presence of stilbene units by a signal of a mass fragment of 242; but no quantification is possible.

The corresponding bromine additive *t*-butylbenzyl bromide does result in a decrease of the molecular weight, but an effect on the yield is not pronounced. In regard to the large amount added compared to the experiments of Hsieh, the effect is not in full accordance. Analysis of the ^{1}H-NMR spectra of the residual

fractions yields the following observations: the signal of stilbene vinylene units is possibly somewhat hidden underneath aromatic additive signals between 7.2 and 7.5 ppm, making irrefutable qualification and quantification of this side product impossible. However, again the presence of a peak at 242 in the corresponding mass spectra reveals stilbene formation. The main signals in the NMR spectra seem to be originating from remaining monomer and additive in a ratio equalling unity. Also in this case oligomer signals emerge at relatively lower intensity, as is supported by TLC analysis.

When 0.5 equivalents of TEMPO are added to the standard reaction mixture no polymer can be recovered pointing at a complete inhibition of polymer formation. ^{1}H-NMR analysis of the residual fraction demonstrates that remaining monomer constitutes the main product. In this case a new, and most intense downfield signal emerges at 9.93 ppm. Integration values show a correspondence with signals at 7.81, 7.30, and 2.95 ppm - a set in good accordance with signals assigned to the dialdehyde perceived by dr. Issaris[7,11]. Putting the monomer intensity at 100%, this product has a relative intensity of 20%, which is relatively high compared to other signals present. Further, some signals of TEMPO can be detected between 2 and 3 ppm, representing less than 3% compared to remaining monomer signals, but so far no detailed adduct structures could be revealed.

The effect of the addition of carbon tetrabromine on the molecular weight of the polymer is explicit: it is decreased by almost a factor of ten. At the same time problems with precipitation after elimination occur – the precipitate is oily instead of fibrous - resulting in very low yields. Currently, a definite explanation for this feature cannot be offered, but the residual fractions are coloured a reddish-brown and, according to NMR analysis, still contain an amount of polymer. Possibly, remaining additive or side products prevent a proper separation of the polymer by addition of methanol. The ^{1}H-NMR spectra of the residual fractions show mainly signals of two products of which the monomer is one. The other is probably a bromine substituted product, because a new signal at 4.45 ppm appears corresponding with aromatic signals between 6.7 and 7.0 ppm – possibly pointing at the presence of a ϕCH_2Br structure. Again oligomer signals can be detected, as is confirmed by tailing and fluorescence of the starting spot in TLC.

The addition of 0.5 equivalents of 2-*tert*-butyl-4-methoxyphenol to the polymerisation mixture results in a somewhat different reaction work up. Although the colour of the reaction mixture, after the elimination procedure, is (only) slightly orange, addition of methanol does not result in precipitation. Only after evaporation of all solvent, addition of methanol results in a yellow-orange solution containing a small amount of finely distributed red polymer particles, which can be recovered by filtration. Clearly, both yield and molecular weight of the polymer are seriously affected. Probably, this additive (**6**) acts, just like TEMPO, as a radical scavenger. Only, in the present circumstances, it appears somewhat less effective. Probably, the additive efficiently blocks polymer formation during the first moments of reaction, but after a while some initiation and propagation can take place, explaining the formation of a small amount of low molecular weight polymer. This time the ^{1}H-NMR spectra of the corresponding residual fractions do not contain any residual polymer signals, thus confirming the low yields. The main signals correspond to monomer and additive structures in a ratio of about 40 over 60. Due to an overlap of signals it is not possible to determine if and which adduct structures are involved.

3.3.3 Conclusions of the study on the Sulfinyl route in THF

The combination of these results yields indications on the nature of the polymerisation mechanism of the Sulfinyl route towards OC_1C_{10}-PPV and stress the complexity of the reactions. One of the most striking observations is the result of the TEMPO experiments. They pretty much resemble those of a similar experiment described in chapter 2 – including the NMR analyses of the residual fractions where signals possibly originating from a derivative of the initiating dimer are present. The fact that this addition experiment leads to a complete inhibition of polymer formation is a strong indication that radical processes occur.

The other results seem to support this idea. The additive *t*-butylbenzyl chloride does not seem to exhibit an effect on the polymerisation, contradicting the experience of Hsieh and the occurrence of an anionic polymerisation mechanism. Except for the lowering of the yield, the effect of carbon

tetrabromine on the molecular weight corresponds with that of a chain transfer agent. Also the effect of *t*-butylbenzyl bromide can in this view rather be attributed to a chain transfer effect – decrease in molecular weight, while yield is unaffected - caused by the carbon-bromine bond, than to an anionic influence. Addition of 2-*tert*-butyl-4-methoxyphenol to the polymerisation mixture clearly affects both yield and molecular weight of the polymer; both decrease significantly. These results can be explained by its function as a radical scavenger, in the present circumstances apparently somewhat less effective than TEMPO.

It can be concluded that these results lie in the line of expectation elaborated in chapter 2, and present strong indications that a radical polymerisation mechanism, yielding high molecular weight polymer, is involved. All this, together with the analyses of the residual fractions can lead to a proposal for the radical polymerisation (figure 3.6) similar to that in chapter 2.
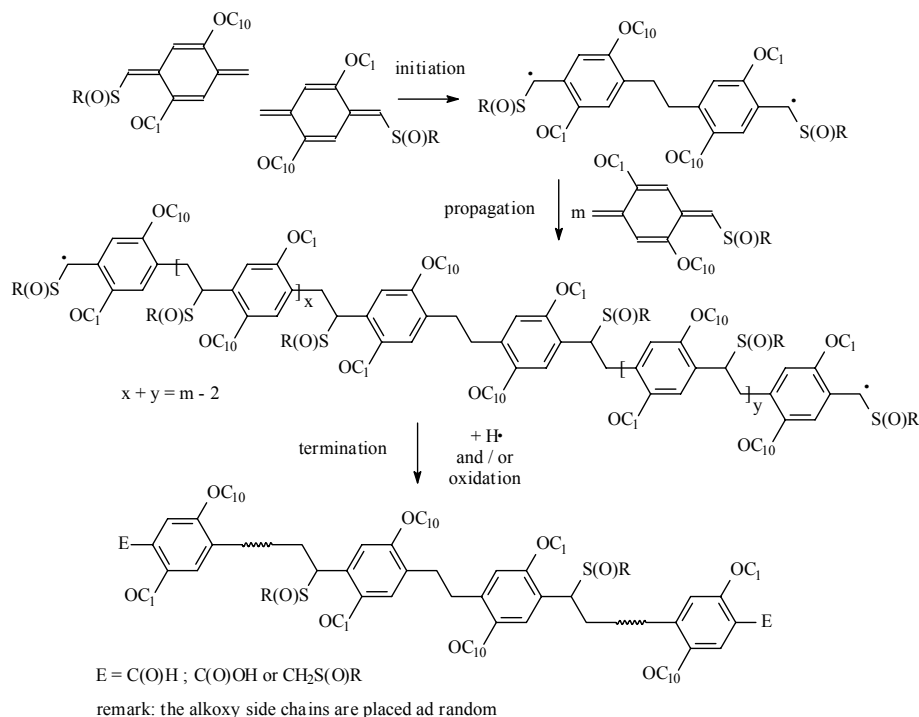
Figure 3.6: A proposal for a radical polymerisation mechanism of the Sulfinyl route towards OC_1C_{10}-PPV

The NMR analysis of the residual fraction of the TEMPO experiment, which contains signals of a dialdehyde – most probably a derivative of the initiating dimer particle -, yields indications for the nature of initiation. The exact nature of the termination reaction remains unclear, but the presence of low intensity carboxyl and / or carbonyl signals in NMR spectra seems to point at some oxidation reactions. All through the experiments no indications for an anionic polymerisation mechanism are found.

3.4 MECHANISTIC STUDY ON THE GILCH ROUTE IN THF

3.4.1 The polymerisation procedure

The polymerisation procedure used for this study resembles the one applied for the experiments described in section 3.3, only this time a basic elimination is performed. Again polymerisation is initiated by addition of 1.3 equivalents of solid base, but after ten minutes a large excess of base is added to execute the conversion to the conjugated polymer. Stirring is continued for 2 hours at ambient temperature. Addition of ice water and neutralisation by aqueous hydrochloric acid under vigorous stirring stops the reaction. The precipitated polymer is recovered by filtration, washed with methanol and dried under reduced pressure at room temperature. Residual fractions are concentrated *in vacuo*.

3.4.2 Results and discussion

Table 3.4 contains the results of the experiments with the additives on the Gilch route in dry THF. All SEC analyses present a monomodal molecular weight distribution, but during sample preparation most of the SEC samples exhibit a feature what is defined by Hsieh[1,12] as 'microgel' formation: filtration through a 0.45 μm filter is (severely) hampered. Experiments are performed ad random to cancel time influences, but the corresponding results clearly demonstrate that this time reproducibility is missing completely.

Table 3.4: Results of standard and additive experiments
on the Gilch route in THF

	Yield (%)	M_w (g/mol)	M_n (g/mol)	PD
Standard (1)	76	633 000	21 000	30
Standard (2)	63	1 462 000	435 000	3
Standard (3)	69	404 000	30 000	14
Standard (4)	65	856 000	19 000	44
Standard (5)	57	973 000	42 000	23
tBuφCH_2Cl (1)	51	1 072 000	566 000	2
tBuφCH_2Br (1)	118	1 473 000	119 000	12
tBuφCH_2Br (2)	69	1 133 000	482 000	2
TEMPO (1)	0	/	/	/
TEMPO (2)	0	/	/	/
CBr_4 (1)	104	999 000	40 000	25
CBr_4 (2)	83	762 000	20 000	59
CBr_4 (3)	97	126 000	25 000	5

These results clearly indicate that for some reason the Gilch route is much more sensitive to reaction conditions than the Sulfinyl route, expressed in irreproducibility. Obviously the precipitated polymer fraction is not pure – as is demonstrated by yields exceeding 100%. Therefore, on the analogy of the Covion procedure[16] a purification method is applied on all polymer fractions. This is done by dissolution of the crude product in THF, heating to 68°C until a homogeneous solution is obtained, cooling to 40°C and next, a dropwise addition of methanol causing the polymer to precipitate. The precipitated polymer is recovered by filtration, washed with methanol and dried under reduced pressure at room temperature. The corresponding results after purification are listed in table 3.5. Again filtration of the polymer solutions through a 0.45 µm filter during sample preparation causes problems, indicating 'microgel' formation.

Table 3.5: Results of standard and additive experiments
on the Gilch route in THF - after one purification

	Yield (%)	M_w (g/mol)	M_n (g/mol)	PD
Standard (1)	38	694 600	66 800	10
Standard (2)	23	1 102 700	71 400	15
Standard (3)	44	529 700	55 100	10
Standard (4)	56	771 600	58 800	13
Standard (5)	43	928 100	52 000	18
tBuϕCH$_2$Cl (1)	39	533 500	34 300	16
tBuϕCH$_2$Br (1)	42	1 276 100	72 300	18
tBuϕCH$_2$Br (2)	50	781 000	57 400	14
TEMPO (1)	0	/	/	/
TEMPO (2)	0	/	/	/
CBr$_4$ (1)	50	335 500	29 300	11
CBr$_4$ (2)	32	266 200	43 300	6
CBr$_4$ (3)	56	426 600	56 000	8

The purification procedure seems to bring polydispersity levels to a more acceptable level, and the obtained results show already an improved reproducibility compared to those before purification, however it is still far from satisfying. Similar results are observed by others[19].

3.4.3 Conclusions of the study on the Gilch route in THF

Due to the poor reproducibility, the number of conclusions to be drawn is very limited. Although ^{1}H-NMR spectra of the polymer fractions all contain the same set of signals corresponding to OC$_1$C$_{10}$-PPV, the complexity of the spectra of the residual fractions clearly indicate that the Gilch route is even more complex than the Sulfinyl route and holds new problems to solve. The behaviour of the polymer solutions during the SEC sample preparation already offers the

possibility that some type of gelation – a physical or chemical network - is involved.

Only the complete inhibition of polymer formation by addition of 0.5 equivalents of the radical scavenger TEMPO is striking and reproducible. However, this is considered to be insufficient to comment on the nature of the polymerisation mechanism of the Gilch route. It is therefore decided to start looking for some adjustments of the synthetic procedure improving reproducibility and hence providing a reliable system to investigate the effect of additives on the Gilch route towards OC_1C_{10}-PPV.

The observation of irreproducibility of the Gilch route in THF poses some questions on the conclusions drawn in publications, in which duplo experiments are not mentioned. This makes a re-examination and / or reinterpretation of the results wishful or appropriate.

3.5 MECHANISTIC STUDY ON THE GILCH ROUTE IN DIOXANE

3.5.1 Scanning for a reproducible polymerisation method

In an attempt to obtain reproducible results with the Gilch route, the solvent is changed to dry 1,4-dioxane, because this is the solvent used in the industrial manufacture of OC_1C_{10}-PPV. Also several other parameters, like base quantity and temperature are evaluated.

3.5.1.1 Variation of base conditions

According to the publication[16] the use of dry dioxane as polymerisation solvent is linked to working at elevated temperature (98°C) under reflux. To compare the effect of the experimental conditions of our method with the one described in the reference, several experiments are set up.

First of all, the effect of the change of solvent is tested, respecting the base quantities of a standard procedure applied in section 3.4. This implies the use of 1.3 equivalents of potassium *tert*-butoxide (K*t*BuO) to initiate polymerisation, after 10 minutes followed by the addition of another 3.3 equivalents of solid base

to proceed with the conversion from the precursor stage to the conjugated polymer.

Next, the base quantities of the publication are applied (2.6 and 2.0 equivalents of solid base for polymerisation and elimination, respectively). Notice that the total amount of base added to the reaction mixture is kept constant.

In a separate experiment the base is added as solution: 1.3 equivalents of K*t*BuO in 4 mL dioxane, and 3.3 equivalents in 7 mL dioxane. The monomer concentration is 0.02 M after addition of the first amount of base. The dilution effect related to the addition of the second portion of base is considered of minor importance, because this mainly concerns the elimination step.

All polymers are purified in THF at 68°C prior to SEC analysis. This has as effect that tailing on the low molecular weight side of the SEC-chromatogram (at higher elution time) is suppressed and the polydispersity of the molecular weight distribution is lowered.

Table 3.6: Results of Gilch polymerisations in dioxane
using various base conditions

Entry	Base condition	Yield (%)	M_w (g/mol)	M_n (g/mol)	PD
1	1.3 / 3.3 eq. (1)	47 (54)	805 000	77 000	10
2	1.3 / 3.3 eq. (2)	33 (36)	748 000	92 000	8
3	2.6 / 2.0 eq. (1)	24 (44)	903 000	80 000	11
4	2.6 / 2.0 eq. (2)	32 (39)	707 000	76 000	9
5	B solution (1)	47 (61)	1 040 000	76 000	14

Third column: between brackets: yield before purification

As is demonstrated by the results listed in the first two entries the transfer to another solvent can be regarded as a success: performing the Gilch route in dioxane at 98°C leads to an improved reproducibility. However, the obtained yields are slightly lower compared to those of the industrial process (54% after purification), possibly due to a larger sensitivity to losses while working with

relatively small quantities. At this time, the reason for the difference in reproducibility between the results obtained in THF and dioxane is still obscure.

Changing the partial amounts of base added – entries 3 and 4 – does not seem to exhibit much effect. The corresponding deviations in molecular weight do not seem to be satisfactorily pronounced to determine a concentration effect, if any.

Similar remarks can be made about the experimental results when the base is added as solution – entry 5. The distinction in molecular weights, listed in the table, is considered not sufficient, compared to entry 1 and 2, to nominate effects with certainty.

As a consequence, the amounts of base used in entries one and two are set as standard conditions for future experiments, even as the addition in solid state. In this way, a link is retained with the experiments in THF as well as with the Sulfinyl experiments.

3.5.1.2 Polymerisations at ambient temperature

Because the experiments in THF are performed at ambient temperature, the effect of this condition is checked on a Gilch polymerisation in dioxane. The corresponding results are listed in table 3.7. Immediately, a new feature arises: within one hour of reaction a phase separation is completed – an orange-red coloured lump of polymer is floating in a light orange solution. Further work up results in complete isolation of the crude lump, representing the major part of reaction products (yield = 94%). The corresponding characterisation of its molecular weight distribution is listed in entry 1. During SEC sample preparation, difficulties with solubility and filtration are encountered, pointing at gel properties of the lump – explaining or resulting in the extremely high numbers for molecular weight and polydispersity.

In an attempt to solve the problem of the phase separation and / or gelation, the lump of crude polymer is subjected to a purification treatment in THF at 68°C. After a short while the contours of the lump begin to faint, some swelling is observed, and the treatment is continued for over 72 hours. As a result, the lump is only slightly dissolved and a continuation of the thermal treatment is considered inadequate. From the precipitated fraction a SEC sample is prepared,

resulting in the values listed in the second entry. The molecular weight as well as the polydispersity is already somewhat lowered, but still the same problems as with the previous sample are encountered.

Because this thermal treatment in THF does seem to exhibit only some effect and because the primary experiments conducted at elevated temperature did not yield any phase separation, dioxane is added once more to the polymer fraction and the mixture is brought at 98°C for two hours. In this relatively short time the lump has completely dissolved and an entirely homogeneous orange solution is obtained. This behaviour is an indication that a physically crosslinked gel is involved. Cooling down does result in an increase in viscosity, however a phase separation no longer occurs. During SEC sample preparation no significant problems with solubility or filtration are encountered. The corresponding results are displayed in the third entry and the SEC data show good correspondence with those of the experiments at elevated temperature (table 3.6, first and second entry).

Table 3.7: Results of Gilch polymerisations in dioxane
at ambient temperature (AT)

Entry	Purification level	Yield (%)	M_w (g/mol)	M_n (g/mol)	PD
1	AT (1)	94	3 158 000	77 000	41
2	AT (1) – pur. 68°C	89	2 024 000	64 000	32
3	AT (1) – pur. 98°C	74	754 000	94 000	8
4	AT (2) – pur. 98°C	78	816 000	130 000	6
5	AT (2) – pur. 68°C	74	813 000	111 000	7

To check the observed influence of temperature another polymerisation is performed at ambient temperature – again resulting in a phase separation / gelation - but this time the temperature is raised till 98°C after the standard reaction time of two hours. In less than 12 hours a completely homogeneous orange solution is obtained and further work up is executed. A sample of the red fibrous polymer is analysed with SEC – no problems encountered during sample preparation - and the corresponding results are listed in the fourth entry. They

already are in good agreement with the results displayed in entry 3. Nevertheless, the polymer fraction is subjected to purification in THF at 68°C, but this does not seem to alter much (entry 5).

From these results it can be concluded that the phase separation – occurring at polymerisations performed at ambient temperature – is apparently due to the formation of a physically crosslinked gel. A temperature treatment in THF at 68°C is not sufficient to undo the gelation. Filtration of the treated polymer still presents problems, and gel particles are still present. Only a thermal treatment of the lump of polymer in dioxane at 98°C for several hours results in a completely homogeneous solution. This process is irreversible: cooling down does not result in a (renewed) phase separation. No presence of gel particles is observed and filtration of the SEC samples causes no problems.

Based on these observations it can indeed be argued that a polymerisation at ambient temperature in dioxane results in a physical network that can only be unravelled by a thermal treatment at a temperature of about 98°C. This will be evaluated and discussed in more detail in section 3.7.

A close comparison with the experimental results obtained in dioxane at elevated temperature yields comparable molecular weight distributions. However, the ambient temperature experiments result in a significant higher yield and therefore this room temperature is set as standard for future experiments.

3.5.2 <u>Results and discussion</u>

The previous experiments have led to a somewhat adjusted polymerisation procedure in order to evaluate the influence of additives on the Gilch route. Polymerisation reactions are performed in dioxane at ambient temperature. The base is added as a solid: 1.3 equivalents to initiate polymerisation and later 3.3 equivalents to eliminate into the conjugated polymer. To solve the feature of phase separation all polymers are subjected to a purification procedure. This can in fact be considered as a double thermal treatment: a first step consists of the heating of the crude reaction mixture to 98°C until a homogeneous solution is

obtained (2-12 h). After appropriate work-up the dried polymer fraction is subjected to a second thermal treatment in THF at 68°C.

The latter procedure results quite often in a suppression of tailing on the low molecular weight side of the SEC-chromatogram, leading to a lower polydispersity value of the molecular weight distribution. To demonstrate this effect a selection of data prior to and after purification is listed in table 3.8 in the even and odd numbered entries, respectively, and an overlay of the corresponding chromatograms of entries 3 and 4 is presented in figure 3.7. For the following experiments only the SEC results after the thermal treatment will be listed, because these are used to evaluate effects.

Table 3.8: The effect of purification in THF on SEC-characteristics of polymers synthesised in dioxane*

Entry	Additive	M_w (g/mol)	M_n (g/mol)	PD
1	none	788 000	46 000	17
2	none	754 000	94 000	8
3	tBuφCH$_2$Cl	606 000	32 000	19
4	tBuφCH$_2$Cl	582 000	60 000	10
5	tBuφCH$_2$Br	667 000	72 000	9
6	tBuφCH$_2$Br	655 000	98 000	7
7	CBr$_4$	59 000	9 600	6
8	CBr$_4$	73 000	19 000	4

* Odd entries: values before purification; even entries: values after purification

Another consequence of this thermal procedure gives rise to two different residual fractions: before and after purification in THF. ^{1}H-NMR analysis of the former residual fraction only shows sharp signals of low molecular weight products, while the spectra of the latter residual fractions also contain broader polymer or oligomer signals, indicating that the treatment causes some polymer to stay in solution during precipitation.
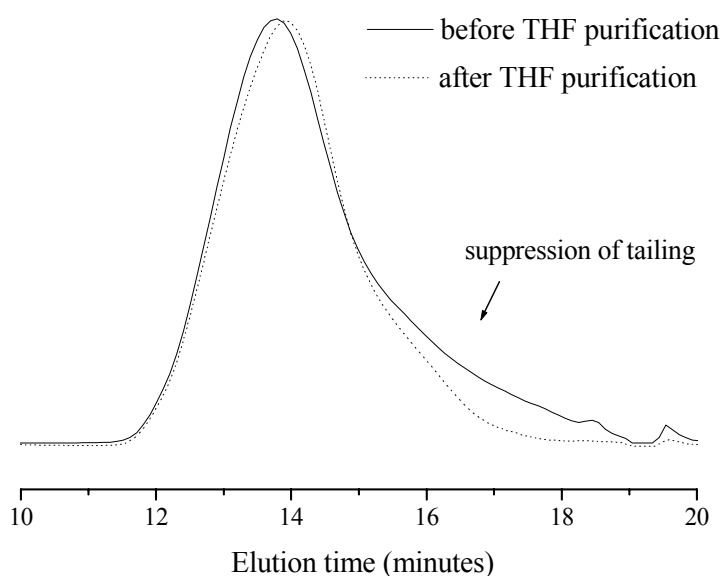
Figure 3.7: An overlay of SEC-chromatograms showing suppression of tailing

As response to a recent publication[2] the additives **5** and **6** are included in the study. All experiments are done in duplicate, except for the experiments with the latter additives, which are executed in triplicate. For all experiments the amount of additive is set at 0.5 equivalents to enhance the visibility of effects and maintain a link with previous experiments. An overview of the obtained results confirms that this polymerisation procedure indeed shows an acceptable reproducibility. Sampling for SEC measurements is performed on these purified polymers. The corresponding SEC results after purification are listed in table 3.9 together with polymer yields. The ^{1}H-NMR spectra of the polymer fractions all are identical and in accordance with the structure of OC_1C_{10}-PPV. Because of the high yields only a small amount of residual fraction is left. Unfortunately, the complexity of the ^{1}H-NMR spectra of these residual fractions does not allow a detailed characterisation of side products. Hence, only a few observations can be made: to some extent monomer and additive signals are present. The low intensity signals neighbouring the monomer peaks are probably originating from an oligomer fraction. Between 10.20 and 10.40 ppm several new minor signals

emerge – possibly pointing at the presence of carbonyl and / or carboxyl groups due to oxidation. Only the residual fraction of the TEMPO experiment shows an additional signal around 9.7 ppm, possibly pointing at a dialdehyde structure. This could be originating from an initiating dimer – as is discussed in chapter 2 (section 2.7.1) and presented in figure 3.4 - but its detailed structure could this time not be confirmed.

Table 3.9: Results of standard and additive experiments on the
Gilch route in dioxane at ambient temperature - after purification

	Yield (%)	M_w (g/mol)	M_n (g/mol)	PD
standard (1)	78 (85)	754 000	94 000	8
standard (2)	74 (78)	797 000	109 000	7
standard (3)	85 (86)	650 000	93 000	7
tBuϕCH$_2$Cl (1)	76 (77)	582 000	60 000	10
tBuϕCH$_2$Cl (2)	80 (83)	720 000	73 000	10
tBuϕCH$_2$Br (1)	80 (83)	655 000	98 000	7
tBuϕCH$_2$Br (2)	80 (83)	533 000	90 000	6
CBr$_4$ (1)	75 (100)	73 000	19 000	4
CBr$_4$ (2)	83 (100)	85 000	26 000	3
TEMPO (1)	21 (33)	179 000	40 000	5
TEMPO (2)	26 (38)	227 000	53 000	4
MeOPhOH (1)	12 (30)	1 513 000	87 000	17
MeOPhOH (2)	3 (22)	16 000	6 200	3
MeOPhOH (3)	10 (39)	679 000	48 000	14
tBuMeOPhOH (1)	8 (14)	479 000	49 000	10
tBuMeOPhOH (2)	2 (20)	58 000	15 000	4
tBuMeOPhOH (3)	3 (40)	190 000	20 000	10

Second column: between brackets: yield before purification in THF

The standard polymerisation procedure leads to polymer with a molecular weight from 700 000 to 800 000 in a yield of over 70%. Addition of 4-*tert*-butylbenzyl chloride or bromide does not affect the polymer yield and result in a small decrease in molecular weight. It can be concluded that these additives – even in the relatively large amount of 0.5 equivalents - do not exhibit the effect experienced by Hsieh and do not act as anionic initiators or end-caps for the polymerisation. This is also confirmed by a Swedish group of researchers[18]. The observed small decrease in molecular weight could, considering the effect of carbon tetrabromine, rather be interpreted as a chain transfer effect. The formation of stilbenes is confirmed by analysis of the residual fractions using mass spectrometry.

The additive carbon tetrabromine results in a serious decrease in molecular weight and a lowering of polydispersity, while the yield is not affected. This is consistent with it acting as a chain transfer agent.

The effect of TEMPO on the polymerisation is in accordance with the inhibition of a radical polymerisation mechanism; the yield of polymer and the molecular weight, both decreased by a factor of about 4. Possible reasons why polymerisation is not completely inhibited are a second initiation of polymerisation by addition of the second portion of base and a decreased efficiency of TEMPO in the present conditions. To distinguish both possibilities an additional experiment is set up in which a second amount of TEMPO (0.2 equivalents) is added to the reaction mixture together with the second base portion. In this case, no polymer is found, supporting the idea of a second initiation. Corresponding ^{1}H-NMR spectra similar to the other TEMPO experiments are found.

The effects of the additives 4-methoxyphenol and 2-*tert*-butyl-4-methoxyphenol are more complex. Reproducibility of molecular weight is poor – explaining the experiments in triplicate - whereas the yield after purification is somewhat more consistent. No phase separation occurs during polymerisation, but the thermal treatment is nevertheless completed. Before purification the resulting polymer is a wet, sticky substance – probably because side products are entrapped – which complicates separation, leading to a spread in yields. Apparently for these reactions the molecular weight of the resulting polymer is

very sensitive to reaction conditions, leading to a large spread in molecular weights. The yields decrease to an extremely low level indicating a huge influence of these additives on the reactions occurring during synthesis. But because the additive 2-*tert*-butyl-4-methoxyphenol (**6**), which has less nucleophilic properties, seems to exhibit a similar effect on the yield as additive **5**, these results do not support the hypothesis of anionic initiation.

To approximate the conditions of Ferraris[2] somewhat more, the additives **5** and **6** could be added together with the base as solution, increasing the probability of them acting as nucleophile or base. Therefore, to have some kind of reference values two polymerisations (without additives) are performed in which the base is added as solution (in amounts of 1.3 and 3.3 equivalents). The corresponding results are listed in table 3.10 and confirm the previous results of table 3.6.

Table 3.10: Polymerisation results with the base added as a solution

	Yield (%)	M_w (g/mol)	M_n (g/mol)	PD
B solution (1)	65	1 021 000	60 000	17
B solution (2)	70	1 189 000	42 000	28

It can be concluded that the polymerisations in which the base is added as solution yield a somewhat higher weight average molecular weight (M_w) value and an increased polydispersity in comparison to reactions where the base is added as a solid (table 3.9, entries 1 to 3).

In the additional experiments, the additives **5** and **6** are added together with the base in solution. This way, they should be deprotonated before addition and are consequently more likely to act as nucleophile or base. Additive **7** is included in the study to obtain additional information on the nature of the effects. If all three additives exhibit a comparable effect on the polymerisation, a radical polymerisation process is more likely than an anionic. On the contrary, when large differences in effects of the distinct additives are obtained, this does present an important indication in favour of anionic processes.

To check if deprotonation occurs, the additives are dissolved in diethyl ether and repeatedly washed with an aqueous solution of NaOH. In case of additives **5** and **6** the aqueous layer colours slightly pink, however, as could be expected, no coloration is visible in case of additive **7**. TLC analyses of the organic layers after separation reveal the presence of original products. These results indicate that additives **5** and **6** can be partly deprotonated in these basic conditions, while the di-*t*-butylated derivative cannot.

During the polymerisation reactions with these additives **5**, **6** and **7** no phase separation occurs, even if the base amounts are adjusted to 2.6 and 2.0 equivalents to enhance the probability of polymerisation. The reaction mixtures do not colour a deep orange, but remain yellow to slightly orange for **5** and **6**, and light orange in case of **7**. The result of the precipitation procedure is dependent on the additive used and will therefore be discussed separately.

In case of the reaction with 4-methoxyphenol (**5**) no polymer precipitates, hence an extraction is performed leading to one yellow-orange fraction containing all organic products formed. For this reason in table 3.11 it is referred to as fraction 'all'.

Precipitation of the reaction mixture resulting from addition of 2-*tert*-butyl-4-methoxyphenol (**6**) yields some kind of reddish oily fraction, in stead of fibres, which can be recovered by filtration (stays behind on the filter). The remains of the reaction mixture is subjected to further work up consisting of extraction and drying under reduced pressure (precipitation does not yield any polymer). This yellow-orange fraction will from now on be referred to as residual fraction.

Polymerisation in the presence of 2,6-di-*tert*-butyl-4-methoxyphenol (**7**) does yield an orange reaction mixture. By precipitation in water and neutralisation a small amount of red polymer separates from the solution. However, this polymer turns out to be unmanageable, complicating its recovery by filtration. It easily spreads out over a large surface, and is very hard to remove although addition of methanol somewhat facilitates collection (similar to the previous experiments with carbon tetrabromine on the Sulfinyl route towards OC_1C_{10}-PPV).

Although no explicit polymer could be separated in the case of additives **5** and **6**, SEC samples from each fraction are nevertheless prepared and analysed.

The corresponding results are listed in table 3.11. In case of the polymerisations in the presence of **5** and **6**, the yield is calculated taking relative peak areas in the corresponding chromatograms together with relative amounts of the fractions (e.g. the ratio residual over oily fraction) into account.

The ^{1}H-NMR spectra of the polymer obtained in reactions in the presence of additive **7** contain signals in agreement with the structure of OC_1C_{10}-PPV. Although other monomer signals - including those of the alkoxy side chains - are present, none of the other spectra seem to contain remaining ϕCH_2Cl signals. The residual fraction resulting from the experiments with **6** do not seem to vary much from the spectra of the corresponding oily fractions. Additive signals all are present, except for the hydroxide signal, which is possibly hidden below other signals or indicates the formation of an adduct structure. However, due to an overcrowding of the NMR spectra in between 2.5 and 4.2 ppm, the identification of such adduct structure is hampered. New intense signals emerge between 5.8 and 7.0 ppm, but currently no reasonable explanation can be offered.

Table 3.11: Results of additives added in combination with the base as solution

Additive	Fraction	M_w (g/mol)	M_n (g/mol)	PD	Yield (%)
MeOPhOH (1)	all	63 600	30 500	2.1	2*
MeOPhOH (2)	all	66 800	29 900	2.2	3*
*t*BuMeOPhOH (1)	residual	50 400	21 600	2.3	2*
	oily	2 500	740	3.4	
*t*BuMeOPhOH (2)	residual	41 300	17 300	2.4	3*
	oily	1 700	740	2.3	
di*t*BuMeOPhOH	PM	47 600	18 100	2.6	8
di*t*BuMeOPhOH	PM	51 000	18 900	2.7	10

* These yields are estimated values, calculated from corresponding SEC chromatograms

Even though no polymer could be separated in case of additive **5** and **6**, the SEC analyses detect the presence of a higher molecular weight species. However, an important remark is that the detector response for these samples is extremely low. The chromatograms have to be strongly enlarged to be able to set limits for

the calculations. This is in accordance with the NMR spectra, where at first no polymer signals could be detected, pointing at very low corresponding concentrations and hence low yields.

Although the various fractions that contain polymer to a certain extent behave differently, it can be stated that the effect of the three additives is comparable. All three result in a substantial decrease in yield together with a significant lowering of molecular weight, pointing at a similar interference in reactions. In combination with the other results reported, it can be concluded that their main effect is probably a strong radical inhibiting one, as described previously for the case of quinones[20].

This makes an anionic polymerisation mechanism less probable and strongly supports the hypothesis of a radical mechanism.

3.5.3 Conclusions of the study on the Gilch route in dioxane

A reproducible polymerisation procedure to synthesise OC$_1$C$_{10}$-PPV via the Gilch route in dry 1,4-dioxane at ambient temperature with a good yield is developed based on the industrial manufacture process. This adjusted polymerisation procedure is used to investigate the influence of different types of additives in an attempt to obtain indications about the nature of the polymerisation mechanism.

The lower polymerisation temperature results in a phase separation between polymer and solution, which is found to be cancelled by a thermal treatment consisting of two consecutive steps. First, a homogeneous solution is obtained by treatment in dioxane at elevated temperature and next, the obtained polymer is somewhat more purified during heating in THF. The feature of phase separation is probably due to a physical network that is irreversibly unravelled by a sufficient temperature increase.

It is stressed that it was and still is not our objective to claim a full understanding of the processes occurring during polymer synthesis, because the involved chemistry has proven to be extremely complex. However, as a whole, the obtained results present a strong indication that the main polymerisation

mechanism of the Gilch route is radical in nature and yields high molecular weight polymer.

3.6 INFLUENCE OF TEMPERATURE TREATMENT ON PHASE SEPARATION AND / OR GELATION

Apart from the effects of the additives, the experiments on the Gilch route have demonstrated a new feature - which is apparently not a public awareness: irreproducibility of polymerisations in the solvent THF. Thanks to the broad range of experiments executed for the present mechanistic study a link can be made between results obtained in 1,4-dioxane and in THF – the former being much more reliable.

When a polymerisation is performed in dioxane at ambient temperature a phase separation occurs: a polymer fraction – looking like a somewhat swollen lump of gel - separates from the solution. This is cancelled by a thermal treatment at 98°C: a homogeneous orange solution is obtained, which appears to be stable until at least 40°C. This is explained as an unravelling of a physical network.

These observations raise a number of questions. Perhaps do polymers in THF exhibit a similar, but less pronounced (with a lower macroscopically visibility) behaviour, explaining their irreproducibility. And what about other publications concerning Gilch polymerisations in THF: were the polymers mentioned subjected to some kind of thermal treatment, or is there a need to question their reliability and reproducibility? What does it mean when it is spoken of gelation: is it an extreme case of physical crosslinking that also can be cancelled by a heat treatment, or are chemical crosslinks involved?

Possible explanations for the cancellation of the phase separation are an unravelling of a physical network - physical crosslinking - and a degradation of the polymer at higher temperatures. The latter is proposed by a group of researchers of the Göteborg University in Sweden, who investigated the influence of polymerisation temperature on molecular weight of a phenyl-substituted PPV using the Gilch route[18]. They observed a more or less halving of

the molecular weight by reaction in THF at –78°C compared to reaction in THF at –35 or 0°C. Reflux in o-xylene for 4 hours of the original polymer resulting from the latter reaction yields similar results and is ascribed to chain scission of the polymer backbones. No specific reasons for this interpretation are given.

Therefore, it is decided to set up some additional experiments in an attempt to trace the origin of the feature of gelation and evaluate if the conclusions drawn from the previous dioxane experiments can be extended to other solvents and monomer concentrations. Gilch polymerisations on the monomer 2,5-bis(chloromethyl)-1-(3,7-dimethyl-octyloxy)-4-methoxybenzene are performed using various concentrations in THF and dioxane. The colour of the OC_1C_{10}-PPV polymer yields a first indication of its solubility: orange in contact with a solvent while in the case of a non-solvent (and in a dry state) the polymer turns red.

3.6.1 Polymerisation in THF at ambient temperature
based on a monomer concentration of 0.2 M

A polymerisation in dry THF at ambient temperature based on a monomer concentration of 0.2 M is known to result in gelation. Indeed an orange gel is formed that seems to occupy all of the solvent capacity.

Addition of a non-solvent results in a floating of the swollen gel in the non-solvent and a red coloration of the outer surface of the gel lump. By cutting a piece of the lump an orange surface is exposed, demonstrating that solvent is trapped inside and that non-solvent cannot intrude. As a consequence, further work up to remove residual base and salts is hampered.

Without exposing the gelly clod of polymer to a stress it remains one piece. By addition of new solvent the lump softens and swells only to a limited extent, and the surrounding solvent slowly turns orange. The process of removal of old and addition of new solvent is repeated several times and eventually the gel has been in contact with an excessive amount of solvent. However, the lump still looks intact - no significant difference in the volume of the gel is observed – and the surrounding solvent becomes orange coloured.

Eventually, two polymer fractions are collected: a gel and a small fibrous fraction. They are both subjected to SEC analysis and the corresponding results

are listed in table 3.12. An approximation for the relative quantities is given, but it should be kept in mind that the gelly fraction still causes additional solvent to turn orange and contains impurities (residual base, salts, monomer). Extraction and precipitation purify the fibrous fraction. SEC samples are subjected to 50°C overnight and as a result the fibrous sample appears to be a homogeneous solution, while the gelly sample still contains gel particles as well as an orange solution. However, by filtration through a 0.45 μm filter the gel particles are withheld by the filter and an orange solution passes without problems. On the other hand it turns out to be impossible to use a 0.45 μm filter for the fibrous sample – it even passes with great difficulty through a 1.0 μm filter.

Table 3.12: Results on the Gilch route in THF
based on a monomer concentration of 0.2 M

Fraction	Yield (rel.%)	Peak	M_w (g/mol)	M_n (g/mol)	PD
Fibrous	1	1	2 060 000	596 000	4
		2	12 000	2 600	5
		1 + 2	1 260 000	7 400	170
Gelly	99	1	1 460 000	573 000	3
		2	35 000	12 000	3
		1 + 2	561 000	19 000	30

Both SEC chromatograms show extremely broad molecular weight distributions of which the signal is roughly build out of 2 overlapping peaks. For this reason, the polymer characteristics are calculated in various ways: both peaks are integrated separately (peak 1, peak 2) as well as together (peak 1 + 2) and the corresponding values are listed as such in table 3.12. The second peak (most to the right hand side of the chromatogram) is in case of the gelly fraction relatively more intense than that of the fibrous fraction, explaining the lower molecular weight of the total signal. However, in both cases this second peak is again build out of more than one peak, but no further division is made.

The fact that the 'soluble' fibrous polymer presents more problems during filtration than the gelly fraction, while actually in both cases a similar soluble polymer fraction is involved, is possibly caused by a concentration difference (of soluble polymer) of both samples.

Later, the gel fraction is torn into smaller parts to obtain a larger contact surface and subjected to a thermal treatment in dioxane at 98°C for over 72 hours. This results in an orange solution containing big, swollen gel particles and these two polymer fractions could not be separated. By cooling down to 40°C – the industrial precipitation temperature – the solution becomes more reddish, pointing at decreasing solubility. A SEC analysis of the combined polymer fractions yields the following numbers: M_w = 583 000, M_n = 22 000 and PD = 26, very similar to the SEC data of the untreated gel. The filter withholds the main part of the polymer fraction (the gel, comprising probably over 90% of the polymer). Apparently the polymer is degraded to a small extent by the high temperature, or loose polymer chains are liberated from the lump. However, it can also be explained by the fact that the lump has been put under stress by tearing it into small pieces or that the gelation hampered a homogeneous distribution of the base resulting in a broad distribution.

Subjection of the gelly polymer fraction to ^{1}H-NMR analysis yields a spectrum containing relatively broad signals in accordance with OC_1C_{10}-PPV. However, the signals of the alkoxy side chains are much more intense than the aromatic and the vinylene signals. This is due to a waiting period between two scans that is too short for the backbone nuclei to relax. Normally, to obtain a good spectrum the waiting period should be at least 5 times T_1 (T_1 being the spin – lattice relaxation time in the direction of the z-axis; figure 3.8). When the waiting period is less than 5 x T_1, the nuclei are still relaxing to their equilibrium state and few can be excited again. This is the case for the backbone nuclei, which are trapped in a network, while the side chains are much more mobile and have a shorter T_1. Apparently the waiting period applied for the recording of the spectra had a value in between 5 x $T_{1, side\ chain}$ and 5 x $T_{1, backbone}$. As a consequence the corresponding backbone signals have a much lower intensity than the alkoxy side chain signals. This effect is much less pronounced for the fibrous fraction.

In a normally resolved spectrum structural defects can be observed when they are present at a minimum concentration of about 5%. However, a crosslinked gel is already obtained at less than 5% branching points. Hence, it is not meaningful to look for structural defects possibly pointing at branching points in these low quality spectra.
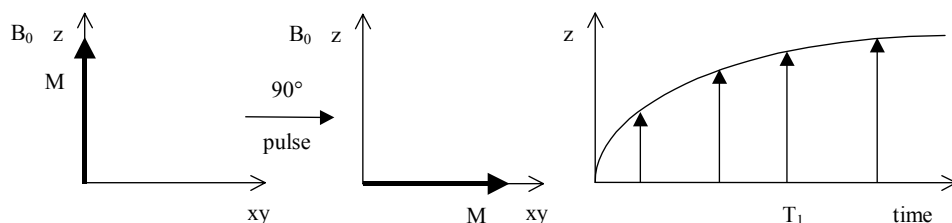
Figure 3.8: A schematic representation of the spin-lattice relaxation time T_1

In a relaxed state the nuclear magnetic moments tend to align with the

magnetic field (B_0) in the z-direction. A 90° pulse rotates the magnetisation (M)

into the xy-plane. The time that is needed to return to the equilibrium (relaxation)

in the z-direction is defined as the T_1 relaxation time.

Two different residual fractions are collected: before and after heating in dioxane. ^{1}H-NMR analysis of the former residual fraction only shows sharp signals of low molecular weight products, while the spectrum of the residual fraction after heat treatment is very similar, but also contains a limited amount of broader polymer and / or oligomer signals.

Unlike the observed physical gel in dioxane at room temperature ([MM] = 0.02 M), subjection of the THF polymer to a thermal treatment in dioxane at 98°C does not have a major effect. Even a temperature increase to 144°C in xylene is not sufficient to obtain a homogeneous solution. Only a relatively small fraction dissolves or liberates from the gel lump and yields a more or less normal weight average molecular weight (M_w) value.

These results indicate that in this case (THF, [MM] = 0.2 M, AT) also a chemically crosslinked gel is involved. Especially the property of swelling

combined with insolubility points in this direction. Subjecting the polymer to a thermal treatment does not seem to have a major effect on the gel lump.

3.6.2 Polymerisation in dioxane at ambient temperature based on a monomer concentration of 0.2 M

A similar experiment – based on a monomer concentration of 0.2 M - is executed in dry 1,4-dioxane at ambient temperature. This time not all volume is taken by a gel, but a phase separation takes place already some minutes after addition of the first amount of base: a polymer lump is floating on a solution. As a consequence, the second base addition is not effective – no homogeneous distribution takes place risking irreproducible results and a broad molecular weight distribution. Nevertheless, the reaction is continued for 2 hours and further work up proceeds as usual, although only the outer surface of the lump is reached. The results of the SEC analysis are listed in entry 1 in table 3.13.

To check the influence of temperature on the polymer, it is subjected to a sequence of thermal treatments. The polymer fraction is successively dissolved in 250 mL of THF, dioxane and *o*-xylene – to obtain concentrations similar to those of a standard purification procedure, discussed in section 3.5 - and heated for three hours at 68°C, 98°C and 144°C respectively. By this consecutive increase of the temperature the gel swells and larger parts of the lump spontaneously break down into smaller gel particles and even dissolve. However, it turns out that the main part remains insoluble – in the shape of multiple smaller particles - and is withheld in the process of filtration during SEC sample preparation. This results in an only slightly coloured solution, while gel particles are visible on the filter surface.

After the treatment in *o*-xylene two polymer fractions could be collected separately: a gelly and a fibrous fraction. Both are subjected to SEC analysis and the corresponding results are listed in entries 4 and 5, respectively.

Table 3.13: Results on the Gilch route in dioxane
based on a monomer concentration of 0.2 M

Entry	Thermal treatment	Yield (%)	M_w (g/mol)	M_n (g/mol)	PD
1	none	108	210 000	14 000	15
2	THF	90	948 000	22 000	44
3	dioxane	86	816 000	17 000	47
4	*o*-xylene	75	449 000	31 000	14
5	*o*-xylene	9	273 000	21 000	13

Actually, these values are easily misinterpreted without an overlay of the corresponding chromatograms (figure 3.9). This overlay is zoomed in the region between 10 and 20 minutes of elution time and the peak around an elution time of 18 minutes results from low molecular weight products – like the monomer or derivatives thereof – while the peak at about 20 minutes originates from toluene.

a ——— before thermal treatment
b ········· THF, 68°C, 3h
c –·–·–· dioxane, 98°C, 3h
d ——— *o*-xylene, 144°C, 3h - fibres
e – – – – *o*-xylene, 144°c, 3h - gel
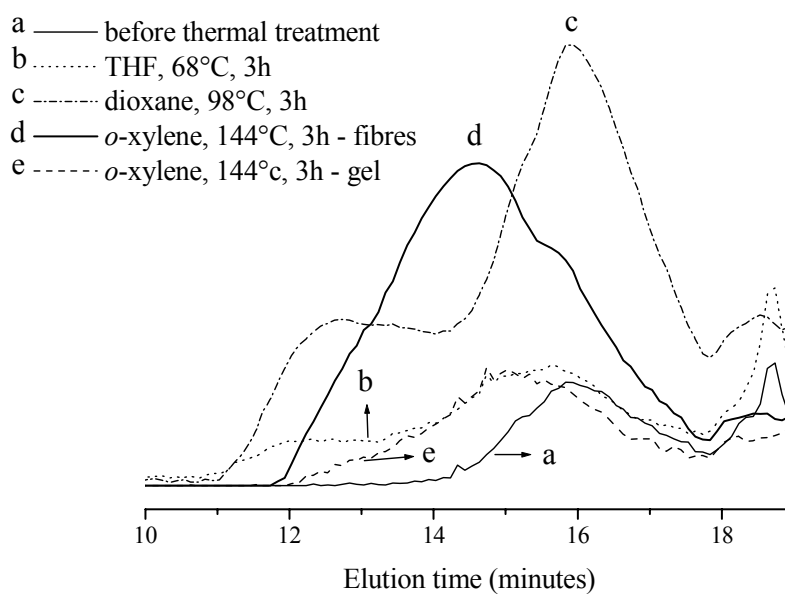
Figure 3.9: An overlay of SEC-chromatograms
visualising effects of thermal treatment

The overlay demonstrates that mainly the fibrous polymer fraction obtained after thermal treatment in *o*-xylene exhibits a normal monomodal molecular weight distribution. The other chromatograms show some kind of broad bimodal molecular weight distribution between an elution time of 10 and 17 minutes. This is possibly due to the presence of aggregates, which constitute the peak on the high molecular weight side of the chromatogram (short elution time). The lower molecular weight signal could be originating from loose chains escaped from the network or from shorter chains resulting from thermal degradation of the polymer.

Residual fractions are collected after each step, leading to four different NMR-samples. Only the ^{1}H-NMR spectrum of the last residual fraction – after thermal treatment in *o*-xylene - does contain some small amount of broader polymer or oligomer signals on top of some sharp signals of low molecular weight products, which constitute the main products of the spectra of the other residual fractions. The ^{1}H-NMR analyses of the gelly fractions all yield spectra with minor backbone and major side chain signals, as is explained in the previous section.

Because similar concentrations of the polymer solutions for the thermal treatment (0.02 M) are adopted, a comparison with the observations discussed in section 3.5 can be made. Even though at first glance these polymerisation conditions (a monomer concentration of 0.2 M, dioxane, ambient temperature) yield a feature of phase separation similar to the reactions with 0.02 M, the effect of a thermal treatment is different. In none of the cases of the 0.2 M polymer the thermal treatment leads to a homogeneous solution. This indicates that in these cases probably different types of network are involved. In fact, the results presented here show a rather good agreement with the experiments discussed in section 3.6.1, confirming the presumption that also here a chemical network is involved.

3.6.3 Polymerisation in THF at ambient temperature
based on a monomer concentration of 0.03 M

According to Hsieh, a Gilch polymerisation towards MEH-PPV in THF respecting a monomer concentration of 0.03 M yields a microgel – which cannot be filtrated through 0.45 μm[1,12]. In order to check this observation a similar polymerisation is performed towards OC_1C_{10}-PPV. To trace the origin of this gelation effect the obtained polymer is subjected to a sequence of various heat treatments and the effect on the polymer characteristics is evaluated using SEC, ^{1}H-NMR and UV-vis analysis. Also, the macroscopical state of the polymer fraction can give a first impression of an effect. If the molecular weight remains constant during prolonged heating, this is considered an indication that a physical network of polymer chains is involved, which is unravelled. On the other hand, a sudden, strong alteration of molecular weight enhances the probability that polymer degradation is involved.

The Gilch polymerisation towards OC_1C_{10}-PPV in THF is initiated by addition of 1.3 equivalents of solid KtBuO to a monomer solution of 0.03 M, resulting in a clear yellow reaction mixture. Addition of the second base portion results in a colour change to orange within one minute. The viscosity increases rapidly to a level at which stirring is strongly hindered and this phenomenon lasts for the remains of the reaction time. Addition of water and neutralisation with aqueous hydrogen chloride yields a red, fibrous polymer lump, which is recovered by filtration, washed with methanol and dried under reduced pressure.

Next, this polymer is subjected to a series of thermal treatments under nitrogen atmosphere consisting of a heating for 2 hours at 68°C in THF; 12 hours at 98°C in dioxane, another 12 hours at 98°C in dioxane, and finally 2 hours at 144°C in *o*-xylene. After each treatment the polymer is precipitated by addition of methanol, recovered by filtration and subsequently dried under reduced pressure. From each polymer fraction a SEC sample is prepared and the corresponding results are listed in table 3.14 together with the yields.

Table 3.14: Results of a series of thermal treatments on Gilch OC_1C_{10}-PPV synthesised in THF based on a monomer concentration of 0.03 M

Entry	Thermal treatment	Yield (%)	M_w (g/mol)	M_n (g/mol)	PD
1	none	71	2 170 000	29 000	76
2	THF	66	2 000 000	66 000	30
3	dioxane (1)	63	1 170 000	67 000	18
4	dioxane (2)	61	1 070 000	82 000	13
5	*o*-xylene	52	120 000	48 000	3

After the standard polymerisation time of 2 hours, a red, fibrous lump of polymer is obtained of which a solution of about 2 mg/mL proves very hard to filtrate through 0.45 μm filters (two filters are necessary). In this way, the observation of MEH-PPV 'microgel' formation in THF by Hsieh is more or less confirmed for OC_1C_{10}-PPV. Possibly, this feature is characteristic for Gilch polymerisations performed in THF applying this concentration. The corresponding SEC data (entry 1) reveal that the obtained polymer has a very high apparent weight average molecular weight and a very broad molecular weight distribution.

By addition of THF to the polymer fraction and a temperature increase to 68°C an apparently homogeneous orange polymer solution is obtained, which refutes the supposition of a chemically crosslinked gel. The THF treatment leads to a lowering in polydispersity, but has little or no effect on the M_w-value (entry 2). The appearance of the polymer is unchanged: it is a red, fibrous lump of polymer. Filtration during SEC sample preparation again is difficult and once more, two 0.45 μm filters are required.

A subsequent treatment in dioxane at 98°C, lasting 12 hours, followed by work up, results in a red powdery to fibrous polymer fraction. Filtration during SEC sample preparation still is hindered, but already to a lesser extent. SEC analysis demonstrates a more or less halving of molecular weight as well as polydispersity (entry 3). However, a repetition of this treatment (another 12 hours at 98°C) does not exhibit a significant effect (entry 4). This observation is of

major importance, because it lowers the probability of a polymer degradation process caused by an increase in temperature. Consequently, the explanation of an unravelling of a physical network by a thermal treatment at 98°C seems to be more plausible and acceptable.

The effect of the thermal treatment in *o*-xylene, even if the heating only lasts for two hours, is much more radical and supports the idea of polymer degradation. Compared to the weight average molecular weight of the polymer after a prolonged heat treatment in dioxane, a decrease in M_w by a factor ten is demonstrated (entry 5). Other indications of a huge change in molecular weight are the almost immediate dissolution of the corresponding SEC sample, while the previous SEC samples of entries 1 to 4 need a few hours to be completely dissolved, together with the disappearance of filtration problems. The change in polymer appearance from red, fibrous into an orange thin film strongly confirms the supposition of a degradation of polymer chains. The macroscopically visible change in colour is confirmed by UV-vis measurements (overlay in figure 3.10). The wavelength of maximum absorption is shifted from about 498 to 466 nm, in case of the polymer solutions corresponding to entries 1 to 4 and entry 5, respectively.
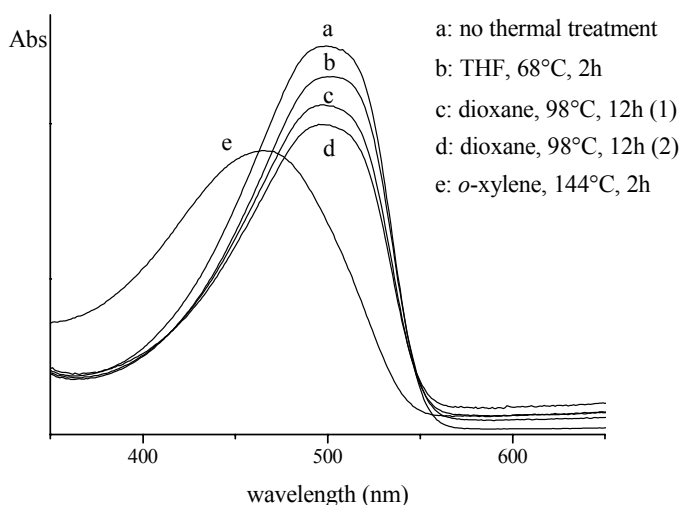
Figure 3.10: Overlay of UV-vis spectra of the various polymer fractions visualising effects of thermal treatment

Also the residual fractions are collected, dried under reduced pressure and subjected to SEC analysis. The corresponding results are listed in table 3.15.

Table 3.15: SEC-results of the corresponding residual fractions

Thermal treatment	M_w (1) (g/mol)	M_n (1) (g/mol)	PD (1)	M_w (2) (g/mol)	M_n (2) (g/mol)	PD (2)
none	640	520	1.2	/	/	/
THF	4 400	2 900	1.5	600	580	1.1
dioxane (1)	2 700	2 100	1.3	610	570	1.1
dioxane (2)	5 100	3 800	1.3	820	720	1.1
o-xylene	21 000	4 700	4.5	/	/	/

The chromatograms show a peak corresponding to a molecular weight value of 600 to 800 g/mol, which possibly originates from remaining monomer or some monomer adduct. Currently, no further data are available. These SEC results show that as soon as the polymer solution is subjected to a temperature increase, also low molecular weight entities ($M_w > 1\,000$ g/mol) are liberated that dissolve in methanol and hence end up in the residual fraction. Most probably, it involves oligomers. The broader signal of the residual fraction from the *o*-xylene experiment is probably build out of multiple overlapping peaks, including the one around 700 g/mol, but no separate calculations are performed.

^{1}H-NMR analysis of the polymer fraction resulting from the *o*-xylene treatment still shows the signals corresponding to OC_1C_{10}-PPV. The spectrum of the corresponding residual fraction seems relatively simple. No polymer or oligomer signals are present with significant intensity. The signals corresponding to the alkoxy side chains are missing. Aromatic signals between 7.15 and 7.50 ppm are present together with a relatively intense downfield signal at 10.25 ppm and new signals around 5 ppm. Currently, for these signals no reasonable explanation can be offered.

3.6.4 Thermal treatment on polymers obtained by the Gilch route in THF (0.02 M)

A question, which is till now still unanswered, is the origin of irreproducibility of Gilch polymerisations performed in THF. The previous experiments indicate that ambient temperature Gilch polymerisations in THF and dioxane (at relative low concentrations) suffer from some kind of gelation behaviour – apparently a physical network is formed. To check if the irreproducibility of the 0.02 M THF experiments originates from this feature a selection of the resulting polymers is subjected to a thermal treatment in dioxane. The polymers of standards 2, 3 and 4 (section 3.4.2 – after purification) are dissolved in 25 mL of dioxane and the temperature is raised till 98°C. The solutions of standards 3 and 4 are maintained under nitrogen atmosphere at this temperature for 12h, while the solution of standard 2 is subjected to two subsequent treatments, each consisting of 6h. The corresponding results are listed in respectively entries 7, 2, 4 and 5 of table 3.16 together with the original SEC values from table 3.5. The resulting polymer from standard 3 is subsequently subjected to an additional treatment in dioxane at 98°C for another 14 hours (entry 8).

Table 3.16: SEC data before and after heat treatment in dioxane at 98°C

Entry	Standard	Yield (%)	M_w (g/mol)	M_n (g/mol)	PD
1	4	56	771 600	58 800	13
2	4[a]	53	587 000	70 000	8
3	2	23	1 102 700	71 400	15
4	2[b]	22	931 000	89 000	10
5	2[a]	20	465 000	62 000	8
6	3	44	529 700	55 100	10
7	3[a]	42	467 000	61 000	8
8	3[c]	39	461 000	63 000	7

[a]: dioxane, 12h, 98°C; [b]: dioxane, 6h, 98°C; [c]: dioxane, 26h, 98°C

The SEC data of the various polymers subjected to a thermal treatment of 12h in dioxane at 98°C are very similar. Apparently, the reproducibility of Gilch polymerisations performed in THF only surfaces after a treatment at 98°C of at least 12 hours. However, the decrease in molecular weight does not always continue by excessive heating to 98°C as is shown by the data in entry 8. This indicates that there exists some kind of "true molecular weight" – molecular weights value - that is insensitive to an extended heat treatment at 98°C. However, it has to be remarked that not all of the studied polymers are subjected to this extended (in time) treatment; hence the listed values do not necessarily correspond to their "true molecular weights". Therefore, only an "apparent" reproducibility is mentioned.

To check the influence of a xylene treatment on a polymer obtained by Gilch polymerisation in THF at a monomer concentration of 0.02 M, a high molecular weight polymer is selected (*t*BuϕCH$_2$Br 1; table 3.5) and subjected to 144°C in *o*-xylene for 2 hours. The corresponding results are listed in table 3.17 together with the original data.

Table 3.17: SEC data of a tBuϕCH$_2$Br polymer subjected to 144°C for 2h in *o*-xylene

	Yield (%)	M$_w$ (g/mol)	M$_n$ (g/mol)	PD
*t*BuϕCH$_2$Br 1	42	1 280 000	72 000	18
*t*BuϕCH$_2$Br 1[*]	38	118 000	47 000	3

[*]: *o*-xylene, 144°C, 2h

After the two hours treatment an orange-red, powdery polymer is collected of which the molecular weight has decreased significantly. UV-vis analysis shows that the wavelength of maximum absorption is shifted from about 498 nm to 479 nm. This observation supports the supposition of degradation proposed in earlier experiments with *o*-xylene and is to some extent in agreement with the proposal of thermal degradation by chain scission of the Swedish group of researchers[18]. An OC$_1$C$_{10}$-PPV polymer chain with a molecular weight of 1 200 000 g/mol corresponds with about 4200 repeat units. According to a ^{13}C-NMR study performed by researchers of Covion Organic Semiconductors a Gilch

OC$_1$C$_{10}$-PPV structure contains about 3% of CH$_2$-CH$_2$ defects[16] (in our case corresponding to about 130 C-C defects in an average polymer chain), which could be more sensitive to thermal degradation. Supposing the polymer chain breaks at these defective points by a thermal degradation process an average conjugation length of about 33 repeat units results. But a molecular weight of 120 000 g/mol corresponds to about 420 repeat units, possibly indicating that not all structural defects degraded or that less than 3% CH$_2$-CH$_2$ defects are present in the studied polymer. However, a difference in UV absorption is only then expected when the conjugation length decreases to an average value of below ten repeat units. This indicates that during a thermal treatment of OC$_1$C$_{10}$-PPV in *o*-xylene at 144°C besides thermal apparently also some chemical degradation occurs.

3.6.5 <u>Conclusions</u>

Apparently, two types of gelation can occur, depending on reaction conditions - especially the influence of the monomer concentration and solvent is tested. So far indications are found for chemical crosslinks when polymerisation is performed in THF and dioxane at ambient temperature using a monomer concentration of 0.2 M. The latter results in a visible phase separation between polymer clod and a solution. The clod or gel swells to a limited extent when the temperature is raised or solvent is added, but even a thermal treatment in *o*-xylene does not cause it to dissolve, supporting the idea of a chemically crosslinked polymer network. A minor part of the clod does dissolve, but it is impossible to determine whether this is due to chain scission or to a liberation of loose polymer chains.

The polymerisations based on a monomer concentration of 0.02 M performed in dioxane at ambient temperature also give rise to a phase separation, only this time a thermal treatment in dioxane cancels the phase separation and results in a homogeneous solution. The corresponding SEC analyses show monomodal molecular weight distributions and calculations yield a molecular weight value of about 700 000 to 800 000 g/mol. These observations are strong

indications that in this case a physical polymer network is involved, which can be unravelled by a treatment at elevated temperature. The origin of this network can be due to an aggregation of polymers. Apparently, this feature is inherent to the Gilch route, because in Sulfinyl polymerisations no such behaviour has ever been observed.

To obtain a link with the publications of Hsieh[1,12] a Gilch polymerisation towards OC_1C_{10}-PPV is performed in THF respecting a monomer concentration of 0.03 M. The stated experience of microgel formation is more or less confirmed by SEC analysis of the resulting red fibrous polymer lump. After a hampered filtration a high M_w together with a large polydispersity value is found. The origin of this gelation effect is traced by a subjection of the obtained polymer to a sequence of various heat treatments. Effects are evaluated using the macroscopical appearance of the polymer together with its SEC, ^{1}H-NMR and UV-vis analysis. Subjection of the polymer to a thermal treatment in dioxane at 98°C, leads to a halving of molecular weight and polydispersity. However, at a prolonged heating this apparent decline is not continued. This observation lowers the probability of a polymer degradation process caused by this increase in temperature and supports the explanation of an unravelling of a physical network. However, when temperature is increased to 144°C in *o*-xylene, polymer degradation does occur. This is derived from a radical decrease in weight average molecular weight by a factor ten, supported by a visible colour change of the polymer as is also confirmed by UV-vis analysis. This colour change indicates that a heating of the polymer in *o*-xylene significantly affects conjugation length. Taking 3% C-C defects in OC_1C_{10}-PPV polymer structure into account, it implies some kind of chemical next to a thermal degradation process.

Additional experiments yield an indication that the reproducibility of Gilch polymerisations performed in THF at a monomer concentration of 0.02 M only surfaces after a thermal treatment of at least 12h in dioxane at 98°C. Extended heating to 98°C does not result in an ongoing molecular weight decrease; at some point a "true molecular weight" seems to be reached that is insensitive to further heating at 98°C.

3.7 GENERAL CONCLUSIONS

This study was undertaken in an attempt to elucidate the nature of the polymerisation mechanism - anionic or radical - of *p*-quinodimethane based polymerisations. A common way to investigate a polymerisation mechanism is to look at the influence of additives on the reaction and its products. For this study a combination of additives is used: some of them were thought to affect anionic processes, while others were expected to exhibit an effect on radical processes. Although *p*-quinodimethane based polymerisations have been investigated by a number of research groups, the nature of the underlying polymerisation mechanism - radical or anionic - is still under discussion, indicating the difficulty of the subject. It was therefore not our objective to claim a full understanding of the processes occurring during polymer synthesis, but merely to offer new material for discussion.

First of all the effect of the additives was studied on the Sulfinyl route in THF towards OC_1C_{10}-PPV. One of the most striking observations is the result of the TEMPO experiments: this addition leads to a complete inhibition of polymer formation, presenting a strong indication that radical processes occur. The additive *t*-butylbenzyl chloride does not seem to exhibit a strong effect, contradicting the experience of Hsieh and the occurrence of an anionic polymerisation mechanism. The effect of carbon tetrabromine on the molecular weight corresponds with that of a chain transfer agent (except for the lowering of the yield). In this view, the effect of *t*-butylbenzyl bromide on the polymerisation can rather be attributed to a chain transfer effect, than to an anionic influence. As a conclusion it can be stated that these results lie in the line of expectation elaborated in chapter 2 and present strong indications that a radical polymerisation mechanism is involved that yields high molecular weight polymer. Together with the analyses of the residual fractions a proposal for the radical polymerisation can be put forward (figure 3.6). The nature of the termination reactions remains unclear. However, no indications for an anionic polymerisation mechanism are found.

The complexity of the NMR-spectra of experiments with additives on the Gilch route clearly indicates that this route is even more complex and presents

new problems to solve. The Gilch route in THF is demonstrated to yield irreproducible results, which invites some questions on the conclusions of some publications, where duplo experiments are not mentioned. Perhaps a re-examination and / or reinterpretation of the results are required.

As a consequence of the poor reproducibility of results in THF it is changed to dioxane – the solvent used for the industrial manufacture of OC_1C_{10}-PPV. A reproducible polymerisation procedure to synthesise OC_1C_{10}-PPV via the Gilch route at room temperature was developed, based on the Covion procedure, and used to investigate the influence of different types of additives. Compared to the Sulfinyl route, the Gilch route is clearly much more sensitive to reaction conditions, but similar conclusions can be drawn. Addition of TEMPO can completely inhibit polymer formation by its function of radical scavenger. Carbon tetrabromine acts as chain transfer agent: molecular weight decreases while the yield is left unchanged. The small decrease in molecular weight by the additives 4-*tert*-butylbenzyl chloride and bromide could in this view rather be interpreted as a chain transfer effect. They do not exhibit the effect experienced by Hsieh and no indications are found for them acting as anionic initiators or end-caps for the polymerisation. The effects of the additives 4-methoxyphenol and 2-*tert*-butyl-4-methoxyphenol are more complex. Apparently for these reactions the molecular weight of the resulting polymer is very sensitive to reaction conditions, leading to a poor reproducibility of molecular weights. In additional experiments the additives **5**, **6** *and* **7** are added together with the base as solution, increasing the probability of them acting as nucleophile or base and approximating the conditions of Ferraris[2] somewhat more. Although the various fractions that contain polymer behave differently to a certain extent, all three additives result in a substantial decrease in polymer yield together with a significant lowering of molecular weight, pointing at a similar interference in reactions. In combination with the other results reported, it can be concluded that their main effect is probably a strong radical inhibiting one. This makes an anionic polymerisation mechanism less probable and somewhat questions the interpretation given by Ferraris. Taken as a whole, the results obtained in this mechanistic study are a strong indication that the main polymerisation

mechanism operating in the Gilch route is radical in nature and yields high molecular weight polymers.

New features during the Gilch experiments – irreproducibility and phase separation raised the question of gelation. A series of experiments demonstrated that apparently, two types of gelation can occur, strongly depending on the monomer concentration. Indications for chemical crosslinks are found when polymerisation is performed in THF and dioxane at ambient temperature using a monomer concentration of 0.2 M. The gel swells to a limited extent when the temperature is raised or solvent is added, and even a thermal treatment in xylene at 144°C is insufficient to dissolve the gel. These observations strongly support the idea of a chemically crosslinked polymer network. A minor part of the clod does dissolve, but it is impossible to determine whether this is due to chain scission or to an escape of loose polymer chains. Never a homogeneous solution is obtained.

The polymerisations in dioxane at ambient temperature based on a monomer concentration of 0.02 M also result in a phase separation, only this time a thermal treatment in dioxane is sufficient to cancel this and results in a homogeneous solution. The observations and SEC analyses yield strong indications that a physical polymer network is involved, which can be unravelled by a treatment at elevated temperature. The origin of this network can be due to an aggregation of polymers. Apparently, this feature is inherent to the Gilch route, because in Sulfinyl polymerisations no such behaviour has ever been observed.

A similar conclusion is found for polymers resulting from a Gilch polymerisation in THF based on a monomer concentration of 0.03 M, which at first exhibit some kind of microgel formation. A thermal treatment in dioxane at 98°C causes a halving of the M_w value, but this decline is not continued over prolonged heating, therefore supporting the idea of the unravelling of a physical network. However, thermal as well as chemical degradation of polymer chains does seem to occur when the polymer is subjected to temperatures of about 144°C in *o*-xylene.

Polymers, obtained from Gilch polymerisations in THF at a monomer concentration of 0.02 M, are subjected to 98°C in dioxane for at least 12h. The

results indicate that the initial irreproducibility of such polymerisations can possibly be improved by a thermal treatment.

3.8 EXPERIMENTAL SECTION

General remarks and instrumentation

^{1}H-NMR spectra were obtained in $CDCl_3$ at 300 or 400 MHz on a Varian Inova spectrometer using a 5 mm probe. Chemical shifts (δ) are expressed in ppm relative to the $CHCl_3$ absorption (7.24 ppm). All spectra were recorded at room temperature. Direct Insert Probe Mass Spectrometry (DIP-MS) analyses were carried out on a Finnigan TSQ 70, electron impact mode, mass range 35-550 and an interscan time of 2 s. The electron energy was 70 eV. Fourier transform infrared spectroscopy is performed on a Perkin-Elmer 1600 FT-IR (nominal resolution 2 cm^{-1}, summation of 16 scans). UV-vis measurements are performed on a Varian Cary Scan 500 spectrophotometer. Solutions have a concentration of about 10^{-4} M. The scan range was set from 200 to 800 nm. Molecular weights and molecular weight distributions were determined relative to polystyrene standards (Polymer Labs) with a narrow polydispersity by Size Exclusion Chromatography (SEC). Separation to hydrodynamic volume was obtained using a Spectra series P100 (Spectra Physics) equipped with two mixed-B columns (10 μm, 2 x 30 cm x 7.5 mm, Polymer Labs) and a refractive index (RI) detector (Shodex) at 40 °C. SEC samples are normally filtered through a 0.45 μm filter, but in case of filtration problems a 1.0 μm filter is used. HPLC grade THF (p.a.) is used as the eluent at a constant flow rate of 1.0 ml/min. Toluene is used as flow rate marker. Thin layer chromatography (TLC) is carried out on Merck precoated silica gel 60 F254 plates using chloroform as eluent.

Materials

All reagents are purchased from Aldrich, unless stated otherwise. Tetrahydrofuran and dioxane are dried over sodium and distilled prior to use. The

monomer 2,5-bis(chloromethyl)-1-(3,7-dimethyl-octyloxy)-4-methoxybenzene - also known as BCDM - (**8**) is put at our disposal by Covion Organic Semiconductors and therefore especially dr. H. Becker and dr. W. Kreuder are acknowledged. All glassware was dried overnight in a drying oven prior to use.
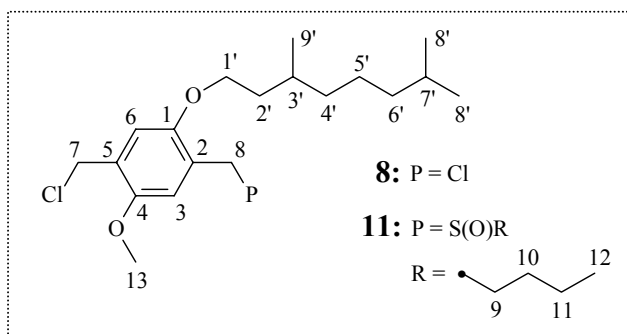
Figure 3.11: Atomic numbering of monomers used

Monomer Synthesis *of 1-[2-[(butylsulfinyl)methyl]-5-(chloromethyl)-4-methoxyphenoxy]-3,7-dimethyloctane (and isomer)* (**11**)

A solution of **8** (70.5 g, 0.195 mol) and tetrahydrothiophene (70 mL, 0.79 mol) in methanol (150 mL) is stirred for 70 hours at ambient temperature. The reaction mixture is precipitated in diethyl ether (1700 mL). The precipitate is collected, washed with *n*-hexane (300 mL), and dried under reduced pressure, yielding the corresponding bis-tetrahydrothiophenium salt (**9**) as a white hygroscopic solid (96.5 g, 85%).

A mixture of Na*t*BuO (7.54 g, 78.4 mmol) and n-butanethiol (7.07 g , 78.4 mmol) in 150 mL methanol is stirred for 30 minutes at ambient temperature. This clear solution is added in one portion to a stirred solution of **9** (46.5 g, 80 mmol) in 250 mL methanol. After one hour the reaction mixture is neutralised with aqueous hydrochloric acid (1.0 M), and concentrated under reduced pressure. The crude product is diluted with chloroform (250 mL) and filtrated to remove precipitate. The filtrate is concentrated *in vacuo*, thus yielding yellowish oil. To remove the tetrahydrothiophene an azeotropic distillation with *n*-octane or petroleum ether (boiling range: 100-130°C) is repeated three times to obtain 1-[2-

[(butylsulfanyl)methyl]-5-(chloromethyl)-4-methoxyphenoxy]-3,7-dimethyloctane (and isomer) (**10**) in a yield of 90%.

To obtain the corresponding sulfoxide an aqueous solution (35 wt.%) of hydrogen peroxide (19.4 g, 0.2 mol) is added dropwise to a solution of crude thioether (32.8 g, 78.4 mmol) in a mixture of 1,4-dioxane (300 mL), TeO_2 (1.55 g, 9.8 mmol) and some drops of concentrated HCl. After 3 hours the reaction is quenched by addition of 250 mL of a saturated NaCl solution. Extraction with chloroform (3 x 200 mL), drying of the combined organic layers over $MgSO_4$, filtration and concentration under reduced pressure affords a mixture of **8** (6%), **11** (86%) and the corresponding disulfoxide (8%) as yellow oil. The reaction mixture is purified by column chromatography (SiO_2, eluent: hexane / ethylacetate 60 / 40) to give pure **11** as a light yellow solid, which solidifies upon standing. ^{1}H NMR ($CDCl_3$, 300 MHz): δ 0.83 (d, J = 6.6 Hz, 6H, H8'), 0.90 (d, J = 6.3 Hz, 3H, H9'), 0.89 (t, J = 7.2 Hz, 3H, H12), 1.12 (m, 2H, H6'), 1.12 + 1.26 (m, 2H, H4'), 1.28 (m, 2H, H5'), 1.41 (m, 2H, H11), 1.46 (m, 1H, H7'), 1.51 + 1.71 (m, 2H, H2'), 1.51 (m, 1H, H3'), 1.71 (m, 2H, H10), 2.58 (m, 2H, H9), 3.65 (s, 3H, H13), 3.95 (m, 2H, H1'), 3.79 + 3.78 (dd, J_{AB} = 9.6 Hz, 2H, H8), 4.63 + 4.55 (dd, 2H, H7), 6.80 (d, J = 2.1 Hz, 1H, H6), 6.89 (d, J = 3.9 Hz, 1H, H3) ppm. IR (KBr): 2959, 2916, 2846, 1443, 1070, 847 cm^{-1}. MS (EI, m/z, rel. int. (%)): 431 ([M+1]$^+$, 100), 395 ([$C_{23}H_{39}O_3S$]$^+$, 10), 325 ([$C_{19}H_{30}ClO_2$]$^+$, 30), 163 ([$C_{10}H_{11}O_2$]$^+$, 30).

Mechanistic study on the Sulfinyl route in tetrahydrofuran

General Sulfinyl polymerisation procedure in THF at ambient temperature:

Preparation of poly[2-(3,7-dimethyloctyloxy)-5-methoxy-p-phenylene vinylene]: OC_1C_{10}-PPV

Prior to reaction a 100 mL three-neck flask with Teflon stirrer, and reflux condenser is flushed with nitrogen gas for about 30 minutes to create a nitrogen atmosphere. To degas the solvent the flask is charged with 20 mL of dry THF, the liquid level is marked, and N_2 gas is passed for about 15 minutes. Due to evaporation the flask has to be partially refilled till the mark is reached. Another 5 mL of dry THF is used to rinse in 0.5 mmol (0.2153 g) of solid **11** providing a monomer concentration of 0.02 M. All additives are added to the monomer

solution in an amount of 0.5 equivalents based on the amount of monomer (0.25 mmol; TEMPO: 0.040 g; CBr$_4$: 0.083 g; tBuϕCH$_2$Br: 0.060 g; tBuϕCH$_2$Cl: 0.046 g; tBuMeOPhOH: 0.0451 g). Polymerisation is initiated by addition of 1.3 equivalents (0.65 mmol, 0.073 g) of solid potassium *tert*-butoxide, maintaining a nitrogen atmosphere. After 2 hours at ambient temperature pouring the mixture in 250 mL of ice water stops reaction. Excess of base is neutralised by addition of 1.0 M aqueous hydrochloric acid, followed by extraction with chloroform (3 x 100 mL). The combined organic layers are concentrated under reduced pressure, and the precursor polymer is redissolved in 25 mL of toluene. Thermal elimination to the conjugated polymer takes place during 3 hours of reflux. The solution is cooled to about 40°C and a dropwise addition of 30 mL of methanol causes the polymer to precipitate (except in the case of additive **6**, where precipitation by addition of methanol only occurs after evaporation of toluene). The precipitated polymer is recovered by filtration, washed with methanol and dried under reduced pressure at room temperature. Residual fractions are concentrated *in vacuo*. ^{1}H NMR (CDCl$_3$, 300 MHz): δ 0.6-2.0 (br, 19H, H2'-H9'), 3.7-4.0 (br, 3H, H13), 4.0-4.2 (br, 2H, H1'), 7.1-7.3 (br, 2H, ϕC$\underline{H}$=C$\underline{H}\phi$), 7.3-7.6 (br, 2H, H3 + H6) ppm. IR (KBr): ν 2957, 2925, 2860, 1510, 1469, 1395, 1217, 1028, 872 cm^{-1}. NMR analyses of the residual fractions are discussed in section 3.3.2. TLC analyses of residual fractions: standard: R$_f$ = 0.93, 0.90, 0.66, 0.54, 0.37, 0.29, 0.16, tailing of starting spot till 0.08. TEMPO: concatenation of spots. tBuϕCH$_2$Cl: R$_f$ = 0.93, 0.88, 0.66, 0.54, 0.36, 0.29, 0.17, tailing of starting spot till 0.08. tBuϕCH$_2$Br: R$_f$ = 0.93, 0.87, 0.67, 0.54, 0.35, 0.29, 0.17, tailing of starting spot till 0.08. CBr$_4$: R$_f$ = 0.96, 0.93, 0.78, 0.70, 0.63, 0.34, 0.20, 0.12, tailing of starting spot till 0.05. Information on SEC results and polymer yields are listed in table 3.4.

Prior to reaction a 100 mL three-neck flask with Teflon stirrer, and reflux condenser is flushed with nitrogen gas for about 30 minutes to create a nitrogen atmosphere. To degas the solvent the flask is charged with 20 mL of dry THF, the liquid level is marked, and N$_2$ gas is passed for about 15 minutes. Due to evaporation the flask has to be partially refilled till the mark is reached. Another 5 mL of dry THF is used to rinse in 0.5 mmol (0.2153 g) of solid **11** providing a monomer concentration of 0.02 M. All additives are added in an amount of 0.5

equivalents based on the amount of monomer (0.25 mmol; TEMPO: 0.040 g; CBr$_4$: 0.083 g; tBuϕCH$_2$Br: 0.060 g; tBuϕCH$_2$Cl: 0.046 g) to the monomer solution. Polymerisation is initiated by addition of 1.3 equivalents (0.65 mmol, 0.073 g) of solid potassium *tert*-butoxide, maintaining a nitrogen atmosphere. After 2 hours at ambient temperature pouring the mixture in 250 mL of ice water stops reaction. Excess of base is neutralised by addition of 1.0 M aqueous hydrochloric acid, followed by extraction with chloroform (3 x 100 mL). The combined organic layers are concentrated under reduced pressure, and the precursor polymer is redissolved in 25 mL of toluene. Thermal elimination to the conjugated polymer takes place during 3 hours of reflux. The solution is cooled to about 40°C and a dropwise addition of 30 mL of methanol causes the polymer to precipitate. The precipitated polymer is recovered by filtration, washed with methanol and dried under reduced pressure at room temperature. Residual fractions are concentrated *in vacuo*. ^{1}H NMR (CDCl$_3$, 300 MHz): δ 0.6-2.0 (br, 19H, H2'-H9'), 3.7-4.0 (br, 3H, H13), 4.0-4.2 (br, 2H, H1'), 7.1-7.3 (br, 2H, ϕC$\underline{H}$=C$\underline{H}\phi$), 7.3-7.6 (br, 2H, H3 + H6) ppm. IR (KBr): ν 2957, 2925, 2860, 1510, 1469, 1395, 1217, 1028, 872

Mechanistic study on the Gilch route in tetrahydrofuran

General Gilch polymerisation procedure in THF at ambient temperature

Preparation of poly[2-(3,7-dimethyloctyloxy)-5-methoxy-p-phenylene vinylene]: OC$_1$C$_{10}$-PPV

A 100 mL three-neck flask with Teflon stirrer, reflux condenser and elbow to add solid base is flushed with nitrogen gas for about 30 minutes. Next, the reactor at room temperature is charged with 21 mL of dry THF, the liquid level is marked, and by passing N$_2$ through for about 15 minutes the solvent is degassed. Due to evaporation the flask has to be refilled till the mark is reached. With about 4 mL of dry THF 0.18 g (0.5 mmol) of solid 2,5-bis(chloromethyl)-1-(3,7-dimethyloctyloxy)-4-methoxybenzene (**8**) is rinsed in. All additives are added in an amount of 0.5 equivalents to the monomer solution (0.25 mmol; TEMPO: 0.040 g; CBr$_4$: 0.083 g; tBuϕCH$_2$Br: 0.060 g; tBuϕCH$_2$Cl: 0.046 g). Polymerisation is initiated by a first addition of 1.3 equivalents (0.65 mmol; 0.073 g) of solid potassium *tert*-butoxide. In most cases the viscosity increases

significantly while the reaction mixture turns from colourless to yellow / orange. After 10 minutes 3.3 equivalents (1.65 mmol; 0.185 g) of solid potassium *tert*-butoxide is added and the reaction mixture becomes a deep orange – except for the TEMPO experiments where a yellow colour with an orange tone is preserved. Stirring is continued for 2 hours. For work-up the solution is poured in 25 mL of ice water under vigorous stirring. 3.5 mL of 1.0 M aqueous hydrochloric acid and 2.5 mL of methanol are added, and the precipitated polymer is recovered by filtration over a P3 glass filter. The red fibrous polymer is washed with methanol and dried under reduced pressure at room temperature. Residual fractions are concentrated *in vacuo*. Characterisation of the polymer fraction is identical to the one described previously.

General purification procedure in THF

The polymers are purified using a similar procedure to that described in reference 16. The polymer is dissolved in 25 mL of THF and heated to 68°C. The solution is cooled to 40°C and a dropwise addition of methanol causes the solution to colour red due to precipitation of the polymer. The precipitated polymer is recovered by filtration, washed with methanol and dried under reduced pressure at room temperature. Again the residual fractions are concentrated *in vacuo*. Information on SEC results and polymer yields are listed in table 3.5.

Mechanistic study on the Gilch route in 1,4-dioxane

Gilch polymerisations in 1,4-dioxane at elevated temperature

Variation of base conditions: added as a solid, in amounts of 1.3 and 3.3 equivalents

A 100 mL three-neck flask with Teflon stirrer, reflux condenser and elbow to add solid base is flushed with N_2. The reactor at room temperature is then charged with 21 mL of dry dioxane, the liquid level is marked, and passing N_2 through it for about 15 min degasses the solvent. Due to evaporation the flask has to be refilled till the mark is reached. With about 4 mL of dry dioxane 0.18 g (0.5 mmol) of solid **8** is rinsed in and temperature is raised until 96°C. Polymerisation is initiated by a first addition of 1.3 equivalents (0.65 mmol; 0.073 g) of solid

potassium *tert*-butoxide. The viscosity increases significantly while the reaction mixture turns from colourless to yellow/orange. After 10 minutes 3.3 equivalents (1.65 mmol; 0.185 g) of solid potassium *tert*-butoxide is added and the reaction mixture becomes a deep orange. Stirring is continued for 2 h and afterwards the reaction mixture is subjected to work-up. The solution is cooled to 40°C and during vigorous stirring 25 mL of water is added slowly. Also 3.5 mL 1.0 M aqueous hydrochloric acid and 2.5 mL methanol are added, and the precipitated polymer is recovered by filtration. It is washed with methanol and dried under reduced pressure at room temperature. The residual fractions are concentrated *in vacuo*. The polymers are subjected to purification in THF, as described previously. Characterisation is identical to the one described under the general Sulfinyl polymerisation procedure in THF at ambient temperature. Information on SEC results and polymer yields are listed in table 3.6.

Variation of base conditions: added as a solid, in amounts of 2.6 and 2.0 equivalents

The polymerisation procedure is identical to the previous, except for the amounts of base added. Polymerisation is initiated by an addition of 2.6 equivalents (1.3 mmol; 0.146 g) of solid potassium *tert*-butoxide. The viscosity increases significantly while the reaction mixture turned from colourless to yellow / orange. After 10 minutes 2.0 equivalents (1.0 mmol; 0.112 g) of solid potassium *tert*-butoxide is added and the reaction mixture becomes a deep orange. Further work up, purification and characterisation is similar to the previous. Information on SEC results and polymer yields are listed in table 3.6.

Variation of base conditions: added as a solution

A 100 mL three-neck flask with Teflon stirrer, reflux condenser and septum is flushed with N$_2$. Two base solutions are prepared: a) 1.3 equivalents (0.65 mmol; 0.073 g) of K*t*BuO in 4 mL dioxane, and b) 3.3 equivalents (1.65 mmol; 0.185 g) of K*t*BuO in 7 mL dioxane. They are stirred for about 1 hour under a nitrogen atmosphere. The reactor at room temperature is then charged with 17 mL of dry dioxane, the liquid level is marked, and passing N2 through for about 15 minutes degasses the solvent. Due to evaporation the flask has to be partially

refilled till the mark is reached. With about 4 mL of dry dioxane 0.18 g (0.5 mmol) of solid **8** is rinsed in and temperature is raised until 96°C. Using a syringe the 4 mL base solution is added via the septum and polymerisation is initiated while the global volume of solvent of 25 mL is reached, together with the 0.02 M monomer concentration. The viscosity increases significantly while the reaction mixture turns from colourless to yellow/orange. After 10 minutes the second base solution (3.3 equivalents in 7 mL) is added via the septum making use of a syringe and the reaction mixture becomes a deep orange. Further work up, purification and characterisation is identical to the previous. Information on SEC results and polymer yields are listed in tables 3.6 and 3.10.

Gilch polymerisations in 1,4-dioxane at ambient temperature

First trials at room temperature

The polymerisation appliance is flushed with N_2 for about one hour. The reactor at room temperature is then charged with 21 mL of dry dioxane, the liquid level is marked, N_2 gas is passed through for about 15 minutes, and afterwards the flask is partially refilled. With about 4 mL of dry dioxane 0.18 g (0.5 mmol) of solid **8** is rinsed in. Polymerisation is initiated by addition of 1.3 equivalents (0.65 mmol; 0.073 g) of solid potassium *tert*-butoxide. The reaction mixture turns yellow. After 10 minutes 3.3 equivalents (1.65 mmol; 0.185 g) of solid potassium *tert*-butoxide is added and the viscosity increases significantly while the reaction mixture becomes a deep orange. Within the hour a phase separation between a red polymer lump and a yellowish solution is completed. Nevertheless, stirring is continued for 2 hours - as far as possible - and afterwards 25 mL of water, 3.5 mL 1.0 M aqueous hydrochloric acid and 2.5 mL methanol are added slowly to the reaction mixture. The precipitated polymer lump is recovered by filtration. It is washed with methanol and dried under reduced pressure at room temperature. The residual fraction is dried under reduced pressure.

In an attempt to dissolve the polymer lump a standard purification procedure in THF is applied, without much success. Next, 25 mL of dioxane is added and the mixture is brought to 96°C until a homogeneous solution is obtained. The solution is cooled to 40°C and addition of 30 mL of methanol caused the polymer

to precipitate as red fibres. These are washed with methanol, collected by filtration and dried under reduced pressure. Information on SEC results and polymer yields are listed in table 3.7.

In a second, similar polymerisation the temperature is raised to 98°C - after the regular 2 hours of reaction - until a homogeneous, deep orange solution is obtained. The solution is cooled to 40°C, methanol is added and causes the polymer to precipitate. It is recovered as red fibres by filtration, washed with methanol, and dried under reduced pressure. Next, the polymer is subjected to a standard purification procedure in THF. Information on SEC results and polymer yields are listed in table 3.7.

General polymerisation procedure in dioxane at ambient temperature towards OC$_1$C$_{10}$-PPV

A 100 mL three-neck flask with Teflon stirrer, reflux condenser and elbow to add solid base is flushed with N$_2$. The reactor at room temperature is then charged with 21 mL of dry dioxane, the liquid level is marked, and passing N$_2$ through it for about 15 min degasses the solvent. Due to evaporation the flask has to be partly refilled till the mark is reached. With about 4 mL of dry dioxane 0.18 g (0.5 mmol) of solid **8** is rinsed in. All additives are now added in an amount of 0.5 equivalents to the monomer solution (0.25 mmol; TEMPO: 0.040 g; CBr$_4$: 0.083 g; *t*BuφCH$_2$Br: 0.060 g; *t*BuφCH$_2$Cl: 0.046 g; MeOPhOH: 0.031 g; *t*BuMeOPhOH: 0.0451 g). Polymerisation is initiated by addition of 1.3 equivalents (0.65 mmol; 0.073 g) of solid potassium *tert*-butoxide. The reaction mixture turns from colourless to yellow. After 10 minutes 3.3 equivalents (1.65 mmol; 0.185 g) of solid potassium *tert*-butoxide is added and the viscosity increases significantly while the reaction mixture becomes a deep orange. Within the hour a phase separation between a red polymer lump and a yellowish solution is completed. Nevertheless, stirring is continued for 2 hours as far as possible and afterwards the reaction mixture is heated to 98°C until a homogeneous solution is obtained (2-12 h). For work-up the solution is cooled to 40°C and during vigorous stirring 25 mL of water is added slowly. Also 3.5 mL 1.0 M aqueous hydrochloric acid and 2.5 mL methanol are added, and the precipitated polymer

is recovered by filtration. It is washed with methanol and dried under reduced pressure at room temperature. The residual fractions are dried under reduced pressure. Information on SEC results and polymer yields are listed in table 3.8 and 3.9.

Additional experiment with TEMPO

Similar polymerisation procedure as for the previous TEMPO experiment in which 0.5 equivalents (0.040 g) of TEMPO are added to the monomer solution (0.5 mmol; 0.1800 g in 25mL of dioxane). Except for this time an additional amount of 0.2 equivalents (0.016 g) of TEMPO is added to the reaction mixture together with the second portion of base (3.3 equivalents, 0.073 g added as a solid). Further work up is identical to the one described previously.

Additional experiments on additives 5, 6 and 7

A 100 mL three-neck flask with Teflon stirrer, reflux condenser and septum is flushed with N_2. Two base solutions are prepared under a nitrogen atmosphere: a first of 1.3 equivalents (0.65 mmol; 0.073 g) of KtBuO in 4 mL dioxane, and a second containing 3.3 equivalents (1.65 mmol; 0.185 g) of KtBuO in 7 mL dioxane.

Additives are added to the first base solution respecting the following concentrations: **a**) 0.5 equivalents (0.25 mmol; 0.031 g) MeOPhOH and 1.3 equivalents (0.65 mmol; 0.073 g) KtBuO in 4 mL dioxane; **b**) 0.25 mmol (0.031 g) MeOPhOH and 2.6 equivalents (1.3 mmol; 0.146 g) KtBuO in 8 mL dioxane; **c**) 0.25 mmol (0.0451 g) tBuMeOPhOH and 2.6 equivalents (1.3 mmol; 0.146 g) KtBuO in 8 mL dioxane; **d**) 0.25 mmol (0.0591 g) di-tBuMeOPhOH and 2.6 equivalents (1.3 mmol; 0.146 g) KtBuO in 8 mL dioxane.

The reactor at room temperature is then charged with 17 mL of dry dioxane, the liquid level is marked, and passing N_2 through for about 15 minutes degasses the solvent. Due to evaporation the flask has to be partially refilled till the mark is reached. With about 4 mL of dry dioxane 0.18 g (0.5 mmol) of solid **8** is rinsed in and temperature is raised until 96°C. Using a syringe, the 4 mL base solution (containing the additive) is added via the septum and polymerisation is initiated. The global volume of solvent of 25 mL together with the 0.02 M monomer

concentration is now reached. After 10 minutes the second base solution (consisting of 3.3 equivalents (1.65 mmol; 0.185 g) of K*t*BuO dissolved in 7 mL dioxane for reaction **a**); and 2.0 equivalents (1.0 mmol; 0.112 g) K*t*BuO dissolved in 7 mL dioxane for reactions **b**), **c**) and **d**)) is added via the septum making use of a syringe.

After the standard reaction time of 2 hours the reaction mixtures still has yellow as the main colour. Addition of water does not result in precipitation for reaction **b**) and **c**), but for the latter an oily fraction is withheld by filtration. Filtrates are extracted with chloroform (3 x 50 mL), and the combined organic layers are dried under reduced pressure, thus constituting residual fractions. Reaction **b**) only results in such a residual fraction, because no polymer could be collected. Information on SEC results and polymer yields are listed in table 3.11.

*Deprotonation test on additives **5**, **6** and **7***

An amount of about 0.5 g of additive is dissolved in 10 mL of diethyl ether and is subsequently and repeatedly washed with 10 mL of an aqueous 2 M NaOH-solution. The aqueous layers are collected and acidified by addition of an aqueous hydrogen chloride solution, resulting in a cloudiness of the solution. In case of additives **5** and **6** a pink coloration of the aqueous layers is demonstrated. The diethyl ether layer is subjected to TLC analysis prior to and after the washing procedure, leading to the observation that in all cases after the washing some remaining additive is present. For the TLC analysis chloroform is used as eluent and yields the following R_f-values: MeOPhOH: 0.08; *t*BuMeOPhOH: 0.37; di*t*BuMeOPhOH: 0.79.

Gelation reactions

In THF based on a monomer concentration of 0.2 M

A 100 mL three-neck flask with Teflon stirrer, reflux condenser and elbow to add solid base is flushed with N_2. The reactor at room temperature is then charged with 21 mL of dry tetrahydrofuran, the liquid level is marked, and passing N_2 through it for about 15 min degasses the solvent. Due to evaporation the flask has to be partly refilled till the mark is reached. With about 4 mL of dry THF 1.8 g (5 mmol) of solid **8** is rinsed in. Polymerisation is initiated by addition

of 1.3 equivalents (6.5 mmol; 0.73 g) of solid K*t*BuO. The reaction mixture turns yellow to orange with some orange parts floating in the solution. After 10 minutes 3.3 equivalents (16.5 mmol; 1.85 g) of solid K*t*BuO is added: the viscosity increases rapidly and within 5 minutes an orange gel is obtained, occupying all of the original space. Nevertheless, only after 2 hours 25 mL of water is added to the reaction mixture. As a result the gel lump colours reddish on the outer surface and starts floating on the yellow solution. Filtration turns out to be impossible. Therefore chloroform is added in an attempt to extract the polymer, but this causes the gel to swell even more, while the surrounding solvent turns orange. The large lump of gel is separated as good as possible, while the orange solution is subjected to precipitation in methanol after concentration under reduced pressure resulting in a small amount of fibrous, red polymer. Both polymer fractions are analysed. Information on SEC results and polymer yields are listed in table 3.12. ^{1}H-NMR characterisation is in accordance with OC$_1$C$_{10}$-PPV, but especially the gel fraction exhibits a broadening of signals as is explained in section 3.6.1.

In 1,4-dioxane based on a monomer concentration of 0.2 M

Similar experimental set up as the previous, only this time dioxane is used as solvent. Reaction is performed on a monomer concentration of 0.2 M (5 mmol of solid **8** dissolved in 25 mL of dioxane). The addition of 1.3 equivalents (6.5 mmol; 0.73 g) of solid K*t*BuO immediately results in a phase separation: a large lump of polymer starts floating on a yellowish solution and covers the whole surface. After 10 minutes 3.3 equivalents (16.5 mmol; 1.85 g) of solid K*t*BuO is added, but the phase separation does not allow a homogeneous distribution thereof. Addition of 25 mL of water to the reaction mixture does not change much. The impenetrable collapsed polymer lump hampers further work up. Only the outer surface is reached. The lump is separated and dried under reduced pressure.

The lump of polymer is subjected to a sequence of thermal treatments: it is successively dissolved in 250 mL of THF, dioxane and *o*-xylene and heated for three hours at 68°C, 96°C and 144°C respectively. Each time precipitation occurs by addition of 250 mL of methanol at 40°C and next filtration yields the polymer

fraction. Information on corresponding SEC results and yields is listed in table 3.13. ^{1}H-NMR analyses are in accordance with OC_1C_{10}-PPV, but they exhibit a broadening of signals as is explained in section 3.6.1.

In THF based on a monomer concentration of 0.03 M

A 100 mL three-neck flask with Teflon stirrer, reflux condenser and elbow to add solid base is flushed with N_2. The reactor at room temperature is then charged with 20 mL of dry tetrahydrofuran, the liquid level is marked, and passing N_2 through it for about 15 min degasses the solvent. Due to evaporation the flask has to be partly refilled till the mark is reached. With about 5 mL of dry THF 0.271 g (0.75 mmol) of solid **8** is rinsed in. Polymerisation is initiated by addition of 1.3 equivalents (0.975 mmol; 0.1094 g) of solid K*t*BuO and the reaction mixture turns yellow. After 10 minutes 3.3 equivalents (2.475 mmol; 0.278 g) of solid K*t*BuO is added: the viscosity increases rapidly and within 5 minutes a strongly viscous but more or less homogeneous orange solution is obtained. The stirrer needs to be set at maximum speed to obtain an effect. After 2 hours 25 mL of ice water is added to the reaction mixture resulting in an orange-red solution. Neutralisation by addition of an aqueous hydrogen chloride (1 M) solution and addition of 3 mL of methanol yield a separation between a red, fibrous polymer lump and a yellow-orange solution. The polymer is recovered by filtration, washed with methanol and dried under reduced pressure.

Thermal treatments

Next, 25 mL of p.a. THF is added to the polymer and temperature is raised to 68°C for 2 hours under a nitrogen atmosphere after which an orange solution that seems to be homogeneous is obtained. Addition of 30 mL of methanol causes the polymer to precipitate in the appearance of a red, fibrous lump. The polymer is recovered by filtration, washed with methanol and dried under reduced pressure.

Subsequently, 25 mL of dioxane is added to the polymer and temperature is raised until 98°C for 12 hours maintaining a nitrogen atmosphere. A homogeneous orange solution is obtained from which polymer precipitation is caused by addition of 30 mL of methanol. A red powdery to fibrous polymer is

recovered by filtration, washed with methanol and dried under reduced pressure. This treatment is repeated once.

At the end, 25 mL of *o*-xylene is added to the remaining polymer and temperature is raised until 144°C for only 2 hours preserving a nitrogen atmosphere. A clear and homogeneous orange solution is obtained. Addition of 30 or more mL of methanol at first only results in a troubling of the solution, but after a difficult, troublesome filtration some orange polymer can be collected in the form of a film, which is then dried under reduced pressure.

After each step about 10 to 15 mg of polymer is withheld to prepare SEC and NMR samples. Residual fractions are dried under reduced pressure. Information on SEC results and polymer yields are listed in tables 3.14 and 3.15. ^{1}H-NMR characterisation of the polymer fractions is in accordance with OC$_1$C$_{10}$-PPV. The mentioned UV-vis measurements are performed on polymer solutions in p.a. THF respecting a concentration of approximately 10^{-4} M.

Thermal treatments of Gilch polymers synthesised in THF based on a monomer concentration of 0.02 M

A selection of the polymers of which the SEC data are presented in table 3.5 is subjected to a thermal treatment in dioxane at 98°C. Each of them is dissolved in 25 mL of p.a. dioxane and the temperature is raised to 98°C under a nitrogen atmosphere for a certain time period specified in section 3.6.4 and table 3.16. Homogeneous orange solutions are obtained and addition of 30 mL of methanol causes the polymer to precipitate as a red, fibrous lump. The polymer is recovered by filtration, washed with methanol and dried under reduced pressure.

To a polymer resulting from a Gilch polymerisation in THF in the presence of 0.5 equivalents of *t*BuφCH$_2$Br 25 mL of *o*-xylene is added and temperature is raised to 144°C for 2 hours, maintaining a nitrogen atmosphere. A homogeneous orange solution is obtained from which polymer precipitation is caused by addition of 30 mL of methanol. An orange-red powdery polymer is recovered by filtration, washed with methanol and dried under reduced pressure. The corresponding SEC-data are listed in tables 3.16 and 3.17.

3.9 REFERENCES

1.   B.R. Hsieh, Y. Yu, A.C. VanLaeken, H. Lee, *Macromolecules*, **30** (1997) 8094.

2.   C.J. Neef, J.P. Ferraris, *Macromolecules*, **33** (2000) 2311.

3.   L. Hontis, M. Van Der Borght, D. Vanderzande, J. Gelan, *Polymer*, **40** (1999) 6615.

4.   H. Becker, H. Spreitzer, W. Kreuder, E. Kluge, H. Schenk, I. Parker, Yong Cao, *Adv. Mater.*, **12(1)** (2000) 42.

5.   a) G.H. Gelinck, J.M. Warman, E.G.J. Staring, *J. Phys. Chem.*, **100** (1996) 5485; b) C.J. Brabec, N.S. Sariciftci, J.C. Hummelen, *Adv. Funct. Mater.*, **11(1)** (2001) 15; c) J. Manca, *LUC-nieuws*, **oktober** (2001) 28; b) L. van der Ent, *Kunststof magazine*, **april 3** (2001) 38.

6.   G. Odian, Principles of polymerisation, 3rd edition, John Wiley & Sons, inc. (1991) p. 243.

7.   a) D. Vanderzande, A. Issaris, M. Van Der Borght, A. van Breemen, M. de Kok, J. Gelan, *Macromol. Symp.*, **125** (1997) 189; b) A. Issaris, *Ph.D. Dissertation*, 1997, Limburgs Universitair Centrum, Diepenbeek, België

8.   L.A. Errede, R.S. Gregorian, J.M. Hoyt, *J. Am. Chem. Soc.*, **82** (1960) 5218.

9.   G. Odian, Principles of polymerisation, 3rd edition, John Wiley & Sons, inc. (1991) p. 259.

10. F.R. Denton III, P.M. Lahti, F.E. Karasz, *J. Polym. Sci. Part A: Polym. Chem.*, **30** (1992) 2223.

11. A. Issaris, D. Vanderzande, J. Gelan, *Polymer*, **38(10)** (1997) 2571.

12. Y. Yu, A.C. VanLaeken, L. Hookun, B.R. Hsieh, *Polymer Preprints*, **39(1)** (1998) 161.

13. a) B.R. Hsieh, Y. Yu, E.W. Forsythe, G.M. Schaaf, W.A. Feld, *J. Am. Chem. Soc.*, **120** (1998) 231; b) B.R. Hsieh, Y. Yu, G.M. Schaaf, W.A. Feld, *Polymer Preprints*, **39(1)** (1998) 163; c) R. Dagani, *C&EN*, **january 19** (1998) 9.

14   ACROS catalogue 2001-2002, p. 625 ; Merck index 12, 1582.

15. M. Valoti, H.J. Sipe, G. Sgaragli, R.P. Mason, *Arch. Biochem. Biophys.*, **March** (1989).

16. H. Becker, H. Spreitzer, K. Ibrom, W. Kreuder, *Macromolecules*, **32** (1999) 4925.

17. A.J.J.M. van Breemen, *Ph.D. Dissertation*, 1999, Limburgs Universitair Centrum, Diepenbeek, België.

18. D.M. Johansson, G. Srdanov, G. Yu, M. Theander, O. Inganäs, M.R. Andersson, *Macromolecules*, **33** (2000) 2525.

19. Personal communication with dr. H. Becker from Covion Organic Semiconductors.

20. Finley, K.T. in 'Chemistry of quinonoid compounds', ed. E.S. Patai, Wiley, New York (1974) p. 339.

4 | Characterisation of Polymers by means of (SEC-)LS

This chapter concerns the characterisation of polymers using the relatively new technique of light scattering – eventually coupled with size exclusion chromatography (SEC) and viscometry. In a first section some background of the light scattering theory from macromolecular solutions is given. Next, in section 2 and 3, it is focussed on the individual instruments and the experimental set up used to give an idea about the complexity of the appliance. In a fourth section the technique is applied on Sulfinyl PPV-precursor polymers, synthesised in different solvents. Further, the results of a light scattering study on Gilch and Sulfinyl OC_1C_{10}-PPV will be discussed. These polymers are also subjected to a branching study to detect possible differences in structure inherent to the synthetic route used.

4.1 THEORETICAL BACKGROUND[1-4]

A typical rapid and convenient means to determine polymer molecular weights and molecular weight distributions (MWDs) is size exclusion chromatography (SEC). Usually, a differential refractive index (RI) detector is placed after the columns to detect the molecular species eluting according to their hydrodynamic volume. A correlation between the RI detector response – which is proportional to the concentration of the eluting species – and the molecular weight of the unknown sample is required for deriving molecular weight data from SEC and a common method for this is the use of a conventional calibration curve. In organic solvents, for example, mostly narrow – monodisperse -

polystyrene standards are used. The set up is simple and concentrations do not have to be known exactly. Unless the polymer in question is polystyrene as well, this method yields only relative values.

In contrast, static light scattering detectors can provide *absolute* molecular weight and size information, or in other words these quantities are determinable without reference to any size or mass reference standards. All the constants required are measured experimentally – they do not depend on empirical relations (as in universal calibration). The phenomena associated with light scattering are encountered widely in every day life. An impressive example of light scattering is the scattering of sunlight on particles in the atmosphere giving rise to the blue colour of the sky and the spectacular colours that can sometimes be seen at sunrise and sunset. The theory of light scattering – among others developed by Einstein[5] and Raman[6] – was extended to macromolecular solutions and suspensions by Debye[7] and Zimm[8], and others.

In general, the interaction of electromagnetic radiation with a molecule can lead either to absorption or scattering of the radiation. The latter can be explained as follows. By exposing a small, isotropic molecule to a vertically polarised, monochromatic light beam, the electrical field causes the electrons of the molecule to oscillate with the same frequency as the incident rays. These oscillating electrons then serve as secondary sources of electromagnetic radiation: the scattered light, which has – in the case of elastic or Rayleigh scattering – a similar wavelength, but a different amplitude than the incident light (figure 4.1). This phenomenon is also called static or classical light scattering.
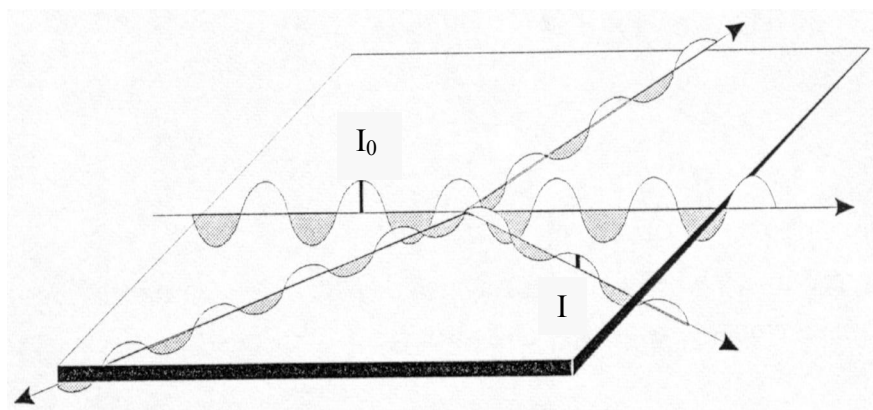
Figure 4.1: **Rayleigh scattering of an isotropic scattering molecule**
irradiated with vertically polarised light

For molecules in solution the quantity measured with static light scattering is the 'excess Rayleigh ratio', $R(\theta)$, which is proportional to the light scattering of the sample at an angle θ (I_θ) above that of the pure solvent ($I_{\theta,S}$), divided by the incident intensity (I_0):

$$R(\theta) \approx \frac{(I_\theta - I_{\theta,S})}{I_0} \qquad (1)$$

The Rayleigh theory assumes that the molecule is much smaller than the incident wavelength ($d \ll \lambda / 20$), which causes $R(\theta)$ to be independent of the angle. For particles with a diameter larger than 5% of the wavelength of the incident light, intramolecular interferences occur and in this case it is mostly referred to as Debye scattering. As a rule of thumb, for molecules > 50 000 g / mol or 10 nm diameter, the intensity of the scattered light varies with angle. The scattering intensity decreases due to increasing destructive interference at higher angles. This is expressed by the particle scattering function $P(\theta)$ - a characteristic that can be used to calculate the radius of the molecule without assumptions about the conformation (rod, random coil or sphere) provided that the scattering intensity is measured at enough (over two) angles.

Tremendous advances in personal computers and new electronics together with flexible and versatile data acquisition and processing software played

significant roles in the returning of light scattering to the arsenal of analytical chemists. In the seventies, Low Angle Laser Light Scattering (LALLS) photometers were launched on the market using one angle - enough to provide molecular weight information for very small Rayleigh scatterers. But advantages are gained from two or more detector angles leading to a commercial introduction of the Multi Angle Laser Light Scattering (MALLS) detector in the eighties. It represents an analytical technique for determining absolute molecular weights and sizes, without making assumptions. The amount of light scattered by a suspension of molecules may be used to determine directly their weight-average molecular weight, while the angular variation of the scattering reveals the molecules' mean square size. The fundamental relationship linking the intensity of scattered light, the scattering angle, and the molecular properties is:

$$\frac{K\,c}{R(\theta)} = \frac{1}{M_w\,P(\theta)} + 2\,A_2\,c \tag{2}$$

Where:
- $R(\theta)$ is the excess intensity of scattered light (excess Rayleigh ratio) at instrument angle θ,
- c is the sample concentration, expressed in g/mL,
- A_2 is the second virial coefficient, which is a measure for the polymer-solvent interaction: the higher and more positive the value, the better is the thermodynamic quality of the solvent for the given polymer,
- K is an optical parameter equal to $4\pi^2 n_0^2\,(dn/dc)^2 / (\lambda_0^4 N_A)$, $\qquad\qquad$ (3)
- n_0 is the refractive index of the solvent at the given wavelength,
- N_A is Avogadro's number,
- and λ_0 is the wavelength of the scattered light in vacuum.
- The particle light scattering function $P(\theta)$ describes the scattered light's angular dependence. The important property of $P(\theta)$ is that it is a function of particle size[4,9]:

$$P^{-1}(\theta) = \frac{R(\theta)}{R_0} = 1 + \frac{16\pi^2 n_0^2}{3\lambda_0^2}\,<r_g^2>_z\,\sin^2(\theta/2) \tag{4}$$

- R_0 is the excess Rayleigh ratio at angle zero,

- the root mean square (RMS) radius $<r_g^2>^{1/2}$ is often called the radius of gyration, and describes the size of a macromolecular particle in a solution, regardless of its shape. To elucidate this parameter the macromolecule is divided into σ small elements of identical mass, with each element at a distance s_i from the centre of gravity. For a flexible chain only the average of r_g has practical meaning:

$$<r_g^2>^{1/2} = \frac{1}{\sigma + 1} \sum_{i=1}^{\sigma} <s_i^2> \tag{5}$$

These equations express the foundation of the theory of light scattering at macromolecular solutions and they are used in the calculations performed by the software. As a consequence of the progress in data collection, processing software and the enhancement of the ease of application, these calculations have receded into the background. However, it is interesting to keep them in mind during interpretation of the results.

4.2 INSTRUMENT SPECIFICATION[9]

Driven by the need to more fully characterise an increasingly complex array of new polymers, there has been an increasing demand to get more information out of SEC. As a result, specialised detectors have been developed to couple with SEC, among which the laser light scattering and the viscometer detector. Because both detector responses depend on the concentration of the sample, neither can operate very well without the nearly universal concentration detector in liquid chromatography: the refractometer. In this section the main parts of the appliance used will be discussed individually.

4.2.1 The Solvent

The solvent (THF) should be degassed to prevent pulsation of the pump and to prevent the occurrence of spikes in the chromatograms. This is done by an in-line degasser system. Particles from the chromatographic system, including the

solvent and the column, can render a static light scattering detector difficult to use by creating an unstable baseline. These detectors are more difficult to stabilise and keep running than other detectors and can be quite sensitive to dirt in the chromatographic system. The quality mostly used for these measurements is HPLC-grade solvent, but a thorough filtration still is necessary to prevent damaging of the pump heads, the columns and interfering scattering by dust particles at the light scattering detector. For this reason the solvents used are filtrated five times: three times over a 0.2 μm and two times over a 0.02 μm filter disc.

4.2.2 The Columns

The most common SEC-columns for organic solvents contain a highly crosslinked spherical polystyrene / divinylbenzene gel as matrix. In our laboratory PL gel 10 μm mixed-bed columns are used - meaning that the particle size of the gel is 8 to 10 μm while the pore sizes vary from Ångstroms to several nanometers. They are designed to provide good resolution with relatively low pressures for enhanced lifetimes and span a wide range of molecular weights (from 500 to 10 000 000 g/mol), with a linear calibration curve. In view of detector stability it is important to use columns of good quality that don't shed particles.

4.2.3 The Light Scattering Detector

The light scattering detector present in our laboratory is a Dawn-F instrument from Wyatt Technology Corporation. It is a multi angle laser light scattering detector, equipped with a Helium-Neon laser as light source, producing vertically polarised light of a constant wavelength (λ_0) of 632.8 nm. The flow cell consists of a massive glass body (with a known refractive index of 1.617) around which eighteen discrete photodetectors are spaced around in a planar, ellipsoid geometry (figure 4.2). The distances of the photodiodes to the cell is such that intensity differences of anisotropically scattering molecules are not too large, ensuring that measurements may be made simultaneously over a broad range of

angles (typically from 15 – 160°, depending on solvent-glass refractive indices). The temperature inside the light scattering photometer is 30°C ± 2°C.
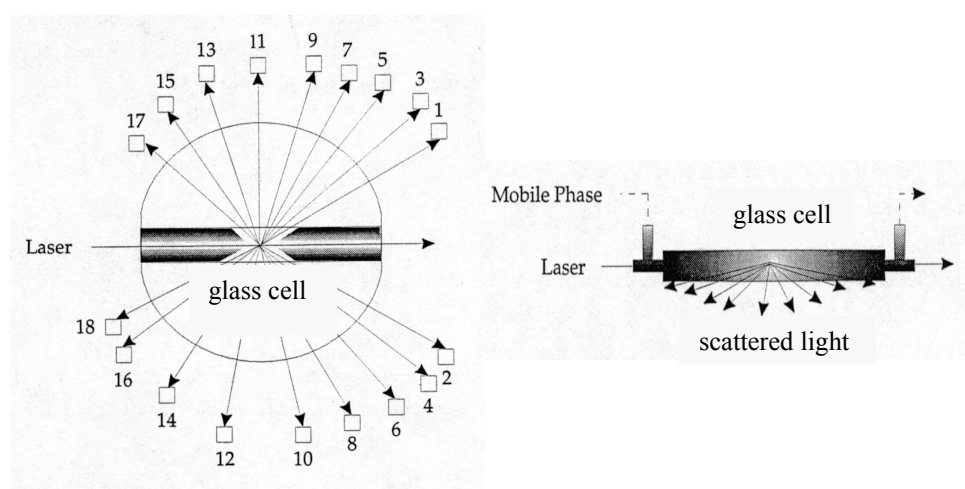
Figure 4.2: Schematic representation of the flow cell and the 18 discrete detectors – right: top view; left: side view

4.2.4 The Concentration Detector

The Optilab DSP from Wyatt Technology Corporation is a differential refractometer (RI detector) that is based upon a special interferometric measurement method to enhance sensitivity and stability (to temperature and pressure changes) (figure 4.3). A collimated light source is plane polarised at 45° to the horizontal and split into two orthogonally polarised components of equal intensity by a first Wollaston prism. The horizontally polarised beam passes through a reference cell, while the vertically polarised beam passes through a sample cell and undergoes a phase shift, due to the extra refractive index, Δn, of the sample. The relative phase shift φ is directly proportional to the refractive index difference and equals $2\pi L\Delta n/\lambda$ where L is the cell path length (1.0 mm) and λ is the optical wavelength in vacuum. The beams are recombined in the second Wollaston prism (and a quarter wave plate) to yield a plane polarised beam, rotated over an angle $\varphi/2$ with respect to the original 45°. By measuring the orientation of the plane of polarised light by a polarisation filter the output is

quantitatively correlated to the refractive index difference between the sample and reference cells.
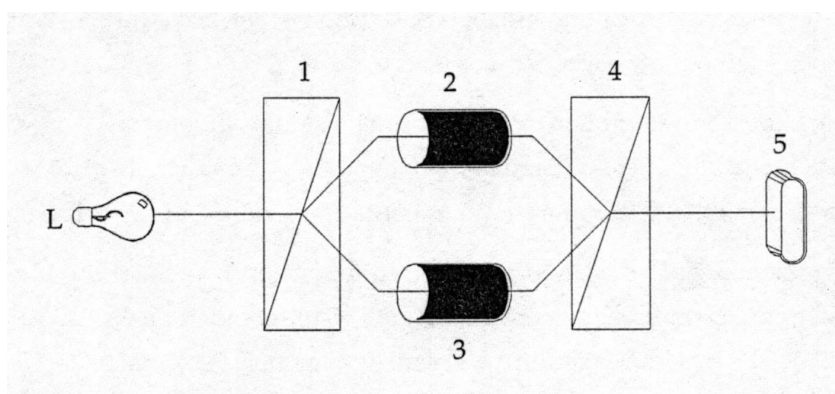
Figure 4.3: Simplified schematic representation of an interferometric differential refractometer. L: light source ; 1,4: Wollaston prisms ; 2: sample cell ; 3: reference cell ; 5: detector

Because refractive indices are strongly dependent on temperature and wavelength of the incident light, the instrument is equipped with an interference filter and a temperature control unit. The former selects light of a specific wavelength, $\lambda = 630$ nm, corresponding well with the 632.8 nm of the light scattering photometer, while the latter is included in the instrument to maintain a constant temperature of $40°C \pm 0.1°C$.

4.2.5 The Viscometry Detector

The working principle of the H 502 B viscometer from Viscotek Corporation is based on the principle of a Wheatstone bridge in electrical circuits, and consists of a bridge of four capillaries of equal resistances as shown in figure 4.4. It is designed for the accurate determination of very small sample volume specific viscosities. The polymer sample flows down both sides of the bridge equally, but half of the sample is strongly diluted in a hold up reservoir (forming the reference line). A differential pressure transducer monitors the resulting pressure drop across the bridge, ΔP, while an inlet pressure transducer measures the pressure drop through the reference capillary, P_i. The specific viscosity, η_{sp}, is

derived directly from the flow of a sample / solvent mixture across one leg of the capillary bridge according to the equation: $[\eta_{sp}] = 2\ \Delta P/P_i$. The compensation reservoir is meant to compensate for temperature and / or compressibility effects. A temperature control unit maintains a temperature of 35 to 40°C.
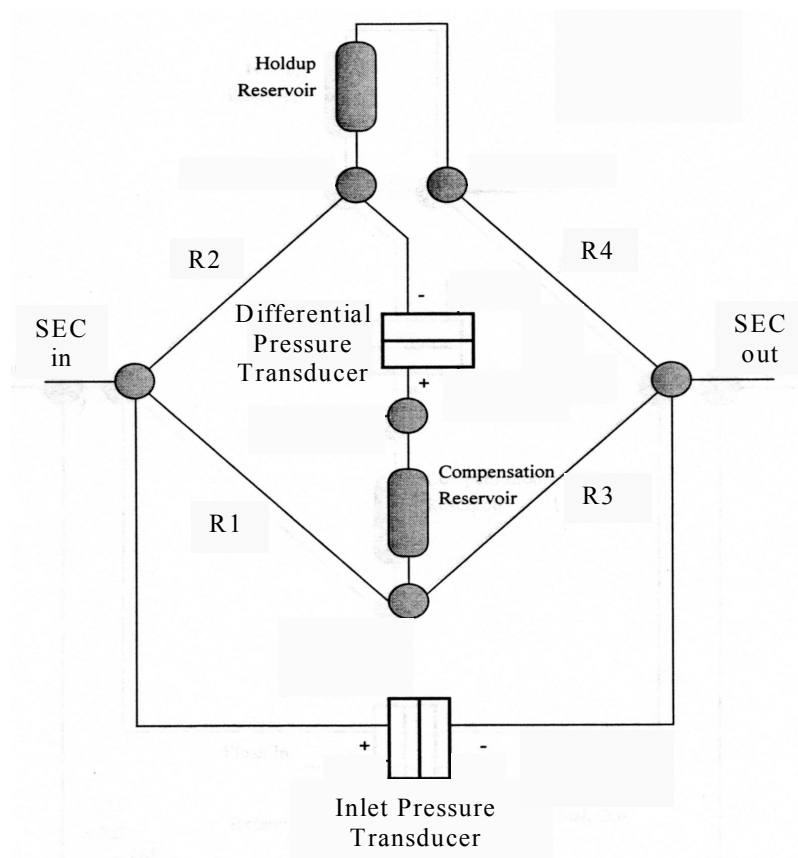
Figure 4.4: Schematic representation of the viscometer based on the principle of a Wheatstone bridge

4.3 EXPERIMENTAL SET UP[10-12]

In our laboratory a multi-detector SEC-LS set up is present that consists out of an isocratic HPLC pump, an autosampler, two PL-gel columns, a light scattering detector, a refractive index (concentration) detector and a viscometer

detector. The solvent used for the measurements is tetrahydrofuran (THF). In this section the different set ups will be discussed in some more detail.

4.3.1 <u>MALLS in Batch Mode – Off-line</u>

By using the Optilab and the Dawn off-line, the specific refractive index increment for a change of solute concentration, *dn/dc*, can be determined for each new polymer, and a Zimm plot constructed. The latter enables determination of the absolute weight-average molecular weight, the z-average RMS radius and the second virial coefficient. In this set up (figure 4.5) a 5 mL injection loop, build in between the HPLC pump and the LS photometer in series with the RI detector, is used to introduce a concentration range of polymer samples. The software packages DNDC 5.10 and Astra 4.50 from Wyatt Technology Corporation are used simultaneously on distinct computers.
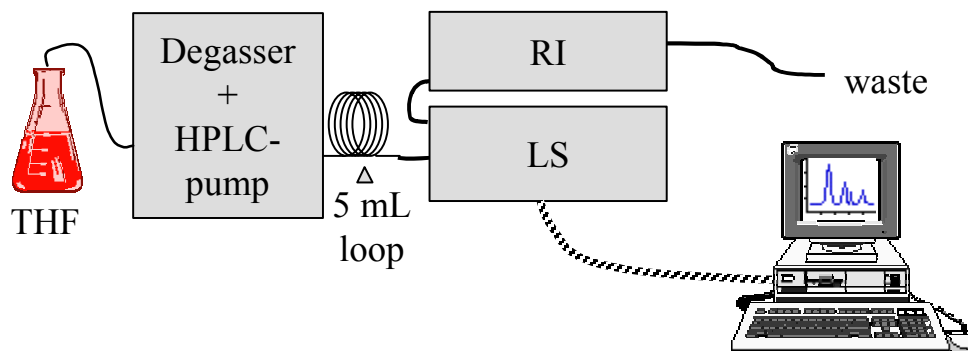
Figure 4.5: Off-line set up

4.3.1.1 Determination of the dn/dc-value

The specific refractive index increment, dn/dc, is a characteristic of prime importance, because its square is found in the equation of K (equation 3). The dn/dc is actually the slope of the dependence of the refractive index, n, of the solution on the polymer concentration. In dilute solutions dn/dc is usually a constant and can be satisfactorily approximated by the ratio $\Delta n/c$, where Δn is the difference between refractive indices of the solution and pure solvent. Measure the refractive index of several solutions of varying concentration, plot the data Δn

versus c, and the value of the slope equals dn/dc. To obtain absolute measurements it is of importance that the dn/dc is determined at the same wavelength as the light scattering photometer operates on.

4.3.1.2 Construction of a Zimm plot

For the analysis of light scattering measurements mostly the method of Zimm is used. Herefore, samples of a polydisperse solution are prepared over a range of low concentrations, and measured over various angles. The corresponding data are displayed in a so-called Zimm plot. To construct a Zimm plot, $y = K c / R(\theta)$ is plotted versus $\sin^2(\theta/2) + k c$ (figure 4.6).
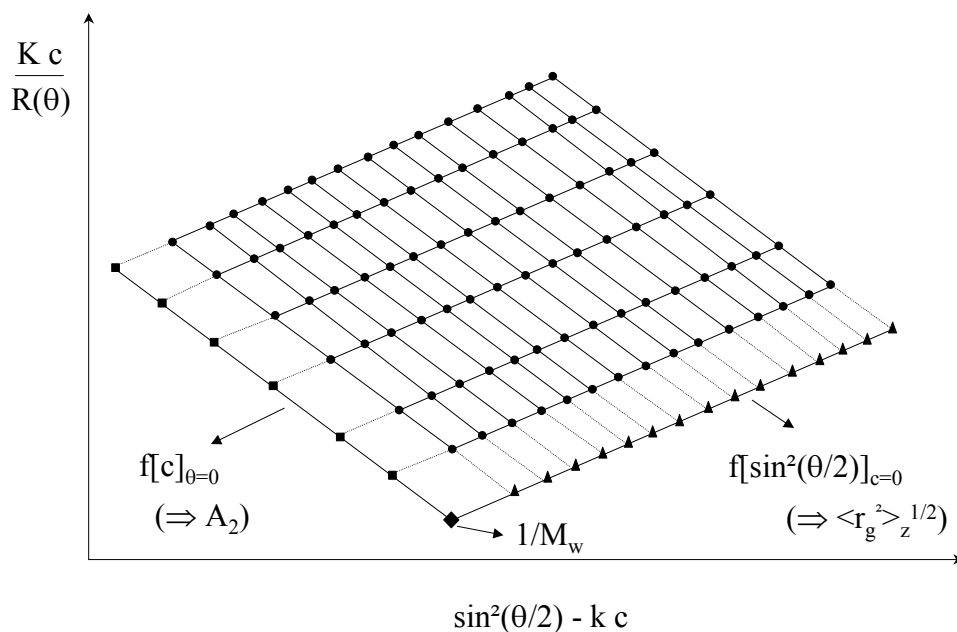
Figure 4.6: Example of a Zimm plot, where:

●: measured data points; ▲: extrapolation function f to c = 0 g/L to determine A_2;

■: extrapolation function f to θ = 0 to determine $<r_g^2>_z^{1/2}$;

♦: point of intersection to determine $1/M_w$

The quantity k is a scaling or stretch factor which scales the contributions from c to be roughly equal to the contributions from $\sin^2(\theta/2)$. Its value or sign has no effect on the numerical results obtained, but a proper choice improves the appearance of the plot. For this reason, the Zimm plots displayed in this work use a negative scale factor.

From the slope of the angular dependent axis at c = 0 g/L the z-average RMS radius is calculated, while the slope of the concentration dependent axis at $\theta = 0°$ is used to determine the second virial coefficient. The double projection to zero angle and zero concentration (the point of intersection) yields the inverse of the weight-average molecular weight.

4.3.2 <u>MALLS Coupled with SEC (SEC-LS) –</u>
<u>In-line Triple Detection</u>

In the coupled set up the LS photometer, the RI detector and the viscometer are put in series after the columns and the loop is replaced by an autosampler (figure 4.7). This detector sequence is maintained because the light scattering detector is the most sensitive to pressure build up. In this set up the light scattering data are limited to one angle, mostly the 90° detector, because this normally shows the maximum sensitivity – hence, the best signal-to-noise ratio - of all detectors.

Figure 4.7: Coupled set up: triple detection

This set up together with the calculation methods enable determination of absolute number, M_n, weight, M_w, and z-average molecular weights, M_z, the various average root mean square (RMS) radii, $\langle r_g^2 \rangle^{1/2}_{n,m,z}$, and polydispersity values. This i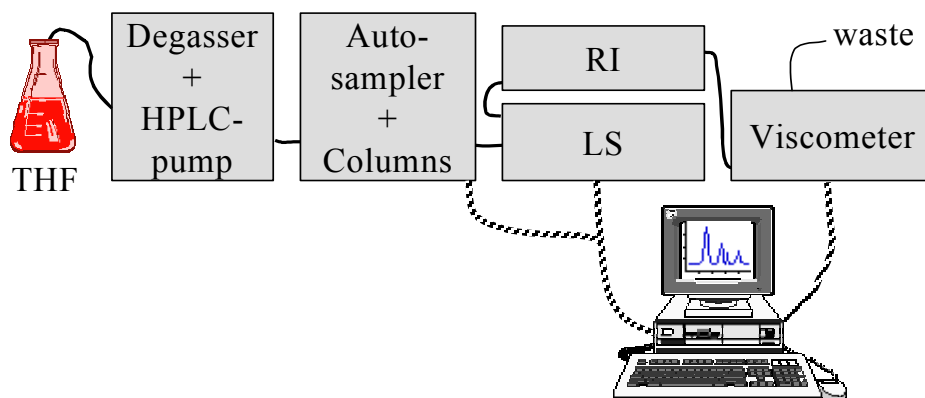s possible thanks to the software that divides chromatograms in slices and calculates the values for each slice. Recordings and calculations are performed using the software packages Astra 4.50 from Wyatt Technology Corporation (dual detection) and Trisec 3.0 from Viscotek Corporation (triple detection). With the latter technique, information on r_g is obtained through the Flory-Fox equation:

$$r_g = \frac{1}{6^{1/2}} \frac{\left([\eta] \, M \right)^{1/3}}{\Phi}$$

(6)

where Φ is a shape factor. Because for all polymers studied the dn/dc-value is measured off-line it was possible to use the recommended calculation method with known dn/dc and known calibration constant (Astra).

4.3.3 Calibration and Normalisation of the Instruments

Before starting to use the set up for the characterisation of polymers, some instrument constants have to be determined to be able to obtain absolute data. The calibration measurements should be made with great care as the accuracy of all other measurements depends upon them. Consequently, both software packages (Astra and Trisec) require special calibration. In both cases a narrow polystyrene standard is used to determine interdetector volume delays to account for tubing volume.

4.3.3.1 LS photometer calibration

This calibration is needed for the Astra software. The quantities measured by the LS photometer are detector voltages proportional to light intensities, leading to a need to calibrate the detectors. Simplified, an instrument constant - independent of geometrical factors and diode sensitivity - is needed to fulfil the relationship $R(\theta) = k \, I(\theta)$. This constant is determined by monitoring the 90° detector signal voltage and the dark offset voltage – obtained with the laser

switched off using toluene as scattering standard. Toluene has the highest Rayleigh ratio of any of the common solvents ($R(\theta) = 1.406 \times 10^{-5}$ cm^{-1} at $\lambda = 632.8$ nm), and thus represents an interesting calibrator.

4.3.3.2 LS photometer normalisation

When the 90° detector is calibrated, each of the other detectors can be related to this by a set of normalisation coefficients. To normalise, an isotropic scatterer (scattering equally in all directions – mostly a low molecular weight polystyrene sample (PS 30 000) with a known radius less than 10 nm) is introduced in the cell, dissolved in the same solvent as is used for the molecular weight measurement. A set of coefficients is computed with the Astra software so that each detector gives the same $R(\theta)$ as the 90° detector when its signal is multiplied by its coefficient.

4.3.3.3 RI detector calibration

The proportionality factor relating detector output voltage to Δn is called the RI detector calibration constant. It is the number required to convert the voltage output into changes in refractive index units. To determine this constant injection of a series of accurately known concentrations (at least 5) of a sample with a known dn/dc value is needed. For this purpose a concentration range of solutions of p.a. NaCl, with a known dn/dc of 0.174 mL/g (at 633nm) is used. For each concentration the change in refractive index dn (equal to known concentration times known dn/dc) is calculated and the detector output (depending on phase difference) is measured. The slope of the plot of Δn versus output voltage yields the RI calibration constant, dn/dV (refractive index change per Volt). This calculation of the constant is performed in DNDC software and exported to the Astra software.

4.3.3.4 Viscometer zeroing and Trisec method construction

The viscometer does not require a separate calibration - only the pressure transducers need to be zeroed at zero flow when all capillaries contain pure solvent. The previously discussed calibrations and normalisation concern the requirements for absolute measurements and calculations using Astra software.

The Trisec software includes the viscometer data and requires the creation of a calculation method file. Injection of several narrow polystyrene standards as well as a broad standard of known dn/dc and known concentration allows calculation of peak parameters (σ and τ) and light scattering, mass and viscosity constants (of which the determinations are based on similar principles as discussed previously).

4.4 CHARACTERISATION OF PPV PRECURSOR POLYMERS

As discussed in chapter one of this thesis PPV is commonly used as a green light-emitting layer in polymer LEDs. Due to insolubility of the conjugated polymer, precursor routes were developed to be able to stop at the soluble precursor stage, enhancing the number of characterisation techniques. One of these precursor routes is the Sulfinyl route, developed in our research laboratory. It is very versatile and allows polymerisation of the same monomer in a range of solvents – as is discussed in chapter two.

The light scattering technique is used to determine absolute molecular weights and sizes of two Sulfinyl PPV-precursors obtained by polymerisation of chloromethyl-4-(*n*-octyl-sulfinyl)methylbenzene in MMF and secondary butanol according to a standard polymerisation procedure. These polymers are delivered by colleague researchers and will be referred to as butanol and MMF polymer, pointing at the solvent of synthesis. A comparison between the light scattering results of both polymers and the conventional SEC characterisation is made. The butanol polymer is also subjected to an in-line dual detector SEC-LS characterisation.

4.4.1 Off-line Characterisation

The off-line experimental set up is used to determine exact dn/dc-values of the Sulfinyl precursor polymers that can immediately be included in the calculations for the construction of a Zimm plot. The obtained data are compared with results of conventional SEC-measurements.

4.4.1.1 dn/dc-determination

In order to obtain accurate absolute values with the light scattering technique the exact value of dn/dc should be measured in a separate experiment using the off-line set up. Hence, for each polymer a series of 7 concentrations is made ranging from 3 x 10^{-4} to 1.2 x 10^{-3} g/mL. The corresponding graphs (dn versus concentration) of both PPV precursor polymers are shown in figure 4.8. The slope, as explained in section 4.3.1.1, determines the dn/dc-value, and the corresponding calculated dn/dc-values are listed in table 4.1.
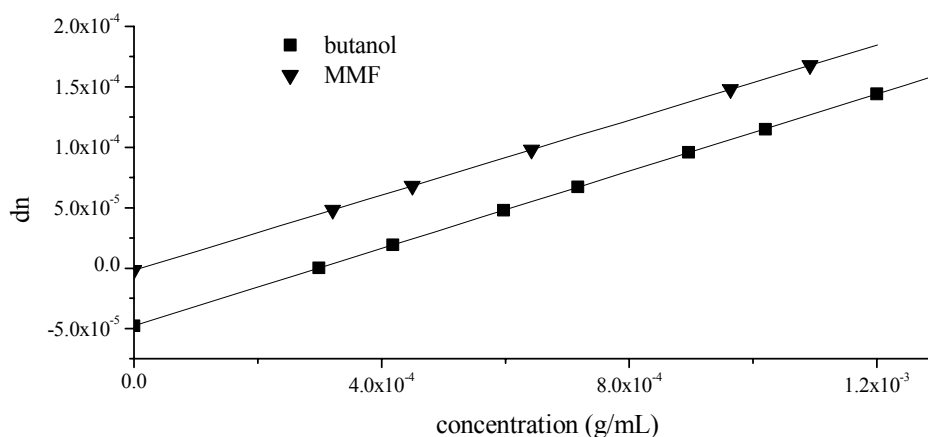
Figure 4.8: The dn/dc curves of the Sulfinyl PPV-precursor polymers

4.4.1.2 Construction of a Zimm plot and comparison
with conventional SEC

Simultaneous with the dn/dc measurement a Zimm plot can be constructed (figure 4.9) from which the absolute weight-average molecular weight, the value of A_2 and the RMS radius can be derived using the previously determined dn/dc value in the calculations. To construct the Zimm plot, first order angular and concentration fits are used, without smoothing or spike removal. The plot is displayed with a negative scaling factor (k = -794) to improve the overview and to spread the data over a larger area.
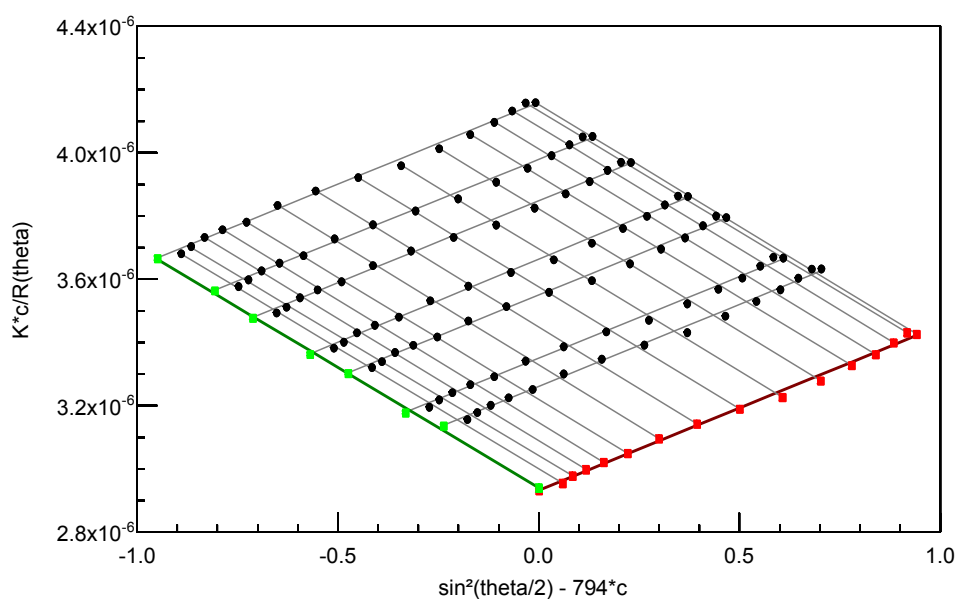
Figure 4.9: Zimm plot of the PPV-precursor polymer synthesised in butanol

The results thus obtained with the light scattering and concentration detector off-line are summarised in table 4.1. The precursor polymers are also subjected to a conventional SEC characterisation in THF using similar columns at 40°C and a standard RI as detector. The determined values for M_w – relative to narrow polystyrene standards - are listed in the third column.

Table 4.1: Survey of the LS results and comparison with conventional SEC

Solvent of Synthesis	dn/dc (mL/g)	M_w (SEC) (g/mol)	PD (SEC)
MMF	0.155 ± 0.004	290 000	2.2
s-butanol	0.156 ± 0.004	250 000	2.1

Solvent of Synthesis	M_w (LS) (10^5 g/mol)	$<R_g^2>_z^{1/2}$ (nm)	A_2 (10^{-4} mol mL/g^2)
MMF	3.27 ± 0.06	27.9 ± 1.7	3.21 ± 0.31
s-butanol	3.41 ± 0.02	26.2 ± 0.2	3.02 ± 0.09

The Astra software calculates uncertainties for all reported quantities determined from statistical fluctuation in each detector's output (by analysis of the baseline data). These uncertainties are statistical only, and do not include possible systematic errors (in dn/dc, calibration constants, or normalisation coefficients).

A comparison between the M_w-values determined by SEC and by light scattering demonstrates that the former technique underestimates the molecular weight, but yields values of the same order. This is a consequence of the fact that the Sulfinyl precursor polymers, as expected, behave somewhat different than polystyrene standards. However, the conventional SEC technique can be used to obtain relative molecular weights. It should be remarked that the conventional SEC technique can be sensitive to time variations due to the need of calibration – daily new calibration curves need to be constructed - and a possible explanation for the spread in SEC data is the fact that they are recorded separately, on different days.

The dn/dc-values determined for the two polymers can be called identical, pointing at a similar structure for the polymers in solution. This is confirmed by the values for the second virial coefficient, which also show a good correspondence, indicating that the two polymers exhibit similar interactions with the solvent. The positive value shows that THF acts as a good solvent for these polymers. The numbers for the weight average molecular weight likewise lie close to one another as well as the values of the radii of gyration. Actually, the large resemblance between all data of the two PPV-precursor polymers - obtained with the off-line light scattering set up – indicates that the structure of both is very similar.

4.4.2 SEC-LS Characterisation

The precursor polymer synthesised in secondary butanol is also subjected to an in-line dual detection set up. A polymer sample with a concentration of 1.2 mg/mL is injected, separated on the columns and detected by a light scattering and a concentration detector (in series). The determined dn/dc-value of 0.156 mL/g is used in the calculations resulting in the following numbers:

$M_w = (3.57 \pm 0.04) \times 10^5$ g/mol

PD = 1.8

$<R_g^2>_z^{1/2} = (23.8 \pm 0.5)$ nm.

The value for polydispersity can be determined thanks to the coupling with SEC. The numbers for M_w and RMS are in good agreement with the results presented in section 4.4.1: both in-line and off-line detection to characterise these polymers yield similar results. This indicates that the determination of constants during set up has been successful.

Thanks to the slicing of the chromatogram in the calculation method of the light scattering technique, the RMS radius can be determined at each elution volume. This way an idea about the conformation of the polymer can be formed by plotting the RMS radius as a function of molecular weight in a so-called conformation plot (figure 4.10). Both axes are scaled logarithmic and the slope, s, of the log-log plot yields information on the polymer's conformation. Theoretical slopes for spheres, random coils and rigid rods are 0.33, 0.50 and 1.0, respectively. Most real random coils have slopes in the range of 0.50 to 0.80[10]. For the butanol precursor polymer a slope-value of 0.55 is derived. This implies that this Sulfinyl precursor polymer behaves as a random coil in THF at 40°C.
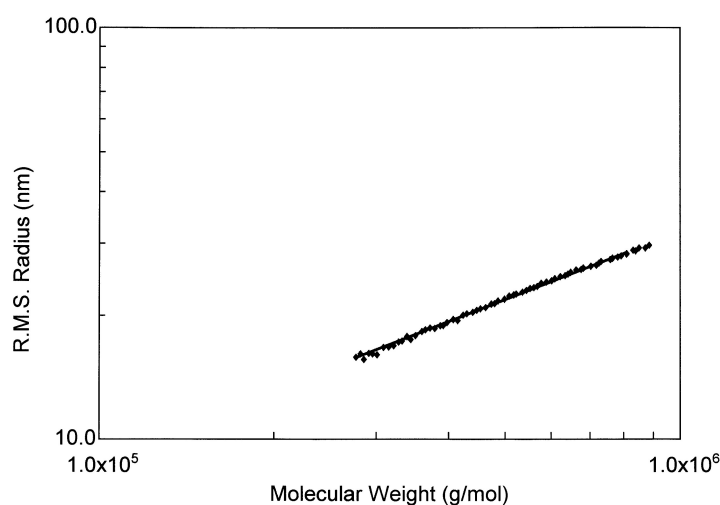
Figure 4.10: Conformation plot of the butanol polymer

4.4.3 Conclusions

Absolute molecular weights and sizes of two Sulfinyl precursor polymers differing in the solvent used for synthesis (secondary butanol and MMF), are determined using the light scattering technique. A comparison with conventional SEC analysis has shown that the latter underestimates the molecular weight of the polymers, but can be used as a means to determine relative numbers. The resemblance of the results of both polymers obtained by off-line detection – dn/dc, RMS - indicates that the structure of the PPV-precursor polymers is independent of the solvent of synthesis. The positive value of A_2 shows that THF at 40°C acts as a good solvent for these macromolecular species.

The in-line dual detection measurements on the butanol polymer demonstrate a good conformity between results of both set ups (in- and off-line). The values of M_w and RMS radius resulting from both experimental set ups are in good accordance. By plotting the RMS radius versus molecular weight using logarithmic scales a slope value of 0.55 is determined, pointing at a random coil conformation of the polymer in THF at 40°C.

4.5 CHARACTERISATION OF OC_1C_{10}-PPV

As described in chapter three of this thesis, this polymer is commonly used as active layer in polymer LEDs and also in plastic solar cells. It is soluble in common organic solvents in its conjugated form due to its alkoxy side -chains. The analysed polymers: Gilch and Sulfinyl OC_1C_{10}-PPV were obtained from Covion Organic Semiconductors and dr. Lutsen, respectively.

4.5.1 Off-line Characterisation

Samples of OC_1C_{10}-PPV, synthesised via the Sulfinyl and the Gilch route, are subjected to an off-line LS characterisation. This is done in order to determine their specific dn/dc-values and possibly construct a Zimm plot.

4.5.1.1 dn/dc-determination

For each polymer series of 4 to 5 concentrations are made ranging from 2 x 10^{-4} to 5 x 10^{-4} g/mL. The corresponding graphs (dn versus concentration) of the Gilch and the Sulfinyl OC_1C_{10}-PPV are shown in figure 4.11. The measurements on the Sulfinyl polymer are repeated thrice while two series of concentrations of the Gilch polymer are measured. The obtained results are listed in table 4.2.

Table 4.2: Dn/dc-values determined for Sulfinyl and Gilch OC_1C_{10}-PPV

OC_1C_{10}-PPV	Sulfinyl	Gilch
dn/dc (mL/g)	0.263 ± 0.002 0.264 ± 0.006 0.266 ± 0.004	0.384 ± 0.008 0.386 ± 0.004

The data show a good reproducibility per polymer, allowing determination of an average dn/dc-value for both polymers. From now on, average dn/dc-values of 0.264 and 0.385 mL/g for the Sulfinyl and the Gilch OC_1C_{10}-PPV, respectively, will be applied in calculations of the Astra software. The variation in dn/dc-value between Gilch and Sulfinyl polymer indicates that both polymers behave differently in these experimental conditions. The Gilch and Sulfinyl OC_1C_{10}-PPV have a rather high dn/dc-value, considering that those values normally lie in the range of –0.1 to 0.2 mL/g. Possibly, this is linked with their orange colour in solution.
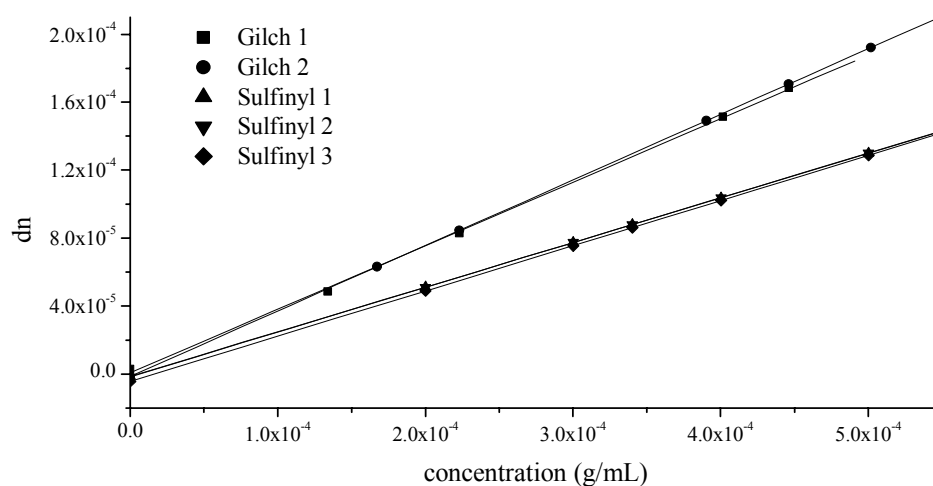
Figure 4.11: Overlay of dn/dc-graphs of the measured OC_1C_{10}-PPVs

4.5.1.2 Zimm plot construction

Simultaneous with the dn/dc-determination, the Astra-software records the data allowing the construction of a Zimm plot. This could be achieved for the measurements on the Sulfinyl polymers leading to the three sets of data listed in table 4.3. Repeated technical breakdowns caused a loss of the corresponding Gilch data. In the Zimm calculations the previously determined dn/dc-value of 0.264 mL/g is applied.

Table 4.3: Survey of Zimm plot results of the Sulfinyl OC_1C_{10}-PPV

Entry	M_w (LS) $(10^5$ g/mol)	$<R_g^2>_z^{1/2}$ (nm)	A_2 $(10^{-4}$ mol mL/g$^2)$
1	2.25 ± 0.04	39.2 ± 0.7	6.27 ± 0.98
2	2.13 ± 0.02	37.4 ± 0.4	4.17 ± 0.56
3	2.14 ± 0.02	37.9 ± 0.5	5.69 ± 0.44

Again the measurements show a rather good reproducibility, leading to a mean weight-average molecular weight value of about 220 000 g/mol, an average

RMS radius of 38 nm and a average second virial coefficient of approximately $5.4e^{-4}$ mol mL/g². The Zimm plot corresponding to the third entry is displayed in figure 4.12 using a negative scaling factor (k = -1898) and is constructed without the use of smoothing or spike removal features. Angular and concentration variations are fitted using first order polynomials. The other constructed Zimm plots (entries 1 and 2) are not displayed, but look very similar.
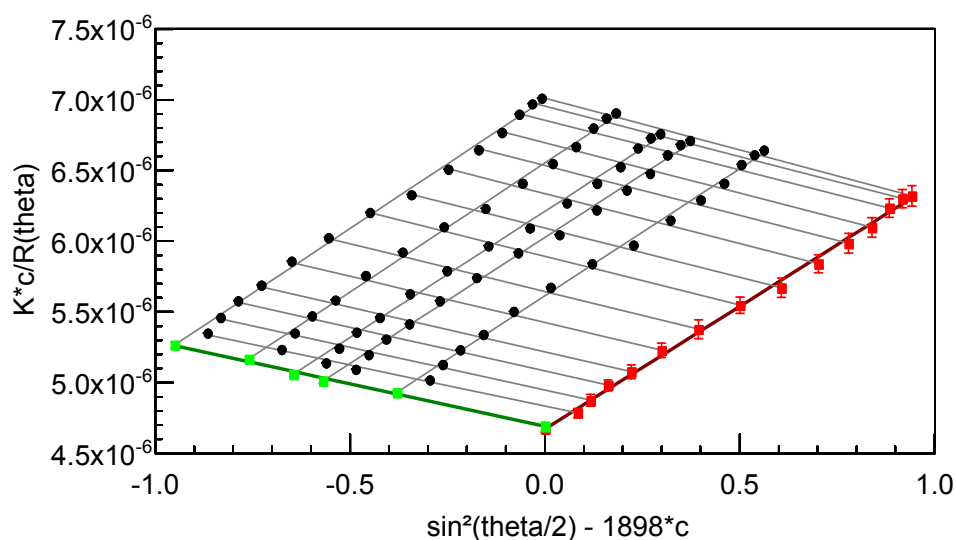
Figure 4.12: Zimm plot of the Sulfinyl OC$_1$C$_{10}$-PPV

4.5.2 SEC-LS Characterisation

Various polymers are subjected to an in-line SEC-LS analysis and the data are compared with the results of conventional SEC-measurements. The studied polymers are the Gilch and the Sulfinyl OC$_1$C$_{10}$-PPV of the previous study, and on top some Sulfinyl OC$_1$C$_{10}$-PPV obtained using variations in reaction conditions.

4.5.2.1 Comparison of Sulfinyl and Gilch OC$_1$C$_{10}$-PPV

During sample preparation it is experienced that filtration of the Gilch polymer causes more problems than the Sulfinyl OC$_1$C$_{10}$-PPV – even if 1.0 μm

filters are used. This is not the case for the off-line measurements, where much lower sample concentrations are used. The chromatogram of the Gilch OC_1C_{10}-PPV does show a strong tailing effect to the low molecular weight side of the chromatogram, possibly pointing at shear degradation. Therefore, another Gilch sample is injected, for which the filtration step during sample preparation is skipped, resulting in an improved chromatogram. A similar comparative experiment is performed on Sulfinyl OC_1C_{10}-PPV, but in this case no major difference between both chromatograms is demonstrated. Apparently, the Gilch polymer is much more sensitive to shear degradation during filtration or the higher molecular weight fraction is partially withheld by the filter material. Figure 4.13 shows an overlay of the corresponding SEC-LS chromatograms.

a : Sulfinyl - before filtration
b : Sulfinyl - after filtration
c : Gilch   - before filtration
d : Gilch   - after filtration

Figure 4.13: Overlay of chromatograms

    As a consequence, the filtration step in sample preparation is omitted in following measurements on the Gilch polymer. The chromatograms clearly demonstrate that the Gilch polymer has a higher average molecular weight and a broader distribution than the Sulfinyl OC_1C_{10}-PPV and this is confirmed by the
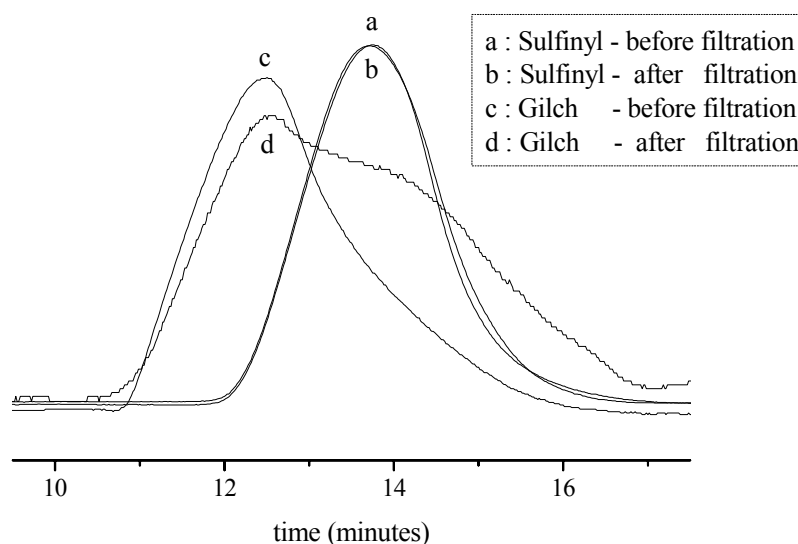
data listed in table 4.4. As could be expected the higher molecular weight is coupled to an increased value of the RMS radius. The SEC-LS data are obtained from non-filtered samples.

Table 4.4: Survey of SEC and SEC-LS results of
Gilch and Sulfinyl OC$_1$C$_{10}$-PPV

OC$_1$C$_{10}$-PPV	M$_w$ (SEC) (g/mol)	PD (SEC)	M$_w$ (LS) (10^5 g/mol)	$<R_g^2>_z^{1/2}$ (nm)	PD (LS)
Sulfinyl	500 000	3.6	1.80 ± 0.01	31.7 ± 0.6	1.40 ± 0.02
Gilch	1 900 000	9.2	5.40 ± 0.20	52.0 ± 7.4	1.88 ± 0.08

A comparison of the absolute data with conventional SEC results demonstrates that the latter technique can (only) be used as a relative molecular weight measure. The absolute values show large deviations with regards to the SEC-data, implying that calibration with polystyrene standards for OC$_1$C$_{10}$-PPV measurements is far from ideal. The large difference between the polydispersity of the Gilch polymer determined with SEC and the corresponding SEC-LS value, can be partially attributed to filtration of the SEC sample, resulting in tailing and hence a broader distribution. However, also the lower sensitivity of light scattering to the low molecular weight fraction of the distribution can lead to smaller (and erroneous) polydispersity values compared to those obtained by conventional SEC.

The in-line data on the Sulfinyl OC$_1$C$_{10}$-PPV demonstrate a rather good agreement with the obtained off-line data (section 4.5.1.2), as should, stressing the difference with conventional SEC.

4.5.2.2 Comparison of different Sulfinyl OC$_1$C$_{10}$-PPVs

A regular Sulfinyl polymerisation comprises the use of secondary butanol as solvent of synthesis, because this results in the highest yield (about 80 to 90%). Previous measurements are performed on this butanol Sulfinyl OC$_1$C$_{10}$-PPV. However, as mentioned previously, the versatile Sulfinyl route allows the use of a broad range of solvents as polymerisation medium, including NMP. A Sulfinyl OC$_1$C$_{10}$-PPV synthesised in this solvent – with conservation of other reaction

conditions - is included in the study to check for influences of solvent on polymer characteristics. Simultaneously, another Sulfinyl polymer is measured to investigate the influence of the experimental conditions of the elimination step. It is synthesised in secondary butanol, but instead of a thermal conversion process of three hours at 110°C in toluene, the solution is subjected to a temperature increase to 125°C for six hours. The corresponding SEC-LS results are listed in table 4.5 together with conventional SEC results. The determined dn/dc-value of Sulfinyl OC$_1$C$_{10}$-PPV of 0.264 mL/g is used in all calculations. As is shown in figure 4.14 the chromatograms are very similar. During sample preparation no filtration difficulties are encountered, and as shown in figure 4.13 (for the butanol polymer) chromatograms before and after filtration of each Sulfinyl polymer sample overlap completely – making a distinction between these results superfluous.

Table 4.5: Survey of SEC and SEC-LS results of various Sulfinyl OC$_1$C$_{10}$-PPVs

Sulfinyl OC$_1$C$_{10}$-PPV	M$_w$ (SEC) (g/mol)	PD (SEC)	M$_w$ (SEC-LS) (10^5 g/mol)	$<R_g^2>_z^{1/2}$ (nm)	PD (SEC-LS)
butanol	500 000	3.6	1.80 ± 0.01	31.7 ± 0.6	1.40 ± 0.02
NMP	200 000	4.1	0.955 ± 0.004	21.5 ± 0.6	1.47 ± 0.02
high T	790 000	3.8	2.83 ± 0.03	39.3 ± 1.0	1.32 ± 0.02

As is demonstrated in section 4.5.2.1 the conventional SEC-data differ significant from the absolute SEC-LS data, showing that a calibration based on polystyrene standards is not representative for OC$_1$C$_{10}$-PPV. However, the SEC values do give a correct relative proportion between the molecular weights.

As is the case with Sulfinyl PPV-precursors, a polymerisation towards OC$_1$C$_{10}$-PPV in secondary butanol results in a higher average molecular weight compared to polymers synthesised in NMP. This is possibly due to a lower momentarily *p*-quinodimethane concentration in the latter, resulting in shorter polymer chains.
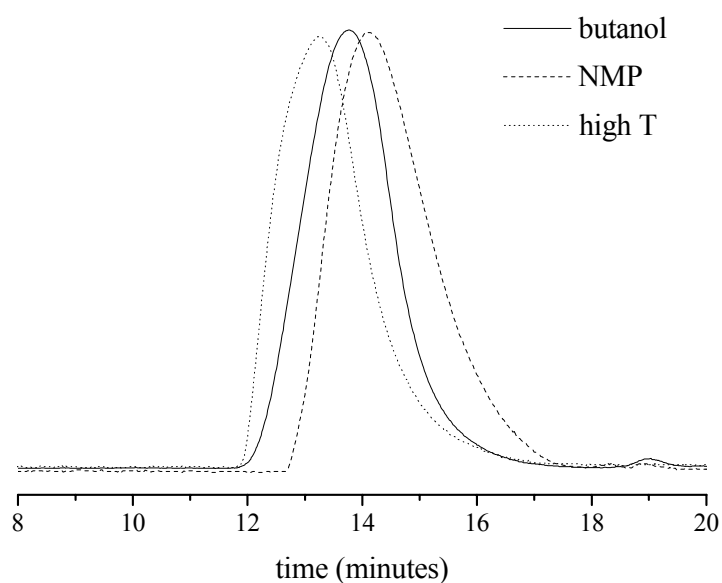
Figure 4.14: Overlay of SEC-LS chromatograms of
various Sulfinyl OC$_1$C$_{10}$-PPVs

Apparently, the combination of a higher elimination temperature and a longer exposure to this thermal treatment results in a higher average molecular weight value and a larger RMS radius. The larger RMS radius can possibly be explained by the execution of a more complete elimination - a polymer eliminated at 110°C for 3 hours still contains some residual sulfinyl groups – leading to a stiffer backbone and hence a larger hydrodynamic volume, eluting at a shorter elution time. However, the LS technique is supposed to be independent of the elution time, hence this can not explain the increase in molecular weight. At the moment a reasonable explanation for this phenomenon, other than synthetic influences, can not be offered.

4.5.3 <u>Branching Study on OC$_1$C$_{10}$-PPV</u>

4.5.3.1 Branching study on Gilch and Sulfinyl OC$_1$C$_{10}$-PPVs

The Gilch route suffers from gelation problems, whereas the Sulfinyl route does not, what could point at a more branched structure of the Gilch OC$_1$C$_{10}$-PPV. The SEC-LS technique with triple detection is used to look for relative differences in branching between both polymers by performing branching calculations on the SEC-LS chromatograms, included in the Astra and the Trisec software packages.
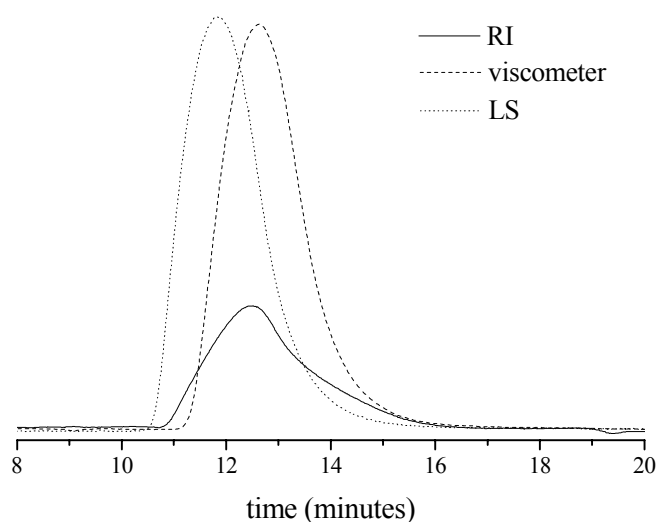
Figure 4.15: Signal overlay of the Gilch polymer: RI, LS and viscometer signals

To get an idea about the obtained chromatograms the signal overlay of the three detectors is shown in figure 4.15. The RI signal is much smaller than the LS and the viscometer detector signal, because it is only dependent on concentration. On the other hand, the light scattering detector yields a response proportional to molecular weight (MW) and concentration, while the viscometer detector response is proportional to the intrinsic viscosity (IV) and concentration, leading to increased intensities.

Traditionally, branching has been determined using a conformation plot, by comparing the slope, s, of the log-log plot RMS radius as a function of molecular weight. Branched molecules may have slopes much smaller than the typical random coil value (between 0.5 and 0.8), making the slope a possible indicator of branching. In figure 4.16 the conformation plots of both polymers are depicted.
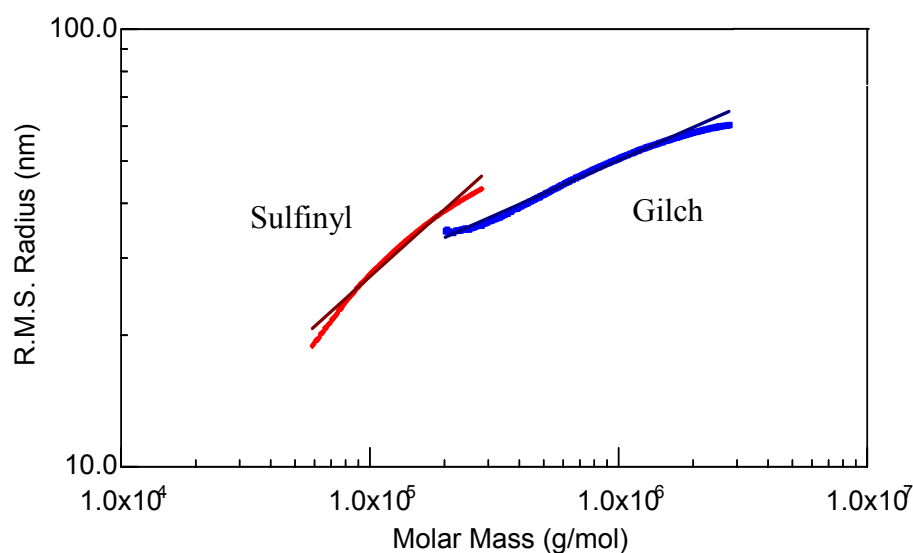
Figure 4.16: Conformation plot of the Sulfinyl and the Gilch OC_1C_{10}-PPV

The calculated slope value of 0.25 for the Gilch polymer clearly deviates from the value of 0.51 for the Sulfinyl and presents a first indication that the Gilch OC_1C_{10}-PPV probably has a more branched structure than the Sulfinyl polymer.

Another method for structural comparison is the Mark-Houwink plot in which intrinsic viscosity is plotted as a function of molecular weight, both on logarithmic scales. Branching indications can be a deviation of linearity at higher molecular weight, or a lower slope value. It is the preferred method over the conformation plot as a larger slope change is exhibited for the branching phenomenon. The Mark-Houwink plot of the Gilch and the Sulfinyl OC_1C_{10}-PPV is shown in figure 4.17 and demonstrates a lower slope value for the Gilch polymer.
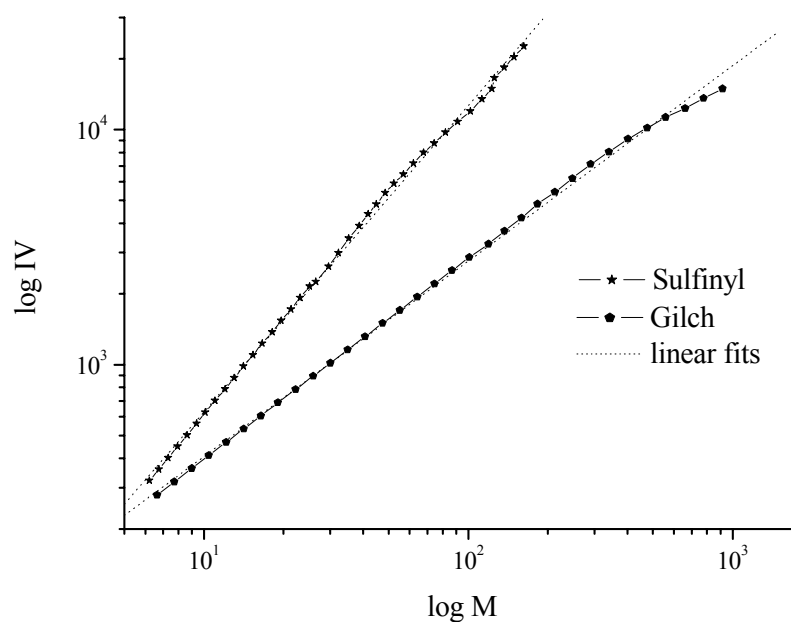
Figure 4.17: Mark-Houwink plot of the Sulfinyl and the Gilch OC_1C_{10}-PPV

The calculated values for the Mark-Houwink constants a and log K are listed in table 4.6 and are obtained from the slope and the point of intersection with the y-axis respectively, according to equation 7.

$$\log[\eta] = \log IV = \log K + a \log M \qquad (7)$$

The Mark-Houwink parameter a can in theory have a near zero value for globular proteins and a value of 1.0 or more for extended rod-like molecules. It is known that for most random coil molecules, a-values between 0.5 for poor solvent and 0.8 for good solvent are found. For polymers containing long chain branching, the a-value can fall significantly below 0.5, depending on the degree of branching.[11]

Table 4.6: The calculated Mark-Houwink values
for the Gilch and the Sulfinyl polymer

OC$_1$C$_{10}$-PPV	a	log K
Sulfinyl	0.98	-3.866
Gilch	0.76	-3.255

These data clearly show that the curve corresponding to the Gilch polymer has a significant lower slope than the curve of the Sulfinyl OC$_1$C$_{10}$-PPV. This again is an indication that the Gilch OC$_1$C$_{10}$-PPV has a more branched structure than the Sulfinyl polymer and confirms the results of the conformation plot. The calculated a-values are somewhat high for random coil molecules, probably due to an overlooked divergent parameter in the Trisec calculation method. However, this presents a minor or no problem, as the values are only used for relative comparisons.

The Mark-Houwink parameter a is related to the slope of the conformation plot s by the equation s = (a+1)/3. In this case, it would lead to s-values of 0.66 and 0.59 for the Sulfinyl and the Gilch OC$_1$C$_{10}$-PPV, respectively. The deviation with the s-values obtained from the conformation plots is probably due to the different ways of calculation with the distinct software packages. The Astra-software calculates the s-value from the slope of the conformation plot, while the Trisec-software derives the Mark-Houwink parameters from the Mark-Houwink plot. However, both methods lead to the conclusion that the Gilch curves have lower slope values than the corresponding Sulfinyl plots.

The construction of these plots can give a relative indication of branching, but there also exist calculation methods to determine numbers of branching frequencies and others. The Zimm branching factor or ratio[8c], g$_M$, is the starting point for branching calculations and is defined as:

$$g_M = \left(\frac{\langle r_g{}^2 \rangle_{br}}{\langle r_g{}^2 \rangle_{lin}} \right)_M \tag{8}$$

where $\langle r_g{}^2 \rangle_{br}$ and $\langle r_g{}^2 \rangle_{lin}$ are the mean square radii of the branched and the linear

polymer samples to be compared. However, the most used method for branching calculations involves viscosity measurements, because these are more sensitive at low molecular weight compared to LS. It was proposed that g_M is related to the intrinsic viscosity ratio by means of an empirical exponent epsilon (usually in the range of 0.6 to 0.8) following the equation:

$$g_M = \left(\frac{[\eta]_{br}}{[\eta]_{lin}} \right)^{1/\varepsilon}_M \tag{9}$$

The ratio's are taken at the same molecular weight (M), and because in general, for a given molecular weight, the branched polymer will have a smaller radius, the resulting g_M value will lie between 0 and 1. In order to obtain useful branching information, the two chromatograms should overlap as much as possible as the branching ratio can only be calculated in the region of overlap.

For randomly branched, polydisperse polymer samples the following equation allows calculation for the number of branches per molecule, B_n:

$$g_M = \frac{6}{B_n} \left[\frac{1}{2} \left(\frac{2 + B_n}{B_n} \right)^{1/2} \ln \left(\frac{(2 + B_n)^{1/2} + B_n^{1/2}}{(2 + B_n)^{1/2} - B_n^{1/2}} \right) - 1 \right] \tag{10}$$

For randomly branched polymers it is mostly preferred to speak of branching frequency, which is simply the number of branches per 1000 repeat units. This is expressed by the equation:

$$\lambda = 1000 \, B_n \frac{R}{M} \tag{11}$$

where M is the branched molecular weight (for the slice) and R is the repeat unit molecular weight. For these branching calculations it is of major importance to choose an appropriate and meaningful repeat unit molecular weight – in case of OC_1C_{10}-PPV the value of R is set equal to 288.

In the performed branching calculations the Sulfinyl OC_1C_{10}-PPV is supposed linear, and the structure constant, ε, is arbitrary set at 0.75, leading to the following values:

$$g_M = 0.267 \text{ ;}$$
$$B_n = 33.483 \text{ ;}$$
$$\lambda = 26.328.$$

These data do confirm the conclusions of the conformation and the Mark-Houwink plot: the structure of the Gilch OC_1C_{10}-PPV is more branched than the Sulfinyl polymer. The number of the branching frequency offers on top an estimated value of about 3% for the degree of branching in the Gilch polymer. This rather low percentage can explain why NMR measurements fail to detect branching points.

However, in an interesting publication of Covion Organic Semiconductors concerning structural ^{1}H- and ^{13}C-NMR studies on labeled (^{13}C enriched) Gilch OC1C10-PPV another possible explanation for the more compact structure is offered. Due to the symmetry of the monomer the Gilch polymers contain defects in the form of triple and single bonds instead of the usual double bonds. It was found that the extent to which these defects occur is about 3%, which remarkably accords with the value of 3% for the branching degree obtained in our SEC-LS measurements. The single bonds could result in some backfolding of the polymer chain, and hence lead to a smaller RMS radius compared to a fully conjugated polymer with a similar molecular weight. However, in the present study it is not possible to distinguish between these structural defects and real branching, hence both explanations should be retained.

4.5.3.2 Branching study on the various Sulfinyl OC_1C_{10}-PPVs

For the various Sulfinyl polymers the mutual Mark-Houwink plots are compared to check for structural differences and are displayed in figure 4.18. The corresponding calculated values for the Mark-Houwink constants a and K are listed in table 4.7.
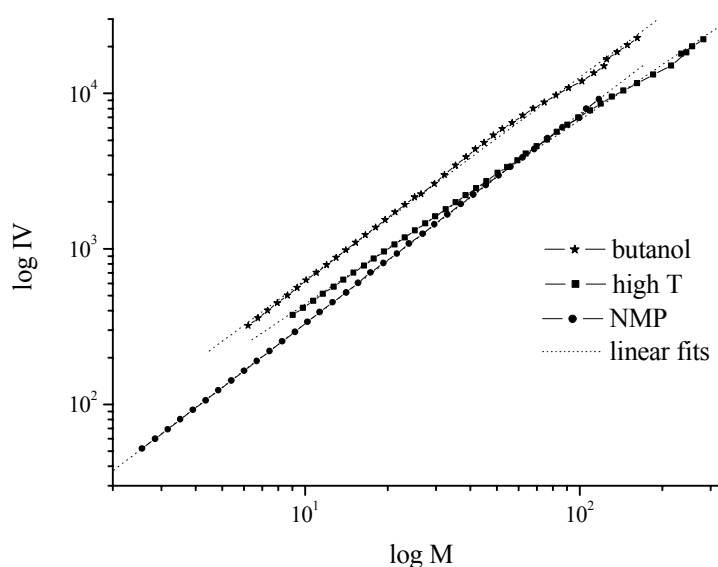
Figure 4.18: Mark-Houwink plot of the various Sulfinyl OC$_1$C$_{10}$-PPVs

Table 4.7: The calculated Mark-Houwink values
for the Gilch and the Sulfinyl polymer

OC$_1$C$_{10}$-PPV	a	log K	S
butanol	0.98	-3.866	0.66
NMP	1.06	-4.020	0.69
high T	0.92	-3.666	0.64

The Sulfinyl OC$_1$C$_{10}$-PPVs synthesised in NMP and butanol differ in molecular weight and hence RMS radius, but seem to have a similar structure, as their Mark-Houwink plots and parameters are very similar. The s-values listed in the last column are calculated from the a parameter by the equation s = (a+1)/3. Similar remarks can be made as for the comparison between Gilch and Sulfinyl OC$_1$C$_{10}$-PPV.

The similarity between the values for the various Sulfinyl OC$_1$C$_{10}$-PPV indicates that the solvent of synthesis does not influence the structure of the Sulfinyl polymer, which can be regarded as a random coil macromolecule. The

curve of the high temperature polymer does show a deviation in slope at the high molecular weight end compared to the other two curves. Apparently, the duration and temperature of elimination does have some effect on the structure of the polymer, but the deviation is so small that further branching calculations are not performed.

4.5.4 <u>Conclusions</u>

Various OC_1C_{10}-PPVs are analysed and characterised by means of the light scattering technique – as well off-line as in-line. The measurements actually can be divided in two parts: firstly, a study of the structural influence of the synthetic route used – the Gilch compared to the Sulfinyl route. Secondly, an investigation into the influence of the solvent of synthesis and a variation in elimination procedure, focussing on the Sulfinyl route. Because it is concentrated on possible structural differences, conformation and Mark-Houwink plots are constructed and both Astra and Trisec software packages are used to perform branching calculations.

The Sulfinyl and Gilch OC_1C_{10}-PPV are subjected to off-line dn/dc-measurements yielding average dn/dc-values of 0.264 and 0.385 mL/g, respectively, values which are used in further light scattering calculations. A concentration range of the Sulfinyl polymer has led to a successful construction of a Zimm-plot, confirming the use of THF as a suitable solvent for OC_1C_{10}-PPV.

The in-line SEC-LS technique is applied to the various polymers and a comparison with conventional SEC analysis has shown that the latter overestimates the molecular weight of the polymers. Hence, the use of polystyrene standards for conventional calibration is not reliable; however, it can be used as a relative means.

A comparison of SEC-LS data of Sulfinyl OC_1C_{10}-PPV synthesised in butanol and NMP reveals a lower molecular weight and RMS radius for the latter as could be expected. The corresponding Mark-Houwink plot does show similar curves pointing at similar structures. An increase in the duration and the temperature of elimination results in an increase in molecular weight, for which currently no reasonable explanation can be offered. The corresponding Mark-

Houwink plot shows a slight deviation of the 'linear' OC_1C_{10}-PPV synthesised according to a standard procedure in butanol, but it appeared too small to perform branching calculations upon. Hence, the solvent of synthesis does exhibit an influence on the molecular weight of the polymer, but not on the structure, whereas a longer duration of the elimination procedure combined with an increased temperature apparently does exhibit an effect on both.

The absolute molecular weights and sizes of the Sulfinyl and Gilch OC_1C_{10}-PPV determined by the SEC-LS technique show that the latter has much higher values, and causes filtration problems. Conformation and Mark-Houwink plots both indicate that the Gilch polymer has a more branched structure compared to the Sulfinyl polymer, by the occurrence of lower slope values. Branching calculations performed lead to a number of 3% as branching degree for the Gilch OC_1C_{10}-PPV. Another possible explanation for this divergent behaviour could be the occurrence of structural defects in OC_1C_{10}-PPV when synthesised via the Gilch route[13]. However, although encountered filtration problems point in the direction of branching at present a combination of both explanations is retained.

4.6 CONCLUSIONS

In conclusion it can be stated that the light scattering technique is successfully applied on different type of polymers. Once the necessary calibration and normalisation of the system is finished and meets the requirements, the technique can be used as a standard characterisation, taking as much time as conventional SEC, but yielding more absolute data.

Dn/dc-values are determined off-line as well for Sulfinyl PPV-precursors as for Sulfinyl OC_1C_{10}-PPV and Gilch OC_1C_{10}-PPV, and are used in further LS calculations. Various Zimm plots are constructed using a series of solutions of varying concentration and lead to absolute values of molecular weights, RMS radii and second virial coefficients.

Different Sulfinyl PPV-precursor polymers are subjected to a SEC-LS analysis. The in-line dual detection measurements on the butanol precursor polymer demonstrate a good conformity with the results obtained by off-line

detection. The derived number for the slope of the conformation plot, points at a random coil conformation of the precursor polymer in THF at 40°C. The positive value of A_2 shows that THF at 40°C acts as a good solvent for these macromolecular species.

Also various OC_1C_{10}-PPVs are analysed and characterised by means of the light scattering technique – as well off-line as in-line. The standard Gilch and Sulfinyl polymers are compared as well as various Sulfinyl OC_1C_{10}-PPVs, differing mutual in solvent of synthesis or elimination procedure. This is done in order to study the influence of the synthetic route and reaction conditions on the polymer characteristics. The absolute molecular weights and sizes of the Sulfinyl and Gilch OC_1C_{10}-PPV determined by the SEC-LS technique show that the latter has much higher values, and causes filtration problems. The SEC-LS data of Sulfinyl OC_1C_{10}-PPV synthesised in butanol and NMP reveal a lower molecular weight and RMS radius for the latter as could be expected. Apparently, an increase in the duration and the temperature of elimination results in an increase in molecular weight, for which currently no reasonable explanation can be offered.

A global comparison between (SEC-)LS results and conventional SEC results shows that the latter technique can be used to obtain relative molecular weights, but large deviations between relative and absolute values have been demonstrated especially in case of Gilch OC_1C_{10}-PPV. Hence, the use of polystyrene standards for conventional calibration is not reliable, however, it can be used as a relative means on condition that one compares similar polymers.

Because for the various Sulfinyl OC_1C_{10}-PPVs it is concentrated on possible structural differences, conformation and Mark-Houwink plots are constructed and both Astra and Trisec software packages are used to perform branching calculations. The Mark-Houwink plots of the butanol and the NMP Sulfinyl polymers show similar curves pointing at similar structures. The corresponding Mark-Houwink plots of the standard and the high temperature polymer show a slight deviation of the latter, but the difference appears too small to perform detailed branching calculations upon. Hence, the solvent of synthesis does exhibit an influence on the molecular weight of the polymer, but not on the structure,

whereas a longer duration of the elimination procedure combined with an increased temperature apparently does exhibit an effect on both.

Conformation and Mark-Houwink plots both indicate that the Gilch polymer has a more branched structure compared to the Sulfinyl polymer, by the occurrence of lower slope values. Branching calculations performed lead to a number of 3% as branching degree for the Gilch OC_1C_{10}-PPV. Another possible explanation for this divergent behaviour could be the occurrence of structural defects in OC_1C_{10}-PPV when synthesised via the Gilch route[13]. However, although encountered filtration problems point in the direction of branching at present a combination of both explanations is retained.

4.7 EXPERIMENTAL SECTION

Materials

The Sulfinyl PPV precursor polymer synthesised in MMF (starting from a 0.2 M monomer concentration) is obtained from dr. Issaris, while the corresponding secondary butanol PPV precursor (based on a monomer concentration of 0.1 M) is delivered by dr. van Breemen. The detailed polymerisation procedures used are described in reference 14 and 15, respectively. The Gilch OC_1C_{10}-PPV is obtained from Covion Organic Semiconductors via a polymerisation procedure described in reference 13, while the various Sulfinyl OC_1C_{10}-PPVs are synthesised by dr. Lutsen according to the following procedures.

In s-BuOH: 0.0163 mol (7 g) of the monomer 1-[2-[(butylsulfinyl)methyl]-5-(chloromethyl)-4-methoxyphenoxy]-3,7-dimethyloctane (and isomer)is dissolved in 60 mL *sec*-BuOH and flushed with nitrogen for 1 hour. A freshly prepared base solution of 0.0214 mol (2.04 g) of NatBuO in 60 mL of *sec*-BuOH is added in one portion resulting in a global monomer concentration of about 0.14 M. Polymerisation is allowed to proceed for 1 hour at ambient temperature under nitrogen atmosphere. The reaction mixture is poured into 300 mL of ice water and neutralised with a 0.1 M aqueous hydrogen chloride solution. After

extraction with chloroform (3 x 150 mL) the organic layers are combined, dried over $MgSO_4$ and concentrated under reduced pressure. The conversion to conjugated polymer is carried out in refluxing toluene at 110°C for 3 hours under nitrogen atmosphere. The conjugated material is obtained by precipitation in methanol, recovery by filtration and drying under reduced pressure.

In NMP: Similar procedure only this time NMP is used as solvent.

At high temperature: Similar polymerisation procedure only this time elimination is carried out at 125°C for 6 hours.

General remarks and instrumentation

In our laboratory a multi-detector SEC-LS set up is present that consists out of an isocratic HPLC pump (TSP 100), a Spectra series P100 (Spectra Physics) autosampler equipped with two mixed-B columns (10 μm, 2 x 30 cm x 7.5 mm, Polymer Labs)autosampler, a light scattering detector (Dawn-F, Wyatt Technology), a refractive index (concentration) detector (Optilab DSP, Wyatt technology) and a viscometer detector (H502B, Viscotek). The solvent used for the measurements is tetrahydrofuran (THF), HPLC grade. In the course of the SEC-LS measurements, calibration and normalisation constants had to be determined more than once, due to technical problems / breakdowns with one of the instruments or computers. Therefore more than one set of constants is used for the measurements.

For the standard SEC-measurements molecular weights and molecular weight distributions are determined relative to polystyrene standards (Polymer Labs) with a narrow polydispersity. Separation to hydrodynamic volume was obtained using a Spectra series P100 (Spectra Physics) autosampler equipped with two mixed-B columns (10 μm, 2 x 30 cm x 7.5 mm, Polymer Labs) and a refractive index (RI) detector (Shodex) at 40 °C. SEC samples are filtered through a 0.45 μm filter, except in case of filtration problems: then a 1.0 μm filter is used. HPLC grade THF (p.a.) is used as the eluent at a constant flow rate of 1.0 ml/min. Toluene is used as flow rate marker.

Filtration of the solvents used

The solvents toluene and THF that are used for calibration and measurements are filtered five times prior to use, to remove dust particles. A special set up is used to filter each solvent three times over a 0.2 μm and subsequently two times over a 0.02 μm Whatman Anodisc filter.

Calibration of the concentration detector

To calibrate the Optilab, the instrument has to be decoupled from the system. Solvent has to be changed from THF over ethanol to millipore water. This is done by means of a syringe pump, which injects solvent at a flow rate of 1 mL/min. In order to determine the Optilab calibration constant, a series of accurately known concentrations of NaCl has to be injected. All glassware is washed three times with millipore water and subsequently three times with ethanol. It is placed upside down to dry at ambient temperature. The p.a. NaCl is placed in the oven to remove possible traces of water. The reference cell must contain pure solvent during the measurement.

A stock solution of NaCl is made by dissolving 130 mg of p.a. sodium chloride in 100 mL millipore water. A series of concentrations is made by dilution of this stock solution, respecting concentrations in the order of 0.129 to 0.645 mg/mL. The concentrations are injected from low to high concentrations to minimise a possible effect of polution between samples. Pure solvent is injected at the start and the end of the measurement to check baselines. A calibration constant of about 1.9880 e-4 is obtained by means of the DNDC software package and is used in all other measurements unless stated otherwise. After this determination the instrument has to be put back in-line after changing solvent from millipore water over ethanol to THF.

Calibration of the light scattering detector

To calibrate the light scattering detector the DAWN-F is put off-line. A syringe pump is used to inject pure, filtered toluene at a flow rate of 1 mL/min. With the calibration function of the Astra software the measurement is repeated 10 to 20 times to obtain a more or less constant value. This way the results can be

averaged in order to increase the accuracy of the determination. A value of 4.4690 e-5 is obtained.

Normalisation of the light scattering detector

To normalise the Dawn laser a narrow standard polystyrene must be injected. It is possible to use the dawn coupled to the pump, as the solvent is THF. The 5 mL loop is used to inject a solution of PS 30 300 of 40 mg / 25 mL. The peak is normalised using a RMS radius of 5 nm and the obtained set of coefficients is saved as default.

To check the accuracy of the determined constants and normalisation coefficients and at the same time construct a method for the Trisec software a series of polystyrene standards (about 1 mg/mL) is injected using the coupled technique (SEC-LS): PS 30 300, PS 70 600, PS 156 000, PS 758 500 and NBS 706.

The narrow standard PS 30300 is used to determine the volume delay for the Astra as well as the Trisec software between the various detectors (= alignment) together with peak parameters for the Trisec method. The broad standard NBS 706 is used to refine those peak parameters of the Trisec method. A narrow polystyrene standard of 70 600 is used to calculate mass, viscosity and light scattering constants. If the Astra calculations on the polystyrene standards deviate significantly from the values on the warranty certificate, it means that the constants used are not accurate, and calibration and normalisation needs to be repeated. If the Trisec calculations show large deviations, a new method has to be constructed.

dn/dc-determination

Measurements are performed in THF at 40°C using the off-line set up. A series of concentrations of polymer solutions is made in filtered THF and measurements are recorded using the DNDC software package. The 4 to 7 concentrations used for each measurement will be listed.

Sulfinyl PPV precursor synthesised in MMF: 5 concentrations (g/mL): $3.21e^{-4}$; $4.50e^{-4}$; $6.42e^{-4}$; $9.63e^{-4}$; $1.09e^{-3}$ (Optilab calibration constant: $2.0563e^{-4}$); dn/dc $= 0.1552 \pm 0.0043$;

Sulfinyl PPV precursor synthesised in s-BuOH: 7 concentrations (g/mL): $2.99e^{-4}$; $4.18e^{-4}$; $5.98e^{-4}$; $7.17e^{-4}$; $8.96e^{-4}$; $1.02e^{-3}$; $1.20e^{-3}$; dn/dc $= 0.1557 \pm 0.0043$;

Sulfinyl OC_1C_{10}-PPV synthesised in s-BuOH: 5 concentrations (g/mL): $2.00e^{-4}$; $3.00e^{-4}$; $3.40e^{-4}$; $4.00e^{-4}$; $5.00e^{-4}$; dn/dc (1) $= 0.2627 \pm 0.0022$; dn/dc (2) $= 0.2637 \pm 0.0064$; dn/dc (3) $= 0.2660 \pm 0.0043$;

Gilch OC_1C_{10}-PPV: (1) 4 concentrations (g/mL): $1.34e^{-4}$; $2.23e^{-4}$; $4.02e^{-4}$; $4.46e^{-4}$; dn/dc (1) $= 0.3841 \pm 0.0080$; (2) 5 concentrations (g/mL): $1.67e^{-4}$; $2.23e^{-4}$; $3.90e^{-4}$; $4.46e^{-4}$; $5.02e^{-4}$; dn/dc (2) $= 0.3858 \pm 0.0035$.

Zimm plot construction

For three different polymers a Zimm plot could be constructed: the Sulfinyl PPV precursors synthesised in *s*-BuOH and MMF, and the OC_1C_{10}-PPV synthesised in *s*-BuOH. For this construction the same series of concentrations as for the dn/dc-measurements are used, as they are recorded simultaneously. The following settings are used in the Astra software: fit method/model: Zimm; angle fit degree:1; concentration fit degree: 1; no spike removal nor smoothing. Because for all polymers studied the dn/dc-value is measured off-line it was possible to use the recommended calculation method with known dn/dc and known calibration constant.

SEC-LS coupling

The SEC-LS measurements are performed using filtered THF as solvent in the in-line dual or triple set up. Both Trisec and Astra software packages are used for the recordings. Of each polymer sample 100 µL is injected onto the columns, maintaining a flow rate of 1 mL/min. and an LS detector angle of 90°. Following concentrations are applied: MMF PPV precursor: 2.46 mg/mL; *s*-BuOH PPV precursor: 1.20 mg/mL; Gilch OC_1C_{10}-PPV: 1.0 mg/mL; *s*-BuOH Sulfinyl OC_1C_{10}-PPV: 2.2 mg/mL; NMP Sulfinyl OC_1C_{10}-PPV: 1.3 mg/mL; high T Sulfinyl OC_1C_{10}-PPV: 1.1 mg/mL.

4.8 REFERENCES

1. Hand-outs of the course organised by Wyatt Technology Deutschland GmbH, entitled: "GPC-LS-Kopplung: Grundlagen und Praxis", Jena (Germany), 17 and 18 May 1999.

2. a) P.J. Wyatt, *Analytica Chimica Acta*, **272** (1993) 1; b) Ŝ. Podzimek, *J. Appl. Pol. Sci.*, **54** (1994) 91.

3. C. Henry, *Analytical Chemistry News & Features*, **January 1** (1998) 59A.

4. L. Jeng, S.T. Balke, T.H. Mourey, L. Wheeler, P. Romeo, *J. Appl. Pol. Sci.*, **49** (1993), 1359; b) L. Jeng, S.T. Balke, *J. Appl. Pol. Sci.*, **49** (1993), 1375.

5. A. Einstein, *Ann. Phys.*, **33** (1910) 1275.

6. C.V. Raman, *Indian J. Phys.*, **2** (1927) 1.

7. P. Debye, *J. Appl. Phys.*, **15** (1944) 338.

8. a) B.H. Zimm, *J. Chem. Phys.*, **13** (1945) 141 ; b) B.H. Zimm, R.S. Stein, P. Doty, *Polymer Bull.*, **1** (1945) 90 ; c) B.H. Zimm, *J. Chem. Phys.*, **16** (1948) 1093 ; d) B.H. Zimm, W.H. Stockmayer, *J. Chem. Phys.*, **17** (1949) 1301.

9. Manuals of the Optilab, the DAWN-F, the H502B viscometer and PL columns

10. Astra Software version 4.2, reference manual.

11. Trisec software version 3, reference manual.

12. M.A. Haney, D. Gillespie, W.W. Yau, *Today's chemist at work*, **3(11)** (1994) 39.

13. H. Becker, H. Spreitzer, K. Ibrom, W. Kreuder*, Macromolecules*, **32** (1999) 4925.

14. A. Issaris, *Ph.D. Dissertation*, 1997, Limburgs Universitair Centrum, Diepenbeek, België.

15. A.J.J.M. van Breemen, *Ph.D. Dissertation*, 1999, Limburgs Universitair Centrum, Diepenbeek, België.

Summary and Perspectives

The discovery of electroluminescence of conductive polymers has led to an impressive list of applications among which photovoltaic (solar) cells and polymer light-emitting devices (P-LEDs). It has moved the dream to create a generation of "plastic electronics" including flat television screens closer to reality. Currently, mainly PPV and its derivatives are used as active layer in these opto-electronic devices. An important number of synthetic routes developed to obtain these conjugated polymers can be classified as *p*-quinodimethane based polymerisations. The aim of this thesis was to gain knowledge of the nature of the polymerisation mechanism of this class of polymerisations, because it would allow an enhanced control on the reaction processes.

In *chapter one* a general introduction into the broad and complex field of conductive polymers, electroluminescence and P-LEDs is presented. The most important precursor routes towards these conjugated materials are summarised and an overview of literature on their mechanism is gathered. This demonstrates the difficulties inherent to such a mechanistic study and the present ongoing discord on the matter.

Chapter two comprises the results and discussion of a mechanistic study performed on the Sulfinyl precursor route towards PPV precursors in dipolar aprotic solvents, solvents that enhance the nucleophilicity. Working in this type of solvent yields the feature of a bimodal molecular weight distribution and constrains an optimisation of the polymerisation procedure. UV-vis and NMR-measurements confirm that the Sulfinyl route indeed belongs to the class of *p*-quinodimethane based polymerisations, while the presence of radicals during polymerisation is demonstrated by means of ESR spectroscopy. However, experiments where the effect of TEMPO and water addition on the polymerisation is investigated indicate that in this type of solvent, two distinct polymerisation mechanisms can occur

simultaneously. Apart from a radical mechanism that is responsible for the formation of a higher molecular weight polymer, also an anionic polymerisation mechanism can take place and results in oligomer formation. A more detailed analysis of residual fractions and a ^{13}C-NMR study of the oligomer fraction allow putting forward proposals for each mechanism. Experiments where the influence of concentration and temperature is checked are conform these proposals and help to gain insight in the competition between both mechanisms and offer ways to control each of them to a certain extent. These findings allowed composing an extension to other monomers and solvents, based on data gathered in our laboratory over the years, to obtain an overall picture of the polymerisation mechanism of the Sulfinyl route.

This knowledge is used in a study, described in *chapter three*, with as aim to link the polymerisation mechanism of the Sulfinyl and the Gilch route - both *p*-quinodimethane based polymerisations. In an attempt to elucidate the mechanism of both routes multiple polymerisations towards OC_1C_{10}-PPV are performed in apolar, aprotic solvents in the presence of different types of additives and the effects are evaluated. The results on the Sulfinyl route performed in THF strongly indicate the presence of a radical mechanism yielding higher molecular weight polymer and lie in the line of expectation elaborated in chapter two. During a similar series of experiments on the Gilch route in THF, unexpected problems with reproducibility surface. As a consequence, it is changed to dioxane – the solvent used for the industrial manufacture of OC_1C_{10}-PPV. A reproducible polymerisation procedure at room temperature is developed, based on the Covion procedure, and used to investigate the influence of different types of additives. Compared to the Sulfinyl route, the Gilch route is clearly more sensitive to reaction conditions. Nevertheless, strong indications are found that the main polymerisation mechanism operating in the Gilch route also is radical in nature and yields higher molecular weight polymers. Moreover, the obtained results make an anionic polymerisation mechanism less probable and question the interpretation of effects given in some publications by other research groups.

New features – irreproducibility and phase separation - during the Gilch experiments raise the question of gelation. A series of experiments demonstrates that apparently two types of gelation can occur, strongly depending on the

monomer concentration. At relatively high monomer concentrations (0.2 M) a chemically crosslinked gel is formed, which appears to be at least stable till temperatures of about 144°C. Lower monomer concentrations (0.02-0.03 M) can give rise to a physical network, possibly originating from an aggregation of polymers. A thermal treatment in dioxane at 98°C causes a decrease in molecular weight, but this decline is not continued over prolonged heating, therefore supporting the idea of the unravelling of a physical network. However, thermal as well as chemical degradation of polymer chains does seem to occur when the polymer is subjected to temperatures of about 144°C in *o*-xylene. Apparently, this feature of gelation is inherent to the Gilch route; in Sulfinyl polymerisations no such behaviour has ever been observed. Preliminary experiments indicate that the initial irreproducibility of Gilch polymerisations in THF can possibly be improved by a thermal treatment in dioxane at 98°C.

In *chapter four* the theoretical and practical background of the SEC-LS technique is described. This characterisation technique is successfully used to determine dn/dc-values of Sulfinyl PPV precursors, and Sulfinyl and Gilch OC_1C_{10}-PPV and these numbers are used in further LS calculations. Various Zimm plots are constructed and lead to absolute values of molecular weights, RMS radii and second virial coefficients. The positive values of A_2 show that THF at 40°C acts as a good solvent for all analysed macromolecular species.

A global comparison between (SEC-)LS results and conventional SEC results demonstrates that the latter technique can (only) be used to obtain relative molecular weights. Especially in the case of Gilch OC_1C_{10}-PPV significant deviations between relative and absolute values are observed.

Various OC_1C_{10}-PPVs are analysed in order to study the influence of the synthetic route and reaction conditions on the polymer characteristics. Conformation and Mark-Houwink plots are constructed and branching calculations are performed. The results indicate that the Gilch polymer has a more branched structure compared to the Sulfinyl polymer, with a number of 3% as branching degree. However, this divergent behaviour could also be explained by the occurrence of structural defects in Gilch OC_1C_{10}-PPV. Indications are found that for the Sulfinyl route the solvent of synthesis does exhibit an influence on the molecular weight of the polymer, but not on the structure, whereas a longer

duration of the elimination procedure combined with an increased temperature apparently does exhibit an effect on both.

As an overall conclusion it can be stated that the mechanistic study is a self-contained unit. The nature of the polymerisation mechanism of *p*-quinodimethane based polymerisations is more or less elucidated: a main radical mechanism is responsible for the formation of high molecular weight polymer, while depending on the monomer and the solvent used also an anionic mechanism can occur which leads to oligomer formation.

It could be interesting to check if this knowledge can be applied to other monomers, e.g. electron-poor systems. The polymerisation could be steered to some extent: reaction conditions can be chosen in order to suppress or favour the anionic polymerisation mechanism. More research is needed to fill in some missing details.

An aspect that is not dealt with in this work is the mechanism behind *p*-quinodimethane formation: E_{1cb} or E_2. Possibly, the stop flow technique in UV-vis spectroscopy can monitor the first moments of reaction and thus allow a detailed kinetic analysis, leading to a better understanding and manipulation of reactions. It could offer ways to adjust reaction conditions to promote *p*-quinodimethane formation for specific monomers.

A more detailed NMR analysis can present a possible way to detect and identify structural defects, initiating particles and / or end groups. However, to compensate for the low abundance of these features working with labelled ^{13}C-enriched materials seems appropriate.

Another interesting feature, especially for industry, is the effect of a thermal treatment in *o*-xylene at 144°C on the Gilch OC_1C_{10}-PPV. More research is required to detect how and which degradation processes occur and if this feature is inherent to the solvent *o*-xylene, the Gilch route and / or the elevated temperature.

These perspectives could provide some missing parts to complete the picture of the complex chemistry of *p*-quinodimethane-based polymerisations.

Samenvatting en Perspectieven

De ontdekking dat geleidende polymeren licht kunnen geven onder invloed van spanning (elektroluminescentie) heeft tot een indrukwekkende lijst van mogelijke toepassingen geleid, waaronder plastic zonnecellen en polymere LEDs. De droom van een generatie van "plastic elektronica" waartoe ook vlakke, flexibele, oprolbare beeldschermen behoren, is hierdoor dichter bij de realiteit gekomen.

Tegenwoordig worden vooral PPV en –derivaten als actieve laag in deze opto-elektronische toepassingen gebruikt. Een belangrijk aantal van de syntheseroutes, ontwikkeld om deze geconjugeerde polymeren te verkrijgen, vallen onder de noemer van *para*-quinodimethaan-gebaseerde polymerisaties. Het doel van dit doctoraatsproefschrift was om meer inzicht te verwerven in de aard van het polymerisatiemechanisme van deze klasse van polymerisaties. Dit zou toelaten om de reactieprocessen beter te sturen en meer controle uit te oefenen op de eindproducten.

In *hoofdstuk 1* werd getracht een algemene inleiding tot en overzicht van het brede en complexe veld van geleidende polymeren, elektroluminescentie en polymere LEDs te bieden. De meest belangrijke precursorroutes naar deze geconjugeerde materialen werden samengevat weergegeven, samen met een literatuuroverzicht over hun mechanisme. Hierdoor werden de moeilijkheden die samengaan met een mechanistische studie en de nog steeds voortdurende onenigheid over de aard van het onderliggende mechanisme aangetoond.

Hoofdstuk 2 bevat de resultaten en discussie van een mechanistische studie uitgevoerd op de Sulfinyl precursorroute naar PPV-precursoren toe in dipolaire, aprotische solventen; solventen die de eigenschap hebben om de nucleofiliciteit te verhogen. Het werken in dit type van solvent bracht het optreden van een bimodale

Samenvatting en Perspectieven

moleculaire gewichtsverdeling met zich mee en vereiste een optimalisatie van bestaande polymerisatieprocedures. UV-vis en NMR-metingen bevestigden dat de Sulfinyl route inderdaad tot de klasse van *p*-quinodimethaan-gebaseerde polymerisaties behoort, terwijl de aanwezigheid van radicalen tijdens de polymerisatie werd aangetoond door middel van ESR-spectroscopie. Experimenten waarbij het effect van de additie van TEMPO en water op de polymerisatie onderzocht wordt, gaven aan dat in dit type solvent twee verschillende polymerisatiemechanismen gelijktijdig kunnen optreden. Naast een radicalair mechanisme dat verantwoordelijk is voor de vorming van polymeer met een hoog moleculair gewicht, kan ook een anionisch polymerisatiemechanisme optreden dat resulteert in oligomeervorming. Een meer gedetailleerde analyse van restfracties, gecombineerd met een ^{13}C-NMR studie van de oligomeerfractie liet toe om voorstellen voor elk mechanisme te formuleren. Experimenten die de invloed van concentratie en temperatuur nagaan, bevestigden deze voorstellen. De resultaten hielpen bij het verwerven van inzicht in de competitie tussen beide mechanismen en bieden in zekere mate mogelijkheden aan om deze te beheersen. Deze bevindingen lieten toe om een uitbreiding naar andere solventen en monomeren samen te stellen, gebaseerd op een hele reeks data die over de jaren in onze onderzoeksgroep werden verzameld. Op die manier werd een globaal beeld van het polymerisatiemechanisme van de Sulfinyl route bekomen.

Deze verworven kennis werd gebruikt in een studie, beschreven in *hoofdstuk 3*, met als doel het polymerisatiemechanisme van de Sulfinyl en de Gilch route – beide *p*-quinodimethaan-gebaseerde polymerisaties - met elkaar te verbinden. In een poging om het mechanisme van beide routes op te helderen werden meerdere polymerisaties uitgevoerd in apolaire, aprotische solventen in aanwezigheid van verschillende additieftypes en werden de effecten op OC_1C_{10}-PPV vorming geëvalueerd. De resultaten van de Sulfinyl route in THF wijzen sterk op een radicalair mechanisme verantwoordelijk voor de vorming van polymeer met een hoog moleculair gewicht en liggen in de lijn van verwachting uitgewerkt in hoofdstuk 2. Tijdens een gelijkaardige reeks van experimenten op de Gilch route in THF traden onverwachte problemen rond reproduceerbaarheid op. Bijgevolg werd er overgeschakeld op dioxaan - het solvent dat gebruikt wordt voor de industriële bereiding van OC_1C_{10}-PPV. Een reproduceerbare polymerisatieprocedure bij

kamertemperatuur werd ontwikkeld, gebaseerd op de Covion procedure. Ze werd gebruikt om de invloed van diverse soorten additieven te onderzoeken. Vergeleken met de Sulfinyl route is de Gilch route duidelijk meer gevoelig voor reactie omstandigheden. Niettemin werden sterke aanwijzingen gevonden dat tijdens de Gilch polymerisatie een radicalair mechanisme optreedt dat verantwoordelijk is voor de vorming van hoog moleculair gewicht polymeer. Sterker nog, de bekomen resultaten maken een anionisch polymerisatiemechanisme minder waarschijnlijk en stellen de interpretatie van effecten in bepaalde publicaties van andere onderzoeksgroepen in vraag.

Nieuwe observaties – een slechte reproduceerbaarheid en fasescheiding – tijdens de Gilch experimenten deden vragen rijzen over het optreden van gelering. Een reeks van experimenten toonde aan dat blijkbaar twee verschillende types van gelering kunnen voorkomen, sterk afhankelijk van de concentratie. Relatief hoge monomeerconcentraties (0.2 M) geven aanleiding tot de vorming van een chemisch gecrosslinkte gel, die stabiel lijkt te zijn tot op een temperatuur van tenminste 144°C. Bij relatief lage monomeerconcentraties (0.02-0.03 M) kan een fysisch netwerk gevormd worden, dat mogelijk te wijten is aan aggregatie van polymeerketens. Een thermische behandeling in dioxaan bij 98°C veroorzaakt een afname in moleculair gewicht, die niet oneindig doorgaat en zo de veronderstelling van een ontrafeling van een fysisch netwerk ondersteunt. Zowel thermische als chemische degradatie treden mogelijk wel op indien het polymeer voor relatief korte tijd onderworpen wordt aan een temperatuur van 144°C in *o*-xylene. Blijkbaar is deze geleringseigenschap inherent voor de Gilch route, want bij Sulfinyl polymerisaties werd zulke gedrag nog niet waargenomen. Inleidende experimenten indiceren dat de slechte reproduceerbaarheid van Gilch polymerisaties in THF mogelijk verbeterd kan worden door de polymeren te onderwerpen aan een thermische behandeling in dioxaan bij 98°C.

In *hoofdstuk 4* komen de theoretische en praktische achtergrond van de SEC-LS techniek aan bod. Deze karakterisatietechniek is met succes toegepast om dn/dc-waarden te bepalen van Sulfinyl PPV-precursoren, en van Sulfinyl en Gilch OC_1C_{10}-PPV. De bekomen waardes werden gebruikt in verdere lichtverstrooiings-berekeningen. Meerdere Zimm plots werden samengesteld wat leidde tot absolute waardes voor moleculaire gewichten, gyratiestralen, en tweede viriaalcoëfficiënten.

Uit de bekomen positieve A_2-waarde blijkt dat THF zich bij 40°C als een goed solvent gedraagt voor alle bestudeerde macromoleculaire oplossingen.

Een algemene vergelijking tussen (SEC-)LS en conventionele SEC resultaten toont aan dat de laatstgenoemde techniek (enkel) kan gebruikt worden om relatieve moleculaire gewichten te bekomen. Vooral in het geval van Gilch OC_1C_{10}-PPV werden significante afwijkingen tussen relatieve en absolute waardes waargenomen.

Meerdere OC_1C_{10}-PPVs werden geanalyseerd om de invloed van syntheseroute en reactiecondities op de polymeereigenschappen na te gaan. Conformatie en Mark-Houwink plots werden samengesteld en vertakkings-berekeningen uitgevoerd. De bekomen resultaten geven aan dat het Gilch polymeer een meer vertakte structuur (berekende vertakkinggraad = 3%) heeft dan het Sulfinyl polymeer. Hierbij dient echter te worden opgemerkt dat dit afwijkend gedrag ook te wijten kan zijn aan de aanwezigheid van structurele defecten in Gilch OC_1C_{10}-PPV. Er werden aanwijzingen gevonden dat het synthesesolvent wel een invloed op het moleculair gewicht van Sulfinyl polymeren heeft, maar niet op de structuur. Dit terwijl een verlenging van eliminatietijd gecombineerd met een verhoogde temperatuur blijkbaar op beide een effect heeft.

Als een algemene conclusie kan men stellen dat de mechanistische studie als een afgerond geheel kan beschouwd worden. De aard van het polymerisatie-mechanisme van op *p*-quinodimethaan-gebaseerde polymerisaties is min of meer opgehelderd. Het hoofdmechanisme is radicalair en is verantwoordelijk voor de vorming van hoog moleculair gewicht polymeer. Gelijktijdig kan, sterk afhankelijk van het monomeer en het solvent, ook een anionisch mechanisme optreden dat aanleiding geeft tot oligomeren.

Het zou interessant zijn om te onderzoeken of deze bevindingen kunnen toegepast worden op andere monomeren, bijvoorbeeld electronenarme systemen. De polymerisatie zou in zekere mate gestuurd kunnen worden door de keuze van reactieomstandigheden in functie van een onderdrukking of stimulatie van het anionisch polymerisatiemechanisme. Verder onderzoek is nodig om de ontbrekende details in te vullen.

Een ander aspect dat niet aan bod is gekomen in dit werk is het mechanisme dat schuilt achter de *p*-quinodimethaanvorming: E_{1cb} of E_2. De stop-flow techniek in UV-vis spectroscopie kan een mogelijkheid bieden om de eerste ogenblikken van de reactie te volgen en zo een gedetailleerde kinetische analyse toelaten. Dit kan tot een beter begrip en manipulatie van de reacties leiden en zo mogelijkheden bieden om reactiecondities in geval van bijzondere monomeren aan te passen in het voordeel van *p*-quinodimethaanvorming.

Om structurele polymeerdefecten, initiërende deeltjes en / of eindgroepen te detecteren en te identificeren zou een meer gedetailleerde NMR analyse aangewezen zijn. Het werken met gelabelde of ^{13}C-aangerijkte materialen kan dan een uitweg zijn om te compenseren voor de lage abundantie van deze structuren.

Een andere opvallende observatie is het effect van een thermische behandeling van Gilch OC_1C_{10}-PPV in *o*-xylene bij 144°C. Meer onderzoek is nodig om te achterhalen hoe en welke degradatieprocessen optreden en of dit afhankelijk is van het solvent *o*-xylene, de Gilch route en / of de verhoogde temperatuur.

Deze perspectieven zouden enkele ontbrekende delen kunnen opleveren die nodig zijn om de complexe chemie van *p*-quinodimethaan-gebaseerde polymerisaties volledig op te helderen.

List of Abbreviations

A_2	second virial coefficient, a measure for the polymer-solvent interaction
AT	ambient temperature
CB	conduction band (band theory)
CBr_4	carbon tetrabromine, chain transfer agent
CCl_4	carbon tetrachloride, chain transfer agent
$Cd\ m^{-2}$	Candela per square meter, unit to express luminance or light intensity
CDT	Cambridge Display Technology
CPR	chlorine precursor route, referred to as Gilch route
CVD	chemical vapour deposition
d	diameter
DAS	dipolar, aprotic solvent
di*t*BuMeOPhOH	2,6-di-*tert*-butyl-4-methoxyphenol
DMF	N,N-dimethylformamide
DMPO	5,5-dimethyl-1-pyrroline-N-oxide, spin trap
DMSO	dimethylsulfoxide
dn/dc	specific refractive index increment for a change of solute concentration
DPPH	diphenyl picryl hydrazine, radical scavenger
DP-PPV	diphenyl poly(*p*-phenylene vinylene)
DSP	digital signal processing
E_g	band gap, energy spacing between the HOMO and the LUMO
EL	electroluminescence
ESR	electron spin resonance
FET	field effect transistor
HCl	hydrogen chloride
HOMO	highest occupied molecular orbital
HPLC	high pressure (/ performance) liquid chromatography
I_0	incident light intensity

I_θ	light intensity at scattering angle θ
IR	infrared (light, spectroscopy)
ITO	indium-tin-oxide
IV	intrinsic viscosity
K*t*BuO	potassium *tertiar*-butoxide, base
L	leaving group
LALLS	low angle laser light scattering
LCD	liquid-crystal display
LDA	lithium diisopropyl amide, base
LEC	light-emitting electrochemical cell
Lm/W	Lumen per Watt, unit to express luminous efficiency
LS	light scattering
LUMO	lowest unoccupied molecular orbital
M	molar, mol/l, unit to express concentration
MALLS	multi angle laser light scattering
MDMO-PPV	poly[2-methoxy-5-(3,7-dimethyloctyloxy)-*p*-phenylene vinylene]
MEH-PPV	poly[2-(2'-ethylhexyloxy)-5-methoxy-1,4-phenylene vinylene]
MeOPhOH	4-methoxyphenol or *para*-methoxyphenol
MMF	N-methyl formamide
M_n	number-average molecular weight
M_w	weight-average molecular weight
MWD	molecular weight distribution
Na*t*BuO	sodium *tertiar*-butoxide, base
NMP	N-methyl pyrrolidinone
NMR	nuclear magnetic resonance spectroscopy
OC_1C_{10}-PPV	poly[2-methoxy-5-(3,7-dimethyloctyloxy)-*p*-phenylene vinylene]
P	polariser
P(θ)	particle light scattering function
PA	polyacetylene
PANI	polyaniline
PD	polydispersity, equal to M_w/M_n
PEDOT	poly(ethylenedioxythiophene)
PEDOT/PSS	PEDOT doped with PSS
PET	poly(ethyleneterephthalate)
PL	photoluminescence [or Polymer Laboratories (chapter 4)]
P-LED	polymer light-emitting device
PPP	poly(*p*-phenylene)
PPV	poly(*p*-phenylene vinylene)
PPX	poly(*p*-xylylene)
PSS	polystyrenesulfonic acid
PT	polythiophene
p-QM	*para*-quinodimethane

224

QE   quantum efficiency
QM   quinodimethane

radius of gyration root mean square radius
$<r_g^2>^{1/2}$ radius of gyration
R(θ)   excess Rayleigh ratio
RI   refractive index
RMS radius   root mean square radius; also called radius of gyration

SEC   size exclusion chromatography
SEC-LS   SEC coupled with LS
$S\ m^{-1}$ Siemens per meter, unit to express conductivity

*t*BuOK   potassium *tertiar*-butoxide
*t*BuONa   sodium *tertiar*-butoxide
*t*BuMeOPhOH   2-*tert*-butyl-4-methoxyphenol
*t*BuϕCH$_2$Br   *t*-butylbenzyl bromide
*t*BuϕCH$_2$Cl   *t*-butylbenzyl chloride
TEMPO   2,2,6,6-tetramethylpiperidinoxyl, radical scavenger
T_g glass transition temperature, transition temperature between
              a polymers' glass and liquid phase
THF   tetrahydrofuran
THT   tetrahydrothiophenium
TLC   thin layer chromatography

UV   ultraviolet (light, spectroscopy)

VB   valence band (band theory)